UNIVERSITÀ DEGLI STUDI DI MILANO

Department of Pharmacological and Biomolecular Sciences

PhD School in Integrative Biomedical Research

XXXI Cycle – Curriculum: Neuroscience

Novel molecular mechanisms underlying GnRH neuron biology and associated reproductive disorders

Roberto Oleari

R11282

PhD Tutor: Prof. Anna Cariboni

PhD School Coordinator: Prof. Chiarella Sforza

Academic Year 2017-2018

Summary

Gonadotropin-releasing hormone (GnRH) neurons regulate the neuroendocrine hypothalamus-pituitary-gonad axis which is the main regulator of reproductive function in many vertebrates. During development, GnRH neurons originate in the nasal placode and migrate along olfactory nerves towards the hypothalamus, where they finally set and integrate in a complex neural network that regulates GnRH secretion. Isolated GnRH Deficiency (IGD) is a rare disorder affecting reproduction characterized by absent puberty onset and infertility. IGD may be caused from either defective GnRH neuron development or function, leading to a wide spectrum of phenotypes which includes normosmic Hypogonadotropic Hypogonadism (nHH), Kallmann Sydrome (KS) and syndromic IGD. Although 35 causative genes have been already identified, IGD genetics remains largely unknown, with up to 50% of overall cases still idiopathic. The identification of novel genes implicated in IGD is fundamental to ameliorate diagnosis and treatment. Here, we have combined screening of IGD patients, together with *in silico*, *in vitro* and *in vivo* experimental models to identify novel IGD causative genes. First, we found a novel homozygous variant in Semaphorin 3G (*SEMA3G*) gene in two brothers affected by an unrecognized form of syndromic IGD, displaying nHH, facial dysmorphisms and mental retardation. We demonstrated both in GN11 cells and in *Sema3g*-null mice that SEMA3G underlies nHH, whereas additional mutations in Rhotekin (*RTKN*) and Natural Killer cell Triggering Receptor (*NKTR*) genes may potentially explain the complex phenotype observed in the two brothers. Then, we showed that Plexin a1 (Plxna1) and Plexin a3 (Plxna3) cooperatively act as signal transducing receptors for Sema3a in the context of GnRH neuron and olfactory system development. Indeed, compound *Plxna1;Plxna3*-null mice, but not single *Plxna1* and *Plxna3* knock out mice, displayed an abnormal phenotype suggesting that the loss of a single Plxna isoform is not sufficient to phenocopy *Sema3a* deletion. Hence, we proposed that not only *PLXNA1* but also *PLXNA3* should be considered as a candidate gene to be screened in IGD patients and in particular in whose affected by KS. Finally, we investigated the genetic causes that lead to an IGD-related disorder known as familial self-limited delayed puberty (DP). By analysing exome sequencing data from a large number of patients who belong to a large and well-characterised cohort of patients, we linked a deleterious heterozygous variant in Heparan Sulphate 6-O Sulpho-Transferase 1 gene (*HS6ST1*) to the onset of familial self-limited DP. These results were corroborated by *in vivo* experiments on *Hs6st1*$^{+/-}$ and wild type showing that haploinsufficiency of Hs6st1 is sufficient to delay puberty onset in mice. Overall, the results presented in this thesis have provided novel insights into the molecular mechanisms that control GnRH neuron biology and into the genetics underlying associated reproductive disorders. These results also provided evidences that the combined access to mutational screenings of patients with the application of *in silico*, *in vitro* and *in vivo* experimental models are effective in the discovery of novel genes implicated in rare and complex inherited disorders such as IGD.

Index

SECTION I – Introduction 1

1. The vertebrate reproductive system: the hypothalamus-pituitary-gonad axis 2

1.1 HPG axis regulation 4

1.2 HPG axis activity during development 6

1.2.1 Puberty 8

1.3 The Gonadotropin-releasing hormone 8

1.4 GnRH-secreting neurons 9

2. GnRH neuron development 11

2.1 Origin of GnRH neurons 13

2.2 Migration of GnRH neurons 16

2.2.1 Factors regulating GnRH neuron migration 17

2.3 Development of GnRH neurons in the forebrain 21

3. Isolated GnRH Deficiency 23

3.1 Normosmic Hypogonadotropic Hypogonadism 25

3.1.1 GNRH1 25

3.1.2 GNRHR 25

3.1.3 KISS1 and KISS1R 25

3.1.4 TAC3 and TACR3 29

3.1.5 LEP, LEPR and PCSK1 29

3.1.6 KLB 30

3.1 Kallmann Syndrome 30

3.2.1 ANOS1 (KAL1) 31

3.2.2 HS6ST1 31

3.2.3 IL17RD 31

3.2.4 NSMF 32

3.2.5 AXL 32

3.2.6 PROK2 (KAL4) and PROKR2 (KAL3) 32

3.2.7 FEZF1 and CCDC141 33

3.2.8 SEMA3A and SEMA3E 33

3.2.9 SEMA7A 33

3.2.10 DCC and NTN1 33

3.3 Syndromic Isolated GnRH Deficiency 34

3.3.1 CHD7 (KAL5) 34

3.3.2 FGF8 (KAL6), FGF17 and FGFR1 (KAL2) 35

3.3.3 SOX10 36

3.3.4 PNPLA6, RNF216, OTUD4, WDR11 and DMXL2 36

3.4 Self-limited delayed puberty 36

4. Experimental tools to study GnRH neuron system 37

4.1 Mutational analysis in affected patients 37

4.2 In silico tools 39
4.2.1 SNPs effect predicting tools 39
4.2.2 Homology modelling 40
4.3 In vitro and ex vivo tools 41
4.3.1 Cell cultures 41
4.3.2 Ex vivo 42
4.4 In vivo tools 44
4.4.1 Mus musculus 44
4.4.2 Danio rerio 45
5. Semaphorin-Plexin signalling 48
5.1 The semaphorin family 48
5.1.1 Semaphorin structure 48
5.2 Semaphorin receptors: Plexins 52
5.3 Semaphorin receptors: Neuropilins 53
5.4 Semaphorin signalling pathways 55
5.5 Semaphorin-Plexin signalling: role in development and disease 58
5.5.1 Nervous system 58
5.6 The role of semaphorins in GnRH neuron development 59
5.6.1 SEMA3A and SEMA3F 59
5.6.2 SEMA3E 60
5.6.3 SEMA4D 62
5.6.4 SEMA7A 62
5.7 Semaphorin 3G 63
5.8 A-type plexins 64
6. Heparan Sulphate 6-*O* Sulpho-Transferase 1 66

SECTION II – Aims 70

SECTION III – Results and discussion 74
1. Semaphorin 3G 75
1.1 Background 75
1.2 Results 77
1.3 Discussion 93
2. Class A plexins 96
2.1 Background 97
2.2 Results 98
2.3 Discussion 107
3. Heparan Sulphate 6-*O* Sulpho-Transferase 1 110
3.1 Background 111

3.2 Results 112
3.3 Discussion 120

SECTION IV – Materials and methods 123

1. Mutational analysis: procedures in patients and *in silico* methods 124

1.1 Homozygosity mapping and Whole Exome Sequencing: SEMA3G case 124
1.2 Self-limited DP cohort 124
1.3 Wole Exome Sequencing and targeted Exome Sequencing: HS6ST1 case 126
1.4 Prediction tools 128

2. *In vitro* methods 128

2.1 Expression vectors and conditioned media 128
2.2 Immunocytochemistry 128
2.3 Immunoblotting 128
2.4 AP-fusion protein binding assay 130
2.5 Migration assays 130
2.6 RT-PCR on GN11 cells 130

3. *In vivo* methods 131

3.1 Mouse strains and procedures 131
3.2 In situ hybridisation 132
3.3 Immunostaining 134
3.4 Histological analysis 135

4. Image processing, quantifications and statistics 135

4.1 Image processing 135
4.2 Quantifications 137
4.3 Statistics 137

SECTION V – Conclusions and future perspectives 138

SECTION VI – References 143

APPENDIX 166

I. List of figures and tables 167

II. List of frequent abbreviations 170

SECTION I
Introduction

1. The vertebrate reproductive system: the hypothalamus-pituitary-gonad axis

Vertebrates, including mammals and humans, are sexually-reproducing organisms and therefore they require the fusion of male and female gametes to generate a zygote, that will give rise to a new organism, to maintain the species. Gametes are produced in sexual organs called gonads and their maturation and functionality are finely controlled by a plethora of genes and pathways highly conserved throughout evolution and across species (Lettieri et al., 2016). The correct development of gonads and therefore gametes critically depends on the endocrine reproductive hypothalamus-pituitary-gonad (HPG) axis (Terasawa and Fernandez, 2001).

The HPG axis is centrally regulated by a releasing hormone, named Gonadotropin-releasing hormone (GnRH), which is synthesized in the hypothalamus by a specific subset of neuroendocrine neurons, called GnRH-secreting neurons or simply GnRH neurons. GnRH neurons are parvocellular neurons[1] as they are characterized by relatively short axons projecting towards the median eminence (ME), an important hypothalamic region surrounding the third ventricle (3v). Here, GnRH is released by axonal terminals contacting the blood vessels (BV) that constitute the hypophyseal blood portal system. Once released, GnRH reaches the anterior pituitary through capillaries and stimulates gonadotrope cells via GnRH receptor (GnRHR) to produce the gonadotropins luteinizing hormone (LH) and follicle-stimulating hormone (FSH) (Figure 1). Gonadotropins act directly on gonads to stimulate the synthesis of sex steroids (androgens and oestrogens), which represent the main hormones involved in sexual maturation and in the regulation of fertility. Specifically, in males, LH acts on interstitial Leydig cells in the testis stimulating steroidogenesis and in particular testosterone synthesis and secretion; in turn FSH binds to specific receptors expressed by Sertoli cells within seminiferous tubules in order to induce spermatogenesis and spermatozoa maturation. In females, steroidogenesis in the ovary is sustained by both LH and FSH. The former acts on theca cells, in the outer layer of the ovarian follicle, in order to induce synthesis and secretion of androstenedione; in turn, the latter stimulates the expression of cytochrome P450 aromatase in granulosa cells, an enzyme that converts androstenedione in estrone, a precursor for oestradiol (E_2). FSH also promotes the maturation of germinal line cells in the ovary, as well as in the testis (Herbison, 2006). In mammals, GnRH secretion has two different modes of release, called GnRH pulse and GnRH surge. The first mode represents the basal secretion of the peptide and in humans it takes place every 90 minutes, while in rodents every 30 minutes (Herbison, 2016).

[1] Parvocellular neurons and magnocellular neurons are neurosecretory cells of the hypothalamus. The former are characterized by relatively short axons that project to the median eminence where they release hormones in the hypophyseal blood portal system in order to stimulate cells of the anterior pituitary; in turn, the latter have long axons projecting directly to the posterior pituitary.

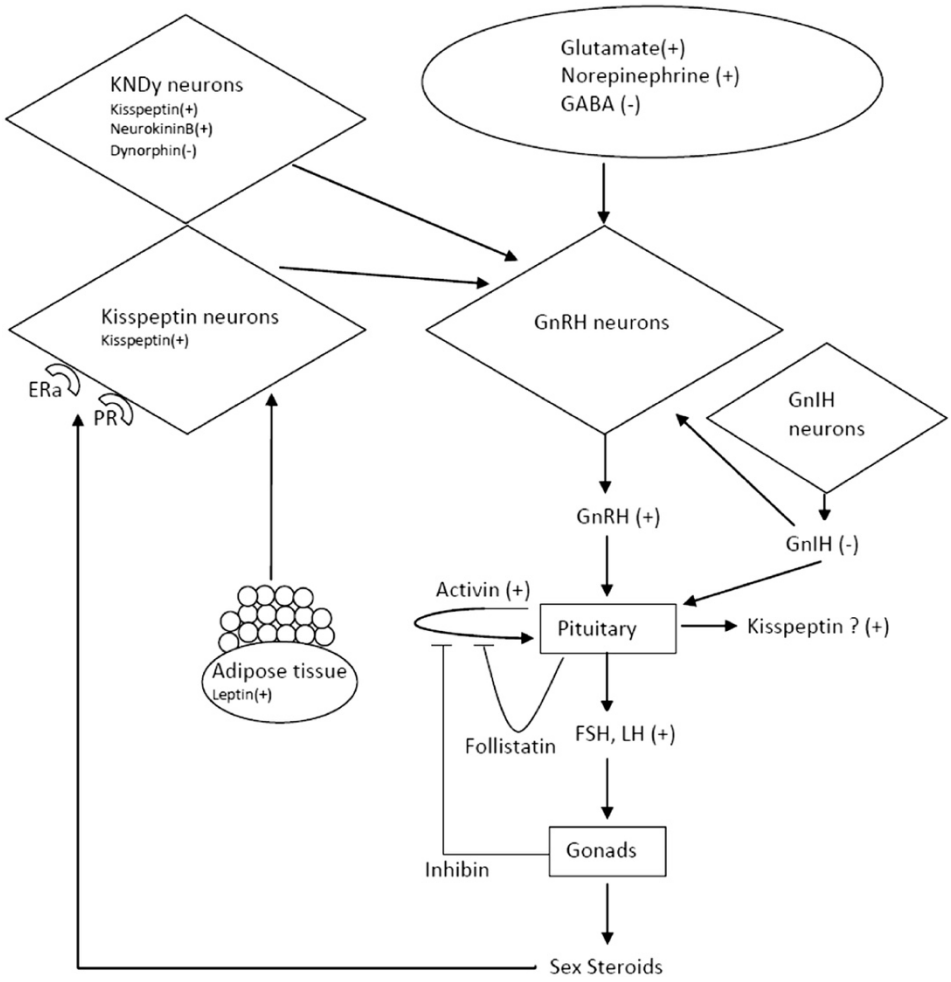

Figure 1 – Schematic diagram of GnRH neuron pathway showing hypothalamic neural networks that regulate GnRH secretion and feedback mechanisms. GnRH, secreted by GnRH neurons, stimulates gonadotrope cells of the pituitary to secrete LH/FSH, which in turn stimulates gonads to produce sex steroids. GnRH has a dual mode of secretion: it pulses every 90 minutes and surges, allowing ovulation in females. GnRH pulses are orchestrated by a plethora of afferent signals from both higher neural circuits and peripheral organs. KNDy neurons in the arcuate nucleus are the main regulator of GnRH pulsatile secretion; additionally, GnIH neurons, GABAergic, glutamatergic and noradrenergic neurons, leptin form peripheral adipose tissues and gonadal peptides (inhibin, activin and follistatin) help to control GnRH secretion. GnRH surges instead are sustained by sex steroids positive feedback loop mediated by Era and PR in anteroventral periventricular nucleus kisspeptin neurons. Abbreviations: (+), stimulatory;(−), inhibitory; Era, oestrogen receptor a; PR, progesterone receptor; GnIH, gonadotropin-inhibiting hormone; KNDy, kisspeptin-neurokinin B-dynorphin A.

Adapted from “The hypothalamus-pituitary-gonad axis: tales of mice and men” by A. Kaprara & I.T. Huhtaniemi, 2018, *Metabolism*, 86:3-17. Copyright 2017 by Elsevier Inc.

This release fashion drives tonic gonadotropins secretion that regulate steroidogenesis in both sex, spermatogenesis in males and folliculogenesis in females. In turn, the second mode of secretion is typical of females and it consists in a massive and prolonged GnRH release that triggers the ovulation via the increase of LH levels (Plant, 2015b). The molecular mechanisms regulating the switch between the two modes of secretion have been extensively studied in many species, from rodents to humans, although they are still not completely understood.

1.1 HPG axis regulation

The HPG axis is characterized by a sexual dimorphic regulation: in males, the control of testes functionality is entirely dependent on GnRH pulses, while spontaneously ovulating females undergo oestrus cycle, that is predominantly under the control of GnRH pulses except for ovulation that occurs after a GnRH surge every 4-5 days in rodents and 28 days in women.

GnRH pulse represents the basal mode of secretion for GnRH and therefore regulates most of reproductive cycle in females and the whole reproductive activity in males. However, the mechanism underlying the generation of GnRH pulses is still under debate. Some researchers believed pulsatility as an intrinsic feature of GnRH neurons (Campbell et al., 2009; Martinez de la Escalera et al., 1992), while others proposed that non-GnRH neurons could drive and synchronize GnRH neuron pulsatility. The latter model has become the predominant view since the discovery of kisspeptin neurons in 2003 by two independent groups (de Roux et al., 2003; Seminara et al., 2003). Kisspeptin, encoded by *KISS1* gene, is a potent secretagogue of GnRH that signals through GPR45 or KISS1R that is highly expressed by GnRH neurons. Interestingly, kisspeptin neurons are localized mainly in the arcuate nucleus (ARC) of the hypothalamus, close to the ME, and their fibres densely innervate GRP45-expressing axons of GnRH neurons. In addition, ARC kisspeptin neurons express neurokinin B (encoded by *TAC3* gene) and dynorphin A (encoded by *PDYN* gene) that stimulate or suppress GnRH secretion, respectively (reviewed in (Maeda et al., 2010)). Taken together, these observations helped to create the nowadays accepted model of GnRH pulse generator, firstly proposed by Navarro and colleagues in 2009 (Navarro et al., 2009): in this model, neurons expressing kisspeptin, neurokinin B and dynorphin A (called KNDy neurons) pace the pulse generation thanks to an interplay of positive and negative stimulations and synchronize GnRH neurons, allowing the pulsatile release of GnRH (Figure 1).

Moreover, pulsatile GnRH secretion is negatively regulated by a distant feedback loop driven by sex steroids produced in the gonads, that can act both at hypothalamic and pituitary level, inhibiting further GnRH or LH/FSH release, respectively. KNDy neurons, and not GnRH neurons, are the mediators of the hypothalamic steroids-driven negative feedback since they express both oestrogen

receptor alpha (ERα) and androgen receptor (AR) whereas GnRH neurons do not (Maeda et al., 2010; Plant, 2015b; Shivers et al., 1983). However, more recent works showed that ERα is dispensable for a correct HPG functionality (Dubois et al., 2015) suggesting that other neuronal population, such as recently discovered hypothalamic nNOS neurons, may be implicated in mediating the action of sex steroids on GnRH neurons (Chachlaki et al., 2017).

The HPG axis is peculiarly characterized also by a positive feedback loop occurring during pre-ovulatory phase of oestrus cycle. Thus, while E_2 normally acts as a negative modulator of GnRH as described above, sustained exposure to high E_2 levels, occurring during late follicular phase, promotes a massive and prolonged release of GnRH and LH, that allows ovulation. The site of action for the E_2-mediated positive feedback has been located in anteroventral periventricular nucleus (AVPV) of the hypothalamus, where a second population of ERα-expressing kisspeptin neurons can be found (Christian and Moenter, 2010) (Figure 1).

In addition to sex steroids, gonads produce three other peptides, namely inhibin, activin and follistatin. Inhibin is secreted exclusively by gonadal tissues and acts as selective inhibitor of FSH release by gonadotrope cells of the anterior pituitary. In turn, activin and follistatin are secreted both by gonads and extragonadal tissues and act in paracrine/autocrine fashions. In particular, activin can modulate HPG axis at different levels: i) it counteracts inhibin action on gonadotrope cells promoting FSH secretion; ii) it up-regulates GnRHR transcription and translocation to the membrane, enhancing gonadotrope cells responsiveness to GnRH; iii) it directly stimulates GnRH neurons to release GnRH. Follistatin instead is an activin binding protein that can neutralize activin effects on gonadotrope cells (reviewed in (Gregory and Kaiser, 2004)) (Figure 1).

A wide range of neuronal systems additionally co-operate in the fine regulation of GnRH neurons, by mediating effects of metabolic status, stress and season (Clarke and Arbabi, 2016; Kaprara and Huhtaniemi, 2018); for these reasons, the HPG axis can be defined an “open” endocrine axis, in contrast to other endocrine axis that are regulated only by signals originating from the axis itself. In particular, metabolic status is strictly intermingled with the HPG axis since reproduction is an energy consuming process and therefore it could be dispensable in extreme metabolic conditions (e.g. caloric restriction, anorexia). First evidence of this correlation came from the discovery that leptin, an anorexigenic hormone released by adipose tissue that normally induces energy expenditure and decreases food intake, has a permissive role on GnRH secretion. It has been shown that leptin, by acting on ARC KNDy neurons that express leptin receptor (*LEPR*), is an essential hormone for the GnRH pulse modulation (Quennell et al., 2009). Conditions of leptin insufficiency (e.g. malnutrition, anorexia) or leptin resistance (e.g. obese with LEPR mutations) are indeed associated

to gonadal and reproductive defects (Vázquez et al., 2015). Further, metabolism and reproduction are linked by other peptides such as neuropeptide Y (NPY), Agouti-related protein (AgRP), orexins, pro-opiomelanocortin (POMC) which can act either directly on GnRH neurons or indirectly via KNDy neurons to modulate GnRH secretion. In agreement with leptin action on reproduction, orexigenic signals negatively modulate the HPG axis, while anorexigenic ones are positive modulators (Manfredi-Lozano et al., 2017). Likewise, stress can negatively affect reproduction. Although response to stressful conditions can be very complex, gonadotropin-inhibiting hormone (GnIH) also named RF-amide related peptides 3 (RFRP3) is emerging as possible intermediate signal connecting stress to reproduction (Clarke and Arbabi, 2016). Further, GnIH may counterbalance excitatory mechanisms driven mainly by KNDy neurons, contributing in the adaptation of reproductive maturation and function to different endogenous and environmental conditions. GnIH-releasing neurons are located mainly in the dorsomedial nucleus (DMH) of the hypothalamus and are able to contact directly GnRH neurons through receptor GPR147, that decrease cAMP production inhibiting GnRH secretion (Clarke, 2011; Tsutsui et al., 2000). GnIH neurons regulate not only gonadotropin synthesis and release, but also finely regulates various neuropeptides, such as dopamine, POMC, NPY, orexin and kisspeptin. GnIH and GPR147 are also expressed in the pituitary and gonads, where they may exert their function in an autocrine/paracrine manner. Moreover, GnIH regulates reproductive development and activity as in female mammals, it may control oestrous cycle and it is also involved in the regulation of seasonal reproduction (Leon and Tena-Sempere, 2015; Ubuka et al., 2012; Ubuka et al., 2016) (Figure 1).

1.2 HPG axis activity during development

In many mammals, the HPG axis sets during embryonic and fetal development and then undergoes a series of dynamic changes that lead to the continuous maturation of the axis until puberty, that represent the starting point for adult life. Although reproductive function is a hallmark of adulthood, the HPG axis presents three different periods of activation (Kuiri-Hänninen et al., 2014) (Figure 2).

The first active phase of the axis coincides with midgestational foetal life and starting just after the settlement of GnRH neurons in the hypothalamus. The biological role of this activation is not completely understood, but it seems fundamental to ensure the complete differentiation of gonads and particularly for the correct development of male genitalia (Clarkson and Herbison, 2016). The second phase occurs within the first six months after birth in humans and between postnatal day (P) 2 and P7 in rodents. This period is called minipuberty. In males, the increase in gonadotropin levels peaks at 3 months and then declines towards the age of 6 months. It is responsible for the establishment of sexually dimorphic brain circuitry (Clarkson and Herbison, 2016).

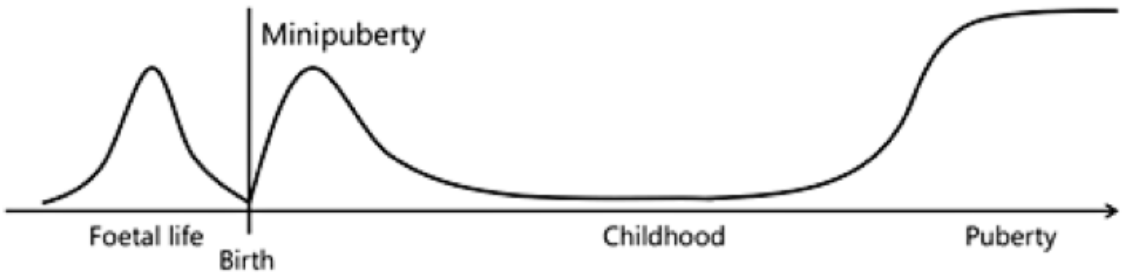

Figure 2 – Periods of activation of HPG axis. Three different windows of activation of the HPG axis can be distinguished during: 1) at midgestation of foetal life, the activity peaks and decreases towards birth, possibly due to the suppressive effects of placental hormones, especially oestrogens; 2) at birth, gonadotropin levels are low, but at around 1 week of age the HPG axis becomes active again. This postnatal gonadotropin surge, or minipuberty, is associated with the activation of gonadal hormone production in both boys and girls; 3) after the peak at 1–3 months of age, hypothalamic-pituitary activity gradually decreases and is then low during childhood until reactivation at puberty.

Adapted from "Activation of the hypothalamic-pituitary-gonadal axis in infancy: minipuberty" by T. Kuiri-Hanninen, U. Sankilampi and L. Dunkel, 2014, *Horm Res Paediatr*, 82:73-80. Copyright 2014 by S. Karger AG.

In both males and females gonadotropin levels peak around 3 months of age, but females show high levels of FSH till the age of 2 years, as FSH is required for ovarian follicles development (Kuiri-Hänninen et al., 2014). After minipuberty, the HPG axis is actively inhibited and therefore becomes silent and inactive throughout childhood until its reactivation just before puberty.

1.2.1 Puberty

Puberty is defined as the period of becoming first capable of reproducing sexually, characterized by complete maturation of genitalia and development of secondary sex features and finally represents the transition to adulthood (Plant, 2015a). The age of puberty onset can vary greatly between individuals and it lasts 3-4 years; on average, girls are more precocious and start puberty at 8-12 years old, whilst boys at 9-14 years old. Menarche (first menstrual bleeding) and spermarche (first spermatozoa release) are considered as final marker of puberty (Abreu and Kaiser, 2016). In mice instead, a peripubertal period can be defined from P30 until vagina opening/first ovulation for females and presence of motile sperm in the testes for males, that are considered as marker of puberty onset (Prevot, 2014). Puberty onset is achieved thanks to the reactivation of GnRH pulse generator after childhood quiescence. Molecular mechanisms underlying the active restraint on HPG axis during childhood and the pubertal activation of HPG axis are, to date, poorly understood.

1.3 The Gonadotropin-Releasing Hormone

The neuropeptide GnRH is the key regulator of the whole HPG axis and its existence was first postulated by Harris since 1955; however, GnRH was isolated from ovine and porcine brains for the first time only in 1971 by two independent groups (Amoss et al., 1971; Matsuo et al., 1971).

The HPG system and therefore GnRH are highly conserved through species (Campbell et al., 2004). To date, in vertebrates, 14 different variants of GnRH have been found and have been recently organized into three groups, namely GnRH1, GnRH2 and GnRH3, based on their phylogenetic tree. The fundamental role of this hormone is highlighted by the high conservation degree amongst variants that all show the same length and 4 of 10 identical residues (Okubo and Nagahama, 2008). Each group represents a paralogue gene of GnRH originated during evolution after two different whole genome duplications; to date, many evidences demonstrate that almost all vertebrates synthesize at least two isoforms of GnRH (Figure 3). GnRH2 (in humans encoded by *GNRH2* gene, located on chromosome 20) represents the ancestral isoform of GnRH. In fish, GnRH2 peptide is mainly found in the mesencephalon, where it might act as neuromodulator in the auditory system or as melatonin-releasing factor in the pineal gland, participating to sleep/wake cycles. Yet, in many tetrapods included humans, this isoform has been silenced or deleted during evolution, so that many questions remain about its biological role in mammals (Forni and Wray, 2015). GnRH1 represents in turn the

main tetrapod variant and it is responsible for the hypophysiotropic role, fundamental for reproduction. The first evidence of the pivotal role of GnRH1 in HPG axis came from Mason and co-workers: they demonstrated that *hpg* mice, carrying a loss-of-function mutation in *Gnrh1* gene, display severe alterations in the HPG axis functionality that can be restored by transgenic overexpression of GnRH1 (Mason et al., 1986). Finally, GnRH3 isoform is mainly expressed by teleosts, while tetrapods lost the gene during evolution. In ancient teleosts, GnRH3 is expressed in olfactory regions where it acts as neuromodulator, whereas in recent teleosts (e.g. *Danio rerio*) it carries out the hypophysiotropic function, since GnRH1 is not present (Forni and Wray, 2015; Okubo and Nagahama, 2008).

In humans, GnRH is released as a decapeptide, whose primary structure is pyroGlu-His-Trp-Ser-Tyr-Gly-Leu-Arg-Pro-Gly-NH2; human GnRH is encoded by *GNRH1* gene that lies on chromosome 8 and is formed by 4 exons and 3 introns (Figure 4). GnRH is synthesized in the endoplasmic reticulum as 92 amino acid prepro-hormone; signal peptide is then cleaved in order to produce the pro-hormone that is further processed in the Golgi apparatus, with a second cut at the level of the highly conserved tripeptide (Gly-Arg-Arg). The latter cleavage generates GnRH decapeptide and GnRH-associated peptide (GAP), whose biological function is still questioned. After enzymatic cleavages, GnRH decapeptide is further processed with an N-terminal pyroglutamate and a C-terminal glycinamide and finally accumulated in vesicles, ready for the release.

1.4 GnRH-secreting neurons

GnRH neurons are at the top of HPG axis and therefore are the first and main regulator of the whole axis. Despite their complex role, GnRH neurons are few in numbers as they constitute a population of 2.000 cells in primate and human adult brains and of 800 cells in rodents (Casoni et al., 2016). They are dispersed in a bilateral continuum throughout the hypothalamus without forming a precise nucleus, even if most of them can be found within the medial preoptic area (MPOA) in preoptic and medial- preoptic nuclei. Interestingly, additional “non-endocrine” GnRH neurons have been recently discovered in extrahypothalamic regions, such as olfactory bulb (OB), amygdala and hippocampus increasing the total number of GnRH neurons up to 10.000 cells, but their role is still unknown (Casoni et al., 2016; Rance et al., 1994). However, because these extrahypothalamic sites are ancient parts of the brain, projections and GnRH cell bodies found in these sites are not surprising, considering that control of reproduction is essential to the perpetuation of species (King and Anthony, 1984).

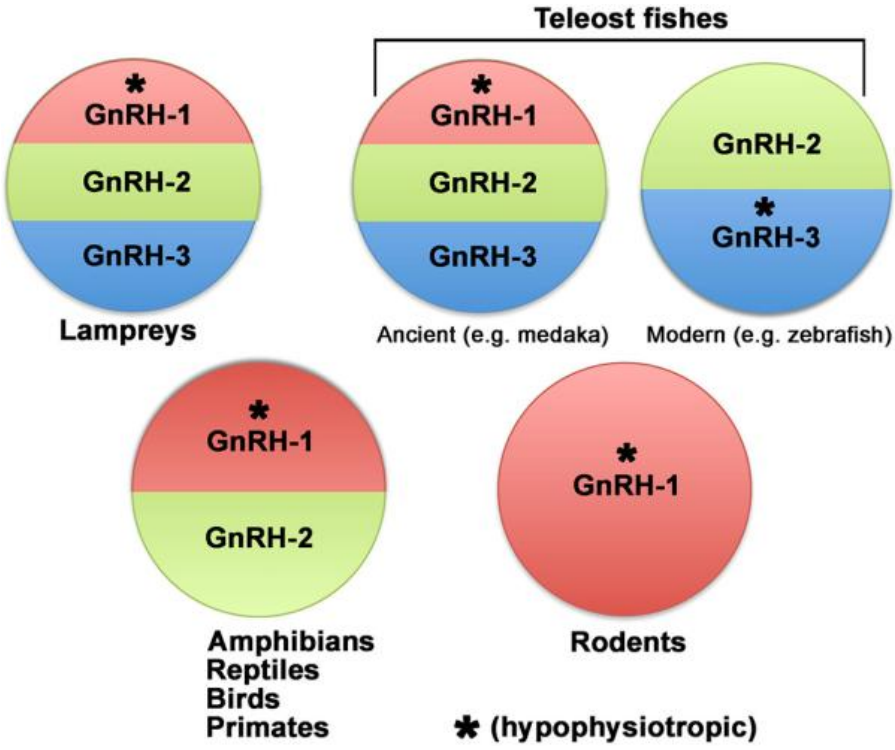

Figure 3 – Schematic illustration showing the different GnRH paralogs expressed by vertebrate species. GnRH1, GnRH2 and GnRH3 paralogue genes originated during evolution subsequently to two different whole genome duplications. Most species lost or silenced non-hypophysiotropic isoforms. Abbreviations: *, hypophysiotropic form**.**

Adapted from "GnRH, anosmia and hypogonadotropic hypogonadism - where are we?" by P.E. Forni & S. Wray, 2015, *Front Neuroendocrinol*, 36:165–177.

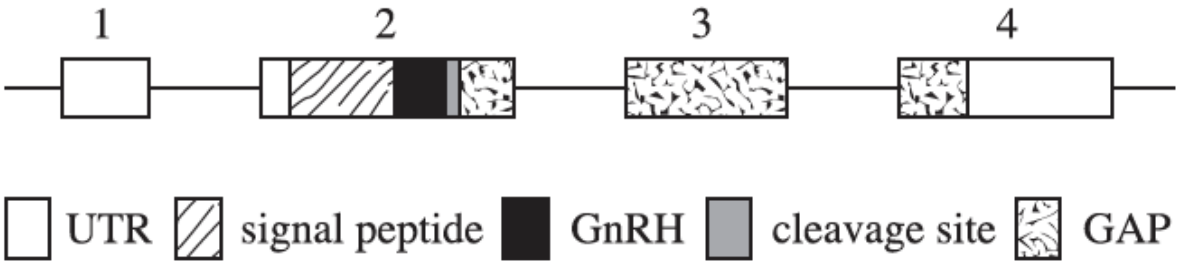

Figure 4 - Schematic diagram illustrating the structural organization of *GNRH1* gene. *GNRH1* gene is composed of four exons (boxes 1-4) and three introns (lines). GnRH is encoded as part of a 92 amino acids precursor polypeptide called prepro-GnRH, which consists of a signal peptide, the GnRH decapeptide, a cleavage site (Gly-Arg-Arg) and the GnRH-associated peptide (GAP). Abbreviations: UTR, untranslated region; GAP, GnRH-associated peptide.

Adapted from "Structural and functional evolution of gonadotropin-releasing hormone in vertebrates" by K. Okubo & Y. Nagahama. 2008, *Acta Physiol,* 193:3–15. Copyright 2008 by Scandinavian Physiological Society.

2. GnRH neuron development

The peculiarity of GnRH neurons is that they originate outside the brain and more precisely in the olfactory placode (OP). During embryonic development, they migrate throughout the nasal septum (NS) towards the basal forebrain where hypothalamus is developing. Just before birth, the migration of GnRH neurons ceases and post-migratory neurons start extending their axons towards ME, where GnRH secretion occurs. GnRH neurons migration has been extensively studied in rodents: in mice, it starts at embryonic day (E) 10.5, peaks at E14.5 and ceases towards E18.5 (Cariboni et al., 2007a; Schwanzel-Fukuda and Pfaff, 1989; Wray et al., 1989a) (Figure 5A). Recently, the study of GnRH neuron migration has been extended to humans, thanks to the availability of human foetuses and tissue clearing technologies, providing evidences that GnRH neuron development is conserved between rodents and primates. First GnRH neurons emerge from OP at Carnegie Stage (CS) 16 (gestation week (GW) 5.5). Migration starts at CS18 (approximately GW 7) and reaches a peak at CS23 (GW8). Around GW12 most of GnRH neurons have already set in the forebrain (Casoni et al., 2016) (Figure 5B).

The OP mainly gives rise to olfactory system. In rodents, the olfactory system is divided into the main olfactory system and the accessory olfactory system. The former is responsible for the detection of odorants through olfactory sensory neurons (OSNs), whose cell bodies reside within the primary olfactory epithelium (OE) whilst axons (OLF nerves) project to the main olfactory bulb (MOB). The latter is in turn formed by VN nerves, whose cell bodies reside in the vomeronasal organ (VNO), project axons to the accessory olfactory bulb (AOB) and recognize pheromones (Forni and Wray, 2012; Sato et al., 2005). The main olfactory system is highly conserved in primates and humans (Müller and O'Rahilly, 2004), whereas the accessory one has been taught to be a vestige for a long time, since recently when researchers have been able to detect the VNO bud in human embryos (Casoni et al., 2016). Thus, GnRH neurons and olfactory system share a common placodal origin and accordingly they are in morphological and functional relationship as during development GnRH neurons migrate along VN and OLF nerves reach the hypothalamus. The common origin shared by GnRH neurons and olfactory system highlights the relationship between olfaction and reproduction and validate the co-segregation of anosmia and hypogonadism often observed in Kallmann Syndrome (KS) (described in paragraph 3.2).

Despite the crucial role played by GnRH neurons in vertebrate reproduction and fertility, many aspects of their development are still questioned. Differentiation, migration, survival, maturation and activity of GnRH neurons are finely tuned by several proteins and molecules making difficult a precise understanding of all developmental processes.

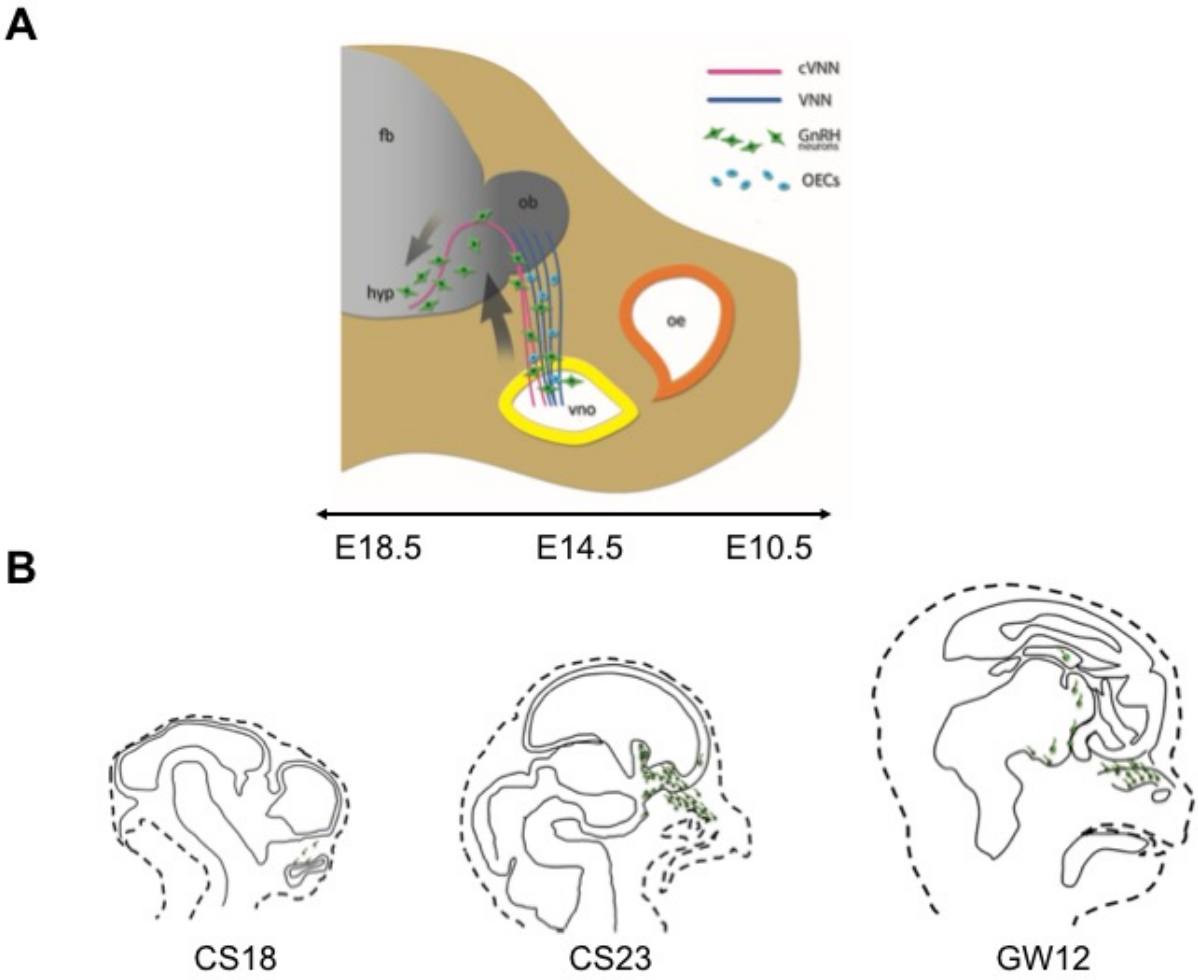

Figure 5 – Schematic representation of GnRH neuron migration. (A) In mouse first GnRH neurons emerge within the VNO at around E10.5 and start migrating in the nasal mesenchyme with along cVN nerves together with OECs. Migration peaks at E14.5 and ceases at E18.5 when GnRH neurons reach their final location in the hypothalamus. **(B)** In humans, GnRH neuron migration takes place during first trimester of gestation. First GnRH neurons are detected at CS18 (approximately during GW7), migration has a peak at CS23 (GW8-9) and at around GW12 most GnRH neurons have reached the hypothalamus. Abbreviations: fb, forebrain; hyp, hypothalamus; ob, olfactory bulb; vno, vomeronasal organ; oe, olfactory epithelium; (c)VN nerve, (caudal) vomeronasal nerves; OECs, olfactory ensheathing cells; CS, Carnegie stage; GW, gestation week.

Adapted from "Development of the neurons controlling fertility in humans: new insights from 3D imaging and transparent foetal brains" by F. Casoni, S.A. Malone, M. Belle et al., 2016, *development*, 143:3969-3981. Copyright 2016 by The Company of Biologists Ltd.

2.1 Origin of GnRH neurons

The origin of GnRH neurons has been controversial for many years, with many regions (e.g. olfactory placodes, ectoderm, neural crest) suggested to be the birthplace of GnRH neurons (Whitlock, 2005). In the last few years several evidences lead to the current and prevailing model that proposes a mixed placodal and neural crest origin for GnRH neurons (Forni et al., 2011).

In mice, OP arises as non-neural ectoderm thickenings at the anterior border of the neural plate at E9.5, just after the neural tube closure. Then, at E10.5 OP starts invaginating to form olfactory pits, that further deepen giving rise to nostrils and nasal cavity by E11.5. OP formation and placodal-derived cell differentiation are finely regulated-processes, hence several factors and signalling pathways are involved. OP formation is sustained by transcription factors such as Pax6, Dlx3/5, Otx2 and Six3/6 (Bhattacharyya and Bronner-Fraser, 2008; Merlo et al., 2007; Moody and LaMantia, 2015) (Figure 6). Shortly after invagination, OP starts differentiating giving rise to neurogenic and non-neurogenic domains. Bmp4 mainly drives non-neurogenic fate leading to the differentiation of respiratory epithelium; conversely, neurogenic domains, such as OE and VNO, are determined by the signalling of Fgf8, Sox2, Pax6 and Hes1/5 (Maier et al., 2014). In particular, Fgf8 plays an essential role for neurogenesis in the developing OP as confirmed by *Fgf8*-null mice that display neuronal precursors apoptosis and absent olfactory neurogenesis (Kawauchi et al., 2005)). GnRH neurons have been demonstrated to arise in neurogenic niches in a region within and at the border of respiratory epithelium and developing VNO, where an intermix of neurogenic and non-neurogenic signals occurs. The first evidence of the placodal origin of GnRH neurons was obtained in 1989 by two independent groups (Schwanzel-Fukuda and Pfaff, 1989; Wray et al., 1989b) that found GnRH immunoreactive neurons migrating out of the VNO at around E11.5 in mice. Consistently, experiments of physical and genetic ablation of olfactory placode in mice confirm that the lack of OP lead to a loss of GnRH neurons. Specifically, several evidences of a placodal origin of GnRH neurons came from transgenic mice. For instance, *Pax6* knockout mice, a model of genetic ablation of olfactory placode, do not show any GnRH immunoreactive neuron (Dellovade et al., 1998). In addition, FGF signalling is critically required for GnRH neuronal fate specification as well, even if it exerts a crucial role also in postnatal maintenance and migration (Chung and Tsai, 2010). In 2004, Gill and co-workers proved that GnRH neurons are responsive to Fgf8 gradients thanks to the expression of Fgfr1 as genetic inactivation of Fgfr1 leads to abnormalities in GnRH neuron development (Gill et al., 2004). As a confirm for the crucial role of Fgf8/Fgfr1 signalling in GnRH neurons differentiation, several mutations have already been identified in Isolated GnRH Deficiency (IGD) patients in FGFs-related genes. Interestingly, recent lineage tracing experiments suggested that loss of FGF signalling

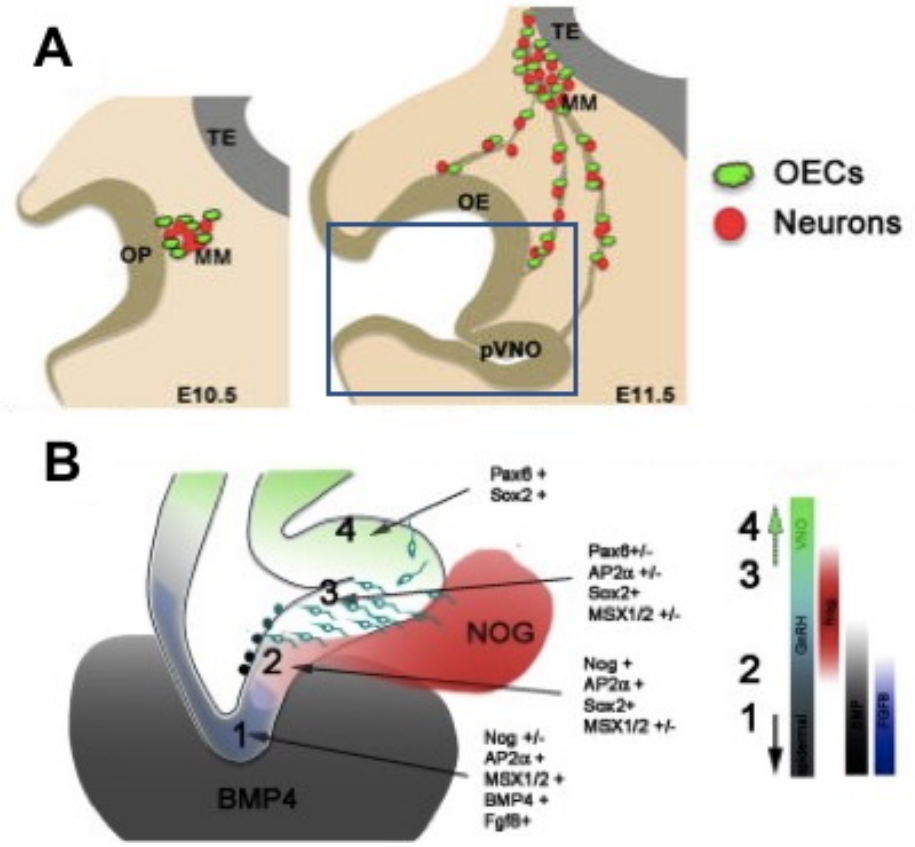

Figure 6 – Olfactory placode formation. (A) Schematic drawing showing OP formation and MM arising from the epithelium at E10.5 and differentiation of OE, pVNO and MM migrating towards TE at E11.5. **(B)** Schematic summarizing molecular expression in the OP (1), transitional area (2), GnRH neurogenic area (3), and VNO (4). Molecules expressed in each area are listed. Colour bars on right side indicate environmental factors associated with the transition from epidermal (1) to vomeronasal (4; +, high expression levels; +/−, low/nonuniform expression; −, non expressed/below detection). Abbreviations: OP, olfactory placode; MM, migratory mass; TE, telencephalon; OE, olfactory epithelium; pVNO, presumptive vomeronasal organ; OECs, olfactory ensheathing cells.

Adapted from "Neural Crest and Olfactory System: New Prospective Paolo" by P.E. Forni & S. Wray, 2012, *Mol Neurobiol*, 46(2):349–360. Copyright 2012 Springer Science+Business Media, LLC.

in the OP is not directly associated with a decreased neurogenesis within the VNO, but rather lack of Fgf8 changes the gradient of cues that drive mesenchymal fate, such as Bmp4 and Noggin, that are crucial factor for craniofacial development and neurogenic niches specification (Forni et al., 2013). In addition, retinoic acid (RA) has an opposite effect on GnRH neuron specification compared to Fgf8, since RA suppresses GnRH neuron differentiation; hence, loss of Fgf8 signalling leads to an expansion of RA signalling and to a failure in GnRH neuron specification (Sabado et al., 2012).

Other factors can potentially play a role in GnRH neuron differentiation during early embryogenesis. For instance, *Sox2* mutant mice display a reduced number of GnRH neurons at early stages (E11.5), indicating an underlying mechanism for Sox2 in OP development and GnRH neuron differentiation (Jayakody et al., 2012). Similarly, Ebf2 (early B-cell factor 2) plays a pivotal role in early GnRH neuron development in a cell autonomous manner. Ebf2 is a transcription factor that mainly regulates immune system, cell migration and neural differentiation. In the developing nose, *Ebf2* is strongly expressed in the OE and in the VNO from E11.5 and *Ebf2* expression is also detectable in GnRH neurons themselves. *Ebf2*-null embryos display massive accumulation of GnRH neurons in the nasal compartment and, consequently, in the adult hypothalamus of knock out mice hardly any GnRH neurons are detected. Yet, olfactory system and VN nerves do not show any abnormalities suggesting a cell-autonomous defect in GnRH neurons (Corradi et al., 2003). Lastly, Otx2 (Orthodenticle homeobox 2) is a homeodomain protein necessary for early development of the head during gastrulation, and later, specifies anterior head structures particularly forebrain; hence, loss-of-function of Otx2 results in malformation of the head and eyes (Hide et al., 2002; Wyatt et al., 2008). Otx2 is among the regulatory proteins that have been shown to control expression of murine GnRH by binding to the conserved Otx2 binding sites in the proximal promoter of GnRH both *in vitro* and *in vivo* (Kelley et al., 2000; Kim et al., 2007; Larder and Mellon, 2009). Generation of conditional knock out mice with Otx2 specifically inactivated in GnRH neurons shows that these mice had fewer GnRH neurons crossing forebrain and entering into the ventral hypothalamus at E14.5 and E15.5 (Diaczok et al., 2011). Yet, no mutations in either *EBF2* or *SOX2* genes have been found in patients affected by IGD (described in details in paragraph 3) so far; mutations in *OTX2* gene have been found in patients affected by compound pituitary hormone deficiency, an IGD overlapping syndrome (Diaczok et al., 2008; Gorbenko Del Blanco et al., 2012).

Recently, a mixed placodal and neural crest origin has been proposed for GnRH neurons. Previously, many evidences about the contribution of neural crest cell (NCC) to sensorial placodes have been generated (Steventon et al., 2014), but not for olfactory placode. The neural crest (NC) is a transient structure generated between the dorsal neural ectoderm and the epidermis; NCC are multipotent cells that delaminate from the NC and migrate towards different target tissues, including

neurons, glia, cranial cartilage, skin, heart. Forni and co-workers first showed that multipotent NCC are localized within the ectoderm-derived developing OP and thanks to lineage tracing demonstrated that NCC can differentiate into olfactory ensheathing cells (OECs) and neurons, including a subpopulation of GnRH neurons. Wnt1-Cre recombination, specific for NC lineage, occurs in about the 30% of GnRH neurons whereas Crect fate mapping, specific for ectoderm, indicates that the remaining 70% has an ectodermal origin (Forni et al., 2011). This mixed origin agrees with the fact that GnRH neurons exhibit heterogeneity at both molecular and morphological levels.

2.2 Migration of GnRH neurons

After differentiation, new-born neurons within VNO and OE start extending their axons towards OB across nasal mesenchyme; the first OLF axon exits OE and crosses the basal lamina at late E10.5. At the same time several cells delaminate particularly from VNO and these migratory cells, together with nascent axons, form the so-called migratory mass (MM) (Suzuki and Osumi, 2015; Valverde et al., 1992). MM comprise heterogeneous populations of cells including OLF/VN extending axons, OEC, GnRH neurons and other poorly characterized cell populations expressing acetylcholinesterase (AChE), Dlx5 and vGlut2 (vesicular glutamate transporter 2). First MM cells delaminate at early E10.5 and these are believed to act as guidepost cells[2] for navigating axons (Miller et al., 2010). The cellular diversity amongst MM guidepost cells suggests that subsets of cells may be associated with specific subsets of axons, perhaps influencing axon sorting and targeting. At E11.5 also OEC and GnRH neurons delaminate from the epithelium and invade nasal mesenchyme: GnRH neurons start their journey towards the hypothalamus, whilst OEC join OLF/VN nerves and wrap axons. By E13.5, when axons have already contacted the developing telencephalon and OB has begun to emerge, MM cells are no longer required since axon-axon interactions within OLF/VN nerves promote axon guidance. Similar to OLF/VN nerve, whose migration is regulated by guidepost cells, extracellular matrix adhesion molecules and guidance cues, during their migration GnRH neurons are physically sustained by the axonal scaffold provided by intermingled OLF/VN nerves and molecularly regulated by several factors composing extracellular matrix or secreted by MM cells. For these reasons, GnRH neuron migration provide a unique example of tangential axonophilic migration (Marín and Rubenstein, 2003).

Once exited the VNO, the prevailing idea is that GnRH neurons migrate along bundles of intermingled OLF/VN nerves throughout the nasal mesenchyme towards the forebrain (Figure 7). These axons, originating from OE and VNO respectively, first invade nasal mesenchyme at the same

[2] namely cells that coalesce with nasal mesenchyme and provide structural and molecular support to extending axons and other migrating cells

time of GnRH neurons at late E10.5. At early developmental stages specific marker for these axons have not yet been found, however when migration starts, OLF nerves express neuropilin 1 (Nrp1), neuropilin 2 (Nrp2), immature neuronal marker Tuj1 and olfactory myelin protein (OMP); VN nerves additionally express peripherin, which is a marker for peripheral nerves. At the dorsal end of nasal mesenchyme, GnRH neurons and OLF/VN nerves cross the cribriform plate (CP) also called nasal-forebrain junction (NFJ), a portion of the ethmoid bone that supports the olfactory bulb and is perforated by foramina that allows the passage of the olfactory nerves. Here, the axonal bundles composed by OLF/VN nerves split into two branches: OLF nerves and a subset of VN nerves proceed in fascicles rostrally and dorsally towards the OB, to contact the MOB and AOB respectively, whereas a subset of VN nerves turn ventrally and caudally without forming fascicles but rather invading in a dispersed manner the developing telencephalon. The caudal branch of the VN (cVN) nerve, in addition to peripherin and Nrp1, specifically expresses PSA-NCAM (polysialic acid rich neural cell adhesion molecule) and TAG-1 (contactin-2). Yet, the cVN seems to be a transient structure that disappear shortly after birth and although it represents a small fraction of the VN nerves, it is virtually the main responsible for GnRH neuron migration (Yoshida et al., 1995). After the crossing of the NFJ, GnRH neuron are indeed associated uniquely to the cVN nerve fibres that extend far into the medio-basal forebrain (Schwanzel-Fukuda, 1999) (Figure 7).

Recently, the peripheral nerve cranial nerve-0, alternatively named terminal nerve (TN), has been pointed out as responsible for GnRH neuron migration as well (Taroc et al., 2017). Similar to VN nerves, the TN emerges from the VNO, intermingles with OLF/VN nerves within the nasal mesenchyme making difficult its identification and finally turns ventrally and caudally in the medio-basal forebrain after crossing the NFJ (Casoni et al., 2016; Vilensky, 2014). TN nerve expresses high levels of peripherin, TAG-1 and Nrp1. Since the cVN nerves and TN nerve share common molecular and morphological features, it is broadly accepted that GnRH neurons migrate within the forebrain along cVN/TN nerve bundles. GnRH neurons migration can be divided into two steps: 1) migration within the nasal mesenchyme along intermingled bundles of OLF/VN nerves; 2) crossing of CP where they follow the caudal branch of VN nerves (Wierman et al., 2011).

2.2.1 Factors regulating GnRH neuron migration

The first migratory step of GnRH neurons is represented by the exit from the VNO and the migration throughout the nasal mesenchyme. This process is strictly regulated by many extracellular matrix protein, adhesion molecules and soluble cues that directly guide GnRH neuron or alternatively guide OLF/VNN/TN axons and therefore GnRH neurons associated to them.

PSA-NCAM (polysialic acid form of neural cell adhesion molecule) is a glycoprotein that

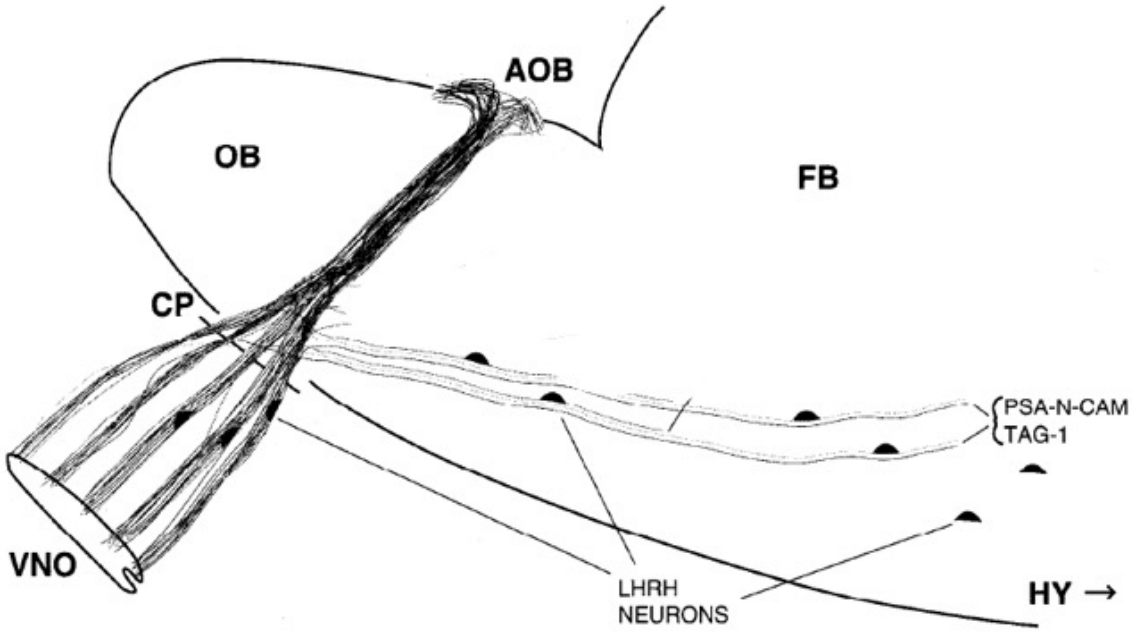

Figure 7 - Schematic diagram of cVN nerve pathways. VN nerves exit from VNO including the proposed pathway for GnRH (also called LHRH) neuron migration towards the HY. The main branch of VN nerves extends to the AOB. The caudal branch of the VN nerves (cVN), marked by PSA-N-CAM and TAG-1, divides from the main branch at the CP and turns caudally and ventrally towards the basal FB. GnRH neurons migrate in association with the PSA-N-CAM+/TAG-1+ subset of VN nerves. Abbreviations: VNO, vomeronasal organ; (A)OB, (accessory) olfactory bulb; CP, cribriform plate; FB, forebrain; HY, hypothalamus; LHRH, luteinizing hormone releasing hormone..

Adapted from "The migration of luteinizing hormone-releasing hormone neurons in the developing rat is associated with a transient, caudal projection of the vomeronasal nerve" by K. Yoshida, S.A. Tobet, J.E. Crandall et al., 1995, *Journal of Neuroscience*, 15(12):7769-7777. Copyright 1995 by Society for Neuroscience.

negatively regulates cell-cell interactions and is widely expressed during embryonic development. Yet, PSA-NCAM is highly expressed by VN nerves along which GnRH neurons migrate. Thus, the enzymatic removal of PSA obtained with endoneuroaminidase N treatment is able to block the migration of half GnRH neurons; surprisingly, the genetic ablation of NCAM do not abolish the migration but rather leads to a switch of migratory route, with GnRH neurons accumulating in the AOB instead of migrating ventrally and caudally toward the hypothalamus (Murakami and Arai, 2002; Yoshida et al., 1999). These discrepant results may have been due to the redundancy of the NCAM subtype system and overall these findings highlight the role of NCAM on migration of GnRH neurons.

Lactosamine-containing membrane glucoconiugates are molecules that are enriched on the OLF/VN nerve and GnRH neuron membranes since early developmental stages. Lactosamine synthesis is dependent on β1,3-N-acetylglucosaminyltransferase (β3GnT1) activity, an enzyme highly expressed in neurons within the OE and the VNO and in those migrating out from the VNO. Interestingly, more than 80% of GnRH neurons is also immunopositive for lactosamine at E13.5 when migration is at its peak and *β3GnT1*-null embryos display GnRH neurons retained in the nasal compartment (Bless et al., 2006).

LIF (leukemia inhibitory factor) is a cytokine, member of interleukin-6 superfamily that regulates many cellular processes by interacting with its receptors gp130 and LIFRβ and activating several kinases pathway. It has been shown to modulate in a dose-dependent manner the migration of immature immortalized GnRH neurons (GN11 cells, (Radovick et al., 1991)) and it is expressed in many hypothalamic nuclei, suggesting a dual role in the migration and maturation of GnRH neurons (Magni et al., 2007).

HGF (hepatocyte growth factor) is a member of the plasminogen regulated growth factor family and proHGF is secreted and cleaved by uroplasminogen (uPA), tissue plasminogen (tPA) or coagulation factors to activate cMet, its coupled tyrosine kinase receptor. It has been demonstrated that HGF creates a chemoattractant gradient within the nasal mesenchyme, from the VNO towards the NFJ. This gradient attracts cMet-expressing GnRH neurons whereas the disruption of HGF gradients leads to a defective GnRH neuron migration both *in vitro* in a chemotactic assay on GN11 cells and *in vivo* in mice lacking *tPA*/*uPA*. Consistently, administration of HGF to nasal explant cultures increases the ability of GnRH neurons to migrate for longer distances (Giacobini et al., 2007).

Ephrins are surface molecules that play a major role in axonal pathfinding and neuronal migration by interacting with their coupled receptor EphA and EphB. The role of ephrins in GnRH neuron development is highlighted by the fact that GnRH neurons express EphA5 receptor and that

abnormalities in EphA5 signalling may result in a reduced migration. In agreement, the overexpression of EphA5 by GnRH neurons in GN23 mice, subsequent to a 67 kb deletion downstream the *Epha5* gene, trigger abnormal adhesion of GnRH neurons to OLF/VN nerves expressing ephrins A3 and A5 during early phases of migration. As a result, the hypothalamus contains less GnRH neurons; however, these few neurons reaching the MPOA are sufficient for puberty onset and adult mice only partially display subfertility or infertility (Gamble et al., 2005).

CXCL12 (CXC-motif ligand 12), also known as SDF-1 (stromal cell-derived factor 1), is a chemokine that act as chemoattractant in several developmental processes. During nose development, CXCL12 is expressed in an increasing rostral to caudal gradient, most intense at the border between nasal compartment and developing telencephalon. The unique CXCL12 receptor CXCR4 has been found expressed by several MM cells, including GnRH neurons and OLF/VN nerves and by neuronal progenitors within the VNO and the OE. Accordingly, GnRH neurons in *Cxcr4*$^{-/-}$ mice fail to exit the VNO at E13.5 and therefore few neurons reach the hypothalamus. The MM is reduced in size as well, suggesting that CXCL12/CXCR4 signalling is fundamental for the migration of many cell types within the developing nose (Schwarting et al., 2006). Recently, CXCR7 has been identified as second CXCL12 receptor by Memi and colleagues. Specifically, they demonstrated that CXCR7 is expressed along the migratory path of GnRH neurons in the nasal cavity and, although not expressed by GnRH neurons, it affects their migration as indicated by the ectopic accumulation of these cells in the nasal compartment in *Cxcr7*$^{-/-}$ mice. CXCR7 regulates CXCL12 availability by acting as a scavenger receptor along the migratory path of GnRH neurons and, thus, absence of CXCR7 influences the migration of these cells in a non cell-autonomous manner by causing abnormal accumulation of CXCL12 that attract CXCR4-positive GnRH neurons (Memi et al., 2013).

Slit ligand and Robo (roundabout guidance receptor) receptor families are axon guidance cues that have been directly implicated in GnRH neuron migration, since *Robo3*- and *Slit2*-null mice exhibit a reduced number of GnRH neurons in the MPOA concomitantly with a normal development of axonal scaffold (Cariboni et al., 2012). Recently, Robo3 has been also implicated in TN navigation and Nell2 (Neural EGFL Like 2) has been proposed as ligand for Robo3 (Taroc et al., 2017).

After the migration within the nasal mesenchyme, GnRH neurons reach the NFJ. Here, the OLF/VN/TN axonal scaffold splits into different branches and GnRH neurons follow cVN/TN nerves that project ventrally and caudally within the forebrain. The crossing of NFJ through the foramina of the CP is a crucial step for GnRH neuron: here, a dramatic environmental change can be observed both at the molecular and anatomical level and therefore cells that cross this region must adapt to these changes. Several researchers demonstrated that GnRH neurons make a pause at NFJ level before

entering the forebrain. Although reasons are still unclear, the prevailing idea is that GnRH neurons undergo maturation and adapt their set of receptor/molecules to adapt to the new environment. Moreover, GnRH neurons must avoid OB and migrate caudally and therefore need to correctly recognize cues that pattern the caudal way (Wray, 2010).

GABA (γ-aminobutyric acid) is the main inhibitory neurotransmitter in adult nervous system, but during embryonic development it regulates several different processes and specifically in the developing GnRH system, it has been shown that GABA acts as modulator of GnRH neuron migration speed. GABA is synthesized by OLF/VN nerves in a spatially and temporally limited window and has profound effects on expressing $GABA_A$. Both GABA and $GABA_A$ agonists are able to stop GnRH neuron migration in nasal explants (Casoni et al., 2012; Fueshko et al., 1998a) suggesting that *in vivo* GABA may be a necessary stop signal that delays GnRH neuron entrance in the forebrain. Consistently, mice lacking glutamate acid decarboxylase (*Gad67* knock out mice), the main enzyme synthesizing GABA, display an increased number at NFJ at E14.5 compared to WT littermates, suggesting that absence of GABA accelerate GnRH neuron migration (Lee et al., 2008).

CCK (cholecystokinin) is a widely distributed entero-hormone that plays important function also in sensory systems, representing one of the most abundant neuropeptides in the central nervous system (CNS). CCK acts via a G-protein coupled receptor, CCK-1R, that is highly expressed by GnRH neurons. CCK is in turn expressed by OLF/VN nerves and acts as negative modulator of GnRH neuron migration, as shown in nasal explant experiments and in *Cck1r*-null mice (Giacobini et al., 2004).

Reelin is an extracellular matrix protein fundamental for cortical neuron migration. Interestingly, reelin is also expressed in the olfactory system and therefore may play a role in its development. Cariboni and co-authors demonstrated that reelin is able to repel directly GnRH neurons and mice lacking reelin (*reeler* mice) display a reduced number of hypothalamic GnRH neurons due to the presence of ectopic neurons in the OB and in the cortex. However, this function does not appear to be mediated by the conventional signalling pathway that involves ApoER2/VLDLR and the cytoplasmic adaptor protein Dab1, as mutant mice for these proteins do not present any alterations in GnRH neuron migration (Cariboni et al., 2005).

2.3 Development of GnRH neurons in the forebrain

GnRH neuron journey finishes within the developing telencephalon. Here, GnRH neurons first follow cVN/TN nerves until the hypothalamus and finally detach from their guiding fibres to disperse in their final location, that is the MPOA. These steps are still poorly studied, even if some factors regulating GnRH neuron survival and maturation have been already identified. For instance, Axl and

Tyro3, two tyrosine kinase receptors, have been demonstrated crucial for the survival of GnRH neurons that reach the MPOA (Pierce et al., 2008). Prok2 (prokineticin 2) and its receptor, Prokr2, are also expressed in the MPOA and may regulate maturation/survival of GnRH neurons. Similarly, the transcription factor Nhlh2, member of the helix-loop-helix superfamily, plays a pivotal role in promoting survival of GnRH neurons in the MPOA between birth and adulthood (Cogliati et al., 2007); Nhlh2 seems to act through its downstream effector Necdin, since analysis of *Necdin* knockout mice shows reduced number of GnRH neurons in the MPOA and a decreased extension of GnRH-positive fibres to the ME (Muscatelli, 2000). ME innervation is also regulated by FGFs/FGFR1: a subset of post-mitotic GnRH neurons expresses Fgfr1 and Fgf2 has been demonstrated to exert a strong neurotrophic role and to promote neurite extension (Gill and Tsai, 2006; Tsai et al., 2005). GABA, in addition to the role exerts at NFJ level, maintains *Gnrh1* mRNA levels, preventing a loss of identity in GnRH neurons (Fueshko et al., 1998b). One of the well-studied molecules acting on mature GnRH neurons is kisspeptin (Kiss1). Kiss1 is a 154 amino acid peptide encoded by *Kiss1* gene. Kisspeptin binds to Gpr54 (also known as Kiss1r) highly expressed by GnRH neurons, promoting a reduction in cell motility (Seminara et al., 2003). Moreover, Kiss1 neurons located in ARC and AVPV nuclei regulate pulsatile GnRH release by contacting GnRH neuron terminals and therefore defects in Kiss1-secreting neurons may result in defective secretion of GnRH. In agreement, both *Kiss1*- and *Kiss1r*-null mice are viable and healthy with no apparent abnormalities but fail to undergo sexual maturation. However, migration of GnRH neurons into the hypothalamus appears normal with appropriate axonal connections to the median eminence and functional HPG axis after Kiss1 replacement, subsequent to peripheral administration of kisspeptin (d'Anglemont de Tassigny et al., 2007). Similarly, neurokinin B and dynorphin A may play a similar role in mature GnRH neurons. Finally, heparan sulphate proteoglycans (HSPG), cell membrane and matrix-associated proteoglycans, may be required for the appropriate establishment, maturation and functionality of hypothalamic GnRH neurons. HSPG have been shown to functionally interact with FGFs and ansomin-1. In FNCB4 human foetal olfactory neuroepithelial cells, anosmin-1 triggered cytoskeletal rearrangement and neurite outgrowth via crosstalk with FGF8/FGFR1/HSPG complex. Hudson and co-workers identified that the heparan sulphate cores that modulate GnRH neuron migration include both syndecan (Sdn-1) and glypican (Gpn-1) (Hudson et al., 2006). These many HSPG complexes modulate multiple factors involved in GnRH neuron migration such as anosmin-1/KAL-1 and FGFs/FGFR1, PROK2, HGF, netrin and perhaps Axl and Tyro3. This raises the intriguing possibility of specificity in the type of HSPG to restrict or amplify crosstalk between cell surface and extracellular matrix factors to modulate GnRH neuron migration and the establishment of GnRH neurons synapses (Condomitti and de Wit, 2018).

3. Isolated GnRH Deficiency

Defects in GnRH neuron development or functionality can lead to a pathological condition known as IGD. This disorder is characterized by inappropriately low serum concentrations of the gonadotropins, LH and FSH, in the presence of low circulating concentrations of sex steroids that lead to absence of puberty, infertility and therefore reproductive failure. Infant boys with IGD often have micro phallus and cryptorchidism (i.e. undescended testes), while adolescents and adults with IGD have clinical evidence of hypogonadism and incomplete sexual maturation. Adult males with IGD tend to have prepubertal testicular volume (i.e. <4 mL), absence of secondary sexual features (e.g. facial and axillary hair growth, deepening of the voice), decreased muscle mass, diminished libido, erectile dysfunction, and infertility. Adult females have little or no breast development and primary amenorrhea (Balasubramanian and Crowley, 1993). IGD can also lead to many co-morbidities and long-term effects, such as psychological and psyco-sexual disorders (Varimo et al., 2015), osteoporosis (Laitinen et al., 2012)and increased risk of metabolic defects like type II diabetes mellitus (Brand et al., 2014). IGD has a male prevalence of 3-5 to 1, however the incidence is uncertain and can vary broadly from 1:4.000 to 1:30.000 males (Marino et al., 2014; Stamou and Georgopoulos, 2018).

The clinical hallmark of IGD is the failure of puberty onset, that is defined as absence of breast development in a 13-years old girl or failure to reach a testicular volume of 4 mL in a 14-years old boy (Topaloğlu, 2017). Diagnosis of IGD is most commonly achieved during adolescence after physical examination of patient sex characteristics and biochemical testing for sex hormones. In boys, mini-puberty represents an additional temporal window to perform early diagnosis, since the failure of HPG axis during foetal life and infancy often results in micro-phallus and cryptorchidism (Dwyer et al., 2016). An early diagnosis is fundamental for a more effective management and treatment of IGD. Treatment options consist of administration of sex steroids, gonadotropins or pulsatile GnRH; therapy is chosen based on the goal of treatment that could be the induction and maintenance of secondary sex features or induction and maintenance of fertility (Balasubramanian and Crowley, 1993). As described above, the HPG axis is a dynamic endocrine axis, and is under the control of sophisticated regulatory mechanisms. This fact makes the HPG axis susceptible to dysfunction due to mutations in several genes; hence, the diagnosis of IGD is made difficult by the high clinical and genetic complexity of IGD

Clinically, IGD could be present solely as GnRH deficiency, in association with absent (anosmia) or diminished (hyposmia) sense of smell, or in multisystemic syndromes. When associated with hyposmia/anosmia, IGD is then referred as KS and represents 50% of overall IGD cases. Instead,

when the sense of smell is intact IGD is referred as normosmic Hypogonadotropic Hypogonadism (nHH). Finally, IGD may be present as clinical trait in multisystemic syndromes or may overlap with multisystemic syndromes sharing only some clinical features. Multisystem syndromes related to IGD include CHARGE syndrome, Bardet-Biedl syndrome, Waardenburg syndrome, Gordon-Holmes syndrome, Dandy-Walker syndrome, Morning Glory syndrome, Hartsfield syndrome, septo-optic dysplasia (SOD), combined pituitary hormone deficiency (CPHD), adrenal hypoplasia, congenital obesity (Boehm et al., 2015; Kim, 2015; Stamou and Georgopoulos, 2018).

IGD is genetically heterogeneous, with both sporadic and familial cases. Several modes of inheritance have been identified, including X chromosome-linked recessive, autosomal recessive and dominant (Boehm et al., 2015). However, IGD is not solely a monogenic disorder as several IGD genes are shown to genetically interact modulating the severity of GnRH deficiency, strengthening the idea that IGD can also be considered a digenic/oligogenic disorder (Marino et al., 2014; Sykiotis et al., 2010b). To date up to 30 genes have been demonstrated to cause IGD but they account only for the 50% of overall IGD cases; genetic causes for the remaining cases are so far still unknown (Boehm et al., 2015). IGD causative genes can be divided into two groups as they disrupt either the development of GnRH neurons (neurodevelopmental genes) or the action/signalling of GnRH in normally developed GnRH neurons (neuroendocrine genes). Mutations in neurodevelopmental genes usually lead to KS, whereas defective neuroendocrine genes usually underlie nHH. Several genes have a dual role both during development and function of GnRH neurons and therefore can cause either KS or nHH. In addition, some genes have a pleiotropic role, controlling many different developmental processes, so mutations lying on these genes can lead to either KS/nHH or syndromic IGD, depending on the nature of the mutation (Boehm et al., 2015; Stamou et al., 2015).

The high degree of phenotypic and genetic variability, in addition to the low penetrance observed for some genes, makes difficult the identification of novel genes implicated in the pathogenesis of IGD. In addition, canonical genetic investigations in affected families are limited by the negative effect of IGD on fertility so that screened patients are few in numbers; finally, our biological knowledge on the HPG axis is still limited. However, in recent years several new IGD causative genes have been discovered following two main approaches: i) screening of patients to discover mutations in novel genes whose role must be studied and confirmed in experimental models such as *in vitro* or *in vivo* models; ii) a basic science-driven identification of candidate genes involved in GnRH neuron physiology that after functional studies in experimental models must be screened in patients in search for mutations. Interestingly, consanguineous families have been very useful for the discovery of novel IGD genes. Further, the recent advances in next generation sequencing (NGS) and

other technologies, such as homozygosity mapping, allowed the identification of several novel causative genes for IGD (Stamou et al., 2015; Sykiotis et al., 2010a).

3.1 Normosmic Hypogonadotropic Hypogonadism

nHH is mainly caused by neuroendocrine defects occurring in GnRH neurons that have correctly reached the hypothalamus, therefore mutated genes are physiologically responsible for GnRH synthesis (*GNRH1*), GnRH action (*GNRHR*) or GnRH pulse generator (*KISS1*/*KISS1R*, *TAC3*/*TACR3*, *PCSK1*, *LEP*/*LEPR*) (Balasubramanian and Crowley, 1993; Bianco and Kaiser, 2009; Boehm et al., 2015; Kim, 2015; Marino et al., 2014; Stamou and Georgopoulos, 2018; Topaloğlu, 2017).

3.1.1 GNRH1

In humans, GnRH is encoded by *GNRH1* gene (chromosomal location chr 8p21.2), thus mutations in this gene are expected to be disease causing. Yet, mutations in *GNRH1* gene are very rare and they account only the 2% of nHH cases. The pattern of inheritance is typically autosomal recessive. Although, the pathogenic potential of variants in GNRH1 was already demonstrated thanks to *hpg* mice, which are sexually immature and infertile and showed complete absence of GnRH, due to a truncating deletion in *Gnrh1* (Mason et al., 1986), first loss of function mutations was found only in 2009 within exons encoding for the GnRH decapeptide (Bouligand et al., 2009; Chan et al., 2009).

3.1.2 GNRHR

GNRHR (chr 4q21.2) mutations are in turn very frequent (5-10% of nHH cases) and can be inherited in autosomal recessive or oligogenic fashion. GNRHR is a 328 amino acids G-coupled receptor deputed to transduce GnRH signalling in gonadotrope cells of the pituitary by mobilising intracellular calcium to stimulate LH and FSH secretion. To date, 25 inactivating mutations have been identified throughout the whole gene, with no hotspot, resulting in a wide range of phenotype, from less severe eunuch fertile syndrome to more severe one (Marino et al., 2014). In agreement with human mutations, *Gnrhr* gene trapped mice have a similar phenotype to the clinical syndrome of hypogonadotropic hypogonadism, presenting small sexual organs, low levels of FSH, LH, and steroid hormones, failure of sexual maturation, infertility, and inability to respond to exogenous GnRH (Wu et al., 2010).

3.1.3 KISS1 and *KISS1R*

Kisspeptins, encoded by the *KISS1* gene, and their canonical receptor, GPR54 (also termed KISS1R), are unanimously recognized as essential regulators of puberty onset and gonadotropin secretion. In humans, kisspeptins refer to a family of neuropeptides resulting from the cleavage of a 145 amino

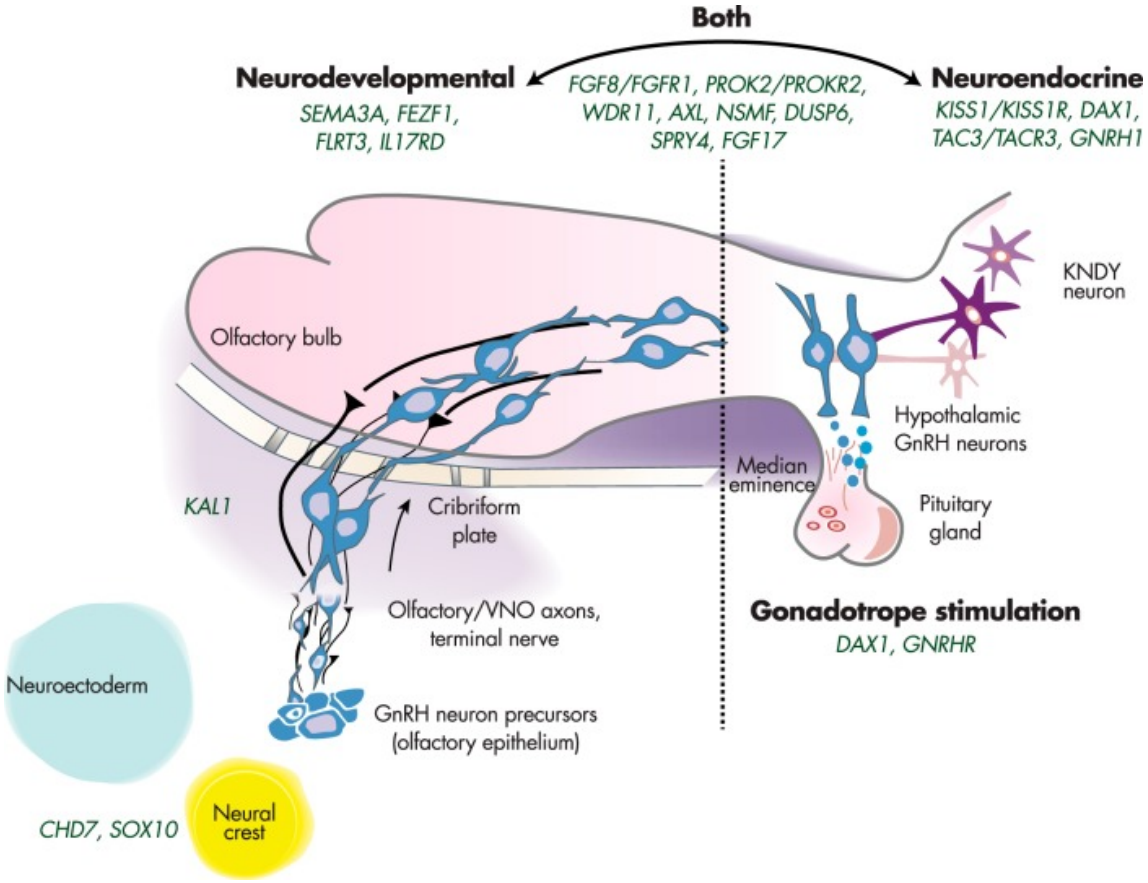

Figure 8 – Neurodevelopmental and neuroendocrine regulation of GnRH neurons. Genes on the left are critical for GnRH neuronal specification and migration and therefore can also affect the development of olfactory system; whereas genes on the right are involved in proper GnRH function. A number of IGD genes, in the centre, are involved in both processes.

Adapted from "Discovering genes essential to the hypothalamic regulation of human reproduction using a human disease model: adjusting to life in the -omics era" by M.I. Stamou, K.H. Cox and W.F. Crowley, 2015, *Endocrine Reviews*, 36(6):603-621. Copyright 2015 by Endocrine Society.

Gene	Location	OMIM	IGD			Inheritance pattern	Biological role
			nHH	KS	syndromic IGD		
ANOS1	Xp22.31	300836		X		X-linked recessive	Extracellular matrix protein modulating FGFR1 and integrin; guidance cues and survival factor for GnRH neurons
AXL	19q13.2	109135	X	X		nd	Receptor containing fibronectin type III domain; GnRH neurons migration
CCDC141	2q31.2	616031		X		nd	Regulate neuron migration; expressed by GnRH neuron
CHD7	8q12.2	612370			CHARGE	AD	Transcriptional regulator essential for neural crest cells development
DCC	18q21.2	120470		X		AD	GnRH neuron migration regulator; receptor for NTN1
DMXL2	15q21.2	616113	X		PEPNS	AR	Synaptic protein involved in GnRH neuron and gonadotrophs homeostasis
FEZF1	7q31.32	613301		X		AR	Zinc-finger transcriptional repressor regulating forebrain development; GnRH neuron migration and survival
FGF17	8p21.3	603725			D-WS	nd	Alternative FGFR1 ligand
FGF8	10q24.32	612702			CPHD	AD	Ligand for FGFR1; placode formation and GnRH neuron specification
FGFR1	8p11.23	147950			CPHD, SOD, HS, SHFM	AD	Tyrosine kinase receptor; placode formation, GnRH neuron specification
GNRH1	8p21.2	614841		X		AR	Decapeptide that stimulate HPG axis; exclusively expressed by GnRH neurons
GNRHR	4q13.2	146110		X		AR	G protein coupled receptor for GnRH, expressed by gonadotrope cells
HESX1	3p14.3	182230		X	CPHD, SOD	AD, AR	Transcriptional repressor for homeodomain-containing genes; placode formation
HS6ST1	2q14.3	614880	X	X		AD	Heparan sulphate modulator; essential for FGFs signalling
IL17RD	3p14.3	606807		X		AD	Negative regulator of FGFR1
KISS1	1q32.1	614842		X		AR	Secretagogue of GnRH, secreted by KNDy neurons in ARC nucleus and Kiss-neurons in AVPV nucleus
KISS1R	19p13.3	614837		X		AD, AR	G protein coupled receptor for Kiss1, expressed by GnRH neurons
KLB	4p14	611135	X			nd	Regulate reproduction and metabolism regulating FGFR1/FGF21 signalling
LEP	7q32.1	614962		X		AR	Anorexigenic adipocyte-specific cytokine regulating food intake; negative modulator of GnRH
LEPR	1p31.3	614963		X		nd	Receptor for leptin

NR0B1	Xp21.2	300200	X			X-linked recessive	Negative modulator of retinoic acid receptor
NSMF	9q34.3	614838	X	X		nd	Guidance molecule for olfactory axons
NTN1	17p13.1	601614		X		nd	Axon guidance cues regulating GnRH neuron migration
OTUD4	4q31.21	611744	X		GHS	AR	De-ubiquitinase
PCSK1	5q15	162150		X		nd	Required for processing of various pre-hormones e neuropeptides
PNPLA6	19p13.2	603197			GHS	AR	Catalyses the de-esterification of membrane phosphatidylcholine
PROK2	3p13	610628	X	X		AD, AR	Olfactory bulb formation and GnRH neuron migration; circadian clock
PROKR2	20p12.3	147950	X	X	CPHD	AD, AR	G protein coupled receptor for PROK2
RNF216	7p22.1	609948			GHS	AR	Zinc-finger protein inhibiting TNF and NF-kB
SEMA3A	7q21.11	614897		X		AD	Guidance cue for GnRH neurons and olfactory axons
SEMA3E	7q21.11	608166			CHARGE	AD	GnRH neuron survival through Plxnd1
SEMA7A	15q24.1	607961	X	X		nd	Membrane anchored guidance cue; GnRH neuron axons outgrowth
SOX10	22q13.1	602229		X	WS	AD	Neural crest development
TAC3	12q13.3	614839		X		nd	Secretagogue of GnRH, secreted by KNDy neurons in ARC nucleus
TACR3	4q24	614840		X		nd	G protein coupled receptor for TAC3, expressed by GnRH neurons
WDR11	10q26.12	614858			CPHD	AD	WD repeat-containing protein; expressed in forebrain and HPG axis

Table 1 – List of known IGD causative genes. Abbreviations: PEPNS, polyendocrine deficiencies and polyneuropathies; CPHD, combined pituitary hormone deficiency; WS, Waardenburg Syndrome; GHS, Gordon-Holmes Syndrome; Dandy-Walker Syndrome; HS, Hartsfield Syndrome; SHFM, split and/foot malformations; SOD, Septo-Optic Dysplasia; OMIM, online mendelian inheritance in man; Ad, autosomal dominant**;** AR, autosomal recessive; nd, not determined.

acid precursor protein, thought to be active predominantly as a 54 amino acid peptide. These key reproductive functions derive from the capacity of kisspeptins to stimulate GnRH release in the hypothalamus (see paragraph 1.1 for kisspeptin action), where two distinct populations of Kiss1-secreting neurons have been identified in ARC and AVPV (Brock and Bakker, 2013). KISS1 and its cognate receptor KISS1R are positive modulator of GnRH release and are essential for the establishment of GnRH pulse generator (de Roux et al., 2003; Seminara et al., 2003), hence mutations in both genes can strongly affect GnRH secretion. Mutations in *KISS1* (chr 1q32) and *KISS1R* (chr 19p13.3) genes are rare, each covering only 2% of nHH cases and can be inherited in autosomal recessive pattern; *KISS1R* variants also contribute to oligogenic inheritance.

3.1.4 TAC3 and *TACR3*

Similarly to KISS1/KISS1R, neurokinin B (NKB encoded by *TAC3* gene, located on chromosome chr 12q13-q21) and its coupled receptor (NK3) encoded by *TACR3* gene (chr 4q25) are key regulator of puberty and fertility. NKB is expressed in the ARC nucleus by KNDy neurons, while NK3 is expressed by GnRH neurons. First pathological variants have been found thanks to homozygosity mapping-driven strategy as patients came from consanguineous families (Topaloglu et al., 2009). To date, several mutations have been discovered and intriguingly those lying on TACR3 gene are as frequent as GNRHR ones. The inheritance pattern should be autosomal recessive, even if both genes contribute to oligogenic inheritance.

3.1.5 LEP, *LEPR* and *PCSK1*

IGD patients may occasionally display a mild obese phenotype, however mutations in genes encoding for leptin (*LEP*, chr 7q31.3), leptin receptor (*LEPR*, chr1p31) or Proprotein convertase subtilisin/kexin type 1 (*PCSK1,* also known as neuroendocrine convertase 1, *NEC1*; chr 5q15-q21) always result in nHH coupled with severe obese phenotype. The inheritance pattern is typically autosomal recessive and mutations in each gene account for less than 5% of overall nHH cases.

Leptin is a 167 amino acids cytokine produced by adipose tissue and exerts a anorexigenic role in the hypothalamus. Leptin-deficient mice (*ob*/*ob* mice, (Zhang et al., 1994)) display obesity and hypogonadism but both conditions are restored by leptin treatment. Leptin is supposed to regulate HPG axis by inhibiting neuropeptide-Y secretion, promoting in turn POMC/α-MSH (proopiomelanocortin/melanocortin) secretion, that have a negative and positive effect on GnRH release, respectively (Landry et al., 2013); furthermore, leptin can positively modulate a subset of KNDy neurons through its receptor LEPR (Cravo et al., 2011). Together, these observations show that leptin has a permissive role for puberty initiation, providing a correlation between energy balance and reproductive function. Mutations in *LEPR* gene (Clément et al., 1998) lead to a less severe

phenotype compared to *LEP* mutations (Strobel et al., 1998) suggesting that leptin may signal redundantly through their receptors.

NEC-1 is required for the processing of large precursor pro-hormones like POMC, insulin and glucagon and therefore for the release of active peptides. So far, the role of NEC-1 in HPG axis is not fully understood, but it may exert the processing of pro-GnRH as well. However, several mutations have been found in *PCSK1* catalytic domain, strengthening this hypothesis (Farooqi and O'Rahilly, 2006; Farooqi et al., 2007; Jackson et al., 1997). The inheritance pattern is uncertain as researchers have been found single heterozygous, compound heterozygous and homozygous mutations.

3.1.6 KLB

Fgfr1 role has been well characterized in several murine studies and it is known to play a dual action on the GnRH neuron system by acting both during embryonic stages and in adult homeostasis. Mouse Fgfr1 mutant show loss of 50% of GnRH neurons in the hypothalamus, delayed puberty and early reproductive senescence (Tsai et al., 2005). Because Fgf8 expression is restricted to embryonic development, researchers have hypothesized the existence of a different ligand for Fgfr1. Fgf21 is mainly secreted in the liver but it has been identified as a central metabolic regulator by acting through Fgfr1 and its obligate co-receptor β-klotho, encoded by *Klb* gene. Interestingly, no mutations have been found in *FGF21* gene, but heterozygous mutations have been found in 4% of nHH patient in *KLB* gene. *Klb* expression is barely detectable at embryonic stages but then increases in the post-mitotic GnRH neurons in adult mice, supporting a postnatal role for Fgf21/Fgfr1/Klb signalling. Consistently, *Klb*-null mice have normal GnRH neuron development but display delayed puberty and subfertility; *in vitro* experiments on GT1-7 cells provide essential evidences of the role of Fgf21 which is promoting neurite extension and GnRH secretion through Klb/Fgfr1 complexes (Xu et al., 2017).

3.2 Kallmann Syndrome

KS was first described by Aureliano Maestre de San Juan in an adult male with testes of prepubertal size and absent olfactory bulbs. Franz Kallmann then demonstrated that hypogonadism co-segregates with anosmia in two families, establishing a genetic basis for this condition. In the last decades, many experimental works showed that patients with KS can display other non-reproductive non-olfactory anomalies including renal agenesis and synkinesia (i.e. mirror movements) (Dodé and Hardelin, 2009). KS is rarer than nHH, having a prevalence of around 1:8.000 in men and 1:40.000 in women. KS is mainly caused by neurodevelopmental defects affecting different steps of migration and development of GnRH neurons (Balasubramanian and Crowley, 1993; Bianco and Kaiser, 2009;

Boehm et al., 2015; Kim, 2015; Marino et al., 2014; Stamou and Georgopoulos, 2018; Topaloğlu, 2017).

3.2.1 ANOS1 (*KAL1*)

ANOS1 (chr Xp22.3) was the first KS gene to be discovered in 1991 (Franco et al., 1991) and several mutations have been identified so far, accounting for 10-15% of overall X-linked KS cases. *ANOS1* gene encodes for anosmin-1, an extracellular matrix glycoprotein of 680 amino acids, with a complex structure that includes four fibronectin-like type III repeats that are homologous to cell adhesion molecules, and several predicted HSPG binding regions. Consistent with its structure, anosmin-1 is able to link cell membranes to HSPG regulating several processes including neural cell adhesion and axonal migration. Dysfunctional anosmin-1 may perturb migration of many cell types, including GnRH and OLF/VN nerves and it was the first protein to be associated to GnRH neuron migration defects. In 1989, a single human foetus affected by KS showed a missense mutation in *ANOS1* gene and exhibited OLF/VN nerves and GnRH neurons tangled in a web of fibres just above the CP (Schwanzel-Fukuda et al., 1989). Anosmin is indeed involved in adhesion of OLF/VN nerves during the early migratory steps, when newly born axons first project out of the epithelium. Thus, dysfunctional anosmin results in an abnormal formation of OLF/VN nerve bundles and therefore has an indirect effect on GnRH neuron migration. Furthermore, it has been shown that anosmin is able to directly stimulate GN11 cells migration whilst mutated anosmin does not (Cariboni et al., 2004). Anosmin-1 however is expressed in many other tissues such as kidneys (Hardelin et al., 1999), hence its variable expression may also explain phenotypic variability observed in patients with *KAL1* mutations (Dodé and Hardelin, 2009).

3.2.2 HS6ST1

Heparan Sulphate 6-*O* Sulpho-Transferase 1 (HS6ST1) is an enzyme that catalyse the specific O-sulphation of HSPG, an important component of extracellular matrix. HSPG are involved in cell migration and cell-cell communication since it regulates gradients of many soluble factors, such as FGFs. Hence, dysfunctional HS6ST1 may result in a mispatterning of gradients followed by migrating cells, including GnRH neurons that become unable to reach their destination. HS6ST1 functionally interact with many other IGD genes such as *ANOS1* and *FGF8*. Despite its developmental role has been studied only in *C. elegans*, autosomal dominant mutations in *HS6ST1* (chr 2q14.3) have been found in both KS and nHH patients (Tornberg et al., 2011).

3.2.3 IL17RD

Interleukin 17 receptor D (*IL17RD*, chr 3p14.3) has been identified as nHH/KS causative gene thanks to protein-protein interaction analysis based on the idea that in addition to

FGF8/FGFR1/ANOS1/HS6ST1, other FGF signalling-related proteins may be implicated in IGD (Miraoui et al., 2013). It has an autosomal dominant inheritance pattern and 2-5% of IGD patients harbour mutations in this gene.

3.2.4 NSMF

NSMF (NMDA receptor Synaptonuclear signalling and neuronal Migration Factor) also known as nasal embryonic LHRH factor (NELF) is a guidance molecule for OLF/VN. Defective formation of these axons lead to a defective migration of GnRH neurons as their axonal scaffold has not been formed correctly (Kramer and Wray, 2000). Mutations in *NSMF* gene (chr 9q34.3) have been discovered both in KS and nHH patients primarily in an oligogenic pattern of inheritance (Miura et al., 2004). NSMF is localized to membrane surfaces of both GnRH neurons and OLF/VN nerves. Its expression pattern presents a peak of expression at around E12.5-14.5 when migration rate is higher and then decreases at E17.5 when most of GnRH neurons have already settled in the hypothalamus. Knock-down of *Nsmf* expression with antisense oligonucleotides leads to abnormal migration of GnRH neurons and defective OB contacts of the OLF/VN nerves. Since Nsmf is localized on the outer side of GnRH neuron and sensory fibre membranes, an homophilic interaction between the two cell types may be suggested (Kramer and Wray, 2000). *nsmf* is also expressed during zebrafish embryonic development in GnRH3 neurons and in their target sites before the initiation of their migration. *nsmf* morpholino-mediated knockdown results in the disruption of the GnRH3 system with absent or misguided GnRH3-positive axons and ectopic positioning of GnRH3-positive perikaryal (Palevitch et al., 2007). These results suggest that NSMF is a highly conserved factor, highlighting its important role in the developmental migration and projection of GnRH.

3.2.5 AXL

Analysis of both *Axl* and its coupled receptor *Tyro3* null mice showed delayed puberty onset and partial loss of GnRH neurons in the hypothalamus (Pierce et al., 2008). Despite described in only one report, the identification of mutations in *AXL* gene (chr 19q13.2) in KS/nHH patients confirm the role of AXL in the neurodevelopment of GnRH neurons (Salian-Mehta et al., 2014).

3.2.6 PROK2 (KAL4) and *PROKR2* (KAL3)

PROK2 (chr 3p13) gene encodes for a small peptide called prokineticin 2 which interacts with its cognate receptor PROKR2 (encoded by *PROKR2* gene, chr 20p12.3), to regulate olfactory system development and neuronal progenitor differentiation. Prok2 is expressed in the mouse OB and acts as chemoattractant for OLF/VN nerves that in turn express Prokr2. Mice lacking either *Prok2* or *Prokr2* display OB hypoplasia and hypogonadism, with GnRH neurons unable to reach and populate the hypothalamus, resembling human KS (Matsumoto et al., 2006; Pitteloud et al., 2007b; Prosser et

al., 2007). After these findings, several pathogenic variants have been found in both genes (Abreu et al., 2008; Dodé et al., 2006; Pitteloud et al., 2007a); patients with *PROK2*/*PROKR2* mutations show a great phenotypic variability, ranging from KS (usually inherited in autosomal dominant or recessive pattern) to nHH (in oligogenicity with other mutated genes) and represents <10% of IGD overall cases.

3.2.7 FEZF1 and *CCDC141*

FEZF1 is a zinc finger transcription factor that regulates neurogenesis and neuronal cell fate, especially within olfactory placode (Eckler and Chen, 2014). Thanks to advances in NGS, it has been possible to identify two mutations lying on *FEZF1* gene (chr 7q31.32) in two independent consanguineous families characterized by KS (Kotan et al., 2014). In one family, a second pathogenic variant harboured on the *CCDC141* gene (chr 2q31.2), which encodes for a coiled-coiled domain containing protein expressed by GnRH neurons. Recently, other mutations affecting *CCDC141* have been found in KS patients (Hutchins et al., 2016; Turan et al., 2017).

3.2.8 SEMA3A and *SEMA3E*

Several studies have demonstrated the fundamental role that class 3 semaphorins exert during GnRH development in mice (Cariboni et al., 2011a; Cariboni et al., 2015; Hanchate et al., 2012). On one hand Sema3a drives OLF/VN nerves towards the olfactory bulb granting the axonal scaffold for GnRH neuron migration; on the other hand, Sema3e promotes survival of GnRH neurons that have reached the hypothalamus. Therefore, dysfunctional Sema3a/Sema3e signalling results in less GnRH neurons reaching or surviving in the hypothalamus, respectively. Accordingly, mutations in both genes have been found: several dominant *SEMA3A* (chr 7p12.1) pathogenic variants have been found in KS patients (6% of overall KS cases; (Hanchate et al., 2012; Känsäkoski et al., 2014; Young et al., 2012)), whilst only one work so far reported mutations in *SEMA3E* gene (chr 7q21.11) into two brothers with KS (Cariboni et al., 2015).

3.2.9 SEMA7A

Lack of Sema7a signalling through b1-integrin was previously associated with a decreased migration of GnRH neurons in mice (Messina et al., 2011). Subsequently, mutations found in KS patients have confirmed the essential role of *SEMA7A* (chr 15q22.3-q23) also in humans (Känsäkoski et al., 2014).

3.2.10 DCC and *NTN1*

Recently, pathogenic variants have been found in two genes, previously identified in mice as key regulator for GnRH neuron migration (Schwarting et al., 2001; Schwarting et al., 2004) thanks to a structure-driven approach. In this case, researchers have searched for novel variants throughout the

whole exome in portions of genes encoding for fibronectin 3 domains, as this specific domain characterized many IGD known genes such as *ANOS1* (Bouilly et al., 2018). Guidance molecule NTN1 (netrin-1) and its coupled receptor DCC (deleted in colorectal cancer) are fundamental proteins that regulate the turning of cVN/TN and GnRH neurons in the hypothalamus avoiding OB. DCC has been found expressed by both OLF/VN/TN nerves and some GnRH neurons and in mice lacking *Dcc* gene trajectories of cVN/TN nerves and GnRH neurons are abnormal. In these mice cVN/TN nerves misproject towards the cortex and consequently ectopic GnRH neurons can be found in the cortex, losing their function (Schwarting et al., 2001). Accordingly, *Ntn1*-null mice show the same phenotype as *Dcc* null mice (Schwarting et al., 2004).

3.3 Syndromic Isolated GnRH Deficiency

Neurodevelopmental genes often have pleiotropic effects since they regulate the development and the differentiation of many different cell types. When mutations underlying IGD occur in such neurodevelopmental genes, IGD may present in combination with a wide range of other non-reproductive non-olfactory anomalies including hearing loss, midline facial defects (e.g. cleft lip/palate), renal agenesis, synkinesia (i.e. mirror movements) and cerebellar ataxia. These clinical features also characterize other complex multi-trait syndromes including CPHD, SOD, CHARGE syndrome, adrenal hypoplasia congenita with HH, Waardenburg syndrome, Bardet-Biedl syndrome, Gordon Holmes syndrome, Morning Glory syndrome, Hartsfield syndrome and Dandy-Walker syndrome. In these cases, the partial overlapping between syndromic IGD and other recognized syndromes represents a huge hurdle for a correct diagnosis and this issue may be overcome with advances in the knowledge of genetics underlying IGD.

3.3.1 CHD7 (KAL5)

The chromodomain helicase DNA-binding protein 7 (*CHD7*, chr 8q12.1) encodes an ATP-dependent chromatin remodeller involved in NCC multipotent precursors that will give rise to several tissues, such as cardiac structures, craniofacial bone and cartilages, skin, peripheral nerves (Rogers and Nie, 2018). Interestingly, CHD7 has been found expressed also in migratory and post-migratory GnRH neurons and in olfactory structures, suggesting a possible role of this protein in GnRH development. Further, many observations strengthen the idea that CHD7 regulates the expression of guidance clues modulating migration of many cell types, including NCC (Schulz et al., 2014).

Dysfunctional CHD7 is the main cause of CHARGE syndrome, a multisystem disease characterized by coloboma of the eye, heart defects, atresia of choanae, growth retardation, genital hypoplasia and ear anomalies. GnRH deficiency and anosmia are secondary but still frequent trait of CHARGE syndrome (Balasubramanian and Crowley, 2017)). Yet, autosomal dominant mutations in

CHD7 have been also found in patients with nHH and KS who were not diagnosed as having CHARGE syndrome (Jongmans et al., 2009; Kim et al., 2008). The prevailing idea is that milder allelic variants could lead to IGD, whilst more severe mutations could result in CHARGE syndrome (Balasubramanian and Crowley, 2017). The precise role of CHD7 in the ontogeny of the GnRH neurons is still under active investigation. Comprehensive human and mouse embryonic expression analysis shows ubiquitous CHD7 expression during early development. Chd7 is widely expressed in the early in the undifferentiated neuroepithelium, neural crest derived mesenchyme, and later in the nasal epithelia, OB and nerves, and also in the anterior and median lobes of pituitary (Bergman et al., 2010; Layman et al., 2009; Layman et al., 2011; Sanlaville et al., 2006). This pattern of expression is consistent with the endocrine phenotypes of HH and other rare anterior pituitary hormone defects in CHARGE. Given the intricate relationship and joint origin of the OLF nerves and the GnRH neurons, studies in a human foetus with CHARGE syndrome has confirmed that the CHARGE foetus showed arhinencephaly (OB agenesis) with absence of GnRH neurons in the forebrain. The migrating olfactory and GnRH neurons accumulated in the fronto-nasal region with the formation of bilateral spherical structures consistent with neuromas near the cribriform plate, implicating a significant migratory defect (Teixeira et al., 2010). In keeping with these observations, *Chd7*-deficient mice display smaller OB, reduced number of OLF nerves, defective senses of smell with loss of odour-evoked electro-olfactogram responses, reduced hypothalamic GnRH neuronal numbers, hypoplastic genitalia, hypogonadotropism, and impaired pubertal timing (Bergman et al., 2010; Layman et al., 2009; Layman et al., 2011). In addition, they show significant defects in neural stem proliferation with reductions in production, proliferation and regeneration of OSN (Layman et al., 2009). These complementary observations in humans and mice provide compelling evidence that the reproductive deficits in CHARGE are secondary to impaired GnRH migration and consequent GnRH deficiency.

3.3.2 FGF8 (KAL6), *FGF17* and *FGFR1* (KAL2)

FGF8 gene (chr 10q24) encodes for the fibroblast growth factor 8, a member of FGF family. FGFs control cell proliferation, migration and differentiation especially during embryonic development by interacting with tyrosine kinase FGF receptors (FGFR). FGF8 is coupled with FGFR1 (encoded by *FGFR1*, chr 8p11.22-p11.23) and regulates patterning of many tissues, including the brain and the olfactory system; the binding affinity is strengthened by the presence of HSPG and other extracellular matrix protein such as anosmin-1. FGF8/FGFR1 are also involved in GnRH neuron migration and development. Autosomal dominant mutations in both genes are frequent (10% of overall cases) in nHH/KS patients (Dodé et al., 2003; Falardeau et al., 2008; Pitteloud et al., 2006b). Patients with mutations in these genes may additionally display cleft lip, corpus callosum aplasia, ear and finger

abnormalities (e.g. polydactyly) and therefore IGD is partially overlapping with syndromes such as Hartsfield syndrome, SOD, Split-hand/foot malformation.

FGF17 (encoded by *FGF17* gene, chr 8p2.3) has been identified as an alternative ligand for FGFR1 due to the high sequence identity with FGF8. Recently, mutations in *FGF17* gene have been reported in nHH/KS patients, showing other abnormalities consistent with Dandy-Walker syndrome (Miraoui et al., 2013).

3.3.3 SOX10

SOX10 gene (chr 22q13.1) mutations are responsible for approximately one third of KS cases with deafness (Pingault et al., 2013). SOX10 (sex-determining region (SRY) box 10) is a transcription factor that controls NCC development. In particular, it regulates NC-derived olfactory cells, such as OECS that provide essential mechanical and chemical support for OLF/VN nerves and GnRH neurons (Barraud et al., 2013). However, defective Sox10 signalling can also result in Waardenburg syndrome and Hirschsprung disease, rare pathological conditions presenting phenotypic features that could be attributed to defective NCC development (e.g. altered skin pigmentation, hearing loss, midline defects, gastrointestinal and cardiac anomalies).

3.3.4 PNPLA6, *RNF216*, *OTUD4*, *WDR11* and *DMXL2*

Mutations in these genes account only for few IGD cases and are all inherited in an autosomal recessive pattern, with the exception of *WDR11* which in turn is autosomal dominant. Furthermore, mutations in these genes are associated to other rare multisystem syndrome.

PNPLA6 (patatin-like phospholipase domain containing protein 6, chr 19p13.2) encodes a phospholipase involved in de-esterification of membrane phosphatidylcholine and it is mutated in Gordon-Holmes and Boucher-Neuhauser syndromes, characterized by IGD and neurological disorders (Topaloglu et al., 2014). Gordon-Holmes syndrome is additionally caused by mutations in *RNF216* gene (Ring finger protein 216, chr 7p22.1), a zinc finger protein involved in ubiquitination (Margolin et al., 2013) and *OTUD4* (OTU domain-containing protein 4, chr 4q31.21), that encodes a de-ubiquitinase found to be mutated in Gordon Holmes syndrome (Shi et al., 2014).

In turn, *DMXL2* and *WDR11* cause polyendocrine polyneuropathy syndrome (Tata et al., 2014) and combined pituitary hormone deficiency (McCormack et al., 2017), respectively.

3.4 Self-limited delayed puberty

In addition to KS and nHH that represent the most severe phenotypes of IGD, there is a broad spectrum of IGD related diseases, such as hypothalamic amenorrhea (HA), self-limited delayed puberty (DP) and adult-onset hypogonadotropic hypogonadism. Self-limited DP, also known as

constitutional delay of growth and puberty (CDGP), is the most common cause of delayed puberty, affecting 53% of the subjects (63% males and 30% females); other delayed puberty causes are IGD, hypergonadotropic hypogonadism, unclassified disorders and delayed but spontaneous pubertal development (Sedlmeyer and Palmert, 2002). Self-limited DP is defined as the lack of sexual maturation at an age >2 s.d. above the mean for a given population. In detail, it is characterized by (i) absence of spontaneous thelarche by the age of 13 years old and spontaneous menarche by the age of 15 years old in girls and spontaneous testicular growth by the age of 14 years old in boys; (ii) spontaneous pubertal development by the age of 18; (iii) evidence of normal rate of pubertal progression; (iv) absence of identifiable underlying causes of delayed puberty. Self-limited DP is often associated with adverse health outcomes including short stature, reduced bone mineral density and compromised psychosocial health (Howard and Dunkel, 2018). One major difference between self-limited DP and IGD is that the onset of puberty in self-limited DP, even though delays, occurs spontaneously before the age of 18 years old in contrast to IGD. Self-limited DP is highly heritable with 50–80% of self-limited DP patients having a positive family history of the same disease. The association between IGD and self-limited DP is suggested by the fact that ~10% of nHH patients have relatives with self-limited DP. In a recent study by Zhu et al., IGD subjects shared their rare variant with the 53% self-limited DP family members and with only 12% of unaffected relatives, suggesting that IGD and self-limited DP may share a common genetic pattern (Zhu et al., 2015). However, more recent studies provide evidences that IGD and self-limited DP have distinct genetic architectures, since mutations in IGD patients have been found in 51% of IGD probands and only in 7% of self-limited DP patients (Cassatella et al., 2018). In support of this view, another recent work by Howard and colleagues, identified *IGSF10* (Immunoglobulin Superfamily Member 10) as a causative gene solely for self-limited DP as no mutations in *IGFS10* gene have been found in IGD patients so far (Howard et al., 2016). In conclusion, whether IGD and self-limited DP share a common genetic pattern is still questioned but the emerging hypothesis is that these two clinical conditions share only in small extent the same the genetic architecture, with the majority of cases that is due to peculiar genetic causes (Howard, 2018).

4. Experimental tools to study GnRH neuron system

4.1 Mutational analysis in affected individuals

Depending on the mode of inheritance of the disease, and the number of affected individuals and their unaffected/carrier family members available, a number of approaches can be taken to identify the Mendelian monogenic disorder causative gene. For rare recessive disorders, particularly those

affecting the product of a consanguineous marriage, the homozygosity mapping method (HZM) is becoming an increasingly popular choice in gene identification. This along with the advent of NGS technologies, such as whole exome sequencing (WES), which makes exome sequencing now possible, gene identification in rare recessive disorders has become more achievable. Often the approach involves a combination of HZM and WES which narrows down the region of interest.

An individual is considered to be homozygous when two identical alleles are present at a particular locus on homologous chromosomes. Normally, outbred populations have short shared homozygous regions due to the increased recombination events which allow paired chromosomal segments to break apart and rejoin with each other, exchanging genetic material. Yet, individuals born from consanguineous parents display long stretches of consecutive homozygous regions, whose size strictly depends on the degree of inbreeding. If parents are first cousins then 1/16 of their offspring's genome will be homozygous, whereas if they are second cousins then the homozygous genome amongst their offspring would be 1/64 (Gibson et al., 2006; Wang et al., 2009). HZM is a method used to identify genes underlying rare autosomal recessive diseases in consanguineous families. This technique, first developed by Lander and Botstein in 1987, has been successfully applied to map the chromosomal loci underlying a number of diseases and syndromes, including Meckel-Gruber syndrome and non-syndromic mental retardation (Lander and Botstein, 1987; Morgan et al., 2002; Rehman et al., 2011). The fundamental principle underlying HZM is that children born from consanguineous parents and affected with an autosomal recessive condition share a common homozygous region spanning the disease locus. Hence through HZM it is possible to identify these long stretches of homozygous regions present only in those family members who are affected by the condition and will not be present in those who are unaffected. Genes found within the HZM region must be subsequently filtered and prioritized in order to narrow down the list of candidate genes. Indeed, HZM will often generate large amount of data with a list of hundreds of possibly causative genes lying in the shared homozygous regions. Numerous tools for gene prioritization are available to search for candidate genes. Endeavour is a freely accessible software providing a computationally curated list of prioritized candidate genes. It collates information from a wide variety of bioinformatic resources when prioritizing the genes, including GO (Gene Ontology) annotations and KEGG (Kyoto Encyclopedia of Genes and Genomes). The key strategy in Endeavour is to prioritize the list of candidate genes based on the training set. The training set is a list of genes known to be associated with similar conditions to the one under study. Endeavour will score the similarity of the candidate genes to the training gene list and give a final overall global ranking of each of the candidate genes. Endeavour has been successful in ranking casual genes for monogenic diseases in the top 16 genes numerous times (Aerts et al., 2006).

Traditional methods of gene discovery (e.g. linkage mapping) and HZM for rare recessive conditions are limited due to a number of factors. Firstly, only a small number of cases and families may be available for the study, particularly for IGD cases where fitness is reduced, and secondly, the disease may be oligogenic, with mutations in two or three different genes, such as in the case of IGD (Bamshad et al., 2011). However, NGS technologies overcome these issues by providing high-throughput sequencing methods for gene identification. As most disease-causing variants are harboured by protein coding regions of a gene, altering the protein product and functionality, focusing on these regions is an efficient gene discovery strategy. Whole exome sequencing (WES), a technique which focuses on sequencing all exons, the protein coding regions of the genome, is thus preferred to whole-genome sequencing, that in turn is aimed in obtaining the sequence of both introns and exons. This allows the identification of thousands of known and novel variants at a relatively affordable cost in comparison to whole genome sequencing, without any compromise in the high coverage of sequence depth. So far, WES has led to the identification of genes underlying numerous monogenic Mendelian disorders and it has been also applied in the discovery of novel mutated genes underlying IGD (Cariboni et al., 2015; Miraoui et al., 2013; Salian-Mehta et al., 2014; Xu et al., 2017). Typically, a filtering strategy is applied to narrow down the list of thousands of variants obtained: first variants in non-coding regions are filtered out, leaving only exonic and splice site variants; then, variants are further filtered according to the ones which affect the protein sequence, i.e. missense and nonsense mutations; finally, from the remaining list, variants which are recognized in any of the single nucleotide polymorphism (SNP) databases, such as dbSNP are filtered out, leaving a list of novel variants.

4.2 In silico tools

4.2.1 Single nucleotide polymorphism effect predicting tools

SNPs are used as markers in linkage and association studies to detect which regions in the human genome may be involved in disease. SNPs in coding and regulatory regions may be implicated in disease themselves; in particular non-synonymous SNPs lead to an amino acid change in the protein product and amino acid substitutions currently account for approximately half of the known gene lesions responsible for human inherited disease. Genome sequencing has brought significant advances in medical sciences since it allows the identification of thousands of SNPs. However, after genomes are sequenced, potentially tens of thousands of missense variations per breed or strain can be identified. Thus, a tool to assist with the prioritization of functional variants is desirable. In general, regions that are evolutionarily conserved tend to be less tolerant toward mutations, and hence amino acid substitutions/insertions/deletions in these regions are more likely to influence protein function.

Several free web tools are available in order to predict the impact of amino acidic or DNA mutations on phenotype including SIFT (Ng and Henikoff, 2003), Mutation Taster (Schwarz et al., 2014), PolyPhen (Adzhubei et al., 2010). In general, algorithms underlying these applications are based on protein sequence homology taking advantage from PSI-BLAST (Position-Specific Iterative Basic Local Alignment Search) alignment tools, that allow to calculate the conservation degree of the amino acid, and on SNPs databases such as 1000 Genomes Project, ClinVar and Whole Human Exome Sequence Space (WHESS), that contain all known disease causing polymorphisms. The output is often divided in four discrete categories: 1) disease causing, probably deleterious; 2) disease causing automatic, known to be deleterious; 3) polymorphism, probably harmless; 4) polymorphism automatic, known to be harmless. These kind of prediction tools have been successfully applied in order to identify causative mutation in IGD and IGD-related disorders, such as self-limited DP (Cariboni et al., 2015; Miraoui et al., 2013; Salian-Mehta et al., 2014; Xu et al., 2017).

4.2.2 Homology modelling

Homology modelling is a tool based on the fact that homologous proteins have similar structure. Proteins evolution tends to conserve structure rather than sequence because change in structure also alters protein function. This tool permits to create a model of a protein, with known sequence but unknown structure, using a homologous protein with a known structure as a template. In order to obtain 3D structures of proteins affected by mutations in patients, a comparative modelling approach can be carried out. The technique viability may depend upon the correlation between the identity sequences percentage and the structures similarity, measured as root mean square deviation between the superposed template and model. Homology modelling requires: i) search and select the template structure on BlastP, scoring the RCSB Protein Data Bank (PDB) database, through a single-sequence search; the selection depends on several factors, such as the presence of the template in PDB, the identity percentage between the target protein and the template, crystallographic condition and quality, resolution and presence or absence of ligand. Looking for homologue templates in the RCSB PDB can be done both through a database search with single sequence and through hidden Markov model; ii) align the target and the template sequence. In this way, the target amino acids are coupled to spatial position on template residues. Difference in identity of 30-40% between two sequences raises the indel, hindering alignment. In this case, multiple alignments of homologous sequences can help to lower the indel and collocate accurately the target residues on the template; iii) create a model, transferring the structural information and spatial coordinates from the template to the model. The importance of homology model prediction is gradually growing as the quantity of distinctive structural folds that proteins assumed are limited due to less number of experimentally determined structures. *In silico* protein modelling is helpful in predicting and generating 3D model

not only of monomers, but also it can be used to model homodimers, heterodimers, multimers and ligand-receptor complexes, whether the complex crystallized exists. Moreover, having a 3D model of the unknown structure of the protein is the first step necessary to compute protein design experiments in order to generate mutants (Khan et al., 2016). A good starting alignment is mandatory for good modelling results and it could be carried out through an accurate family multiple alignment. Moreover, model quality has to be checked by evaluating stereochemical and energetic parameters, e.g. Ramachandran plot. In addition to comparative analysis between wild-type and mutated proteins, 3D protein models obtained homology modelling can serve as a starting point for further analysis, such as protein::protein docking analysis and molecular dynamics, such as solvation and patch analysis.

Semaphorins and plexins have been extensively characterized from a structural point of view, especially by X-ray crystallography, therefore several 3D models are already available in online databases (e.g. PDB Protein Data Bank). Additionally, models of homodimers, heterodimers, multimers and ligand-receptor complexes, such as the trimeric complex semaphorin-neuropilin-plexin have been determined. Overall, homology modelling can thus be a reliable tool to determine unknown structures of other members of semaphorin and plexin families and this technique may be also applied to model mutant proteins and to study their interactions within protein complexes. Homology modelling has been successfully applied in the discovery of novel genes underlying IGD, in particular in generating mutant proteins that allow to predict the biological effect of mutations (Cariboni et al., 2015; Marcos et al., 2017).

4.3 In vitro and ex vivo tools

4.3.1 Cell cultures

GN11 (Radovick et al., 1991) e GT1-7 (Mellon et al., 1990) cell lines represent well-established and most used models to study GnRH neurons physiology *in vitro*. GT1-7 and GN11 cell lines were obtained by dispersion of brain tumors developed in transgenic mice expressing an hybrid gene; this was formed by the coding region of the SV40 large T-antigen oncogene fused with a portion of the promoter region of rat (for GT1-7 cells) and human (for GN11 cells) GNRH1 gene. Although they are immortalized cell lines, they retain many of the phenotypic characteristics of GnRH neurons. Specifically, GT1-7 cells derive from a hypothalamic tumor and therefore they derive from GnRH post-migratory neurons that have already reach their final destination; on the contrary, GN11 cells were obtained from a mouse having a tumor in the olfactory bulb, i.e. they originate from immature GnRH neurons blocked at an early stage of their migration. The different origin of these cell lines leads to diverse functional and morphological features between GN11 and GT1-7 cells. GT1–7 cells

appear as neuronal-like polygonal cells, with small soma, which are interconnected through neuritic processes. They grow mainly in colonies, which establish connections during the time of culture. In contrast, GN11 cells show a homogeneous growth on the whole surface of the culture dishes without forming clusters; they appear bigger than the GT1–7 cells and show generally a bipolar morphology with a distinctive leading process, peculiar of immature migrating neurons. Furthermore, GN11 cells, representing immature migratory GnRH neurons, retain migratory behaviour as shown by several assays, whereas GT1-7 cells do not show any motility (Maggi et al., 2000) (Figure 9). On the contrary, GT1-7 cells, that represents mature hypothalamic neurons, have an intrinsic pulsatile secretory activity of GnRH and therefore are well-established models to study the regulation of GnRH secretion (Wetsel et al., 1992). An immortalized cell line of human GnRH neurons has also been established (FNC-B4, (Vannelli et al., 1995)) but its use is limited as it represents a mixed cell line also containing immature olfactory neurons.

Both GN11 and GT1-7 cells have been extensively used to unravel the role of several molecules implicated in GnRH neurons development. In particular, GN11 cells have been applied in studying the effect of several guidance cues, including semaphorins, on GnRH neurons migration. To test chemoattractant or chemorepulsive potential of these cues, Boyden's chamber assay is the most used assay: it consists in a multi-well composed by two chambers separated by a porous membrane that allows the migration of cells from the upper chamber towards the lower chamber, where media enriched by chemotactic cues is placed (Cariboni et al., 2007b; Cariboni et al., 2011a; Giacobini et al., 2008). In turn, GT1-7 cells have been recently used as an *in vitro* model to test the anti-apoptotic potential of Sema3e on post-migratory GnRH neurons (Cariboni et al., 2015). In addition, molecules regulating GnRH secretion, such as kisspeptin or neurokinin, have been deeply studied in GT1-7 cells (reviewed in (Kanasaki et al., 2017)).

4.3.2 Ex vivo tools

Due to difficulties in accessing the nasal region of embryos *in utero*, a nasal explant system was generated as a model to study migration of GnRH neurons (Fueshko et al., 1998b) and this model has been successfully used to study early development and physiology of the GnRH neuron system and olfactory system. When generated at E11.5 from thin slice of embryonic nose, nasal explant cultures can maintain OSN, OECs and large numbers of GnRH neurons. Depending on the age of the starting material, it is possible to examine cell interactions important for placode formation or neuronal migration and axonal outgrowth (Klenke and Taylor-Burds, 2012). For instance, nasal explants have

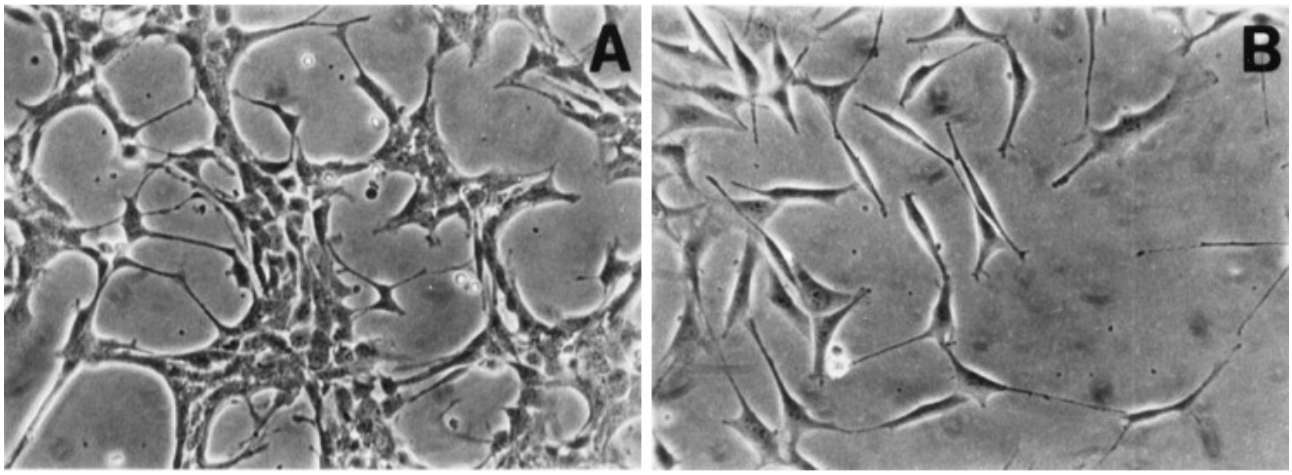

Figure 9 - Phase-contrast photomicrographs of immortalized cell lines of GnRH neurons. (A) GT1–7 and (B) GN11 cells cultured on plastic dishes (20X objective).

Adapted from "Immortalized luteinizing hormone-releasing hormone neurons show a different migratory activity in vitro" by R. Maggi, F. Pimpinelli, L. Molteni et al., 2000, *Endocrinology*, 141(6):2105-2112. Copyright 2000 by The Endocrine Society.

been successfully applied to study the effect on Cxcl12 and GABA on GnRH neuron migration speed rate (Casoni et al., 2012) and OEC role in GnRH neuron physiology (Geller et al., 2013).

Organotypic slices of embryonic heads were developed in 1996 and provided an alternative model to study GnRH migration as GnRH neurons normally developed in cultured slices compared to *in vivo* models (Tobet et al., 1996). This technique consists in culturing 200-300 μm thick slices to monitor GnRH neuron migration in conditions that well mimic the whole embryo; hence, slices can be co-cultured for example with COS-7 cell aggregates expressing exogenous molecules in order to perturb GnRH neuron migration. Hgf role on GnRH neuron migration has been indeed determined by applying aggregates of Hgf-expressing COS-7 cells close to head slices (Giacobini et al., 2007)

Finally, primary GnRH neurons can be easily obtained from transgenic mice (Spergel et al., 1999; Suter et al., 2000) and rats (Kato et al., 2003) in which GnRH neurons have been tagged with green fluorescent protein (GFP), that allows the sorting of GFP-positive GnRH neurons from all the other GFP-negative cells. Primary GnRH neurons constitute an important tool as it is possible to delineate a transcriptomic profile of GnRH neurons along with development (Cariboni et al., 2007b; Xu et al., 2017). Furthermore, isolating single GnRH neuron makes them accessible for electrophysiological recordings (Kato et al., 2003).

4.4 In vivo tools

4.4.1 Mus musculus

In 1986 Mason and colleagues, generated a transgenic mouse with a truncating deletion in *Gnrh1* gene (*hpg* mouse), providing the first example of murine model of hereditary hypogonadism (Mason et al., 1986). Most of subsequent studies on GnRH neurons have used mice as *in vivo* experimental models, both to study the physiological mechanisms underlying GnRH neuron development as well as models to study the role of candidate genes implicated in IGD. For example, mice carrying GFP-tagged GnRH neuron have been obtained allowing an easy visualization and isolation of GnRH neurons (Spergel et al., 1999; Suter et al., 2000), that allowed to study the expression of genes in single cells (Cariboni et al., 2007b). Few years later GnRH-Cre mice, which have *Gnrh1* promoter controlling Cre recombinase, have also been generated (Spergel et al., 2001), allowing the study of factors that intrinsically regulate GnRH neuron development and overcoming the lethality of some mutant mice.

However, GnRH neurons development mostly depends on proteins that exert their role in a paracrine manner rather than autocrine molecules, thus several transgenic mouse models with loss-of-function mutations or gene deletions have been generated in last decades. In particular the role of factors involved in GnRH neuron development, including semaphorins and plexins, has been

unravelled by taking advantage from specific knockout mouse lines carrying deletion or missense mutations in crucial receptor domains (Cariboni et al., 2011a; Cariboni et al., 2011b; Cariboni et al., 2015; Giacobini et al., 2008; Marcos et al., 2017). Overall, knockout mice have been previously used to predict possible IGD candidate genes to be screened in patients and after the introduction of exome sequencing technologies to validate human mutations. Despite few exceptions (e.g. Anos1, see next paragraph), most of the genes underlying IGD are highly conserved across species with particular regard to humans and mice and moreover mouse models usually recapitulate in a reliable manner phenotypic features observed in patients.

Additionally, fate mapping experiments in transgenic mouse models have revealed particularly useful to determine GnRH neuron embryonic origin. Indeed, the generation of neural crest specific (Wnt1) and ectoderm specific (Crect) GnRH neuron mouse lines have allowed for example to identify the origin of GnRH neurons (Forni and Wray, 2015; Forni et al., 2011).

4.4.2 Danio rerio

Zebrafish (*D. rerio*) is a fresh water fish, member of Cyprinidae family. Similarly to recent teleost fishes, it has two paralogue GnRH genes, namely *gnrh3* and *gnrh2*, with the former that represents the hypophysiotropic GnRH, whereas the latter seems to act as midbrain neuromodulator. The zebrafish HPG axis is similar to mammal one, although some differences exist; for example the hypophyseal portal blood system is not present in zebrafish and therefore anterior pituitary cells, such as gonadotrope cells, are directly innervated by hypothalamic neurons (Abraham et al., 2009).

Zebrafish embryos are large in numbers, they are accessible, since egg fertilization is external, and they are transparent; particularly, embryo transparency makes zebrafish a good model to create reporter fish to study *in vivo* gene function and expression pattern. In 2007, Palevitch and co-workers generated a transgenic zebrafish line in which GFP was under the control of *gnrh3* promoter (Tg(*gnrh3*::GFP) line). Hence, they were able to demonstrate that in zebrafish GnRH neurons arise in the nasal placode as well and then migrate caudally along OLF/TN nerves in order to reach the pituitary. First *gnrh3* expression occurs at 24 hpf (hours post-fertilization) in the nasal placode, whereas first projections towards the hypothalamus appear at 36 hpf; first GnRH neuron soma reach the hypothalamus around 12 dpf (days post fertilization) and the migratory processes end by 24 dpf (Palevitch et al., 2007) (Figure 10).

Most factors regulating GnRH neuron physiology and development are conserved in zebrafish and several studies have been performed by applying both forward and reverse genetics. In particular, reverse genetics in zebrafish can be pursued in two different modes: morpholino knock down and CRISPR-Cas9 knock out. Morpholinos are antisense oligonucleotides that knock down gene function

by binding and inactivating specific mRNA. They have been extensively applied to study GnRH neuron development, particularly in Tg(*gnrh3*::GFP) line since it allows a quick and easy evaluation of gene knock down effects. For example, Anos1 role in GnRH system development was first described in zebrafish, as mice lack *Anos1* ortholog gene (Ardouin et al., 2000; Yanicostas et al., 2009).

Then, morpholino oligos have been used to study other genes such as *nelf* and *dlx5* (Garaffo et al., 2015; Palevitch et al., 2009) and to study the confirm the effect of mutations found in human affected by IGD or related disorders, such as mutations in *IGSF10* found in self-limited DP patients (Howard et al., 2016). However, morpholinos display several disadvantages, such as high toxicity and off-target effects, therefore morpholino gene knock-down is not sufficient by itself (Stainier et al., 2017). To overcome these limitations, CRISPR-Cas9 genome editing technique can be applied to obtain knock-out and knock-in transgenic lines. Yet, recent gene knock-out studies provide evidences about the controversial role of gnrh3 and kiss/kissr in controlling zebrafish reproduction. *gnrh3*$^{-/-}$ zebrafish are fertile, displaying normal gametogenesis and reproductive performance in males and females (Spicer et al., 2016). Knock out zebrafish for either kiss1/kiss2 or kissr1/kissr2 display normal spermatogenesis and folliculogenesis as well as reproductive capability (Tang et al., 2015). Taken together, these results suggest that kiss/kissr signalling is not absolutely required for zebrafish reproduction and that fish and mammals have evolved different strategies for neuroendocrine control of reproduction; furthermore these results indicate that a compensatory mechanism should be activated to overcome gnrh3 deficiency in zebrafish. In conclusion, zebrafish lines are powerful models to study GnRH neuron development but several limitations may impact their usage.

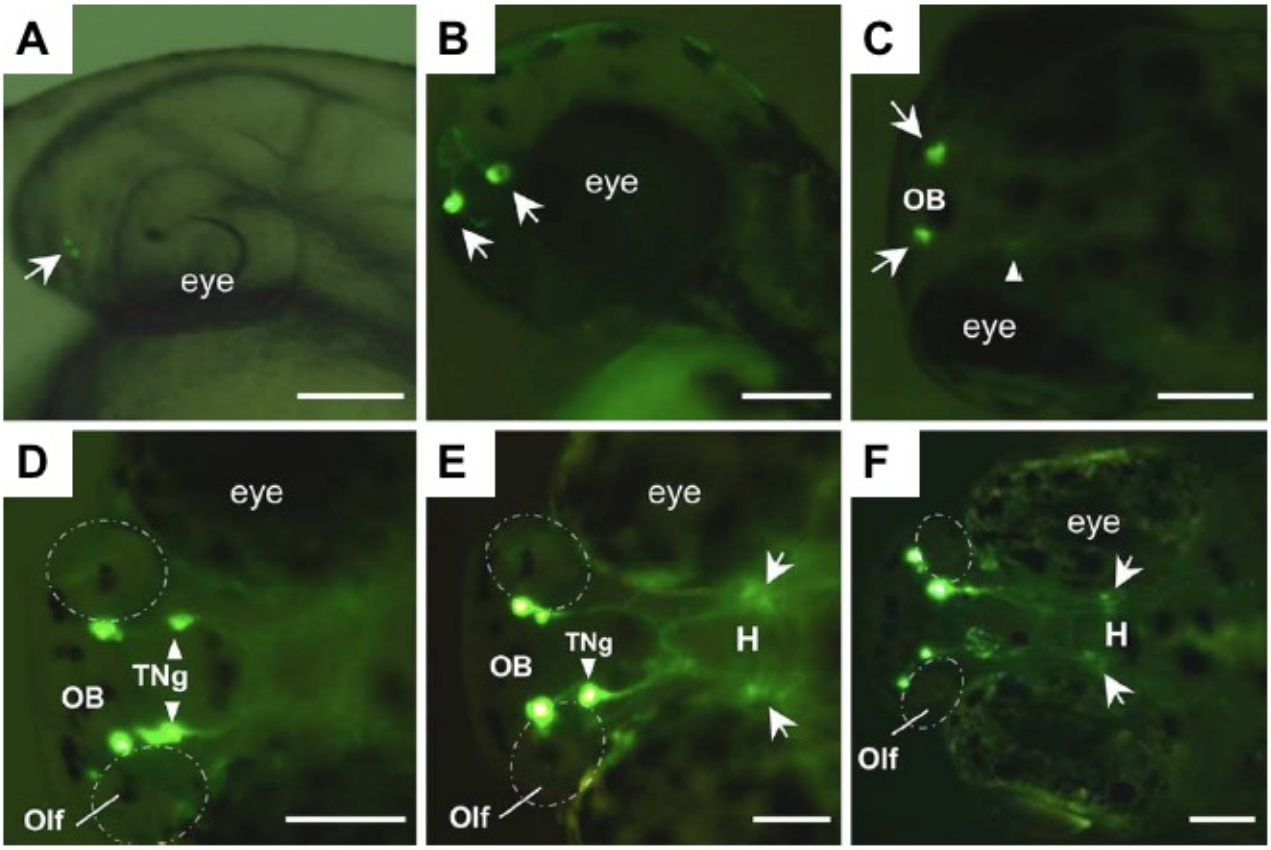

Figure 10 – GnRH3 neuron development observed in a live Tg(*gnrh3*:EGFP) zebrafish larva. (A-B) Lateral and (C-F) dorsal views of the migration path of EGFP-expressing cells. **(A)** EGFP expression is firstly seen at 24 hpf close to the developing Olf (arrow). **(B-C)** After hatching at 2 dpf and 3 dpf neurons expressing EGFP (arrows) start sending projections caudally toward the developing brain and a few positive cells can be found within the telencephalon at 3 dpf (arrowhead). **(D)** By 6 dpf, clusters of cells migrate backward to the presumptive TNg (arrowheads) and additional cells are seen in the telencephalon in association with the projection pathway. **(E)** At 10 dpf initial EGFP-positive cells is detected in the presumptive hypothalamus (H, arrows). **(F)** The entire migration path of the EGFP-expressing cells from the Olf through the TNg to the hypothalamus is seen at 15 dpf. Abbreviations: OB, olfactory bulb; TNg, terminal nerve ganglion; Olf, olfactory organ; H, hypothalamus. Bars 100 μm

Adapted from "Ontogeny of the GnRH systems in zebrafish brain: in situ hybridization and promoter-reporter expression analyses in intact animals" by O. Palevitch, K. Kight, E. Abraham et al., 2007, Cell Tissue Research, 327:313-322. Copyright 2006 by Springer-Verlag.

5. Semaphorin-Plexin signalling

The semaphorin superfamily contains three protein families: semaphorins, their receptor plexins and the MET tyrosine kinase receptor. They are all characterized by a common and evolutionary conserved sequence of about 500 amino acids that folds in an N-terminal extracellular domain called SEMA-domain. The molecular phylogeny of the semaphorin superfamily was identified using the SEMA-domain sequences of 77 semaphorins and plexins, and 12 sequences of MET. It appears striking that all semaphorin sequences, except *C. elegans* sema7a, cluster in the subfamilies defined by their overall domain organization suggesting that the semaphorin family underwent an early expansion and divergence in vertebrates.

5.1 The semaphorin family

Semaphorins constitute one of the largest families of guidance cues, highly conserved across species, including *C. elegans*, *D. melanogaster*, *D. rerio*, rodents, primates and humans. Semaphorins were first discovered as growth cone collapsing factors and therefore as repulsive neuronal guidance cues, but they are broadly expressed both inside and outside the CNS. Vertebrate semaphorins are expressed in most tissues and their expression varies considerably with developmental stage and physiological conditions. The expression patterns of semaphorins has been best characterized in the nervous system, particularly during development, where most, or perhaps all, semaphorins are expressed by both neuronal and non-neuronal cells. Semaphorins are also widely expressed in many other organs, including the cardiovascular, endocrine, gastrointestinal, hepatic, immune, musculoskeletal, renal, reproductive, and respiratory systems. Each of the different classes of semaphorins are not defined by a specific patter of expression, instead many semaphorins are dynamically expressed in specific areas during development, and this expression often decreases with maturity. Interestingly, changes in the adult expression levels of semaphorins have been described following injury in neuronal and non-neuronal tissues, during tumorigenesis, and in association with other pathological conditions (Yazdani and Terman, 2006).

To date, more than 20 semaphorins have been identified and grouped into 8 classes, based on their structural homology and phylogenetic relationship (Messina and Giacobini, 2013). Class 1 and Class 2 comprise invertebrates semaphorins, Class 3-7 semaphorins are in turn vertebrates semaphorins, whereas viral semaphorins are grouped in Class V) (Bamberg et al., 1999) (Figure 11).

5.1.1 Semaphorin structure

The eight main classes of semaphorins differ in sequences and overall structural features, but all members of the semaphorin family contain the characteristic SEMA domain that is essential for

semaphorin function. Close to the SEMA domain, they display a PSI (Plexin-Semaphorin-Integrin) domain, which is enriched in cysteine residues. Semaphorins can further contain other distinct domains such as immunoglobulin-like (Ig-like) domain, thrombospondin domain and basic C-terminal domain. Class 1 semaphorins are transmembrane proteins lacking the Ig-like domain and characterized by a short intracellular C-terminal domain; in contrast Class 2 semaphorins are secreted proteins and display all the three peculiar semaphorin domains, SEMA domain, PSI domain and Ig-like domain. Similarly, Class 3 semaphorins are secreted proteins and present a stretch of basic amino acids composing a basic domain at their C-terminal in addition to the three canonical domains. Class 4-5-6 semaphorins are transmembrane proteins while Class 7 semaphorin are membrane-anchored protein thanks to a C-terminal GPI (glycosylphosphatidylinositol) moiety; however, both Class 4 and Class 7 semaphorins can be secreted after enzymatic cleavage. Class 5 are characterized by seven type I thrombospondin repeats whereas Class 6 semaphorins lack Ig-like domain like Class 1 proteins and its C-terminal intracellular domains are longer in Class 6 compared to Class 1 semaphorins (Figure 12). All semaphorins exhibit redundant structural features such as a distinctive ~500 amino acids SEMA domain. The SEMA domain allows both the dimerization between two semaphorins, and the binding to receptors, two essential molecular events for semaphorin function. The 3D structure of semaphorins was first identified in 2003 for Sema3a and Sema4d (Antipenko et al., 2003; Love et al., 2003).

These findings confirmed that SEMA domain is characterized by a seven-blade β-propeller fold, a common structure for both extracellular and cytosolic proteins that comprise a folded topology. The β-propeller comprises a series of seven four-strand antiparallel β-sheets (also called blades) that are arrayed sequentially around a central axis creating a compact and robust structure. However, semaphorin β-propeller can be distinguished from other similar architecture thanks to a 70 amino acid insertion that is called “the extrusion” located between β-sheets C and D of the fifth blade (Siebold and Jones, 2013). The fold is stabilized by hydrophobic contacts amongst sheets and by a “loop and hook” or velcro-like closure system between the first and the last blade, in which the N-terminus of the outer sheet (D) of blade 7 contributes to the final C-terminal of blade 6. Furthermore, four disulfide bonds contribute to stabilize the structure (Gherardi et al., 2004). Interestingly, all the other members of semaphorin superfamily (i.e. plexins and Met receptors) also exhibit the same architecture for the β-propeller fold. The central cavity has a conical shape that allows to distinguish a top face at the N-terminus and a bottom face at the C-terminus. Subsequent to the SEMA domain C-terminus, the PSI domain can be clearly recognized. This domain is characterized by a high percentage of cysteine residues that resemble the β chain of integrins; cysteines create a central knot based on three highly conserved disulphide bonds.

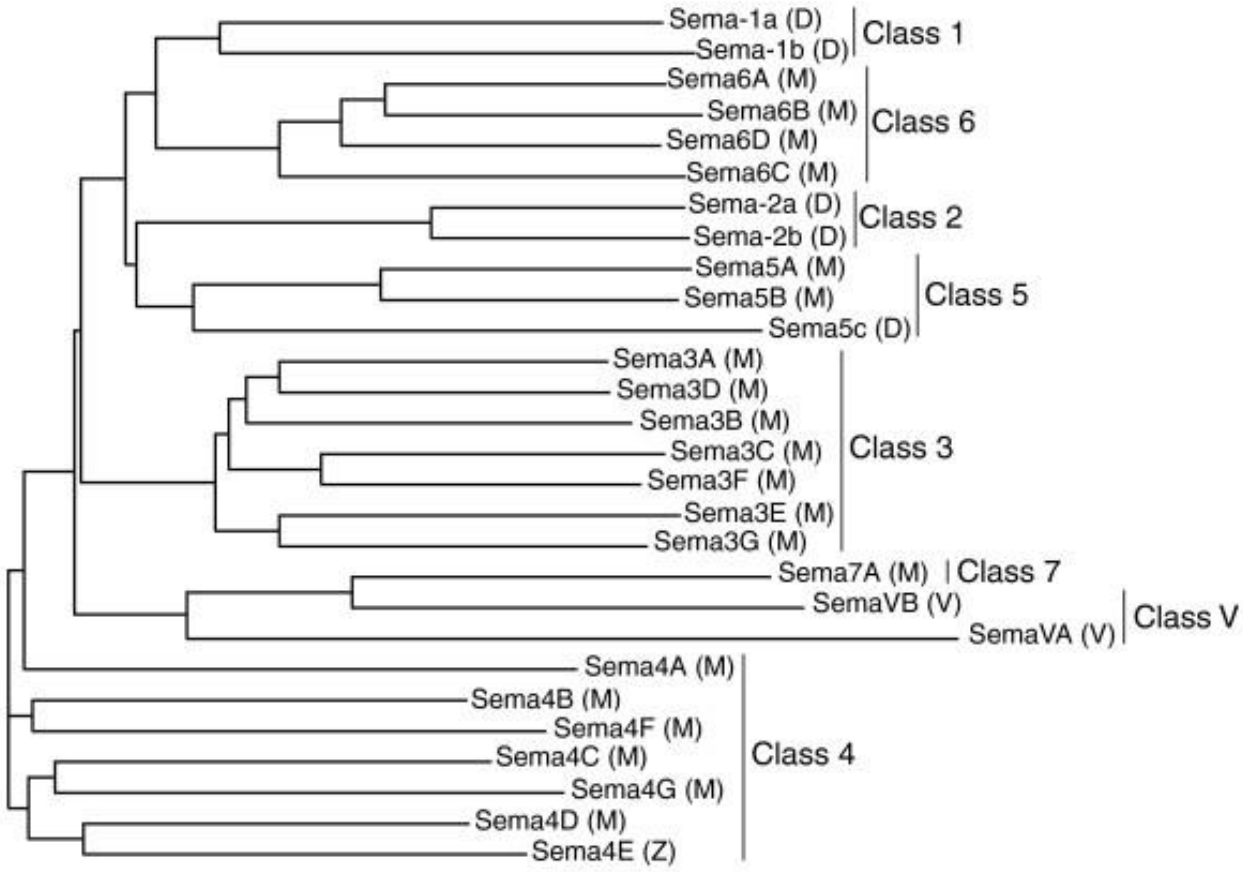

Figure 11 – Phylogenetic tree of semaphorin sequences. Protein sequences were aligned using ClustalW and the tree was generated using the neighbour-joining method. This tree shows groups of related semaphorins organized in clusters that correspond to different classes. Semaphorins are divided into eight classes: Class 1 and 2 semaphorins are found in invertebrates, Class 3–7 semaphorins are found in vertebrates whilst Class V is typical of viruses. Abbreviations: D, Drosophila; M, mouse; V, viral; Z, sequence identified only in zebrafish and not in mammals.

Adapted from "The semaphorins" by U. Yazdani & J.R. Terman, 2016, *Genome Biology*, 7(3):211. Copyright 2006 by BioMed Central Ltd.

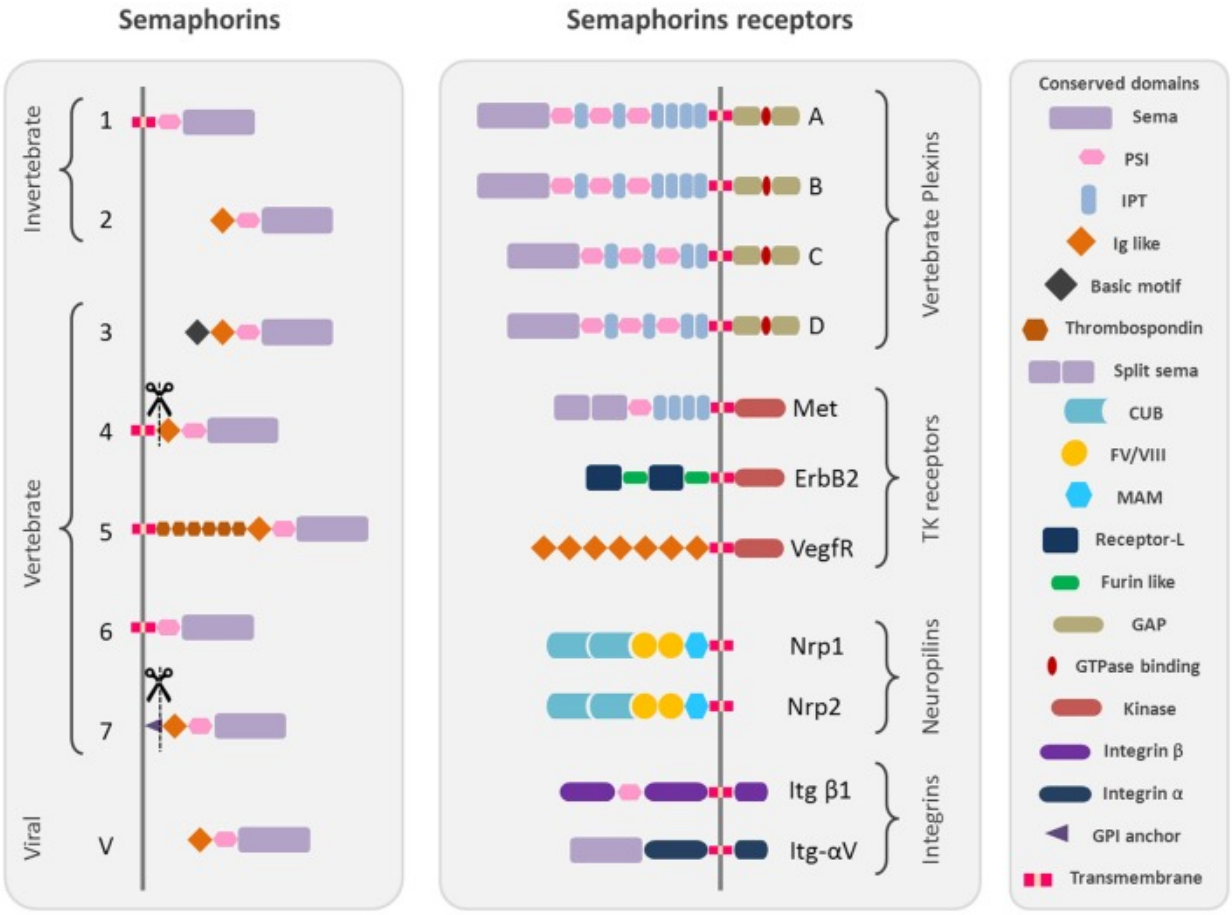

Figure 12 – Schematic representation of the protein structure of semaphorins and their receptors. Semaphorins and plexins are characterized by SEMA domains. Additional domains present in semaphorins and plexins include PSI domains (plexin, semaphorin, and integrin) and immunoglobulin (Ig)-like domains. The structural conserved domains are drawn in different shapes and colours as indicated in the figure. Abbreviations: PSI, plexin semaphorin integrin; IPT, Ig-like Plexin Transcription factors; Ig-like, immunoglobulin like; CUB, complement C1r/C1s, Uegf, Bmp1; FV/VIII, coagulation factor V/VIII homology like; MAM, meprin like; GPI, glycosylphosphatidylinositol.

Adapted from "Semaphorin signalling in the development and function of the gonadotropin hormone-releasing hormone system" by A. Messina & P. Giacobini, 2013, *Frontiers in Endocrinology*, 4:133. Copyright 2013 by Messina and Giacobini.

Semaphorins can undergo post-translational modifications such as N- glycosylation at specific consensus sites; however, little is known about the biological significance of these post-translational modifications. Moreover, several secreted and transmembrane semaphorins can be proteolytically cleaved by furin (Proprotein convertase subtilisin/kexin type 3, PCSK3). For example, SEMA3A display three highly basic regions that constitute consensus sites for furin-dependent proteolytic processing: amino acids 551-555 within the C-terminus of SEMA domain (RRTR**R**), amino acids 731-735 (RKQR**R**) at the N-terminus of the basic domain, amino acid 758-761 (RNR**R**) at the C-terminus of the basic tail (Adams et al., 1997). These furin consensus sites are highly conserved among Sema3s and across species and it has been shown that furin-mediated cleavage is modulating the effects of Class 3 semaphorins in axon guidance, growth-cone collapse, cell migration, invasiveness and growth. Sema3s are indeed synthesized as precursors and, after signal peptide removal, secreted as full-length 95 kDa proteins, that display a repulsive biological activity on axons. Further, the cleavages operated by furin generate a smaller isoform of 65 kDa that is less active compared to full-length one.

Another important feature for functional semaphorins is homodimerization. This is a distinctive characteristic of the semaphorin SEMA-domain, not shared by other members of the superfamily, i.e. plexins and Met receptors. Semaphorins present several conserved cysteine residues in both the SEMA domain and the C-terminal domain which establish intermolecular disulfide bridges that allow dimerization; in particular, SEMA3A cysteine at position 723, located between the Ig-like domain and the basic tail, is essential for dimerization and the only SEMA domain is not sufficient to promote semaphorin pairing. To date, all available crystal structures of semaphorins have revealed the same homodimeric architecture. Interestingly, the furin proteolytic removal of C-terminus that generates the 65kDa SEMA3A isoform strongly affects the dimer formation and, consequently, down regulate the biological effect of SEMA3A (Koppel and Raper, 1998). Transmembrane semaphorins are also able to form homodimers thanks to a highly hydrophobic surface within the SEMA domain. Structure analysis reveals that hydrophobic residues responsible for the dimerization of SEMA4D (Phe223, Val224 and Phe225) are not conserved in Class 3 semaphorins (Janssen et al., 2010). Yet, it seems that transmembrane semaphorin dimerization is required only for receptor signal triggering but not for receptor binding.

5.2 Semaphorin receptors: Plexins

The major signal transducing receptors are the plexins, a large family of type I single, transmembrane-spanning cell surface receptors. To date, nine different plexins have been identified and have been divided into four families, according to structure similarity: Plexin A1-4 (PLXNA1-4), Plexin B1-3

(PLXNB1-3), Plexin C1 (PLXNC1), PlexinD1 (PLXND1) (Tamagnone et al., 1999). Like semaphorins, plexins share a common basal architecture that consists in a N-terminal ectodomain containing the SEMA domain and a variable number of PSI and IPT (Ig-like fold shared by plexins and transcription factors) domains, a single transmembrane region that should be an α-helix and a C-terminal intracellular region composed by a Rho GTPase binding domain (RBD) flanked by two GAP (GTPase activating protein) domains (Figure 10). Class B plexins peculiarly possess an additional PDZ (PSD-95/Dlg/ZO-1) domain that constitute a binding site for GEF (GTPase exchange factor) (Swiercz et al., 2002). PLXNB1 and B2 only present a cleavage site for furin in the ectodomain that allows the generation of heterodimer PLXNB1/PLXNB2 receptor complexes (Capparuccia and Tamagnone, 2009). Plexin SEMA domain shares the same structural features of semaphorin one, with the same seven-bladed β-propeller fold including the 70 amino acids extrusion; however, differently from its counterpart, plexin SEMA domain displays no or little propensity to dimerize. The first PSI domain, close to the SEMA domain, is similar to the semaphorin one, with a cysteine knot topology, whereas the IPT domain is highly enriched in glycine and proline. The large cytoplasmic region is highly conserved through species and amongst plexins; it consists in a R-Ras and M-Ras GAP domain, that is divided into two segments by a RBD.

Plexins bind to semaphorin dimers in a head-to-head interaction at SEMA domain level through the β-propeller fold. After the coupling between ligand and receptor, intracellular plexin domains dimerize to activate downstream effectors. PLXNAs usually serve as receptors for Class 3 and Class 6 semaphorins, whereas Class 4 and Class 5 semaphorins preferentially binds to PLXNBs and SEMA7s to PLXNC1; PLXND1 in turn binds to some SEMA3s independently from neuropilins (Kruger et al., 2005). Yet, plexins and semaphorins show a high degree of redundancy, thus a single semaphorin can bind to and signal through different plexins according to the tissue and the action that is needed.

Since plexins are the main receptors for semaphorins, primarily recognized as axon guidance cues, the role of plexins was first acknowledged in the CNS. However, plexins are not expressed only by neurons but are widely expressed in many other organs, especially during embryogenesis. Plexins play a pivotal role in cardiovascular system, skeletal and renal development but also in immune system physiology and cancer progression, mediating a variety of signals to guide cell migration and adhesion (Perälä et al., 2012).

5.*3 Semaphorin receptors: Neuropilins*

NRP1 and NRP2 are essential type I transmembrane receptor that serve as co-receptor for Class 3 semaphorins in concert with A-type Plexins, with the exception for SEMA3E, that directly binds to

PLXND1. Neuropilins are highly conserved through vertebrates, displaying 40% of identical amino acids. Structurally, both NRP1 and NRP2 exhibit an extracellular region, comprising five well-characterized domains, a transmembrane helix and a short intracellular region composed of a PDZ domain. The extracellular N-terminal region possesses two calcium-binding C1r/C1s/Uegf/Bmp1 (CUB) domains (also termed a1 and a2), two coagulation factor V/VIII-like discoidin domains (b1 and b2) and a Meprin/A5-antigen/ptp-Mu (MAM) domain (briethly c) (Figure 10). Extracellular domains are necessary and sufficient for ligand binding. In particular, the a1 domain has been shown to interact with the SEMA domain of Class 3 semaphorins ligands, whereas the b1 domain contains a specific arginine binding pocket that is essential for the binding to both VEGF and Sema3s ligands. Additionally, b1 and b2 domains together form an extended stretch of positively charged basic residues that is able to bind heparin, a highly sulphated member of the glycosaminoglycan (GAG). The c domain is dispensable for ligand binding but essential for ligand-dependent signalling. The transmembrane helix possesses a conserved GXXXG repeat that confers a high dimerization potential. The intracellular PDZ domain can interact with PDZ domains of several cytoplasmic and transmembrane protein, conferring to neuropilins the ability to transduce intracellularly some signals (Parker et al., 2012). NRPs can be also alternatively spliced with the insertion of an intron that introduce a premature stop codon between c and b2 domains, resulting in the production of a secreted protein that prevents ligand binding. *N*- and *O*-glycosylations and heparan-sulphate coupling can enhance binding capacity of neuropilins.

SEMA3 ligands first bind to neuropilins and then required PLXNAs to transduce downstream signals. NRPs bind to semaphorins in a region that is close to dimerization site within the SEMA domain and that is peculiar for class 3 semaphorins. In 2012 Janssen and co-workers determined the 3D structure of the ternary complex Sema3a::Nrp1::Plxna2 that was postulated ten years before by Antipenko and colleagues. In this structure, semaphorin and plexin contact each other via their SEMA domains, while the a1 domain of neuropilin cross-braces the whole complex (Antipenko et al., 2003; Janssen et al., 2010). Other ligands include members of VEGF, some FGFs, PDGF, TGF-β1 and HGF by coupling with VEGFR, FGFRs, PDGFR, TβRs and c-Met. In particular, the interaction with VEGF/VEGFR critically controls angiogenesis and neuron migration. NRPs, similarly to PLXNs, are broadly expressed in various tissues and organs both during embryogenesis and adult life, participating in multiple cellular signalling cascades and thus having pleiotropic function in vertebrate homeostasis, both in physiological and pathological processes. However, they were first identified and functionally characterized as receptors for SEMA3s in axon guidance during embryonic life for the correct patterning of dorsal root ganglia, cranial nerves, sensory systems including the olfactory one, cortical and hippocampal nerves and GnRH neurons (Guo and Vander Kooi, 2015).

5.4 Semaphorin signalling pathways

Semaphorins preferentially signal through plexins: Class 1, 4, 6, 7 and viral semaphorins can directly bind plexins through head-to-head interactions involving their SEMA domains; in turn, secreted semaphorins, such as Class 2 and 3 semaphorins, need the recruitment of an obligate co-receptor, NRP1 and NRP2. All semaphorins exert their function in a homodimeric form, even if heterodimerization cannot be ruled out. Responsible for dimerization is the SEMA domain together with the Ig-like domain that confers stability to the complex. The SEMA domain is also responsible for the binding to the receptor; each subunit of the semaphorin dimer binds a monomeric receptor (Siebold and Jones, 2013). Semaphorin–plexin (-neuropilin) signalling mediates diverse functions by regulating small GTPase activities and cytoplasmic/receptor-type protein kinases, and regulates integrin-mediated attachment, actomyosin contraction, and microtubule destabilization (Takamatsu and Kumanogoh, 2012).

By contrast to other transmembrane proteins the intracellular domains of plexins interact directly with Rho and Ras family small GTPases. Like other GTPases, the Rho and Ras proteins are understood as on/off switches for signalling, depending on the nature of the nucleotide, GTP or GDP, that is bound. Active (i.e. GTP bound) GTPases associate with effector proteins, typically changing their conformation in order for the signal to be transduced. Alternatively, regulatory proteins bind to the GTPases and effect the rate of nucleotide hydrolysis and exchange such as GTPase-activating proteins (GAPs) and guanine exchange factors (GEFs). Rho family small GTPases (e.g., Rac1, Cdc42, RhoA) are actin cytoskeleton remodeller and thus intimately control motility and adhesion of cells. Rho GTPases directly interact with RBD region of plexins, but the effect of this coupling is not fully understood. Rho binding might result in a reduced GTPase activity with effects on downstream effectors such as kinases involved in cell motility and cytoskeleton remodelling; alternatively, binding of Rho to plexins may activate plexins GAP domains. Ras-family GTPases in turn regulate the transcription of certain genes, including genes for cell growth, and they also influence cell attachment via integrins. An involvement of Ras proteins in plexin signalling was initially inferred from the homology of plexin cytoplasmic regions to the GAP family of regulatory proteins. Later, GAP activity, aimed to silence Ras signalling, was demonstrated for members of all four human plexin families against R-Ras GTPase. GAP activity in both PLXNA1 and PLXNB1 with the subsequent downregulation of R-Ras inhibits PI3K (Phosphoinositide 3-kinase) and results in a dephosphorylation of AKT (that become less active) and GSK-3β (that becomes more active) in neuronal growth cone collapse. Moreover, decreased Ras activity leads to decrease integrin-mediated cell attachment. In addition to intrinsic GAP activity, plexins can recruit the p190 RhoGAP that participate in down-regulating Rho GTPases. PLXNBs have an additional PDZ domain that has been

demonstrated to interact with PDZ domain containing-RhoGEF, an exchange factor for Rho GTPases. Activating Rho GTPases should be important for plexin's to determine stress fibre formation and collapse. However the downstream signalling networks are not yet known in the case of plexins and similarly to other GAP proteins, plexins appear to be multifunctional and activities against different substrate Rho/Ras-family GTPases are likely to be controlled by different mechanisms and environments (Alto and Terman, 2017; Hota and Buck, 2012; Kruger et al., 2005; Swiercz et al., 2002). The outcomes of semaphorin-plexin (-neuropilin) signalling are cytoskeletal rearrangements involving both actin filaments and microtubules and integrin-mediated adhesion. Yet, the precise molecular mechanism by which plexins directly influence cytoskeleton are still poorly understood. Recently, researchers propose two mechanisms: i) the multidomain oxidoreductase enzyme Mical (Molecules Interacting with CasL), which interacts with plexins, is a F-actin disassembly factors that reduce actin polymerization by oxidizing an actin methionine residue critical for polymerization; ii) plexins induces actin depolymerization by regulating levels of active cofilin. Moreover, plexins can recruit CRMP (collapsin response mediator protein) preventing microtubules assembly and inhibit integrin-mediated adhesion by silencing Ras through their GAP domain (Hung and Terman, 2011). Semaphorin-mediated signalling also involves many intracellular proteins and second messengers, such as cytosolic tyrosine kinases including Fak, Fyn and Src that somehow initiate signalling cascades of PI3K/AKT and MAPK/ERK (Figure 13).

To make more complicate the semaphorin-plexin signalling pathways, other molecular mechanisms have been described. First, semaphorins can bind plexins in *cis* (on the same cells), altering the availability of both protein for *trans* signalling and therefore silencing intercellular signalling; this has been demonstrated in dorsal root ganglia, sympathetic axons and in the retina for Sema6a and plexin As. Second, transmembrane semaphorin can act as receptors triggering the so called "reverse signalling" as happen during ventricular trabeculation of chick heart in a process that involves Sema6d and neural circuit assembly in *D. melanogaster* involving Sema1a, that shows high homology to Sema6s (Jongbloets and Pasterkamp, 2014).

Finally, semaphorins can exert their function through other holoreceptor complexes associated to plexins. The ability of semaphorins to bind to different types of receptor makes possible a wide range of effects. Examples of non-canonical semaphorin receptors are cell adhesion molecules (e.g. Nr-CAM and L1-CAM) that associate to neuropilins to transduce Sema3 signals, several tyrosine kinase receptors, including VEGFR2 (vascular endothelial growth factor receptor 2), Met, ErbB2 and off-track (OTK) vascular endothelial growth factor receptors (Vegfr1-2), tyrosine kinase receptors (Met, ErbB2) and integrins (Itgβ1) that specifically bind to Class 7 semaphorins (Alto and Terman, 2017).

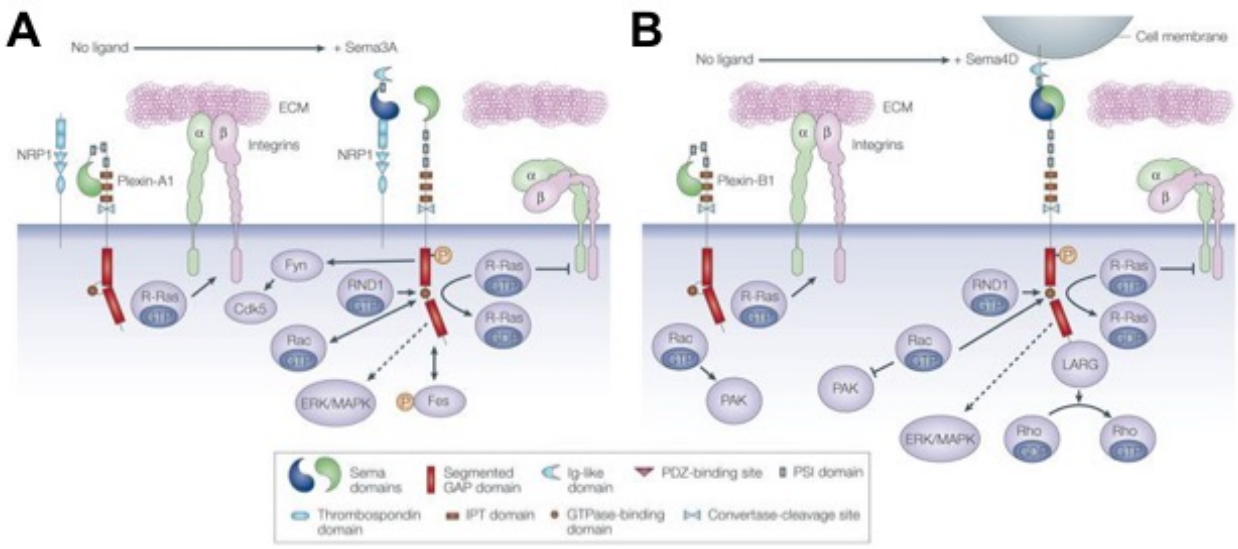

Figure 13 – Semaphorin-plexin complexes signalling pathways. Components of plexin downstream signalling are depicted for Plxna1 **(A) and Plxnb1 (B) as** representatives of the two main plexin subclasses. **(A)** Semaphorin binds to Nrp1 and initiates plexin signalling, causing the inactivation of R-Ras and resulting in the detachment of integrin from the extracellular matrix (ECM). The GAP activity of plexin requires RND1 and promotes the intrinsic GTPase activity of R-Ras. The increase in GDP-bound (inactive) R-Ras leads to a decrease in integrin-mediated attachment to the ECM. Fyn becomes activated and stimulates cyclin-dependent kinase-5 (CDK5). Plxna1 also mediates activation of extracellular signal-regulated kinase (ERK)/mitogen-activated protein kinase (MAPK). Signalling between Plxna1, Fes and Rac might be bidirectional. **(B)** Binding of Sema4d to Plxnb1 directly activates the receptor. Additionally, the GAP activity of Plxnb1 requires RND1 binding. The plexin GAP activity promotes R-Ras•GTP exchange to R-Ras•GDP. Without bound semaphorin, active Rac promotes the activation of p21-activated kinase (PAK). Binding of Sema4d also sequesters active Rac, suppressing PAK activity. Leukaemia-associated Rho-GEF (LARG) and PDZ-RhoGEF (PRG) activity (not shown) is stimulated on Sema4d binding, leading to an increase in Rho•GTP. ERK/ MAPK stimulation also results from the Sema4d–Plxnb1 interaction.

Adapted from “Semaphorins command cells to move” by R.P. Kruger, J. Aurandt and K. Guan, 2005, *Nature Reviews Molecular Cell Biology*, 6:789. Copyright 2005 by Nature Publishing Group.

5.5 Semaphorin-Plexin signalling: role in development and diseases

Semaphorin-plexin signalling is characterized by a high degree of promiscuity because some semaphorins bind to several different plexin families in a tissue-specific manner and the effect originated by this interaction can be positive or negative according to the environmental context or according to the type of co-receptor involved (e.g. neuropilins, tyrosine kinases, integrins). Therefore, making a complete overview of all the developmental and pathological processes regulated by a single semaphorin-plexin complex results highly complicated and further criteria, such as state of the tissue and subcellular localization, should be considered. In general, the biological outcomes of semaphorins-plexins signalling are mainly cell motility and adhesion, even if cell survival and proliferation have been also shown to be regulated by semaphorin-plexin signalling.

5.5.1 Nervous systems

Semaphorins-plexins mediated signalling is involved since early stages of nervous systems development, regulating migration and targeting of neuronal precursors. Then, semaphorins act as axon guidance cues and are therefore responsible for neuronal network formation but also for axonal branching, (de)fasciculation, and pruning back. Finally, they can regulate synaptogenesis and dendritic spine formation.

Class 3 and Class 6 semaphorins are the main regulators of nervous systems development by acting through A-type plexins (class 6, class 3) and neuropilins (class3). For example, the expression of Plxna4 on hippocampal mossy fibres prevents them from entering the Sema6a-expressing supra-pyramidal region of CA3 (*Cornus ammonis 3*) and restricts them to the most proximal part, where Sema6a repulsive activity is attenuated by Plxna2 (Suto et al., 2007). In turn, Sema3a/Plxna4/Nrp1 and Sema3f/Plxna3/Nrp2 complexes mediate bundling and projections of facial branchiomotor axons whereas facial visceromotor axons selectively required Sema3a/Plxna4/Nrp1 (Schwarz et al., 2008). Sema3a mediates growth cone collapse of many cell types through Plxna1 (Takahashi et al., 1999), while Plxna3 is involved in pruning hippocampal fibres (Bagri et al., 2003). Precise synaptic targeting is mediated by Sema6c and Sema6d coupled with Plxna1 in the dorsal horn of vertebrate spinal cord (Yoshida et al., 2006).

Plexin B family members as well play important roles in nervous system development. For instance Plxnb1 together with Sema4d functions in neurite outgrowth, axonal growth cone collapse and arborization of dendrites and axons (Vodrazka et al., 2009) Interestingly, Plxnb2 deletion alone is sufficient to perturb nervous system development in mice, whilst lack of either Plxnb1 or Plxnb3 do not reveal neuronal defects in mice, suggesting compensatory mechanisms among same class plexins (Deng et al., 2007). Plxnc1 role is recently emerging with particular focus in the hypothalamus

(Xu and Fan, 2007), whereas Plxnd1, mostly known for its role in cardiovascular development, has also functions in the central nervous system, with particular regard to sensory neuron and motorneuron connectivity, axonal attraction/repulsion and synapse formation by coupling with Sema3e (Bellon et al., 2010; Chauvet et al., 2007).

The involvement of semaphorin-plexin signalling in several developmental processes makes these molecules particularly implicated also in diseases of the nervous system, such as Parkinson Disease, Alzheimer Disease, schizophrenia, anxiety, autism and mental retardation. For instance, the presence of either a cleaved form of Sema3a or Plxna1 and Plxna2 complexes have been detected in Alzheimer patients and these proteins may be used as early marker for the disease. Instead, loss-of-function mutations in Plxna2 and in its ligands Sema3d and Sema6a have been associated to schizophrenia and anxiety in mice, whereas autism and mental retardation have been linked to B-type plexins and Nrp2. More severe and systematic syndromes, such as Cri du chat and CHARGE syndromes are related to alterations in Sema5a and Sema3e genes. Finally, brain malignancies progression (i.e. angiogenesis, cell survival and proliferation, invasiveness), including highly aggressive glioblastoma, is controlled by several semaphorins and plexins (Pasterkamp and Giger, 2009).

5.6 The role of semaphorins in GnRH neuron development

Several semaphorins result to be expressed along migratory route of GnRH neurons leading researchers to investigate their roles on motility, survival and axonal plasticity of GnRH neurons. To date, three semaphorins, SEMA3A, SEMA3E and SEMA7A, have been found mutated in IGD patients but others, such as SEMA3F and SEMA4D, have been associated to GnRH neuron development, although mutations have not been found yet.

5.6.1 SEMA3A and SEMA3F

Sema3a and Sema3f were first suggested to be involved in GnRH neuron migration by *in vitro* and *in vivo* studies that determined the role of Nrp2 in the same system. Specifically, *Nrp2* knock out mice display severe cVN nerve defasciculation and are subfertile due to a reduced number of hypothalamic GnRH neurons; moreover, both primary GnRH neurons and GN11 cells express Nrp1, Nrp2 and Plxna1 and therefore are able to respond to Sema3a and Sema3f repulsive activities (Cariboni et al., 2007b). Since the phenotype observed in *Nrp2*$^{-/-}$ mice was not so severe, suggesting a redundant role amongst semaphorins and neuropilins, and in order to unravel the exact mechanisms involving class 3 semaphorins and neuropilins in GnRH migration, Cariboni and co-workers have performed further studies using different genetic mouse models for class 3 semaphorins and neuropilins. Accordingly, the combined loss of both *Nrp1* and *Nrp2* lead to a more severe phenotype,

suggesting that Nrp1 can supply for Nrp2 loss. Interestingly, the aberrant phenotype displayed by *Nrp1*$^{sema/sema}$*/Nrp2*$^{-/-}$ -null mice is fully phenocopied by *Sema3a*-deficient mice but not by *Sema3f* knock out mice. Consistently, *Sema3a* knock out mice show several defects in the migration of GnRH neurons due to aberrant formation of cVN nerve projections with a nearly complete loss of neurons in the forebrain during embryonic development (Cariboni et al., 2011a) (Figure 14). Shortly after and in agreement with these findings, two independent groups described mutations in *SEMA3A* gene in KS patients (Hanchate et al., 2012; Young et al., 2012). Recently, analysis on cVN nerve has provided further insights into the essential role of Sema3a. Sema3a is highly expressed at NFJ level and on one side prevents OLF/VN nerves from invading the forebrain whereas on the other side attracts both GnRH neurons and the cVN/TN nerve (Taroc et al., 2017). The double role of Sema3a can be explained by the presence of different sets of receptors and co-receptors on each cell population: according to this working hypothesis, cVN/TN nerve, as well as GnRH neurons, which express high levels of Nrp1, are attracted by Sema3a, whereas OLF/VN, which express both Nrp1 and Nrp2, are repelled by Sema3a, preventing brain invasion. In addition to differential expression of Nrps, different combinations of Plexin As may contribute to the diverse response to Sema3a signalling; yet, the Plexin A that mediates Sema3a signal in GnRH neuron system is still unknown and one of the aims of this PhD thesis is to unravel the role of PlxnAs in GnRH and olfactory systems. Further studies demonstrated that Sema3a exerts a crucial role also in adulthood by remodelling GnRH fibres that project to the ME during the oestrus cycle. Specifically, brain endothelial cells released Sema3a that promotes GnRH neuron axonal sprouting through Nrp1 expressed by GnRH neuron axon terminals; in addition, the amount of released Sema3a increases dramatically during proestrus, when GnRH is released in massive surges to sustain LH surge (Giacobini et al., 2014).

5.6.2 SEMA3E

Sema3e is involved in many developmental dynamics, such as nervous and cardiovascular system formation, and it was demonstrated exerting its function through either Plxnd1 or Vegfr2. Hence, differently from all the other class 3 semaphorins, Sema3e binds to Plxnd1 directly and independently of neuropilins (Oh and Gu, 2013). In a recent work, it has been shown that both Plxnd1 and Sema3e are strongly expressed in the nasal compartment and in the MPOA. However, although Plxnd1 is dispensable for the correct vascular patterning and axonal pathfinding in the embryonic nose, it is essential to maintain GnRH neurons once within the MPOA. Indeed, GnRH neurons express high level of Plxnd1 after the NFJ in order to correctly respond to the pro-survival stimuli of Sema3e. This is confirmed by *in vitro* studies performed on immortalized post-migratory GnRH neurons, GT1-7 cells, in which it has been shown that Sema3e has an anti-apoptotic effect on starved GT1-7 cells. Interestingly, SEMA3E has been linked to CHARGE syndrome (Lalani et al., 2004), a complex

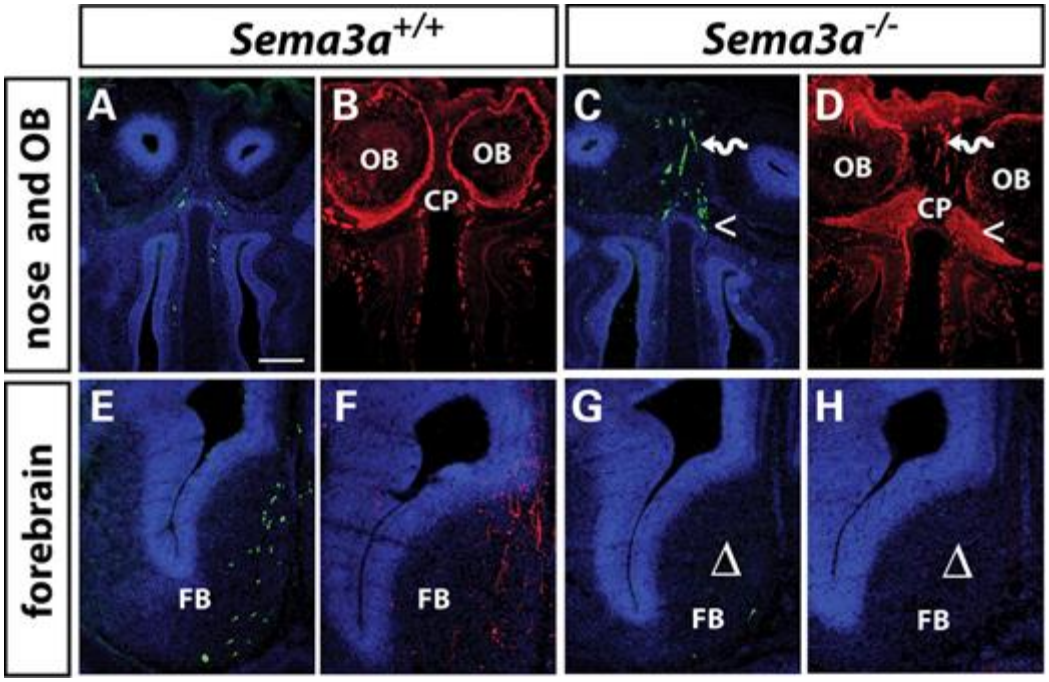

Figure 14 – *Sema3a*-deficient mice aberrant phenotype. (A–H) Cryosections from E14.5 mouse embryo heads immunolabeled for Gnrh (green) and peripherin (red) in order to reveal GnRH neurons and OLF/VN nerves respectively in the nasal compartment/OB **(A-D)** and the basal FB **(E-H)** of wild type and *Sema3a*$^{-/-}$ littermates. Lack of Sema3a leads to mistargeted axons and associated ectopic GnRH neurons (wavy arrows) between the OB; misguided axons form axon tangles that retain GnRH neurons at the level of the CP (open arrowheads). In the basal FB the lack of Sema3a cause a decreased number of GnRH neurons due to the lack of the caudal branch of VN nerves. Abbreviations: OB, olfactory bulbs; CP, cribriform plate; FB, forebrain.

Adapted from "Defective gonadotropin-releasing hormone neuron migration in mice lacking SEMA3A signalling through NRP1 and NRP2: implications for the aetiology of hypogonadotropic hypogonadism" by A. Cariboni, K. Davidson, S. Rakic et al., 2011, *Human Molecular Genetics*, 20(2):336–344. Copyright 2010 by the authors.

syndrome whose phenotypic spectrum also include syndromic IGD. Few years later, in 2015, Cariboni and co-workers prove that missense mutations in *SEMA3E* gene are responsible for KS (Cariboni et al., 2015).

5.6.3 SEMA4D

Sema4d is a membrane-bound semaphorin that is proteolytically cleaved to bind Plxnb1 in combination with Met tyrosine kinase receptor (Conrotto et al., 2005). These interactions are generally known to mediate growth cone collapse of developing axons, induce chemotaxis of epithelial and endothelial cells. Interestingly, the Sema4d receptors Plxnb1 and Plxnb2 are highly expressed in the developing olfactory structures (Perälä et al., 2010). Recently, it has been shown that Sema4d is able to regulate GnRH neuron migration through Plxnb1-Met receptor complex (Giacobini et al., 2008). In this work, researchers demonstrated that Plxnb1 and Ncam expression colocalized in the nasal mesenchyme only at early stages of development (E12.5 but not E14.5 nor E17.5). Consistent with a localized effect early in GnRH neuron migration, *Plxnb1*-null mice showed a reduced number of GnRH neurons reaching the forebrain with accumulation in the OB region. Decreased GnRH neurons in the adult brains resulted also in decreased GnRH fibres in the median eminence. Yet, *Sema4d* knock out mice do not have a reproductive phenotype, with normal migration of GnRH neurons, suggesting that there may be compensation by different semaphorins and no human mutations in this pathway have been documented so far.

5.6.4 SEMA7A

Sema7a is the only glycosylphosphatidylinositol (GPI)-anchored semaphorin and it can act either as a membrane-bound protein or secreted factor, after proteolytic cleavage. Sema7a binds with equal affinity to Plxnc1, reducing the integrin-mediated cell adhesion, and to β1-integrin (Itgβ1), to promote integrin clustering and therefore cell attachment. Since Sema7a is expressed in nasal pits and in the OB, a role for Sema7a was postulated. Indeed, in 2011 Messina et al. demonstrated that Sema7a promotes migration of GnRH neurons in nasal compartment, whereas its expression is turned off in the MPOA. Sema7a is expressed by OLF/VN nerves during the embryonic development whilst the expression pattern of the two Sema7a receptors in GnRH neurons is strictly temporally and spatially regulated: in the nasal mesenchyme GnRH neurons express Itgβ1 and migrate along the $Sema7a^{+}$ axonal scaffold, instead once crossing the NFJ they begin to express Plxnc1 to cease down migration. Consistently *Sema7a*-null mice display defective GnRH migration and, as a consequence, less innervated ME and dysfunctional gonads (Messina et al., 2011). Moreover, Sema7a exerts an additional function in ME plasticity, similarly to Sema3a. Sema7a is indeed expressed by tanycytes, specialized glial cells lining the 3v; here, it induces retraction of GnRH fibre terminals and promotes

the expansion of tanycytes end feet by acting through Plxnc1 and Itgβ1 respectively (Parkash et al., 2015). In agreement with the essential role exerted by Sema7a in the development and functionality of GnRH neurons in mice, mutations in *SEMA7A* have been found in both KS and nHH (Känsäkoski et al., 2014).

5.7 Semaphorin 3G

In 2005 Taniguchi and co-workers identified a novel human class 3 semaphorin, namely *SEMA3G*, mapped on chr 3p21.1 and 725 amino acid long. In parallel, they cloned the mouse ortholog *Sema3g* that exhibits an 86% identity with human one and it is constituted by 780 amino acids, with an estimated molecular weight of 87 kDa. They also investigated the expression pattern of *Sema3g* transcript in rodent and found that Sema3g is strongly present in highly vascularized tissues, such as lung, kidney, heart and placenta and only slightly in the brain, particularly in the cerebellum. Finally, they established that Sema3g canonically signals through Nrp2 to promote repulsion of dorsal root ganglion and sympathetic neurons (Taniguchi et al., 2005).

Subsequently, full *Sema3g* knock out mice were generated and described by Kutschera and co-workers. Specifically, a lacZ/Neo cassette was subcloned in the *Sema3g* gene between exon 2 and exon 16 thanks to gene targeting technology. Breeding of heterozygous mice lead to a normal Mendelian ratio offspring and no significant difference in the number of offspring can be observed between wild type and heterozygous breedings. LacZ reporter tracing allowed a more detail analysis of Sema3g expression, especially during embryonic development thanks to whole-mount staining (Figure 15). This analysis reveals that Sema3g is a primarily vascular-expressed class 3 semaphorin but few positive cells can be identified also in β cells of Langerhans islets of the pancreas and glomerular podocytes in the kidney. To confirm the limited expression of Sema3g in the brain, only ganglions and cerebellum are positive for Sema3g. Furthermore, *in vitro* experiments using plasmids encoding for Sema3g demonstrated that full length Sema3g (100 kDa) binds to Nrp2, confirming previous results, whereas 95 kDa and 65 kDa fragments, originated by furin proteases cleavage, can also bind to Nrp1. Finally, by treating smooth muscle cells and endothelial cells with Sema3g, researchers were able to assess that Sema3g exerts a pro-angiogenic effect (Kutschera et al., 2011).

Although these two works provide fundamental insights on Sema3g, many aspects of Sema3g activity during embryonic development and physiology remain still unknown. Few other papers suggest opposite effects for Sema3g: on one side, Sema3g promotes endothelial cells migration in HUVEC cells (Liu et al., 2015), while on the other side it prevents migration and invasion of U251MG glioma cells (Zhou et al., 2012) and lymphatic endothelial cells (Liu et al., 2016; Uchida et al., 2015). Interestingly, Sema3g has been shown to bind to Plxnd1 and Nrp2 complexes to inhibit lymphatic

endothelial cells sprouting and migration. The high degree of heterogeneity amongst signalling receptor complexes for Sema3g is consistent with the high variability that can be found in the signalling pathway of all the other class 3 semaphorins, that is strictly dependent by tissues, cell types and microenvironment (Liu et al., 2016). However, the expression and the role of Sema3g in GnRH neuron and olfactory systems have not been studied yet and will be object of this dissertation (see Section III, paragraph 1).

5.8 A-type plexins

A-type plexins are the main signal transducing receptor for class 3 and class 6 semaphorins, with the exception for Sema3e that binds to Plxnd1. The interactions between Sema6s and family A plexins are direct, established through contacts within the SEMA domains of both semaphorins and plexins. In turn, Sema3s bind to Nrp1-2 which associate with plexin As forming a trimeric complex (Janssen et al., 2010). Many studies have focused on the identification of receptor complexes for each of the class 3 semaphorins but assessing which receptor combination is needed for each semaphorin has been hard to achieve due to the high degree of redundancy amongst semaphorins, neuropilins and plexins. Moreover, it has become now clear that according to the biological system, the same semaphorin can exert a different function by signalling through a different receptor complex. In conclusion, different combinations of plexins and other co-receptors can produce a different biological outcome depending on cell populations and micro-environmental conditions

In agreement with the plethora of response mediated by class 3 and class 6 semaphorins, type A plexins are involved in several developmental and pathological processes, such as CNS development, angiogenesis, heart development, skeletal and kidney morphogenesis and tumour invasiveness and survival. Plexin As role has been extensively studied in the CNS, where they are predominantly expressed, but plexin As result to be broadly expressed during embryonic development and early postnatal life in many other non-neuronal tissues (reviewed in Perälä et al., 2012). Interestingly, early studies by Murakami and colleagues pointed out that *Plxna1*, *Plxna2* and *Plxna3* transcripts are present in most developing sensorial systems such as auditory, visual and olfactory systems, as well as in the developing neocortex, in the hippocampus and in many peripheral ganglia (Murakami et al., 2001). Shortly after, researchers of the same group first described Plxna4 and reported *Plxna4* mRNA expression in the CNS as well, with several Plxna4-positive cells in peripheral ganglia, sensorial systems including the olfactory one, neocortex and hippocampus (Suto et al., 2003). Thus, plexin As are expressed in overlapping but largely distinct populations of the developing neurons in both CNS and PNS. However, these studies provide the first and unique

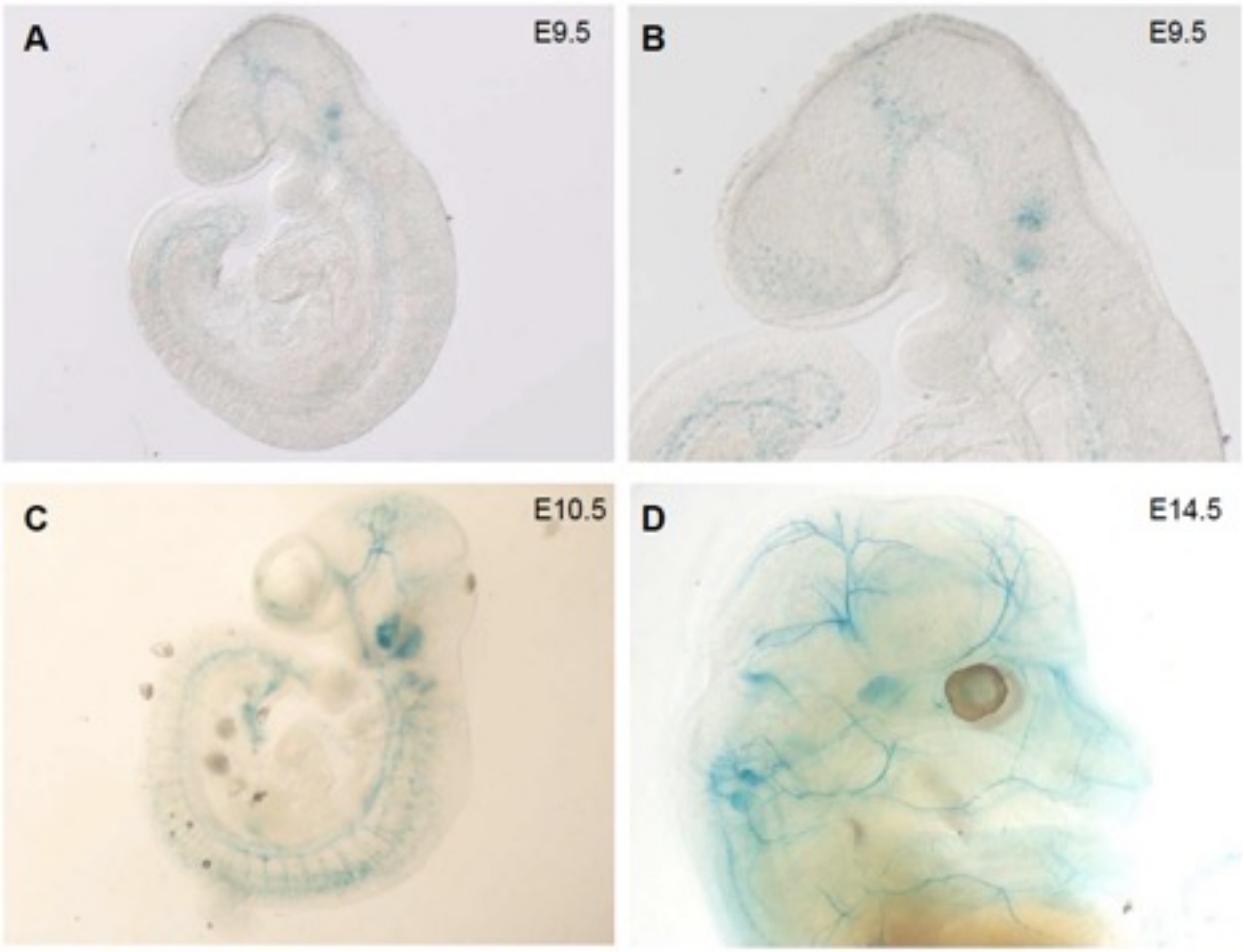

Figure 15 – LacZ staining revealed *Sema3g* expression during mouse development. *Sema3g* is mainly expressed by cardiovascular system and in particular in the aorta since E9.5 **(A, B)** and later on in the spreading of major trunk and brain arteries from E10.5 **(C)** to E14.5 **(D)**.

Adapted from "Differential endothelial transcriptomics identifies semaphorin 3G as a vascular class 3 semaphorin" by S. Kutschera S, Weber H, Weick A et al., 2011, *Arterioscler Thromb Vasc Biol*, 31(1):151-9

evidence of an involvement of A-type plexins in the development of olfactory system. In particular, Plxna1 and Plxna3 are mainly expressed in the accessory olfactory system, with positive cells in the VNO and AOB but also in the OE; in contrast, Plxna2 and Plxna4 are expressed in a complementary manner, with higher expression degree in the main olfactory system, i.e. OE and MOB (Murakami et al., 2001; Suto et al., 2003). All these data suggested that A-type plexins may regulate OLF/VN nerves development, with Plxna1-3 that preferentially regulate VN nerves whereas Plxna2-4 control OLF nerves axonal pathfinding. In agreement with this hypothesis, a recent work by Marcos and colleagues confirm Plxna1 expression in mouse embryo development and provide the first functional correlation between A-type plexins and olfactory and GnRH neurons systems. Specifically, Plxna1 expression was detected in the VNO at E11.5 and later on at E13.5, concomitantly to Nrp1-2 expression, along VN nerves, suggesting a role for Plxna1/Nrp1-2 holoreceptors in VN nerve axon guidance. By analysing *Plxna1*$^{-/-}$ mice, they demonstrated that the lack of Plxna1 results in misrouted VN nerves, unable to contact the AOB and stacked at NFJ level. In particular, the cVN/TN nerve is absent in KO embryos. As a consequence of misrouted VN nerves, GnRH neurons fail to enter the forebrain and therefore *Plxna1*-null embryos display a reduced number of hypothalamic GnRH neurons compared to WT littermates and consistently adult KO mice show a less innervated ME and dysfunctional testes (Marcos et al., 2017). Interestingly, *Plxna1*$^{-/-}$ mice aberrant phenotype well phenocopies defects observed in *Sema3a*$^{-/-}$ and *Nrp1*$^{sema/sema}$*/Nrp2*$^{-/-}$ mice. These findings are strengthened by heterozygous mutations found in KS patients harboured by *PLXNA1* gene. However, the aberrant phenotype has been observed only in 5 mice out of 18, suggesting either incomplete penetrance or a compensatory role amongst class A plexins. Redundancy between A-type plexins has been indeed demonstrated by several authors: for instance, Plxna1 together with Plxna3 are responsible for Sema3a signalling in stato-acoustic ganglion neurons (Katayama et al., 2013), while the combined loss of Plxna3 and Plxna4 impairs facial branchiomotor axon guidance more severely than loss of either plexin alone, suggesting that Sema3a and Sema3f signals, even though both essential, are partially redundant (Schwarz et al., 2008).

6. Heparan Sulphate 6-*O* Sulpho-Transferase 1

HSPGs are glycoproteins that contain one or more chains of heparan sulphate (HS) glycosaminoglycan covalently attached. Cells produce a relatively small set of HSPGs (~17) that can be divided into three groups according to their location: membrane HSPGs, such as syndecans and glycosylphosphatidylinositol-anchored proteoglycans (glypicans), the secreted extracellular matrix HSPGs (agrin, perlecan, type XVIII collagen), and the secretory vesicle proteoglycan, serglycin

(Sarrazin et al., 2011). HSPGs participate in many cell processes and in several different tissues thanks to their structural and chemical properties: 1) they synergise with other extracellular matrix protein to provide an extracellular scaffold for cell migration; 2) they regulate secretory vesicles processes and maintain in an active state proteases; 3) they bind to cytokines, chemokines, growth factors and morphogens to prevent their proteolysis and to guarantee gradient formation and interactions with their receptors; 4) they can act as coreceptors for many tyrosine kinase receptors; 5) they mediate cell adhesion (Bishop et al., 2007) (Figure 16). Structurally, each proteoglycan consists of a core protein and one or more covalently attached HS chains, composed of N-acetylated and N-sulphated glucosamine units. The HS chains are assembled on core proteins by enzymes in the Golgi that confers a high degree of heterogeneity in terms of length, size, epimerization and extent of sulphation (Figure 17).

Amongst the enzymes responsible for HS synthesis, Heparan Sulphate 6-*O* Sulpho-Transferase 1 (Hs6st1) has been the only one to be associated to defective GnRH neurons development (Tornberg et al., 2011). Hs6st1 promotes the *O*-sulphation of *N*-acetylated glucosamines. Hs6st1 is widely expressed in many different tissues during all developmental phases and is also expressed together with Hs6st3 in the developing olfactory epithelium at E14.5 (Sedita et al., 2004). It has been previously shown to regulate axon guidance in mouse CNS and PNS (Tillo et al., 2016) (Pratt et al., 2006). Furthermore, 6-*O* sulpho-transferases have been already implicated in VEGF, FGF and WNT signalling (reviewed in Sarrazin et al., 2011). Specifically, Hs6st1 promotes the formation of VEGF/VEGFR and FGF/FGFR signalling complexes in vascular endothelial cells (Ferreras et al., 2012) and, interestingly, it is also required for the function of Anos1 and Fgfr1 in olfactory system (Bülow et al., 2002; Hu et al., 2009; Tornberg et al., 2011). In a *C. elegans* model, it has been demonstrated that Hs6st1 regulates in an Anos1-dependent manner the neural branching of AIY interneurons by enhancing Fgfr1 signalling. Overexpression of *kal-1*, the *C. elegans* ortholog for *ANOS1*, resulted in interneurons branching, whereas null mutations in *hst-6*, ortholog for *Hs6st1*, are able to suppress axonal branching; moreover, transgenic introduction of human *HS6ST1* mutation found in nHH patients are less able to rescue the phenotype of *hst-6* mutant compared to WT *HS6ST1* expression (Tornberg et al., 2011). However, Hs6st1 mutations may also impact on the HPG axis via Anos1-independent pathways, as HS modifications of many different proteoglycans in the extracellular matrix have the potential to affect multiple signalling pathways (Bishop et al., 2007) previously implicated in the neuroendocrine control of fertility (Condomitti and de Wit, 2018).

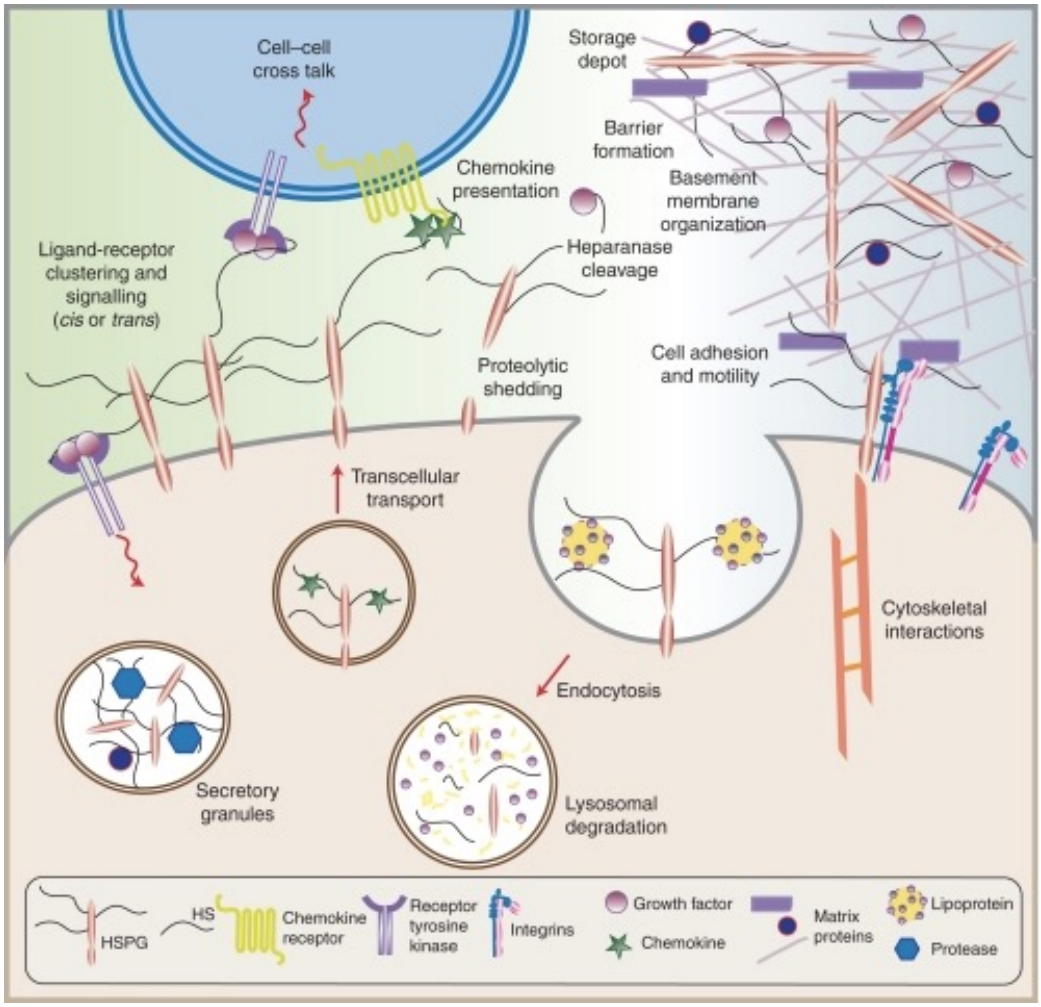

Figure 16 – HSPG have multiple activities in cells and tissues. HSPG are extracellular matrix components and can regulate several biological processes such as ligand-receptor interactions, cells adhesion and motility and endocytosis.

Adapted from "Heparan sulphate proteoglycans" by S. Sarrazin, W.C. Lamanna and J.D. Esko, 2011, *Cold Spring Harb Perspect Biol*, 1;3(7). Copyright 2011 by Cold Spring Harbor Laboratory Press.

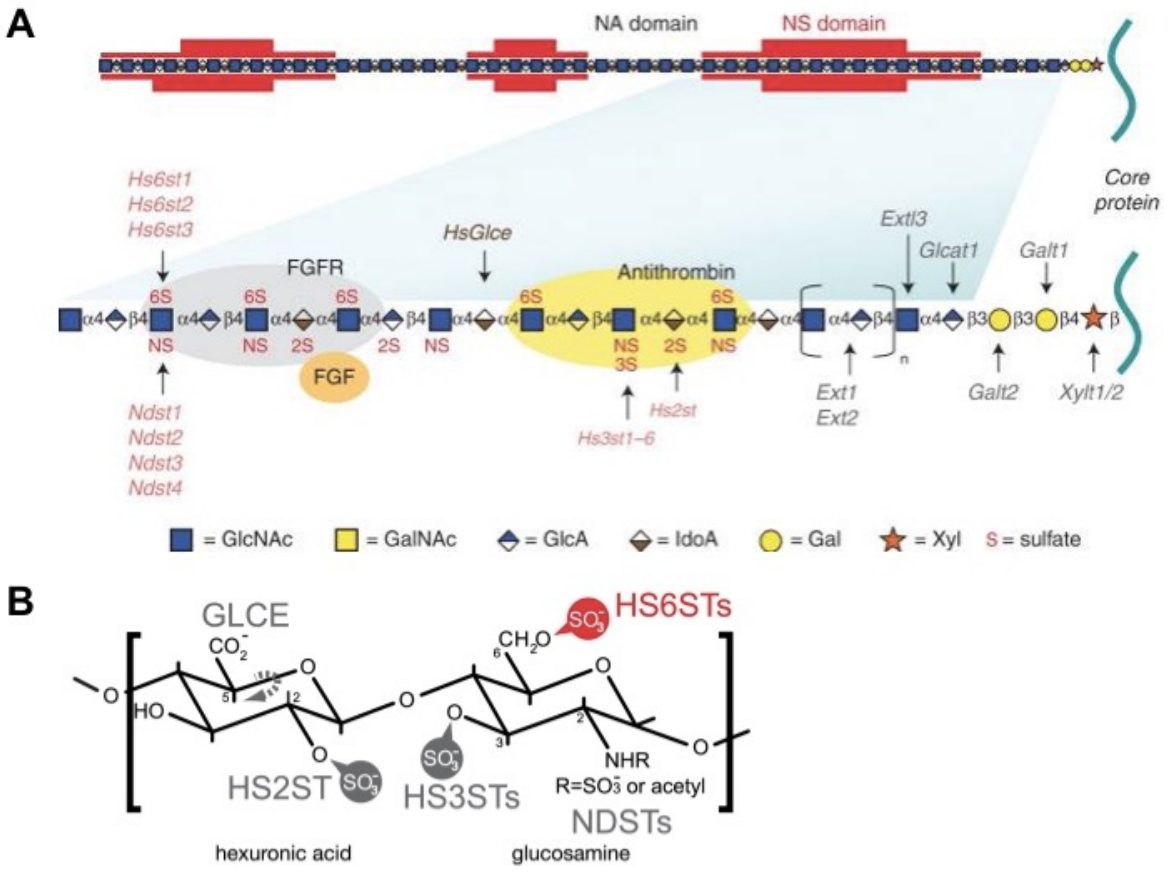

Figure 17 – HSPG structure and enzymatic modifications. (A) HSPG biosynthesis initiates by the attachment of xylose to HSPG core proteins followed by a saccharide linkage (galactose-galactose-glucuronic acid; GlcA-Gal-Gal) and a chain of alternately GlcA and GlacNAc (N-acetyl-D-glucosamine). The chains simultaneously undergo a series of processing reactions, in particular, sulphation and epimerizations that create N-sulphated domains (NS domains in red) interspersed by unmodified domains (NA domains). The modified domains make up binding sites for protein ligands as depicted for antithrombin, FGF and FGF receptor. **(B)** Characteristic disaccharide of HSPG (GlcA and GlcNAc) can be modified by HS-modifying enzymes (grey) such as HS6ST1 (in red) at indicated positions.

(A) Adapted from "Heparan sulphate proteoglycans" by S. Sarrazin, W.C. Lamanna and J.D. Esko, 2011, *Cold Spring Harb Perspect Biol*, 1;3(7). Copyright 2011 by Cold Spring Harbor Laboratory Press.

(B) Adapted "Heparan sulfate 6-O-sulfotransferase 1, a gene involved in extracellular sugar modifications, is mutated in patients with idiopathic hypogonadotrophic hypogonadism" by J. Tornberg, G.P. Sykiotis, K. Keefe et al., 2011, *PNAS USA*, 108(28):11524-11529. Copyright 2011.

SECTION II
Aims

IGD is characterised by complex genetics, with several causative genes being identified. Further, IGD is often manifests as an oligogenic disorder, with two or more genes co-operating to produce a phenotype. These two aspects are thought to be responsible for the heterogeneous nature of the phenotypes among the affected individuals. Identified genes underlying IGD regulate different aspects of GnRH neuron development and function including specification and differentiation of GnRH neurons, their migration from the olfactory placode to their final destinations in the MPOA of the hypothalamus, their maturation and survival within the MPOA, their activation to initiate puberty and their regulation in the response of pituitary gonadotropes to GnRH stimulation. In humans, IGD can be found either in isolated conditions with normal ability to smell (nHH) caused by dysfunctional neuroendocrine genes, along with anosmia/hyposmia (KS) or along with multisystemic phenotypes due to mutations in pleiotropic neurodevelopmental genes. So far, mutated genes underlying IGD have been identified only in 50-60% of overall cases; moreover, there are several IGD-associated disorders, such as self-limited delayed puberty, whose genetic causes are still largely unknown despite the fact that self-limited DP is about 500-fold more frequent compared to IGD. This lack of knowledge about IGD genetics represents a big limitation for a timely diagnosis and an effective treatment, which represent key points to restore the HPG axis functionality and limit potential co-morbidities such as type II diabetes mellitus, osteoporosis and psychosocial disorders.

The main aim of my thesis has been the study of some molecular and cellular mechanisms that regulate GnRH neuron differentiation and migration, with the final goal to identify novel causative genes of IGD and related disorders and ameliorate diagnosis and treatment timing. To achieve this goal, two different approaches have been pursued: i) search for novel mutations in IGD patients, taking advantage by advances in *-omics* techniques especially in next generation sequencing and exome sequencing, and study the functional role of mutated genes in different experimental models in order to validate their involvement in the pathogenesis of IGD; ii) study the expression and the role of candidate genes identified thanks to a basic science-driven approach in experimental models in order to assess a potential role in GnRH neuron physiology and finally search for mutations in IGD patients.

Three different objectives have been established:

1. Functionally validate the role of *Sema3g* gene in GnRH neurons development by combining *in silico*, *in vitro* and i*n vivo* approaches to confirm the involvement of *SEMA3G* homozygous

mutation in the pathogenesis of a novel form of syndromic IGD affecting two Pakistani brothers, born from consanguineous parents;

2. Study the role of A-type plexins along with GnRH neuron and olfactory systems in genetically modified mice, since plexinAs are the signal-transducing receptors for SEMA3A, a well-studied KS gene, and therefore may represent candidate genes underlying IGD;

3. Determine the role of *HS6ST1*, an already known KS gene newly found mutated in a cohort of patients with self-delimited DP, by applying *in vivo* methods in order to define its role and expression in GnRH neuron physiology.

OBJECTIVE 1

To evaluate the role of the guidance molecule SEMA3G in the development of the GnRH system in mice and confirm its potential role in the pathogenesis of syndromic IGD in humans, the following specific aims have been pursued:

1. To study the behaviour of wild type and mutated human SEMA3G in cell lines such as COS-7 and GN11 cells;

2. To study the expression pattern of *Sema3g* mRNA in wild type mice during embryonic GnRH development;

3. To study the reproductive phenotype of *Sema3g*-null mice both at embryonic stage and adult stage.

OBJECTIVE 2

To determine the role exerted by SEMA3A receptors, PLXNA1-4, in GnRH neuron and olfactory systems taking advantage from single and compound genetically modified mice in order to provide evidences of an involvement of A-type plexins in IGD pathogenesis. The following specific aims have been pursued:

1. To elucidate the expression pattern of four A-type plexins *in vivo* in wild type murine and human embryonic tissues;

2. To study the effect of the deletion of one or more PLXNAs in genetically modified mice, both at embryonic and adult stage.

OBJECTIVE 3

To unravel the genetic architecture of self-limited DP by studying the role of *HS6ST1*, already known as KS causative gene, newly found mutated in a cohort of patients with self-delimited DP. The following specific aims have been pursued:

1. To study the expression pattern of *Hs6st1* in wild type adult mouse brains;

2. To determine the effect of heterozygous loss of *Hs6st1* in a genetically modified mouse model.

SECTION III
Results and discussion

1. Semaphorin 3G

Summary

Syndromic IGD is characterized by reproductive defects and can be defined as nHH or KS; in addition, IGD patients can display a broad spectrum of non-reproductive non-olfactory symptoms that can vary depending on the nature of the causative gene. Syndromic IGD is characterized by high clinical heterogeneity and poorly characterized genetics that co-operate to make complex the phenotype-genotype correlations and the subsequent diagnosis in affected patients. Here, we have combined mutational analysis in affected individuals with *in vitro* and *in vivo* experimental models to identify Semaphorin 3G (*SEMA3G*) gene as a novel gene underlying IGD and to study its role in the GnRH neuron system development. Specifically, by applying homozygosity mapping (HZM) and whole exome sequencing (WES), we found a novel non-synonymous mutation harboured by *SEMA3G* gene in two brothers affected by a previously undescribed form of syndromic IGD, characterized by normosmic hypogonadotrpic hypogonadism (nHH), facial dysmorphic features, growth delay and mental retardation. To evaluate the biological relevance of dysfunctional SEMA3G signalling, we demonstrated that the mutation alters GnRH neuron migration due to a failure in Akt activation in GN11 cells. As a confirm of these findings, mice lacking *Sema3g* display a reduced number of hypothalamic GnRH neurons and reduced fertility. Further, in the present study we show evidences for the co-presence of additional mutations in two genes that might contribute to the pathogenesis of this novel form of syndromic IGD.

1.1 Background

In collaboration with clinicians, we have identified two brothers affected by an unusual form of syndromic IGD that present GnRH deficiency concomitantly with facial dysmorphic features, developmental delay and mental retardation. Noteworthy, these two brothers are born from consanguineous parents and therefore share a large region of homozygosity on their DNA. Thus, by combining HZM with WES, bioinformatics, functional *in vitro* studies and phenotyping of a transgenic mouse model we have identified a novel mutation in the *SEMA3G* gene and demonstrated that this gene is important for a correct GnRH neuron migration.

SEMA3G belongs to the family of secreted class 3 semaphorins which represents a class of proteins regulating several developmental processes, with particular regard to nervous system formation. Class 3 semaphorins have been deeply studied in relationship with GnRH/olfactory systems physiology (Cariboni et al., 2011a; Cariboni et al., 2015; Giacobini

et al., 2014) and in line with their essential role in these biological events, mutations in *SEMA3A* and *SEMA3E* genes have been found in KS patients (Cariboni et al., 2015; Hanchate et al., 2012; Känsäkoski et al., 2014; Young et al., 2012). Interestingly, *SEMA3E* mutations have been associated also to syndromic IGD, overlapping with CHARGE syndrome (Lalani et al., 2004).

As a member of Sema3s, SEMA3G is able to bind to both NRP1-2 (Taniguchi et al., 2005) and PLXNA1-4, with the latter being obligate receptors to transduce intracellular signalling (Sharma et al., 2012). Previous reports showed that SEMA3G exerts its function mainly during embryonic development and in particular during vascular patterning as observed in mouse embryo, where *Sema3g* is strongly expressed in highly vascularized tissues, such as lung, kidney, heart and placenta (Kutschera et al., 2011). Yet, expression of *Sema3g* has been also reported in the adult nervous system such as in the cerebellum and in the developing OB (Taniguchi et al., 2005), but no reports on Sema3g role in the establishment of the neuroendocrine reproductive axis are available so far. Moreover, Sema3g biological activity during embryonic development and physiology is still under profound debate as different studies suggest opposite effects for Sema3g. Sema3g acts as positive modulator for endothelial cell motility (Liu et al., 2015), while on the other side it prevents glioma and lymphatic cell migration (Liu et al., 2016; Uchida et al., 2015; Zhou et al., 2012). However, the high degree of heterogeneity amongst receptor complexes is consistent with the high variability that can be found in other semaphorin-mediated biological responses, which are strictly dependent on tissue, cell type and cellular microenvironment.

Here, we demonstrated that *SEMA3G* mutation found in the two brothers affected by syndromic IGD is predicted to be disease causing by different online prediction tools and consistently reduces neuronal migration of GN11 cells and AKT phosphorylation. *In vivo*, we found transient *Sema3g* expression in cells migrating together with GnRH neurons in mouse embryos and by analysing mice lacking *Sema3g*, we showed that loss of Sema3g leads to defective GnRH neuron migration, reduced ME innervation and gonadal misfunctioning. Further, by re-examining exomes of probands we discovered two additional novel mutations occurring in rhotekin (*RTKN*) and Natural Killer cells Triggering Receptor (*NKTR*) genes, both lying in shared homozygous regions. Expression experiments on mouse embryos provided evidences that these two additional mutated genes might explain non-reproductive symptoms observed in the two proband brothers, concurring to the pathogenesis of this complex syndrome.

1.2 Results

Two siblings from consanguineous parents show nHH, facial dysmorphism and developmental delay.

In collaboration with Prof. Khalid Hussain and Dr. Sophia Tahir from UCL Great Ormond Street Institute of Child Health, we identified two brothers with an unusual syndrome characterized by nHH with cryptorchidism, poorly developed scrotum and microphallus in combination with facial dysmorphic features, developmental delay and mental retardation. Patients belong to a consanguineous family of Pakistani origin in which parents are first cousins and they have two normal and healthy elder sisters unaffected by this condition (Figure 1).

The index patient (patient 1) is a 20-year-old male, who was born at 41 weeks of gestation after a normal delivery, with a birth weight of 2.84 kg. At birth, he displayed bilateral undescended testes, a poorly developed scrotum, but normal phallus. Although bilateral orchidopexy was performed at 4-years of age, he maintained very small bilateral atrophic underdeveloped testes and a small hypoplastic scrotum. Dysmorphic facial features noted in the patient include unusual prominent staring eyes, prominent nasal bridge, brachycephaly, synorphrys, a beaked nose, small mouth and chin, a high palate and pointed ears with an over folded helix. A human chorionic gonadotropin (hCG) test was performed at the age of 3 years and showed normal testosterone response with a peak at 14.5 nmol/L from a basal level of less than 0.69 nmol/L, confirming testes functionality and testosterone production upon stimulation. A subsequent hCG test performed for 3 weeks at 11 years of age confirmed a normal gonadal response. Clinical examination at the age of 15-years determined the patient's height velocity to be 5.4 cm per year and a 5 mL right and 4 mL left testes, indicating that the patient had still not started puberty. Testosterone injections (50 mg every four weeks) lead to linear growth and development of secondary sexual characteristics, (i.e. pubic and axillary hair growth and an increase in penile size in the patient).

Patient 2 is a 15-year old male and represents the youngest sibling in the family. He was born at 36 weeks of gestation with an emergency lower segment caesarean section. The birth weight does not figure on records. Antenatal scans showed a dilated large bowel, oligohydramnios and microcephaly, whilst at birth, he showed an anorectal malformation resolved with a colostomy performed at day 2 of life. Subsequently, posterior sagittal anorectoplasty was performed at 1 year of age, followed by colostomy closure in the same year. The patient had bilateral small phallus, hypoplastic scrotum and undescended testes and a small

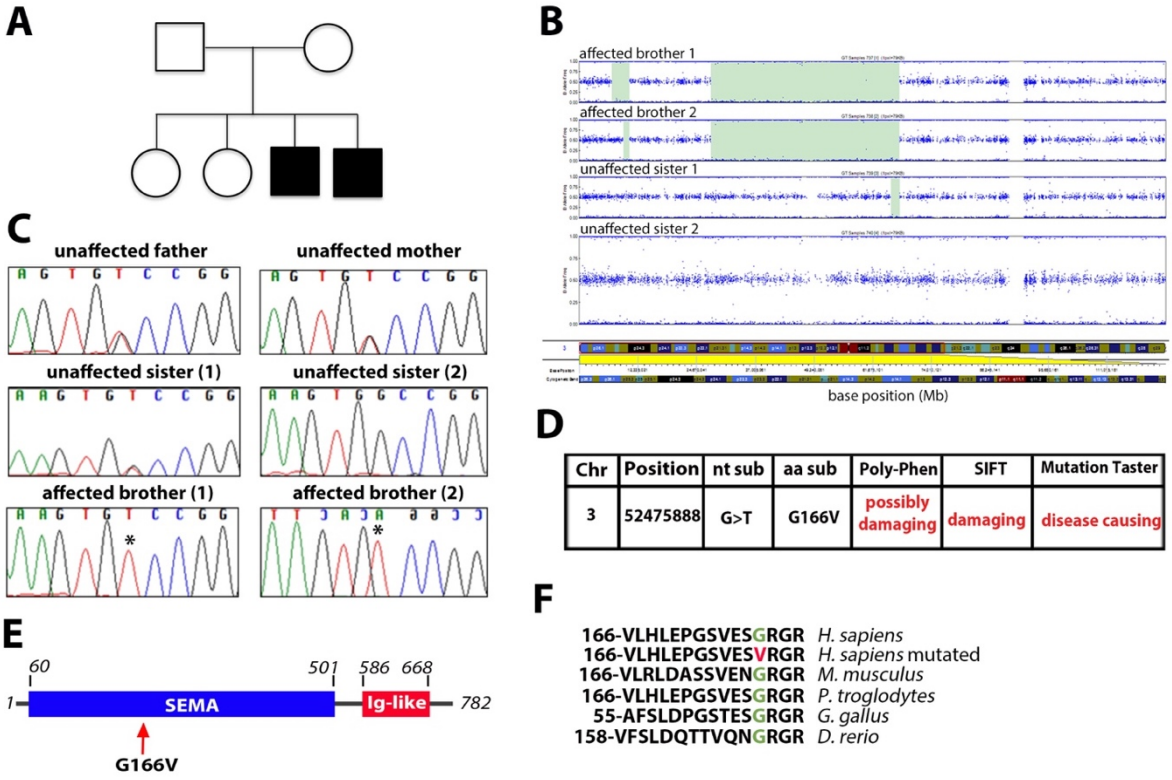

Figure 1 – Homozygosity mapping identifies a *SEMA3G* mutation in two brothers with syndromic IGD. (A) Family tree of brothers affected by IGD. Circle denotes female; square denotes male; black square denotes affected male. **(B)** The panel shows a B-allele frequency plot of chromosome 3, with heterozygous SNPs plotted at 0.5, and homozygous SNPs plotted at either position 0 or 1. Highlighted in green are the homozygous regions. As seen from the image, a large region spanning base pair positions 27663546 to 65514406 (approximately 38 Mb) is shared between the two affected patients. This homozygous region is absent in the unaffected siblings. A small homozygous region of 1.3 Mb is also presented in the figure. This represents the largest shared homozygous region on chromosome 3. **(C)** Chromatograms of nucleotides 492 to 501 of the *SEMA3G* coding sequence from 2 brothers carrying a nucleotide substitution in exon 5 (left side, forward strand; right side, reverse strand; the positions of the G>T and corresponding C>A change are indicated with asterisks) and from the unaffected parents and sisters. **(D)** *In silico* analysis identified *SEMA3G* on chromosome 3 as a potential candidate gene, with nucleotide change c.497G>T and protein change p.Gly166Val. PolyPhen-2, SIFT and Mutation Taster were used to predict structural and functional effects of G166V amino acid substitution on SEMA3G protein structure and function. The mutation was predicted to be possibly damaging (Poly-Phen), damaging (SIFT) and disease causing (Mutation Taster) with probabilistic scores above 0.99. **(E)** Diagram of the SEMA3G functional domains: SEMA and Ig-like. Their position and the position of the mutated amino acid residue within the protein sequence are indicated. **(F)** Alignment of partial protein sequences of vertebrate SEMA3G orthologues shows that the G166 residue is evolutionarily conserved in humans and several other vertebrate species.

phallus: right orchidopexy was initially performed, while left orchidopexy was performed later at the age of 9 years as the left testis was not palpable before. Facial dysmorphic features include a small round head, beaked nose, and thin upper lips; in addition, the left helix is slightly unfolded and the ear is slightly protruding. Glucagon stimulation test revealed growth hormone (GH) deficiency and therefore GH treatment was started at the age of 6 years.

Interestingly, both patients were noted to have some mental retardation. Patient 1, at 5 years of age had a general development quotient of 60, rating in the severely delayed range. In particular, he showed significant learning difficulties and was unable to speak in sentences; at 8 years of age was enrolled in a specialized school. Patient 2 began to walk at 2 years and 7 months and was not speaking by the age of 3 years. The combination of the clinical features described above suggests that the two brothers may have a novel IGD syndrome, as the constellation of these features has not been previously described.

A point mutation in the SEMA3G gene of two brothers with syndromic IGD

We suspected that the two brothers are affected by an autosomal recessive disease with a homozygous genetic pattern of inheritance, due to the unique presenting features in particular the birth from consanguineous parents. HZM was performed on the two patients and their two unaffected sisters to identify candidate genes and was followed by WES. The shared homozygous regions (> 2 Mb) found in the affected patients and absent in the unaffected siblings are listed Table 1. Overall, the affected brothers share approximately 85 Mb of unique homozygous region which houses over 600 protein-coding genes, with the largest shared region, of around 38 Mb, located on chromosome 3 (Figure 1B).

Variants obtained from WES (Table 2) were filtered to narrow down the list of possible causative genes. Firstly, biological relevance of variants has been evaluated and only variants causing gene function disruption (i.e. non-synonymous changes, stop gain/stop loss changes or changes affecting a splice site) were identified, with remaining variants been filtered out. The HZM data was next used in conjunction with the WES filtered variants to identify those lying in the shared homozygous regions and among those variants, only homozygous mutations were considered as we hypothesized an autosomal recessive disorder. Finally, the variants found in a homozygous state in SNPs databases (dbSNP130 and 1000 Genomes project) were filtered out, leaving those unique to the patients.

Specifically, this analysis identified *SEMA3G* gene (ENSG00000010319), located on chromosome 3p21.1, as a potential candidate gene, with nucleotide change c.497G>T

Chromosome	Start	End	Size (bp)	Size (Mb)	Number of protein coding genes
2	64824348	80045133	15220785	15.220785	110
3	9200375	10528910	1328535	1.328535	30
3	27663546	65514406	37850860	37.85086	337
3	158583584	162058440	3474856	3.474856	17
10	26778606	38995349	12216743	12.216743	45
10	42816816	58885646	16068830	16.06883	88
12	126501464	126548335	46871	0.046871	0

Table 1 – List of all homozygous regions identified in affected patients by HZM.

Variant type Type dbSNP Novel	Total	dbSNP	Novel
Essential splice site	27	11	16
Heterozygous	23	7	16
Homozygous	4	4	0
Non Synonymous coding	1788	1074	714
Heterozygous	1501	808	693
Homozygous	287	266	21
Stop codon gained	36	26	10
Heterozygous	30	21	9
Homozygous	6	5	1
Stop codon lost	9	8	1
Heterozygous	4	3	1
Homozygous	5	5	0
Within mature microRNA	2	1	1
Heterozygous	2	1	1
Homozygous	0	0	0
All variants	**1862**	**1120**	**742**
Heterozygous	**1560**	**840**	**720**
Homozygous	**302**	**280**	**22**

Table 2 – List of variants obtained from Patient #2 WES.

(NM_020163.2) and protein change p.Gly166Val (G166V). As class 3 semaphorins and their receptors have been extensively implicated in the pathogenesis of IGD and in the GnRH neuron physiology (Cariboni et al., 2011a; Cariboni et al., 2015; Giacobini et al., 2014; Hanchate et al., 2012; Young et al., 2012), we considered *SEMA3*G as the main candidate to explain the nHH phenotype in our patients. Sanger sequencing confirmed the novel change to be present in the homozygous state in the two affected patients. Both parents and the eldest sister were heterozygous carriers for the mutation, and the second sister was homozygous for the normal reference allele (Figure 1C). The G166V mutation substitutes an ambivalent glycine residue with a hydrophobic valine residue and is predicted to be possibly damaging and disease causing according to PolyPhen (Adzhubei et al., 2010), SIFT (Ng and Henikoff, 2003) and MutationTaster (Schwarz et al., 2014) bioinformatic tools, respectively (Figure 1D). The G166V mutation lies in the SEMA domain, a high conserved domain enriched in cysteine residues that form four disulphide bonds to stabilize 3D structure (Figure 1E). The mutated residue affects a glycine residue that is conserved between vertebrates (Figure 1F).

Wild type SEMA3G, but not SEMA3G G166V, promotes GnRH neuron migration by activating PI3K signalling

To define the cellular and biochemical mechanisms by which wild-type and mutated SEMA3G affect GnRH neurons, we took advantage of GN11 cells, a model of immortalised GnRH neurons that migrate *in vitro* (Maggi et al., 2000). Previous works had already validated this cell line as useful tool to identify molecular pathways involved in GnRH neuron development, since they overcome the challenge to isolate primary GnRH neurons in sufficient quantity for biochemical and cell biological assays, due to their low number and scattered distribution throughout the nose and the brain (Cariboni et al., 2007b; Cariboni et al., 2011a; Cariboni et al., 2015; Giacobini et al., 2007; Zhang et al., 2013). GN11 cells express both neuropilins (*Nrp1-2*) as well as *Plxna1-4* receptors (Figure 2A), thus these cells represent a suitable model to study effects of wild type (WT) vs. mutated SEMA3G. As a source of soluble SEMA3G for *in vitro* studies, we used conditioned medium (CM) of COS-7 cells transfected with human SEMA3G WT and SEMA3G G166V expression vectors. Immunostaining and immunoblotting using an anti-cMyc antibody established that both proteins were expressed and effectively secreted (Figure 2B-C). We engineered recombinant SEMA3G as an alkaline phosphatase (AP) (AP)-conjugated ligand and found that SEMA3G WT and SEMA3G G166V bound GN11 cells in a binding assay (Figure 2D). Taken together, these results suggest that G166V mutation does not compromise neither the production, secretion or binding capacity of the protein.

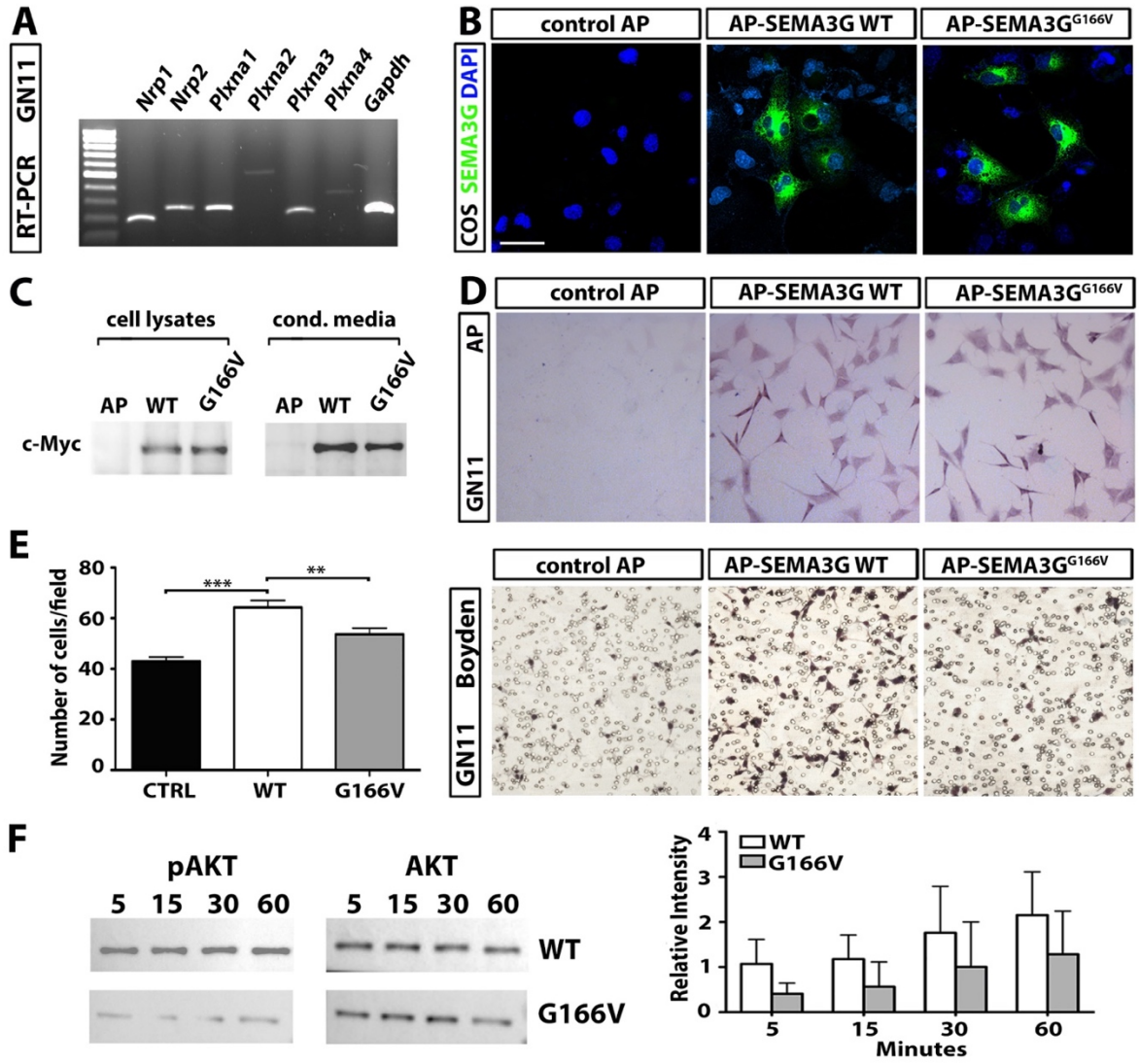

Figure 2 – Diminished signalling activity of SEMA3G protein harbouring the G166V mutation. **(A)** RT-PCR analysis performed on mRNA extracted from GN11 cells showed the presence of specific transcripts for *Nrp1*, *Nrp2*, *Plxna1*-4 and the standard *Gapdh* with amplicons of 188, 260, 250, 485, 195, 320 and 189 bp, respectively. **(B)** Wild type (WT) and mutated SEMA3G were produced in COS-7 cells in serum-free DMEM. **(C)** Western blot analysis of conditioned media from transfected COS-7 cells producing WT or mutated SEMA3G proteins. **(D)** The p.G166V mutation did not alter the protein secretion and protein binding evaluated by AP-assay. **(E)** Chemotactic response of GN11 cells to SEMA3G in a Boyden's chamber assay. SEMA3G^{G166V} concentrated conditioned medium induced significantly less migration compared to SEMA3G WT and control (n=3, ** P<0.01, *** P<0.001, One-way ANOVA). **(F)** Left panel: representative western blots for the phosphorylated and total forms of AKT in GN11 cells following incubations with serum-free media at different time points: 5, 15, 30 and 60 minutes. Right panel: bar graphs illustrate means and standard deviations of 3 independent experiments. Signal intensity was calculated for each western blot. Quantification of relative band intensities (expressed as a ratio of pAKT over total AKT) was made using ImageJ software. Immunoblotting shows decreased levels of pAKT, relative to total AKT, in serum-starved GN11 cells treated with mutated SEMA3G protein at each time point. Scale bar: 50 µm (B, D, E).

GN11 show a strong chemomigratory behaviour *in vitro*, so we used them cells to study the effects of SEMA3G on the migratory activity of GnRH neurons (Cariboni et al., 2007b; Cariboni et al., 2011a; Maggi et al., 2000). For these experiments, GN11 neurons were exposed to control conditioned media or to conditioned media of COS-7 cells transfected with WT or mutated SEMA3G for 2 hours. We found that the chemomigration of GN11 cells was significantly increased in the presence of SEMA3G WT compared with control media, whereas the mutated SEMA3G stimulated the migration to a lower extent in GN11 cells (mean of migrated cells/field ± s.e.m.; CTRL 42.9±1.7; SEMA3G WT 64.2±2.8; SEMA3G G166V 53.6±2.4; $P<0.001$ CTRL vs SEMA3G WT; $P<0.01$ SEMA3G WT vs SEMA3G G166V; One-way ANOVA) (Figure 2E).

Activation of PI3K and its effector AKT plays a key role in migration and survival signalling in many cell types, including neurons (Brunet et al, 2001). Thus, to investigate whether the G166V mutation impaired GnRH neuron migration by impairing intracellular pathways, we studied AKT activation upon stimulation of GN11 cells with WT or mutated SEMA3G. GN11 cells were serum-starved overnight and then treated with concentrated conditioned media (SEMA3G WT and SEMA3G G166V) for 5–60 minutes. We observed that SEMA3G WT could induce AKT activation with a peak after 5 minutes, whereas SEMA3G G166V was less effective in inducing AKT activation (O.D. ratio pAKT/AKT mean ± s.e.m.; SEMA3G WT: 1±0.5 vs SEMA3G G166V: 0.4 ± 0.2) (Figure 2F). Even though SEMA3G G166V could bind to GN11 cells, it failed to promote migration. This may be due to a defective AKT signalling pathway activation. Taken together, these observations suggest that SEMA3G signalling through AKT promotes the migration of immature GnRH neurons, whilst the SEMA3G G166V mutation interferes with this function.

Sema3g expression is expressed during mouse embryonic development consistently with GnRH neuron migration

To determine the expression pattern of Sema3g and to confirm *in vivo* the functional requirement observed in GN11 cells for GnRH neuron migration, we used the mouse as a model organism. In wild-type mice, GnRH neurons are first detected at embryonic day (E) 10.5 in the nasal pit, migrate first in the nasal compartment starting from E11.5 and then in the basal forebrain where they reach the hypothalamus, completing the process just before birth at E18.5. We performed *in situ* hybridization (ISH) experiments using specific riboprobes for *Gnrh* and *Sema3g* on adjacent sections, at three different developmental time points (E12.5, E13.5 and E14.5) to get insights into the expression pattern of *Sema3g* along with GnRH neuron

development. As shown in Figure 3A, *Sema3g* transcript is expressed in the nasal compartment by cells exiting the VNO and migrating along the nasal septum between E12.5 and E14.5, with an expression pattern that resembles *Gnrh* one. To check whether the Sema3g^{+} cells were GnRH neurons, we performed double ISH-immunofluorescence protocols by using the anti-*Sema3g* probe and an anti-Gnrh antibody. We demonstrated that these two cell populations are actually distinct with no co-expression of *Sema3g* in GnRH neurons, although Sema3g^{+} cells migrate in close relationship with GnRH neurons (Figure 3B). These results provide evidences for a possible involvement of Sema3g in the navigation of GnRH neurons within the nasal compartment.

Sema3g loss affects GnRH neuron migration in the developing mouse head.

Because we observed that SEMA3G stimulates the chemomigration of GN11 cells (Figure 2) and we detected expression of *Sema3g* mRNA in the nasal compartment (Figure 3), we next asked if *Sema3g*-null mice (Kutschera et al., 2011) showed impaired GnRH neuron migration. To assess defects in the migration of GnRH neurons, we performed immunostaining with an antibody specific for Gnrh on murine cryosections at E14.5, a time point representing the peak of GnRH neuron migration, as well established by previous work (Cariboni et al., 2011a; Cariboni et al., 2011b; Cariboni et al., 2015; Giacobini et al., 2008). We next counted total number of GnRH-positive cells in each head demonstrating a reduced number of GnRH neurons in mutants compared to wild type mice at E14.5 (Figure 4; number of GnRH neurons/head ± s.e.m.; *Sema3g*$^{+/+}$: 1172.0±80.3 vs. *Sema3g*$^{-/-}$: 811.3±44.8; $P<0.05$; n=3 for each group). Further, we determined the relative number of neurons in each anatomical compartment, i.e. nose, NFJ and FB. We observed a similar number of GnRH-positive cells in mutants' nose (GnRH neurons number ± s.e.m.; *Sema3g*$^{+/+}$: 366.0±68.0 vs. *Semag3*$^{-/-}$: 342.0±42.7; $P>0.05$) and NFJ (GnRH neurons number ± s.e.m.; *Sema3g*$^{+/+}$: 295.3±27.2 vs *Semag3*$^{-/-}$: 244.7±15.6; $P>0.05$) compared to wild types. In turn, FB of *Sema3g*$^{-/-}$ contains a significantly reduced number of GnRH^{+} cells compared to wild type mice (GnRH neurons number ± s.e.m.; *Sema3g*$^{+/+}$: 511.0±31.3 vs. *Sema3g*$^{-/-}$: 224.7±34.1; $P<0.01$, Student's t-test; Figure 4A-B). Interestingly, we observed the presence of aggregates of faintly GnRH^{+} cells in the NFJ of mutants (Figure 4A, wavy arrow in NFJ mutant panel), that are reminiscent of dead cells. This might explain the reduced number of GnRH neurons reaching the FB.

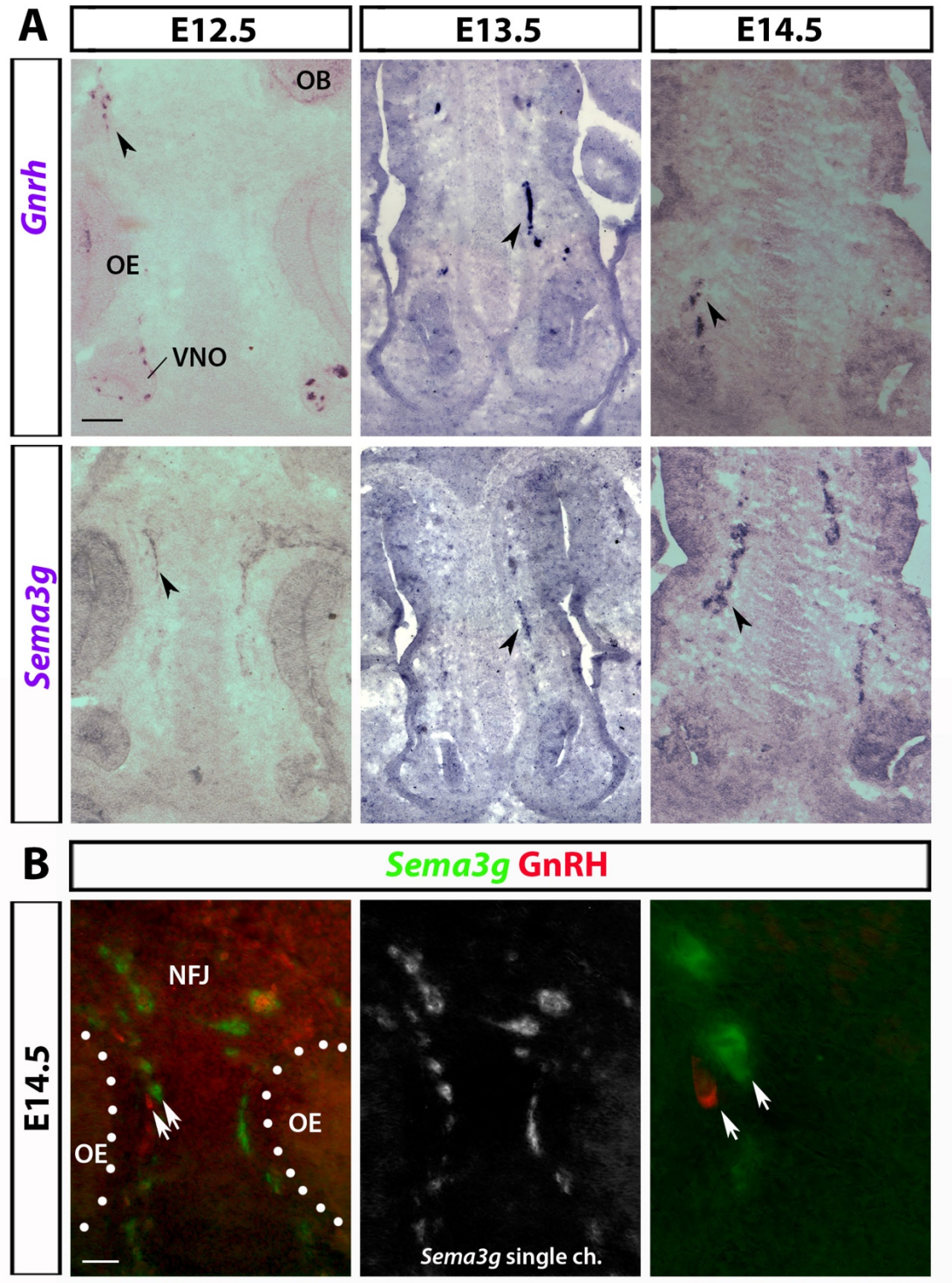

Figure 3 – *Sema3g* mRNA expression during GnRH neuron development. (A) ISH for *Gnrh* and *Sema3g* on coronal sections of mouse heads at the indicated developmental stages; arrows indicate examples of migrating GnRH neurons and of Sema3g^{+} cells. **(B)** *Sema3g* ISH (green signal) of coronal sections from E14.5 heads at the level of the nasal region followed by immunolabelling for GnRH (red signal) revealed that *Sema3g* is expressed by cells that are co-migrating with GnRH neurons (white arrows). Scale bars: 150 µm (A), 100 µm (B). Abbreviations: OB, olfactory bulb; OE, olfactory epithelium; VNO, vomeronasal organ; NFJ, nasal forebrain junction.

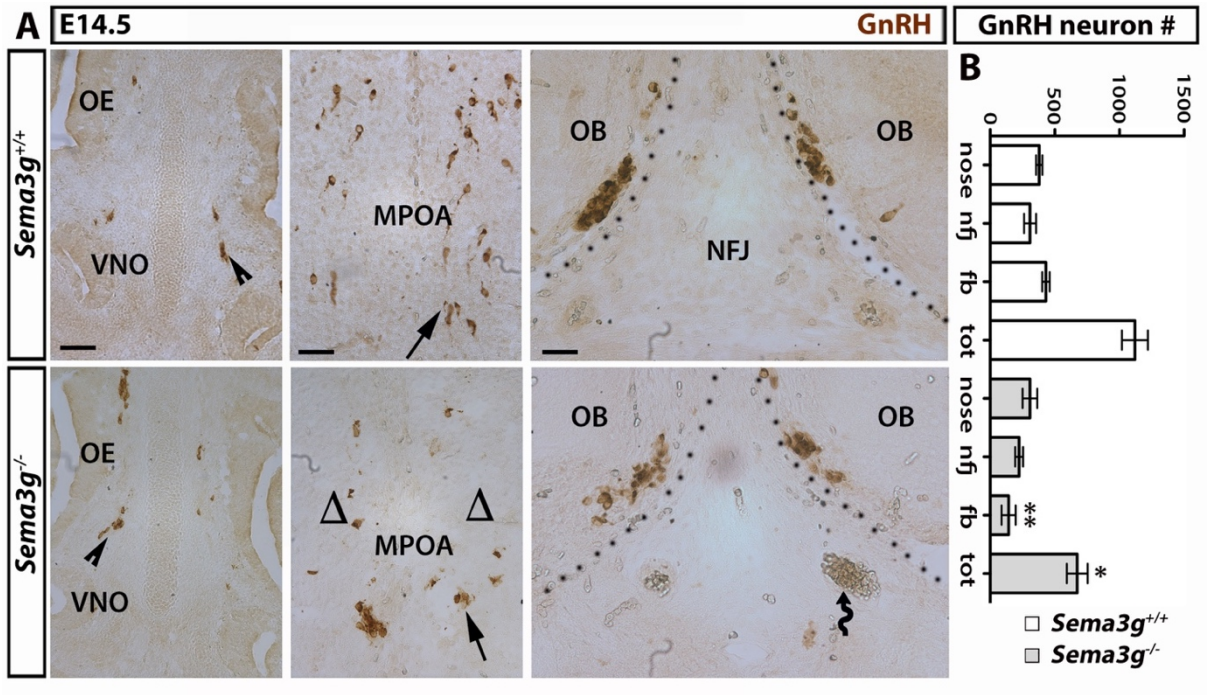

Figure 4 – Reduced GnRH neuron numbers in the *Sema3g*-null embryos. (**A**) Coronal sections of E14.5 mouse heads of the indicated genotypes were immunolabelled for GnRH to reveal GnRH neurons in the nasal compartment (panels in first column), in the MPOA (panels in second column) and in the NFJ (panels in third column). Black dots indicate border with OB. Black arrowheads indicate examples of migrating GnRH neurons in the nose, black arrows indicate examples of neurons in the MPOA. Presence of faintly labelled GnRH neurons accumulating at the level of the NFJ are seen in the mutant mice and indicated with a wavy arrow. (**B**) Quantitative counting analysis showing a significant reduction in the total number of GnRH neurons in *Sema3g*-deficient mouse heads at E14.5, which is explained by a significant reduction of GnRH neurons reaching the FB, but not nose (n=3, * $P<0.05$, ** $P<0.01$ Student's *t* test). Scale bars: 150 µm. Abbreviations: OB, olfactory bulb; OE, olfactory epithelium; VNO, vomeronasal organ; NFJ, nasal forebrain junction; MPOA, medial preoptic area; FB, forebrain.

Yet, altered GnRH neuron migration can be subsequent to defects in OLF/VN nerves patterning or to malformations in BV (Cariboni et al., 2011a; Cariboni et al., 2011b). We explored these possibilities in *Sema3g*-null mice and we analysed the patterning of BV and OLF/VN nerves by performing immunofluorescence experiments using Isolectin-B4 (IB4) and an antibody anti-peripherin, respectively. However, no obvious differences in the anatomy of BV (Figure 5A) nor OLF/VN nerves (Figure 5B) have been reported.

Overall, these data suggest that Sema3g acts independently by BV and OLF/VN nerves on GnRH neuron migration and therefore are consistent with a primary cell-autonomous role for Sema3g signalling in GnRH neurons.

Loss of Sema3g decreases adult median eminence innervation by GnRH neurons and impairs testes functionality.

Having confirmed that lack of Sema3g impairs GnRH neuron migration during foetal life, we investigated the impact of Sema3g loss in adult mice, where ME innervation by GnRH neuron neurites and testes size are reliable outcome of hypothalamic defects. Consistently, with embryonic defects, we observed a reduced number of GnRH-positive neurites at the ME in adult *Sema3g*-null compared to wild type males (Figure 6A-B; GnRH pixel intensity reduction in ME neurites in mutants relative to wild type littermates of 36±0.8%).

To investigate whether the reduction in the number of GnRH neurons is reflected in alterations in the gonads, we analysed the testes of adult male *Sema3g*-null and wild type mice (n=2 for each type). No major differences in the weight, volume or morphological appearance of testes have been observed between the wild-type and mutant mice. However, histological examination revealed a small but significant reduction in the density of seminiferous tubules (mean count/mm^2 ± s.e.m.; *Sema3g*$^{+/+}$ 16.3±0.8 vs. *Sema3g*$^{-/-}$14.2±0.5; P<0.05, Student's t - test). Although spermatogenesis appeared complete in the seminiferous tubules of both groups, we noticed in H&E stainings a decreased area of the interstitial tissue in the mutant testes compared to wild type littermates, which could be due to a reduced number of Leydig cells, and a general loss of cell density in mutant tubule walls, ascribable to lack of Sertoli cells (Figure 6C-D). To get further insights into testes functionality, we stained wild type and mutant testes paraffin-embedded sections with specific antibodies for markers of Leydig cells (Cyp17A1) and Sertoli cells (Sox9) (Wang et al., 2015) and then quantified the number of Cyp17A1$^+$ and Sox9$^+$ cells. In agreement with our preliminary observations, testes of mutant mice show a decreased and significant number of Sertoli cells (Figure 6E-F, mean Sox9$^+$

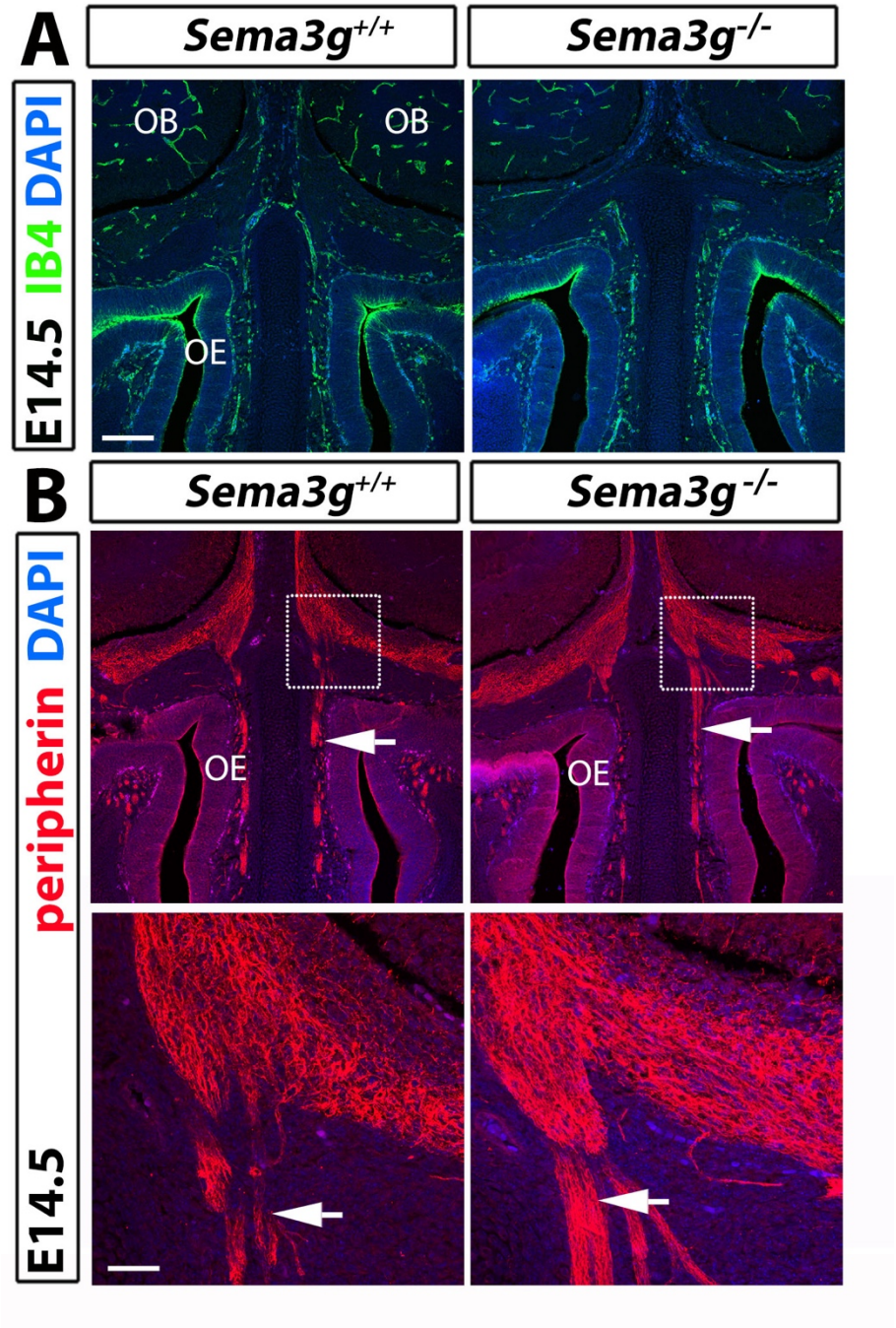

Figure 5 – Sema3g is dispensable for axonal and vascular patterning in the embryonic nose. (A) Normal nasal axon and (B) blood vessel patterning in *Sema3g*-null mutants. Coronal sections of E14.5 mouse heads of the indicated genotypes at the level of the nose were labelled with the blood vessel marker IB4 (A) or immunolabelled for peripherin (B). Nuclei were counterstained with DAPI. White arrowheads indicate examples of normal axonal branches projecting to the OB. Scale bars: 150 µm (A–B), 50 µm (higher-magnification images of boxed areas in B). Abbreviations: OB, olfactory bulb; OE, olfactory epithelium.

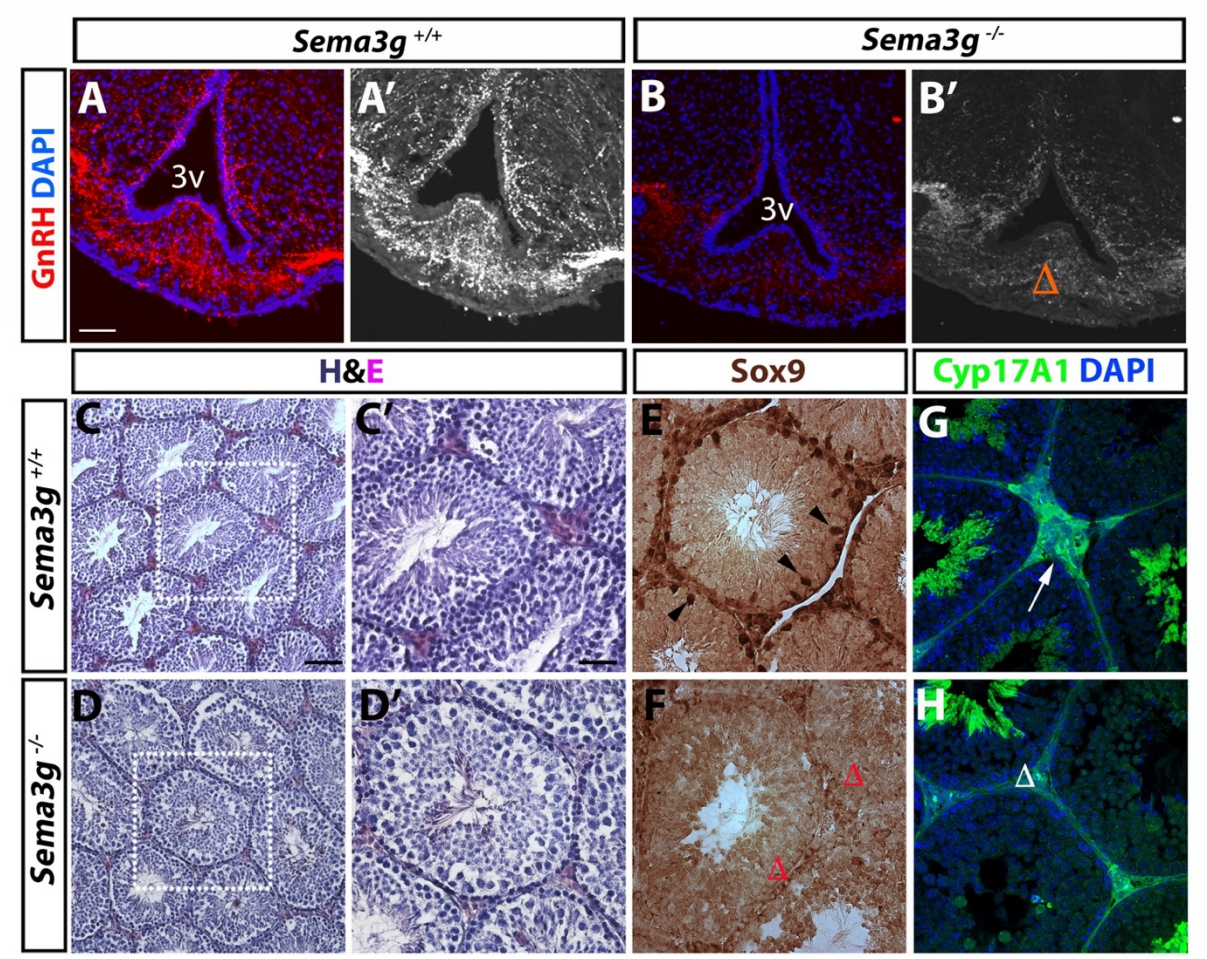

Figure 6 - Sema3g deficiency reduces GnRH neuron projection to the median eminence and impairs testes function. (A-B) Coronal sections of adult hypothalamus of the indicated genotypes were immunostained to identify GnRH-positive axons projecting to the wild type ME; innervation was poor in mutants compared to wild types (indicated by a red delta). Single-channel images of GnRH staining are shown in panels A' and B'. **(C)** H&E staining of seminiferous tubules from wild-types and Sema3g null mice show no gross alterations in the differentiation of spermatozoa. High magnifications of the boxed areas are shown in C' and D'. **(E-F)** Immunostaining for the Sertoli cell marker Sox9 reveals a lack (red delta symbols) of Sertoli cells in the *Sema3g* null testes compared to wild-types. Examples of $Sox9^{+}$ cells are indicated with black arrowheads in E. **(G-H)** Immunofluorescence staining of tubules seminiferous for the Leydig cell marker Cyp17A1 reveals a decrease of Leydig cells in mutant testes compared to controls. Nuclei were counterstained with DAPI. Abbreviations: 3v, third ventricle; H&E, haematoxylin and eosin Scale bars: 100 µm (A-B); 150 µm (C-D); 100 µm (C'-D', E-H).

cells/tubule ± s.e.m.; *Sema3g*$^{+/+}$ 12.8±0.8 vs. *Sema3g*$^{-/-}$ 4.7±1.5; P<0.001, Student's t–test) and a significant decreased expression of Cyp17A1 (Figure 6G-H, mean Cyp17A1^{+}/DAPI^{+} cells/field ± s.e.m.; *Sema3g*$^{+/+}$ 26.3±1.7 vs. *Sema3g*$^{-/-}$ 9.6±1.1; P<0.001, Student's t–test) compared to wild type littermates.

Based on these findings in the genetic *Sema3g*-null mouse model, combined with the identification of a *SEMA3G* mutation in two brothers with IGD and our tissue culture studies using recombinant human SEMA3G, we demonstrated that loss of SEMA3G, either through genetic deletion or mutation, may contribute to the pathogenesis of IGD.

Rhotekin and Natural Killer cell Triggering Receptor genes are expressed in the embryonic mouse head and are additionally mutated in the probands.

Although mice lacking *Sema3g* display GnRH deficiency, they do not recapitulate the other phenotypic features (e.g. facial dysmorphic features and mental retardation) that are in turn peculiar phenotypic feature of the two affected brothers. Hence, we hypothesised that this novel syndrome might result from a synergistic effect of mutated genes in addition to *SEMA3G*. Amongst homozygous variants lying in shared homozygous regions, two additional unreported novel mutations have been identified and they occur in Rhotekin (*RTKN*, chr 2p13.1; ENSG00000114993; NM_001015056, c.1143T>G; p.Ile381Met) and Natural Killer cell Triggering Receptor (*NKTR*, chr 3p22.1; ENSG00000114857; NM_005385.3, c.22600C>T; p.Arg754X) genes (Figure 7A). *RTKN* encodes for a downstream effector of Rho GTPases that has been previously associated to a role in neuroblast differentiation *in vitro* (Thumkeo et al., 2013); *NKTR* instead has been identified as a co-receptor for target recognition of natural killer cells (Anderson et al., 1993; Frey et al., 1991). In both cases, no information is available regarding their role in mouse head differentiation and development.

Thus, to get insights into the possible relevance of these genes in causing some of the developmental defects observed in the two brothers including facial dysmorphic features and mental retardation, we firstly performed ISH on E14.5 mouse embryo cryosections using specific riboprobes for *Rtkn* and *Nktr* transcripts. Interestingly, we found that both genes display a peculiar pattern of expression, completely different from *Sema3g* one. No expression of both genes was detected in the VNO, within nasal mesenchyme and in the MPOA. In turn, we found that *Rtkn* mRNA is expressed mainly in the developing OB (Figure 7B, upper panel) and in the proliferative area of the developing forebrain as ventricular and subventricular zones of the ventral (Figure 7B, lower panel) and dorsal (not shown) forebrain. In addition, *Rtkn* is

A

Chr	Position	Gene	nt sub	aa sub	Poly-Phen	SIFT	Mutation Taster
2	74654363	RTKN	A>C	I381M	possibly damaging	damaging	disease causing
3	42679456	NKTR	C>T	R754X	-	neutral	-

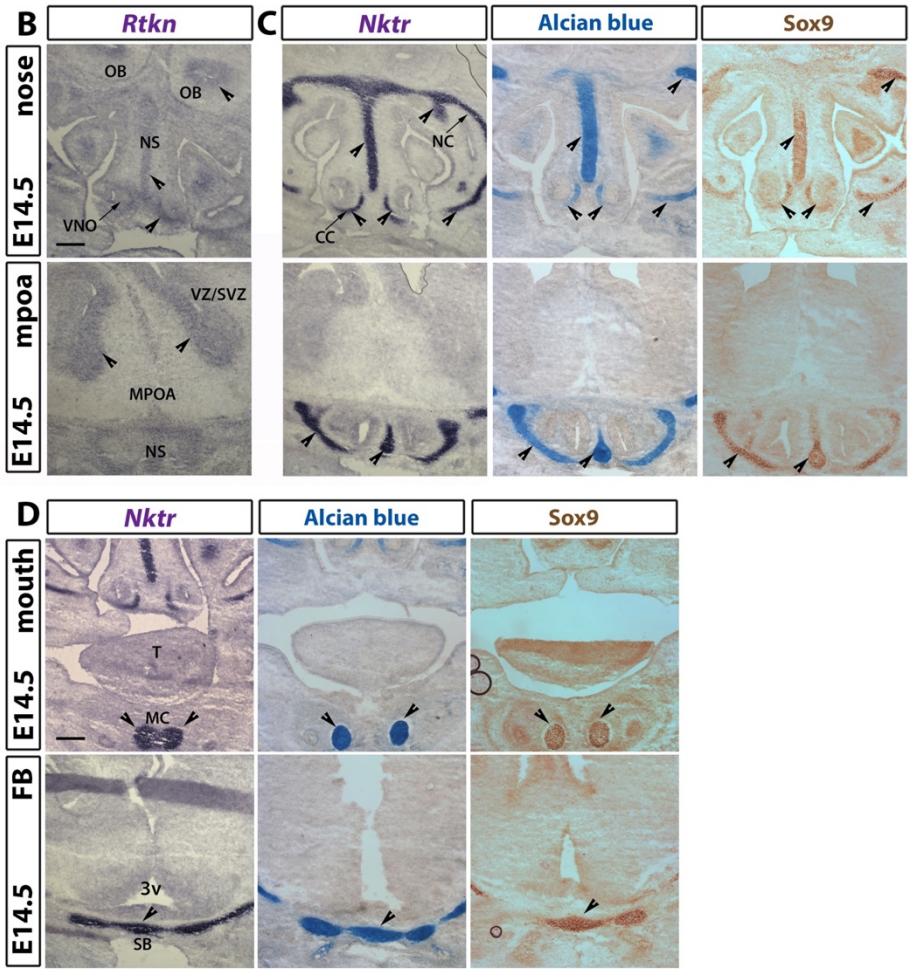

Figure 7 – *Rtkn* and *Nktr* mRNAs are expressed in the mouse embryonic head in the brain and in chondrogenic areas, respectively. (A) *In silico* analysis identified *RTKN* and *NKTR* on chromosome 2 and 3 respectively as additional candidate gene. Nucleotide changes c.1143A>C and c.22600C>T result in protein changes p.Ile381Met and a stop codon gain p.Arg754X. PolyPhen-2, SIFT and Mutation Taster were used to predict structural and functional effects of both amino acid substitutions on proteins structure and function. **(B)** ISH on coronal sections of wild type mouse embryo at E14.5 using antisense riboprobes for *Rtkn* in the nasal compartment (upper panel) and in the FB (lower panel) reveals *Rtkn*-expression in OB and FB (arrowheads). **(C)** ISH for *Nktr* (panels in first column), Alcian blue staining (panels in second column) and Sox9 immunolabelling (panels third column) on coronal sections of wild type mouse embryo in the nasal compartment (upper panels) and FB (lower panels). **(D)** *Nktr* expression overlaps with Alcian blue and Sox9 (arrowheads) in chondrogenic areas of the head both at mouth level (upper panels) and FB level (lower panels). Abbreviations: VNO, vomeronasal organ; CC, capsula cartilaginea; NS, nasal septum; NC, nasal capsule; OB, olfactory bulb; MPOA, medial preoptic area; VZ/VSZ, ventricular zone/subventricular zone; SB, sphenoid bone, MC, Meckel's cartilages; T, tongue; 3v, third ventricle. Scale bar: 250 µm.

also expressed at low levels in the nasal septum and around the VNO (Figure 7B, upper panel). Instead, *Nktr* mRNA shows a highly specific pattern of expression within the mouse embryonic head that is typical of chondrogenic areas. Specifically, we found that *Nktr* is expressed in the nasal septum, in the nasal capsule, in cartilage capsules of the VNO, in Meckel's cartilages and in sphenoid bone primordium (Figure 7C-D).

Interestingly, the analysed stage (E14.5) represents that starting point of facial cartilages development and chondrogenic tissues can be easily visualised by Alcian blue staining or by immunostaining with marker for cranial NCC such as Sox9 (Mori-Akiyama et al., 2003; Pavlov et al., 2003; Suzuki et al., 2016). Thus, to confirm our expression studies for *Nktr*, we stained adjacent sections of embryonic mouse heads at E14.5 with Alcian blue or with an anti-Sox9 antibody and found a precise overlapping pattern of expression among the three stainings. Interestingly, *Nktr* mRNA is exclusively expressed in Sox9/Alcian blue-positive territories, not only restricted to nasal cartilages (Figure 7C) but also in the sphenoid bone cartilage primordium and Meckel's cartilages, which give rise to mandible bone (Figure 7D). Taken together these results provide evidences for a possible role for *Rtkn* and *Nktr* in brain and craniofacial development, respectively and therefore these findings are consistent with a probable involvement of these genes may underlie non-reproductive features observed in our novel form of syndromic IGD.

1.3 Discussion

In the present work, we identified two brothers born from consanguineous parents and affected by a novel syndrome characterised by nHH, facial dysmorphic features, short stature and mental retardation. According to the pattern of inheritance, the composition of the family trio, composed by unaffected and affected siblings, and the consanguinity of parents, we hypothesized an autosomal recessive syndrome. Thus, we applied HZM in combination with WES to identify one or more mutations composing the genetic architecture underlying this peculiar disorder. In particular, HZM was used to narrow down the list of variants obtained from WES, as our hypothesis lead us to consider only variants in a homozygous state within shared homozygous regions of the two brothers. This filtering strategy successfully revealed three novel variants within the shared homozygous regions on chromosome 2 (*RTKN*) and on chromosome 3 (*SEMA3G*, *NKTR*).

We first focussed on *SEMA3G* G166V because nHH is the predominant phenotypic feature in our probands and because Class 3 semaphorins have been already found to regulate

essential roles in GnRH neuron development and mutations in some Sema3s members have been found responsible for the pathogenesis of IGD (Cariboni et al., 2015; Hanchate et al., 2012; Känsäkoski et al., 2014; Young et al., 2012).

Here, we combined different approaches to study the role of SEMA3G along with GnRH neuron physiology and development. First, *in silico* classical prediction tools of mutation pathogenicity confirmed that the *SEMA3G* G166V mutation affects a residue that is highly conserved in various vertebrate species. Then, taking advantage from immortalized GnRH cell line (GN11 cells), we studied *in vitro* the effect of the mutation. We observed that the G166V mutation did not alter synthesis, secretion or binding properties of SEMA3G; yet, although this method has often been used to determine semaphorin binding to receptor-expressing cells (Cariboni et al., 2015; Gu et al., 2005) or tissues (Cariboni et al., 2011b; Giacobini et al., 2008), no reports of this technique measuring differences in affinity between mutated and wild type forms to their specific receptor are available. In turn, G166V mutation significantly affects the chemoattractant activity of SEMA3G WT leading to a reduced GN11 cells migration in a Boyden's chamber assay. Moreover, immunoblotting analysis revealed that the G166V mutation is less able to activate AKT signalling pathway.

Our findings from *in vitro* experiments have also been informative to predict the possible role of SEMA3G *in vivo*. Consistently, mice lacking *Sema3g* exhibit a significant reduced number of GnRH neurons in the FB, since they fail to migrate that far during embryonic development. Along with these data, we found an abnormal accumulation of faintly labelled GnRH neurons at the level of the NFJ. *Sema3g* seems to be highly expressed at this level and moreover we found that Sema3g^{+} cells migrate in close relationship with GnRH neurons within the nasal mesenchyme. Thus, Sema3g-expressing cells may be component of the MM and may provide essential cues for GnRH neuron migration and survival. In agreement with our hypothesis, other semaphorins have been shown to be expressed by MM cells, such as Sema4d by OECs (Geller et al., 2013). As a consequence of reduced hypothalamic GnRH neuron number, we found that *Sema3g*-null mice display a significantly less innervated ME. At gonad level, we did not observe gross differences in testes size and anatomy, but we found morphological changes after histological analysis that showed a significant decrease in the number of Sox9 and Cyp17A1-positive cells in the mutant testes compared to controls. It has been previously demonstrated that IGD mouse models can exhibit normal sized testes even despite the mice being hypofertile or infertile and this appear to be due to additional defects in

androgens production or secretion resulting in unbalanced gonadotropin and/or androgen levels (Marcos et al., 2017).

However, our patients do not only show nHH but they also present non-reproductive symptoms such as facial dysmorphic feature and mental retardation, that are not phenocopied by the *Sema3g* knock out mouse model analysed. Specifically, facial dysmorphism features include defects in the nose and in the chin, which could be caused by mutations in genes implicated in craniofacial development. Further, the two brothers present some learning difficulties and microcephaly that might be explained by mutations of genes affecting brain development. Interestingly, dysmorphic features of the face can be concomitantly present with IGD in known syndromes such as CHARGE and Prader-Willi syndromes. However, we excluded the possibility that our patients are affected by these disorders as they do not show severe ear abnormalities, coloboma and hypotonia, which represent major features associated with CHARGE and Prader-Willy syndromes respectively.

Hence, we hypothesized that additional mutations harboured by *NKTR* and *RTKN* might concur to the onset of this novel multi-trait syndrome. Indeed, by studying the expression pattern of these genes in mice embryos we found that Nktr is strongly and exclusively expressed in chondrogenic areas of mouse embryonic head (i.e. nasal capsule and septum, sphenoid bone cartilage primordium and the Meckel's cartilage). This peculiar pattern of expression goes along with a possible involvement of Nktr in craniofacial development, which heavily depends on the contribution of chondrogenic precursors from the cephalic NC (Cordero et al., 2011; Minoux and Rijli, 2010). Interestingly, NKTR presents a cyclophilin-like domain and mutations in the cyclophilin B gene (*PPIB*), which encodes for a protein involved in collagen hydroxylation, underlie bone formation defects (Pyott et al., 2011); yet, very little is known about Nktr and no reports on Nktr in the context of mouse development are available. Overall, R754X mutation on *NKTR* may underlie craniofacial malformations reported in the two affected siblings, which include prominent nasal bridge, beaked nose, small chin and high palate. On the other side, we found that *Rtkn* is mainly expressed in the developing olfactory bulb and in the proliferative region of the developing forebrain. Interestingly, this protein, which is an effector of Rho GTPases, has been associated with synapse formation and neuroblast differentiation *in vitro* (Iwai et al., 2012; Yuasa et al., 2012). Interestingly, mutations in other members of the Rho GTPases signalling pathway have been previously associated to intellectual disabilities (Ba et al., 2013; Ravindran et al., 2017). Together, these findings strengthen the idea of a possible involvement of I381M mutation on *RTKN* in causing brain

related disorders such as mental retardation observed in our patients. Further, we found weak *Rtkn* expression also in the NS and around the VNO, supporting a role of this gene in craniofacial development as well even because Rho-GTPases and their down-stream effectors have been already associated with osteoblast and chondrocyte differentiation (Strzelecka-Kiliszek et al., 2017). However, these hypotheses should be necessary confirmed by functional studies, such as the generation of knockout mouse models for *Nktr* and *Rtkn* (presently unavailable) or by acute experiments of gene knock-down with shRNAs. Further, the identification of additional mutations in patients affected by similar disorders will allow us to analyse the functional and clinical relevance of these genes, and the possible genetic interactions with *SEMA3G*.

In conclusion, in our study we have identified two brothers affected by a novel syndrome characterized by nHH, facial dysmorphic features and intellectual disabilities. Because they were born from unaffected consanguineous parents, we hypothesize an autosomal recessive pattern of inheritance and therefore we combined HZM with WES to identify three novel mutations in *SEMA3G*, *NKTR* and *RTKN* genes. *In silico*, *in vitro* and in *vivo* models allow us to demonstrate that defective SEMA3G signalling underlies nHH and to anticipate that synergistic effects of RTKN and NKTR may contribute to the complex nature of this novel form of syndromic IGD.

2. Class A plexins

Summary

It is well established that SEMA3A represents an essential axon guidance cue for the development of the VN nerves and therefore for GnRH-neuron migration. Further, mutations in *SEMA3A* have been found in up to 6% of overall patients affected by KS. However, class A plexins that act as signal transducing receptors for SEMA3A have been poorly investigated in the context of GnRH/olfactory systems development. Here, we defined the expression pattern of the four PLXNAs in the nasal and hypothalamic compartments during mice embryonic development and we determined that Plxna1 and Plxna3 are expressed by the VN nerves that compose the axonal scaffold that allows a proper migration of GnRH neurons. Then, we functionally determined the requirement of Plxna1 and Plxna3 in GnRH/olfactory systems by using genetically modified mouse models. Single deletions of *Plxna1* or *Plxna3* did not show any obvious defects in the development of GnRH neuron/olfactory systems, whereas mice

lacking both *Plxna1* and *Plxna3* displayed a severe hypogonadal phenotype, with strongly reduced hypothalamic GnRH neurons, less innervated ME and hypoplastic gonads. Overall, these findings help to identify which PLXNA is conveying SEMA3A signalling in GnRH/olfactory systems and to unravel the role of A-type plexins in GnRH neuron physiology. Moreover, our results will help to predict novel candidate genes to be screened in patients affected by KS.

2.1 Background

KS is caused by neurodevelopmental defects of GnRH neurons that do not reach the MPOA of the hypothalamus and this defect is usually subsequent to a failure of OLF/VN/TN nerves to contact the OB (Boehm et al., 2015; Taroc et al., 2017). During embryonic development, GnRH neurons follow an axonal scaffold composed by intermingled OLF/VN/TN nerves in order to navigate first across nasal mesenchyme and then in the basal FB. These nerves arise from OE (OLF nerves) and from VNO (VN/TN nerves) and then extend their axons towards main and accessory OB respectively, forming bundles of fibres within the nose. At NFJ level, a subset of peripherin-expressing VN/TN nerves (also called cauda branch of VN nerves or cVN nerve) turns caudally and ventrally, avoiding OB and invading the basal FB. GnRH neurons follow this transient branch in order to migrate across the basal FB as well (Yoshida et al., 1995). First evidence of this correlation has been provided by Prof. Donald Pfaff group that analysed a single human foetus affected by KS has that was found to have accumulated GnRH neurons at the level of the CP, which separates the nasal cavity from the brain (Schwanzel-Fukuda et al., 1989). This distribution of GnRH neurons strengthened the possibility of disrupted GnRH neuron guidance perhaps due to a malformed axonal scaffold. Accordingly, mouse mutants with disrupted axon guidance such as *Sema3a*-null mice, demonstrated that Sema3a is essential for GnRH neuron migration by guiding OLF/VN/TN nerves during embryogenesis. Thus, *Sema3a* knockout mouse embryos display GnRH neurons accumulated at the NFJ, outside the FB, as observed in the human KS foetus (Cariboni et al., 2011a). Subsequent genetic analysis of others confirmed these findings revealing the presence of heterozygous mutations lying on the *SEMA3A* gene in a subset of patients with KS (Hanchate et al., 2012; Känsäkoski et al., 2014; Young et al., 2012).

To exert its biological function of axon guidance cue, SEMA3A needs to bind to a complex of transmembrane receptors composed by a ligand binding subunit, either NRP1 or NRP2, and a signal transducing subunit, typically one of the members of the A-type plexin family, termed PLXNA1-4 (Alto and Terman, 2017). We found that SEMA3A-mediated

guidance of the cVN nerves required the presence of either NRP1 or NRP2, as mice lacking Sema3a signalling through both Nrp1 and Nrp2 phenocopied *Sema3a*-null mice regarding cVN/TN nerves and GnRH neuron defects (Cariboni et al., 2011a). Specifically, the cVN/TN nerves do not enter the forebrain in mutants, but instead is misrouted projecting to an area adjacent to the OB. However, which specific PLXNA protein is responsible for SEMA3A/NRP-mediated cVN nerves guidance and therefore GnRH neuron migration into the forebrain has not yet been determined with certainty. So far, only a recent work has investigated the role of class A plexins in the context of neuroendocrine reproductive axis, highlighting the possible involvement of PLXNA1 in the pathogenesis of KS. Heterozygous *PLXNA1* mutations have been found in KS patients alongside mutations in *SEMA3A*, *NRP1* and *NRP2* (Marcos et al., 2017). Moreover, mice with a homozygous *Plxna1*-null mutation showed a phenotype that resembles the KS in humans, although with a very low penetrance as it affects only 1/3 of analysed mice and in ales severe form compared to *Sema3a*-null mice. The KS-like phenotype manifests itself in male mice (P40) as low fertility index, subsequent to less innervated ME and smaller seminal vesicles, and embryonic abnormal OB (Marcos et al., 2017). This observation raises the possibility that PLXNA1 may act as the axonal SEMA3A co-receptor important for cVN/TN nerves and therefore GnRH neuron guidance into the brain.

PLXNAs are expressed in redundant and various pattern depending on developmental stage and tissue. Interestingly, we found that only Plxna1 and Plxna3 are detectable in VN nerves in the nasal region and the sole Plxna1 in the cVN/TN nerves within FB. Hence, we analysed single and compound mouse mutants for *Plxna1* and *Plxna3* and found that single *Plxna1* or *Plxna*3-null mice do not show any defects either in GnRH neurons or in cVN/TN nerves. In turn, compound deletion of *Plxna1;Plxna3* lead to a severe KS-like phenotype, characterized by a strong reduction of GnRH neurons reaching the FB, subsequent to aberrant cVN/TN nerves formation. Different from single *Plxna1*-null mice described in Marcos and co-workers work, *Plxna1;Plxna3*-null mice strongly phenocopy *Sema3a* knockout mice, confirming the role of Plxna1 in GnRH system and indicating Plxna3 as a novel regulator of GnRH neuron development. Therefore, mutational analyses for *PLXNA3* in patients with KS and related fertility disorders should be considered.

2.2 Results

Plxna1 and Plxna3 are co-expressed during GnRH neuron migration

To determine whether PLXNA1 acts in partial redundancy with other(s) A-type plexin to mediate cVN/TN nerves and GnRH neuron guidance, we have first compared the expression pattern of *Plxna1-4* mRNAs in the developing mouse by ISH using specific antisense riboprobes. In agreement with prior reports (Marcos et al., 2017; Murakami et al., 2001; Suto et al., 2003), we confirmed that *Plxna1* was expressed at E12.5 both in the VNO and OE, where VN and OLF axons originate, respectively (Figure 1A) and additionally found that *Plxna3* mRNA displayed a similar expression pattern (Figure 1A). Intriguingly, *Plxna1* and *Plxna3* transcripts were detected in cells of the MM within the nasal mesenchyme (Figure 1A), which compose a mixed population of cells that includes neurons and OECs (Miller et al., 2010). In contrast, *Plxna2* and *Plxna4* mRNA were more weakly expressed in the VNO/OE and by MM cells (Figure 1A). At E14.5, when GnRH neuron migration is at its peak, *Plxna1* and *Plxna3* mRNAs were still expressed in the OE and VNO, whereas the expression of *Plxna2* and *Plxna4* was absent in the VNO and weak in the OE (Figure 1B). Based on these expression patterns, Plxna3 emerged as best candidate for cooperating with Plxna1 in transducing Sema3a signals for cVN nerves axon guidance.

To better characterized cells expressing Plxna1 and Plxna3 and to determine which cell types express Plxna1 or Plxna3 in territories relevant to GnRH neuron migration, we immunostained E12.5 and E14.5 mouse wildtype heads with specific antibodies for Plxna1 or Plxna3, tested on *Plxna1* and *Plxna3* knock out tissues (Figure 2E). Double labelling for both Plxna1/a3 with a marker for neuronal cells, i.e. anti-Tuj1 antibody for neuronal-specific beta 3 tubulin (Tubb3), showed that both Plxna1 and Plxna3 was expressed at E12.5 and E14.5 by neuronal cells arising from VNO and OE and migrating within the nasal mesenchyme (Figure 2A-B). On the other side, double labelling for the OECs marker S100 at E12.5 and E14.5 showed that neither Plxna1 nor Plxna3 are expressed by OECs, but instead Plxna1^{+} and Plxna3^{+} axons were surrounded by OECs that envelope axons (Figure 2C-D). Furthermore, to assess whether GnRH neurons or VN nerves express one of these two plexins, double labelling with antibodies for peripherin and for Gnrh were performed. Peripherin-expressing VN nerves also showed expression of Plxna1 and Plxna3 in the nose; in turn, expression of the only Plxna1 was detectable in peripherin-positive cVN nerves within the basal FB (Figure 3-B, lower panels). Instead, double labelling with an antibody for Gnrh did not detect Plxna1 and Plxna3 on GnRH neurons neither in the nose nor in the ventral FB at E14.5 (Figure 3A-B, upper panels).

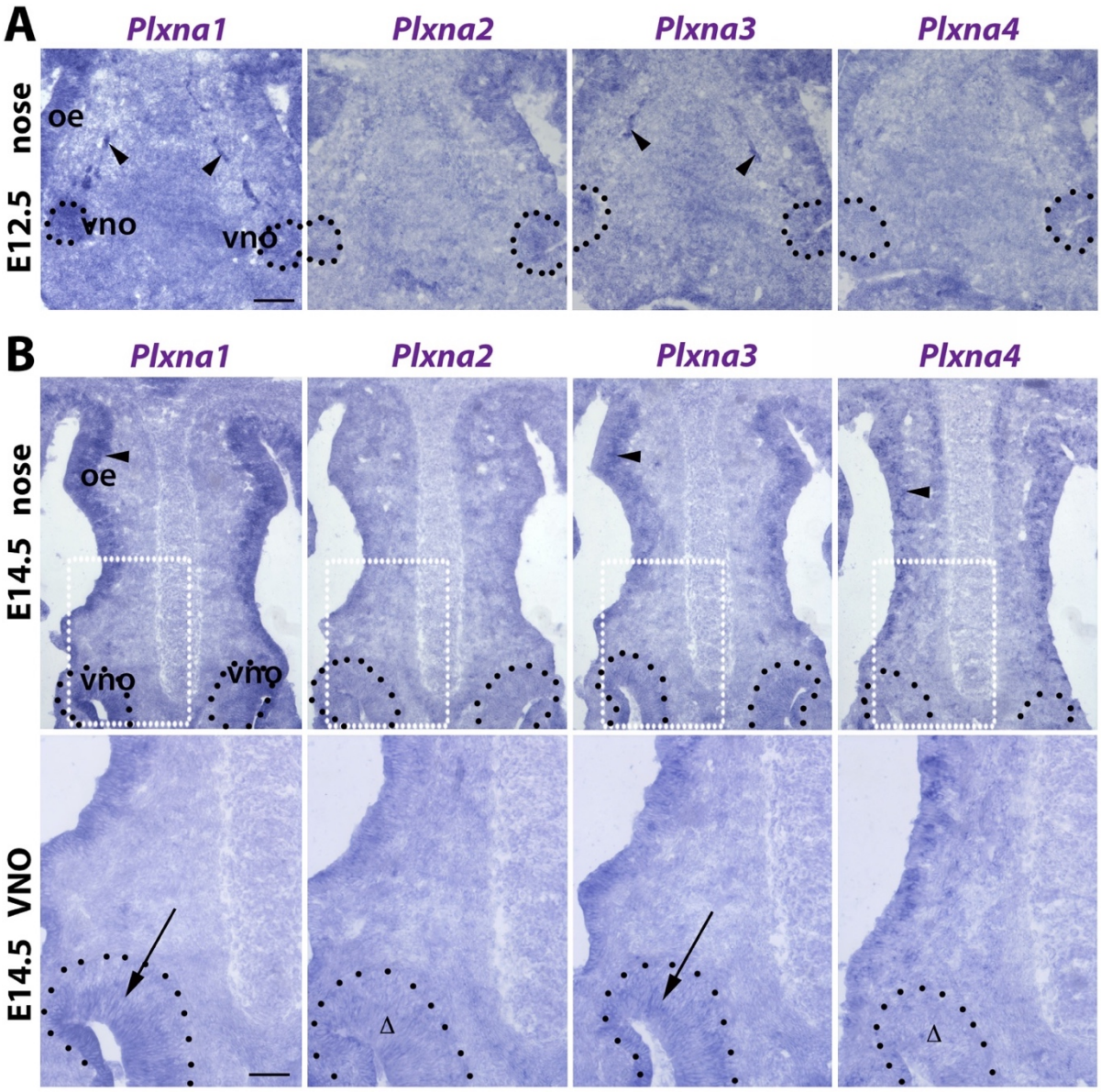

Figure 1 – Differential expression of *Plxna1-4* transcripts during mouse embryonic development in the nasal region. (A) Coronal sections of E12.5 mouse heads at nose level RNA-labelled with specific riboprobes for *Plxnaa1-4* mRNA; *Plxna1* and *Plxna3* are detected in vomeronasal organ (vno) and in the nasal mesenchyme (arrowheads). **(B)** Coronal sections of E14.5 mouse heads at nose level RNA-labelled with specific riboprobes for *Plxna1-4* mRNA; *Plxna1* and *Plxna3* are detected in VNO (arrows in lower panels) and OE while *Plxna2* and *Plxna4* only in the OE (arrowheads in upper panels) and not in the VNO (Δ in lower panels). The black dots delineate the vno; white dots represent high magnification areas. Abbreviations: VNO, vomeronasal organ; OE, olfactory epithelium. Scale bars: 150 μm (A. B upper panels), 100 μm (B lower panels).

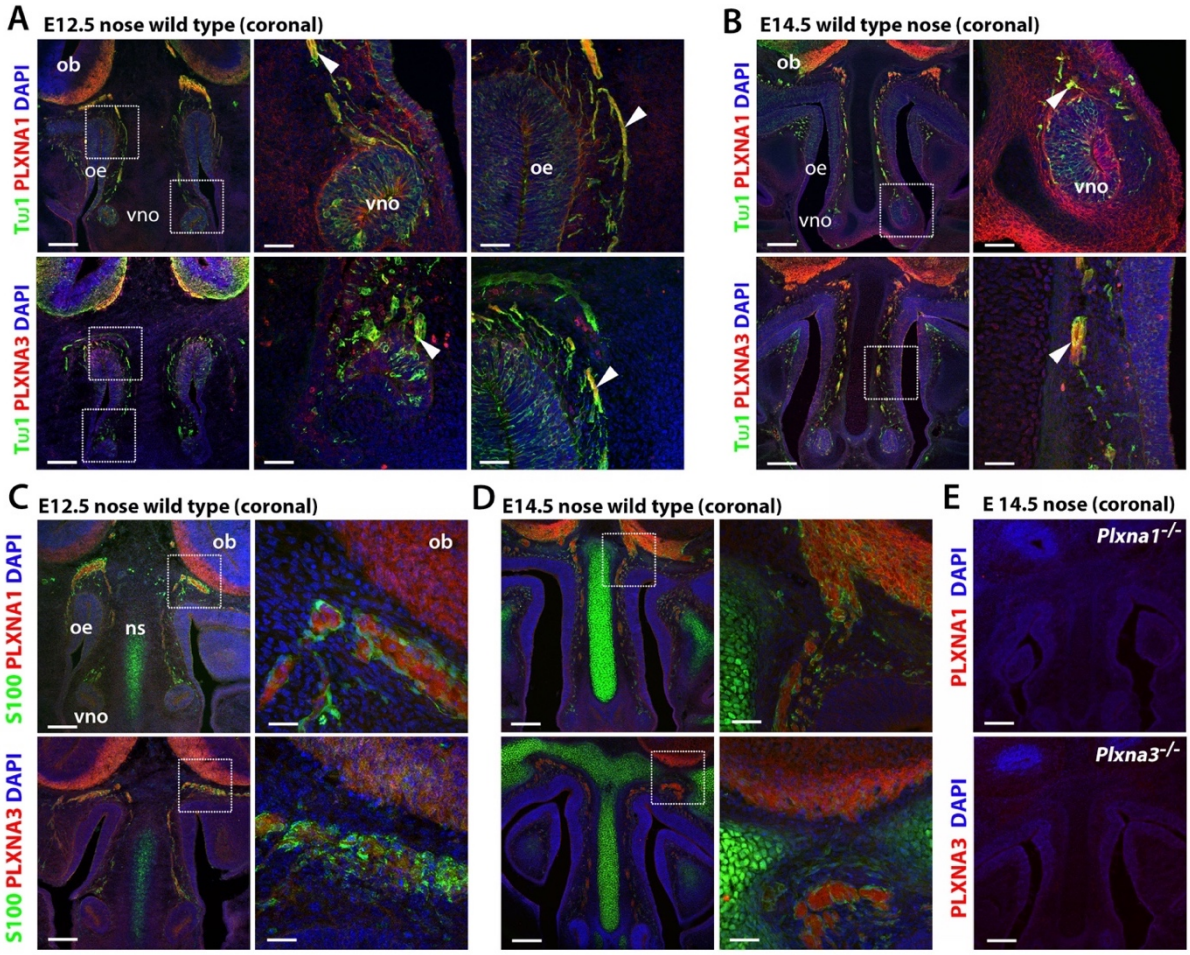

Figure 2 – Plxna1 and Plxna3 are expressed by neuronal progenitors and not by OECs. (A-B) Expression of Plxna1 and PlxnA3 on Tuj1^{+} neurons and fibres. Coronal sections of mouse heads at E12.5 (A) and E14.5 (B) at the level of nasal area were immunolabeled for Tuj1 (in green) and Plxna1 or Plxna3 (in red). White squares represent magnified images on the right. Arrowheads indicate examples of Tuj1^{+}/Plexina1^{+} and Tuj1^{+}/Plexina3^{+} neurons and axons. **(C-D)** Plxna1 and Plxna3 are not expressed by S100^{+} OECs. Coronal sections of mouse heads at E12. 5 (C) and E14.5 (D) at the level of the nasal area were immuno-labelled for S100 (in green) and Plxna1 or Plxna3 (in red). White squares represent magnified images on the right. No colocalization was detected between OEC labelled for S100 and Plxna1^{+} or Pxna3^{+} cells. **(E)** Plxna1 and Plxna3 antibodies were tested for specificity on sections from *Plxna1* and *Plxna3* null mice, respectively. Abbreviations: OE, olfactory epithelium; NS, nasal septum; VNO, vomeronasal organ; OB, olfactory bulb. Scale bars: 150 µm (low magnifications), 50 µm (high magnifications).

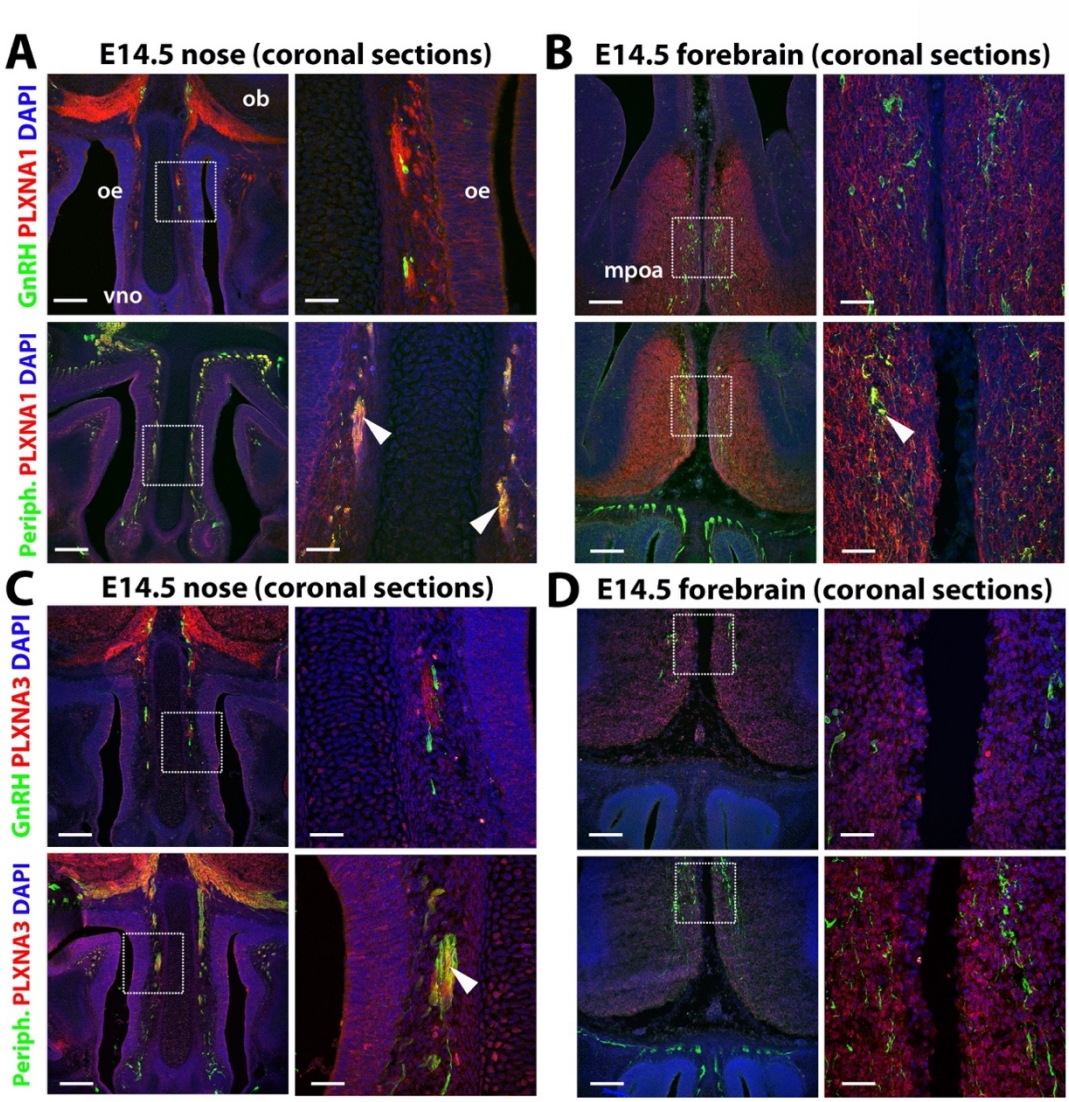

Figure 3 – Expression of Plxna1 and Plxna3 on VN nerves. (A-B) Coronal sections of mouse heads at E14.5 at the level of the nasal area (A) and at the level of the MPOA (B) were immuno-labelled for Plxna1 (in red), GnRH (in green, upper panels) and peripherin (in green, lower panels); white squares represent magnified images on the right. Arrowheads indicate examples of peripherin^{+}/Plexina1^{+} found both in the nose and in the MPOA. **(C-D)** Coronal sections of mouse heads at E14.5 at the level of the nasal area (C) and at the level of the MPOA (D) were immuno-labelled for Plxna3 (in red), GnRH (in green, upper panels) and peripherin (in green, lower panels); white squares represent magnified images on the right. Arrowheads indicate examples of peripherin^{+}/Plexina3^{+} found only in the nose. Abbreviations: OE, olfactory epithelium; VNO, vomeronasal organ; OB, olfactory bulb; MPOA, medial preoptic area. Scale bar: 150 µm (low magnifications), 50 µm (high magnifications).

Additionally, thanks to a collaboration with HDBR (Human Developmental Biology Resources) we had the possibility to analyse the expression of human PLXNA1 and PLXNA3 on human foetus heads. Migration of GnRH neurons in human foetuses is reported to occur between CS18, corresponding to GW5, and GW12. We analysed a human embryo at CS19, a stage representing initial phases of GnRH neuron migration and similar to E12.5 in mice, in order to confirm the expression pattern of PLXNA1 and PLXNA3 in humans. We stained sagittal cryosections using the same antibodies since they exhibit cross-reactivity and we demonstrated that both PLXNA1 and PLXNA3 are expressed in cells emerging from the OE and migrating towards the OB through nasal mesenchyme (Figure 4).

Plxna1;Plxna3-null mice display abnormal GnRH neuron embryonic development and adult median eminence innervation

To compare the distribution and number GnRH neurons in wild type, *Plxna1*$^{-/-}$ and *Plxna3*$^{-/-}$ mutant mice, we immunostained coronal sections though entire E14.5 heads for GnRH, as previously described (Cariboni et al., 2011a; Cariboni et al., 2015). Single knock out mice contained a total number of GnRH neurons comparable to wild type littermates and, more importantly, GnRH neurons reaching the FB in wild type and single mutant mice were similar (Figure 5 and Table 1). Nevertheless, although not statistically significant maybe due to the small sample size that do not allow to detect small differences between genotypes, a small increase of GnRH neuron density was observed at the NFJ of *Plxna1*$^{-/-}$ and *Plxna3*$^{-/-}$ mutants, suggesting a possible delay in forebrain entry (Table 1). These findings raised the possibility that both Plxna1/a3 contribute to the guidance of GnRH neurons, even though each on its own is largely dispensable for this process. Accordingly, E14.5 *Plxna1*$^{-/-}$*;Plxna3*$^{-/-}$ double mutants contained a significantly larger proportion of GnRH neurons in the nose than wild-type littermates, concomitantly to a corresponding significant decrease in the forebrain (Figure 5 and Table 1). The overall similar number of GnRH neurons in double mutants compared to wild-types corroborated our hypothesis that lack of hypothalamic GnRH neurons is due to defective migration, rather than decreased formation or survival (Table 1).

Consistently with the severe phenotype observed in compound *Plxna1;Plxna3*-null embryos, ME innervation by GnRH neuron axonal terminals, was strongly decreased at P10 in double mutant mice compared to wild type and single knock out mice (Figure 6).

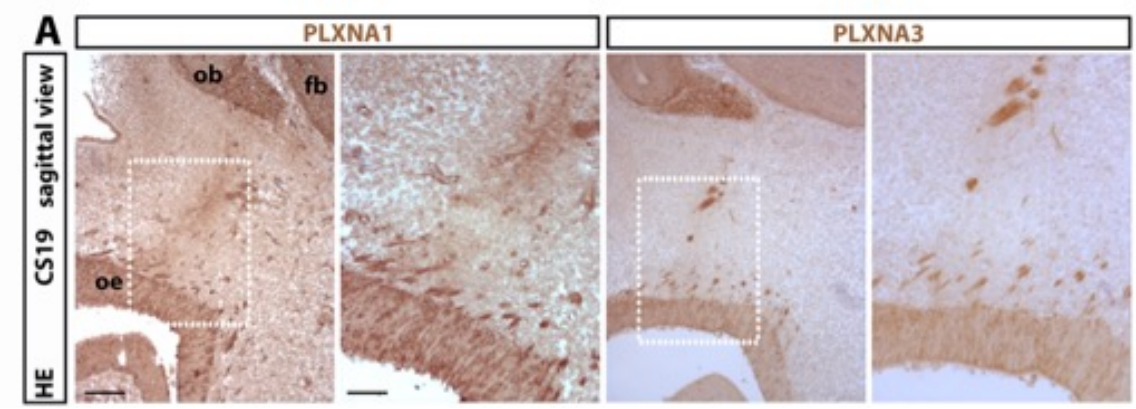

Figure 4 – Expression of PLXNA1 and PLXNA3 in human foetus at CS 19. Sagittal paraffin-embedded sections of human embryo at CS19 (6th gestational week) immunostained for PLXNA1 and PLXNA3 revealed expression in cells emerging from developing OE and in axons contacting OB. White squares represent high magnification on the right. Abbreviations: HE, human embryo; OE, olfactory epithelium; OB, olfactory bulb; FB, forebrain. Scale bars: 150 μm (low magnifications), 100 μm (high magnifications).

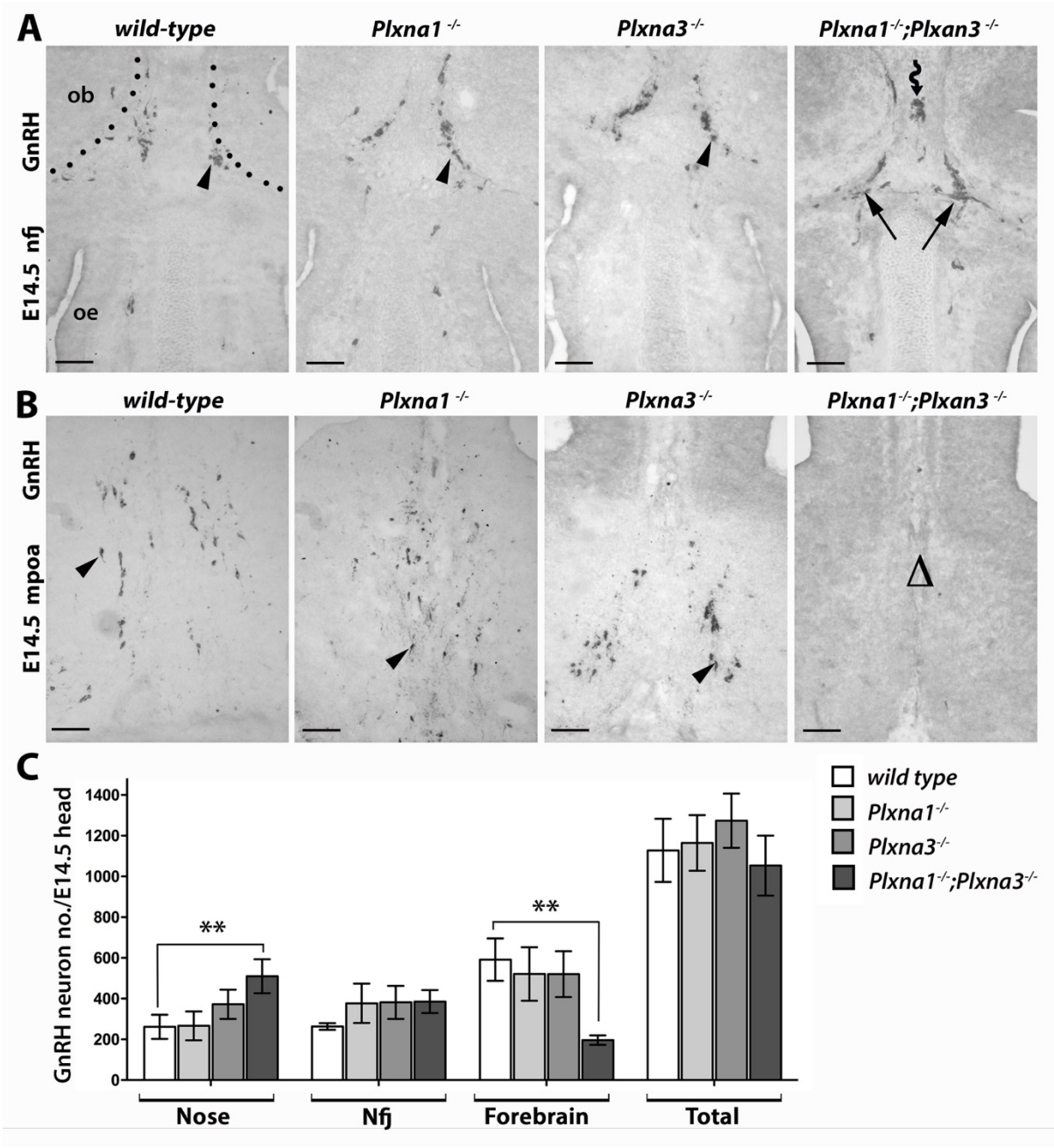

Figure 5 – Abnormal migration of GnRH neurons in the nose and decreased GnRH neuron number in the developing hypothalamus of *Plxna1;Plxna3* compound-null mutants. (A-B) Coronal sections of E14.5 heads from wild type, *Plxna1*$^{-/-}$, *Plxna3*$^{-/-}$ and *Plxna1*$^{-/-}$*;Plxna3*$^{-/-}$littermate embryos were immunolabelled for GnRH to reveal migrating neurons in the NFJ (A) and in the MPOA (B). Black arrowheads indicate examples of migrating GnRH neurons at the level of the NFJ and MPOA. The boundary of each OB is indicated with a black dotted line. Black arrows indicate accumulating GnRH neurons and the wavy arrow points at ectopic GnRH neurons in the meninges tissue between the OB. The lack of GnRH neurons in the mutant MPOA is indicated with Δ. **(C)** Graph showing number of GnRH^{+} neurons per embryo's head at E14.5 as mean ± s.d.; **P<0.01; One way ANOVA/Dunnett's test. Abbreviations: OE, olfactory epithelium; NS, nasal septum; OB, olfactory bulb; MPOA, medial preoptic are; NFJ, nasal-forebrain junction. Scale bar: 150 μm (A, B).

Genotype	Nose	Nasal-forebrain junction	Forebrain	Total
WT (n=4)	261.5 ± 59.04	263.5 ± 16.18	591.8 ± 104.0	1228 ± 154.9
Plxna1 $^{-/-}$ **(n=6)**	266.3 ± 71.16	377.0 ± 96.71	521.0 ± 131.3	1164 ± 136.6
Plxna3 $^{-/-}$ **(n=3)**	372.0 ± 71.63	381.7 ± 81.38	520.3 ± 112.5	1274 ± 133.1
Plxna1/a3 $^{-/-}$ **(n=3)**	510.0 ± 83.52 **	347.0 ± 58.51	196.3 ± 23.59 **	1053 ± 147.5

Table 1 – Total and partial numbers of GnRH^{+} neurons counted in E14.5 mouse heads. GnRH neuron numbers of the indicated genotypes are indicated as mean ± s.d.; significant P-values were calculated by One way ANOVA followed by Dunnett's test, **P<0.01.

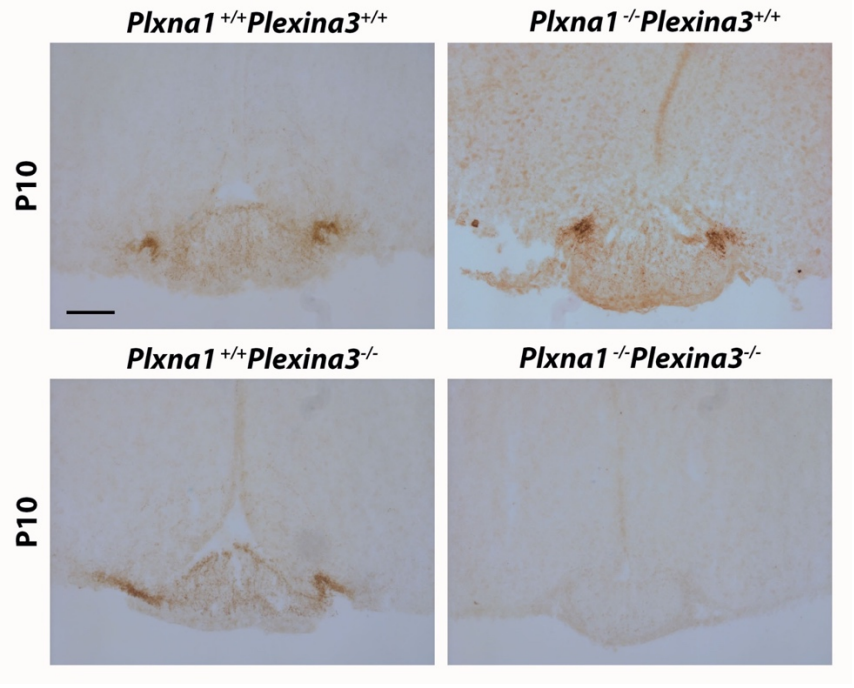

Figure 6 – Combined but not single loss of Plxna1 and Plxna3 reduces GnRH neuron innervation of the median eminence. Coronal sections of adult hypothalamus of the indicated genotypes were immunostained to identify GnRH-positive axons projecting to the ME. ME innervation was poor in double mutants compared to wild type and single mutant mice. Scale bar: 150 µm.

Mispatterned OLF/VN nerves cause migration defects of Plxna1;Plxna3 compound-null mice

To prove that the failure of GnRH neurons to enter the FB in the *Plxna1;Plxna3*-null mice is due to aberrant patterning of the VN/cVN nerves similar to the *Sema3a*-null and *Nrp1*^{sema}*/Nrp2* compound null mice, we performed immunofluorescence experiments by using anti-Gnrh and anti-peripherin antibodies on adjacent sections at E14.5.

Consistent with this hypothesis, we found that the position of ectopic GnRH neurons coincided with the location of ectopic peripherin^{+} axons (Figure 7). Thus, the nearly complete absence of GnRH neurons in the MPOA of these mice is due by the lack of perpherin^{+} fibres in the same position. Further, *Plxna1;Plxna3*-null mice exhibited bundles of accumulated axons that failed to contact the OB.

Overall, our results demonstrated that both Plxna1 and Plxna3 are necessary to ensure the extension of the cVN nerves towards the hypothalamus to guarantee the correct positioning of GnRH neurons. Further, our findings support the concept that Sema3a signals through Plxna1 and Plxna3 to control the patterning of VN nerves and the cVN nerves, that associate with GnRH neurons.

2.3 Discussion

In the present work, we combined ISH and immunohistochemical expression studies together with genetically modified mouse models in order to identify which A-type plexin is involved in SEMA3A signalling pathway in the context of GnRH neuron development and olfactory system formation. SEMA3A is a well-known KS causative gene that exerts a role of axon guidance cue for OLF/VN/TN nerves navigating in the head by coupling with NRP1-2 (Cariboni et al., 2011a). However, the recruitment of obligate signal transducing receptor PLXNA1-4 has been poorly characterized, therefore the identification A-type plexins involved in the correct establishment of HPG axis will help to clarify the role of A-type plexins in this peculiar biological context and may also suggest PLXNAs as candidate genes to be screened in IGD, especially in KS, patients. Prior to us, a recent study by Marcos and colleagues has reported the involvement of Plxna1 in VN nerves and GnRH neuron migration in mice and described heterozygous mutations in KS patients harboured by *PLXNA1* gene (Marcos et al., 2017). Nevertheless, mice exhibited a KS-like phenotype at low penetrance, maybe due to compensatory effects by other A-type plexins and *PLXNA1* mutations found in patients were always in a heterozygous state, suggesting the possibility of genetic interactions with other mutated gene.

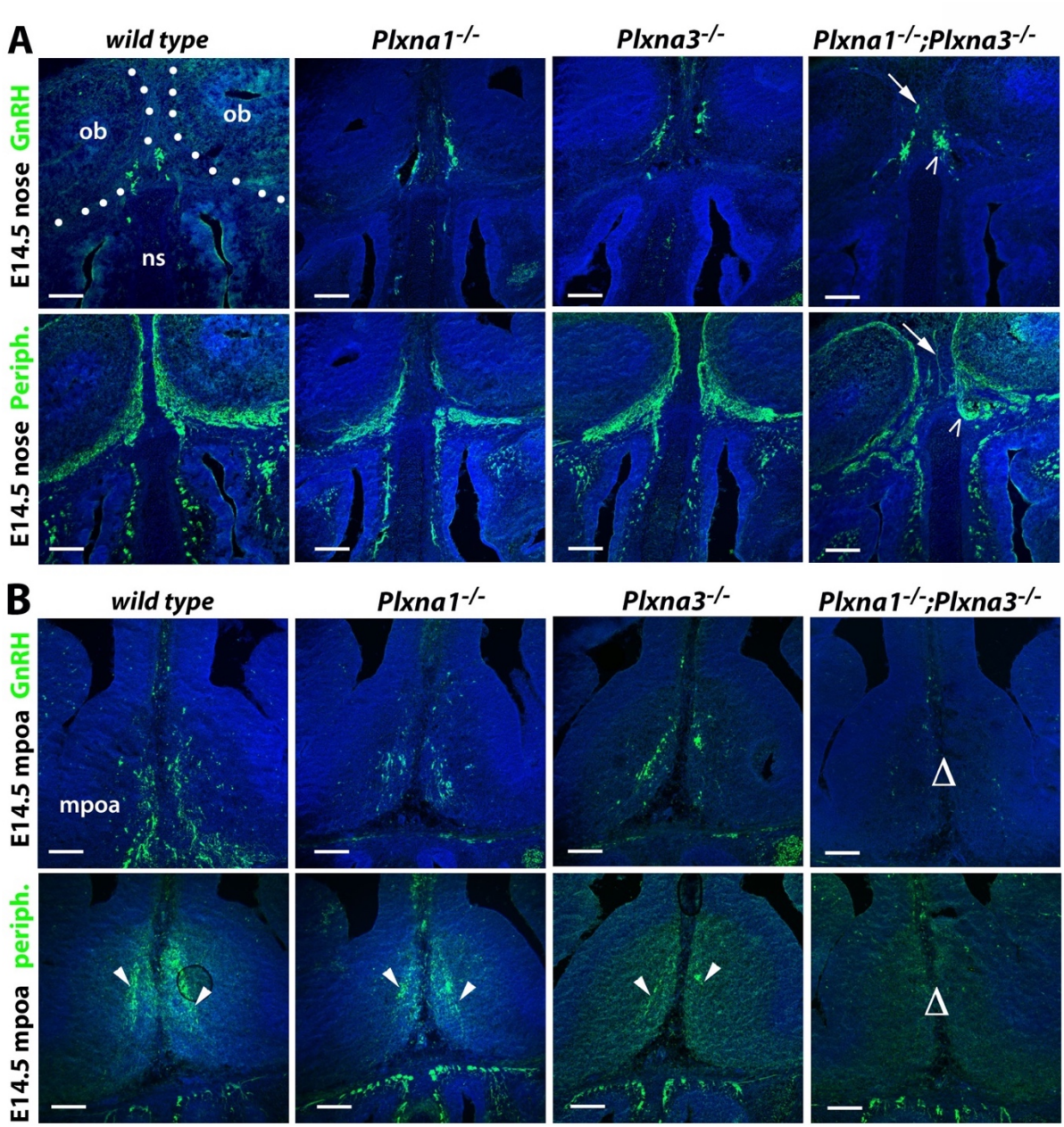

Figure 7 – Aberrant VN nerves patterning and GnRH neuron migration in *Plxna1/a3* compound-null mice. (A) Adjacent coronal sections of E14.5 mouse heads of the indicated genotypes were immunolabelled to reveal GnRH neurons (upper panels) and VN nerves (lower panels) in the nasal compartment/OB. White arrows in *Plxna1*$^{-/-}$;*Plxna3*$^{-/-}$ nasal area indicate mistargeted axons and associated ectopic GnRH neurons between the OB; open arrowheads indicate axon tangles and excess GnRH neurons at the level of the NFJ. **(B)** Adjacent coronal sections of E14.5 mouse heads of the indicated genotypes were immunolabelled to reveal GnRH neurons (upper panels) and VN nerves (lower panels) in the MPOA. Arrowheads indicate normal cVN nerves extending through the MPOA. The lack of GnRH neurons and cVN nerves in the MPOA of *Plxna1*$^{-/-}$;*Plxna3*$^{-/-}$ is indicated with Δ. Abbreviations: NS, nasal septum; OB, olfactory bulb; MPOA, medial preoptic area. Scale bar: 150 μm.

We first determined the expression pattern of all four family A plexins during mouse head development. We interestingly found that only *Plxna1* and *Plxna3* transcripts are expressed in the VNO, where VN/TN nerves originate, and in the nasal mesenchyme, where axons navigate in order to contact OB. These results are in line with previous reports (Marcos et al., 2017; Murakami et al., 2001; Suto et al., 2003). Further double immunofluorescence analysis confirmed our hypothesis since Plxna1 and Plxna3 are expressed by neuronal cells and in particular by peripherin-expressing VN/TN nerves. These results partially agree with expression studies performed by Marcos and co-workers that showed expression of Plxna1 in VN nerves as well but also by some GnRH neurons at E12.5. However, they used mouse monoclonal antibodies for Plxna1 to stain mouse tissues without testing specificity of the antibody, whilst we validated the specificity of our goat polyclonal antibodies and staining protocol as tissue sections from *Plxna1* and *Plxna3* knockout mice lack Plxna1 and Plxna3 immunostaining respectively. Yet, even though we did not observe Plxna1 protein in GnRH neurons, we have previously detected low levels of *Plxna1* transcripts in primary FACS-sorted GnRH neurons at E13.5 (Cariboni et al., 2007b). We can therefore conclude that GnRH neurons might express very low levels of Plxna1 at mRNA or possibly protein level, but still Plxna1 and Plxna3 are much more prominently expressed on the axons that guide migrating GnRH neurons through the nose and into the forebrain. Thanks to HDBR collaboration, we also studied expression on PLXNA1 and PLXNA3 in human foetuses and we found that they are expressed at CS19, an early phase of GnRH neuron migration, in cells migrating out of the OE and contacting OB, accordingly to results obtained in mouse. However, further co-localisation studies are needed to fully characterize the nature of PLXNA1 and PLXNA3 positive cells in humans.

In order to confirm our hypothesis, built up on expression data, that suggests a redundant recruitment of Plxna1 and Plxna3 in GnRH/olfactory systems, we analysed genetically modified mice lacking either single *Plxna1* and *Plxna3* or both the isoforms (*Plxna1;Plxna3*-null mice). We first assessed if lack of PlxnAs can perturb GnRH neuron migration. Analysis of single and double mutants revealed that Plxna1 and Plxna3 cooperate to ensure a proper migration of GnRH neurons, in fact, only when both isoforms are deleted, GnRH neurons fail to enter the FB and accumulate at the frontonasal region. Interestingly, either Plxna1 or Plxna3 loss does not or slightly affect (but not significantly) GnRH neuron position in the NFJ and FB. Taken together, these observations support a cooperative role of Plxna1 and Plxna3 in these systems, with a fully penetrant hypothalamic loss of GnRH neurons

occurring only when both isoforms are deleted. Consistently with results at embryonic stage, ME of mice at P10 resulted less innervated by GnRH neuron neurites only in double mutant mice and not in single mutant mice compared to wild type littermates. Further studies to be performed on adult mice are needed to confirm these preliminary findings, though. Differently, Marcos and colleagues have reported that, at very low frequency, newborn single *Plxna1*-null mice showed a normal number of total GnRH neurons, but a different distribution of GnRH within the FB, with some ectopic cells set in the dorsal and lateral FB. However, in this study they used mice in a mixed C57Bl/6 and CD-1 background, whereas our study is performed using pure C57Bl/6 mice.

Finally, we tested if GnRH neuron defective migration is subsequent to defects in VN/TN nerves formation similarly to what is exhibited by *Sema3a*-null mice. As expected, we found that only the deletion of both Plxna1 and Plxna3 is able to perturb the proper formation of VN/TN nerves with particular regard to cVN formation, strengthening the idea of a cooperative role of Plxna1 and Plxna3. As for GnRH analysis axonal defects were reported in *Plxna1* single knock out mice although at low penetrance, by Marcos and co-authors.

In conclusion, our work demonstrate that Sema3a signalling receptor involved in GnRH neuron and olfactory systems development are Plxna1 and Plxna3 and that loss of single Plxna1 is not sufficient to cause KS-like phenotype in mice and this is due to cooperative roles amongst A-type plexins. Further, these findings provide an example of basic science-driven approach to determine novel candidate genes. This strategy is based on a precise examination of targeted mutant mice that may reproduce human abnormal phenotypes and then on the search for mutations within target genes in humans. In this case, the analysis of compound *Plxna1;Plxna3*-null mice together with the expression studies in human foetuses showing co-expression of both PLXNA1 and PLXNA3 in the GnRH territories suggest that not only *PLXNA1* but also *PLXNA3* genes should be considered as candidate gene to be screened in IGD patients and in particular in whose affected by KS.

3. Heparan-sulphate 6-O sulfotransferase

Summary

Self-limited delayed puberty (DP) usually segregates in an autosomal dominant pattern, but genetic architecture is largely unknown. Although DP can be sometimes observed in relatives of patients affected by with IGD, mutations in IGD causative genes which segregate with the

trait of familial DP have not been identified yet. Here, we took advantage of a WES screening of 125 probands and 35 unaffected relatives (collaboration with Professor Dunkel, QMUL, London) in order to assess the contribution of mutations in genes known to cause IGD to the phenotype of DP. A potentially pathogenic gene variant segregating with DP was identified in 1 of 28 known IGD genes examined. This pathogenic variant occurs in Heparan Sulphate 6-*O* Sulpho-Transferase 1 (*HS6ST1*) gene in one pedigree and segregates with DP trait in the six affected members with heterozygous transmission. To evaluate the biological relevance of Hs6st1 in puberty onset, we performed *in vivo* expression analysis on WT mice and functional studies on *Hs6st1*$^{+/-}$ mice. These experiments showed that *Hs6st1* mRNA was expressed in peri-pubertal WT mouse hypothalamus. Further, we found that GnRH neuron counts were similar in *Hs6st1*$^{+/-}$ and *Hs6st1*$^{+/+}$ mice, but vaginal opening was significantly delayed in heterozygous mice despite normal postnatal growth. Overall, we have linked a deleterious mutation in *HS6ST1* gene to familial DP and showed that heterozygous *Hs6st1* loss causes DP in mice. In this study, the observed overlap in potentially pathogenic mutations contributing to the phenotypes of DP and HH was limited to this one gene.

3.1 Background

Abnormal puberty onset affects over 4% of adolescents and can be associated with adverse health and psychosocial outcomes (Day et al., 2015; He et al., 2010; Ritte et al., 2013). However, in most patients with early or late onset of puberty, the underlying genetic architecture is so far unknown. Self-limited DP represents an extreme variant of normal pubertal timing and has been shown to segregate in an autosomal dominant pattern within families (Sedlmeyer et al., 2002; Wehkalampi et al., 2008b), suggesting a mono- or oligo-genetic inheritance pattern conferred by haploinsufficiency or a gain of function mutation. Thus, pedigrees with familial DP represent a precious resource to investigate the genetic regulation of puberty onset. To date, most significant insights into the genetic control of the HPG axis have come from the discovery of causative genes underlying rare disorders as IGD (Beate et al., 2012). In particular, perturbed migration of GnRH neurons from nose to hypothalamus during embryonic development has been shown to be a major cause of IGD both in humans and in animal models (Wray, 2010). Alternatively, IGD may arise through mutations that occur in genes regulating GnRH secretion or function in the presence of a normal GnRH neuron number in the hypothalamus (Seminara et al., 2003). In view of the possible overlap between the pathogenesis of DP and conditions of GnRH deficiency, only few studies have examined the contribution of mutations in IGD causative genes to the pathogenesis of DP (Lin

et al., 2006; Pugliese-Pires et al., 2011; Vaaralahti et al., 2011). Potentially pathogenic variants in a small number of genes causing IGD (*GNRHR*, *TAC3*, *TACR3*, *IL17RD* and *SEMA3A*) were identified by WES in a few cases of DP, including those with CDGP (Zhu et al., 2015). In line with the idea of a shared genetic architecture between DP and IGD, WES of this cohort of patients (analysis performed by collaborating group of Professor Dunkel, QMUL, London) helped to identify deleterious mutations in *IGSF10* gene, which affect GnRH neuronal migration and can cause DP; however, no *IGSF10* mutation in IGD patients have been found so far (Howard et al., 2016). In this study, we applied the same experimental design and interrogated the same WES data to assess the contribution of mutations in genes known to cause IGD to the phenotype of familial DP. This approach provided evidence that heterozygous mutations of *HS6ST1*, an already known IGD causative gene, can contribute to the pathogenesis of DP.

3.2 Results

Exome sequencing of families with self-limited delayed puberty identifies an HS6ST1 variant

WES of 67 informative families from an accurately phenotyped cohort with self-limited DP identified 20 variants in 12 genes known to cause IGD (Table 1). However, only *HS6ST1* (ENSG00000136720) showed to segregate with trait and therefore was the only one retained as a candidate gene (see Section IV, Paragraph 1.3). The proband and his affected relatives carried a rare and probably damaging *HS6ST1* variant (NM_004807.2: c.1124G>A, rs182882999, p.Arg375His, R375H; Figure 1C) which leads to a non-synonymous amino acid substitution in the coding sequence. This proband carried an additional potentially pathogenic variant in FEZF1 (NM_001024613.3: c.1010T>A, p.Iso337Lys), but this variant did not segregate with DP in any other affected individual from this family and was filtered out. The rare (MAF < 1%) heterozygous missense variant R375H is predicted to be deleterious to protein function with online-available prediction tools, as the affected amino acid residue lies in a coiled-coil domain that is highly conserved among species, as revealed by multiple sequence alignment (Figure 1D). This specific variant was present at low MAF in some public databases, but whole gene rare variant burden testing showed significant enrichment of four *HS6ST1* rare predicted pathogenic variants in our cohort as compared to ethnically-matched controls from the ExAC database (adjusted p-value = 3.01×10^{-5}). Then, targeted exome sequencing was applied in additional 42 families from this cohort and two additional variants in *HS6ST1* were identified in three further affected probands (NM_004807.2: c199A>T, rs202247387, p.Lys67X; c585G>A p.Trp195X). However, Sanger

Gene	No. of rare and predicated damaging variants filtered from whole exome sequencing data	
	Not Segregating with the DP trait	Segregating with the DP trait
ANOS1	0	0
AXL	3	0
CHD7	3	0
DAX1	0	0
FEZF1	3	0
FGF8	0	0
FGFR1	2	0
GNRH1	0	0
GNRHR	0	0
HESX1	0	0
HS6ST1	**1**	**1**
KISS1	0	0
KISS1R	0	0
LEP	0	0
LEPR	0	0
LHX3	1	0
LHX4	1	0
NELF	0	0
PCSK1	0	0
PROK2	0	0
PROKR2	2	0
PROP1	1	0
SEMA3A	0	0
SF1	0	0
SPRY4	1	0
TAC3	1	0
TAC3R	0	0
WDR11	1	0

Table 1 – IGD gene filtering. 28 'HH genes', mutations in which have been identified as causal or potentially causal in patients with GnRH deficiency, used for filtering post whole exome sequencing. Details given of number of variants in these genes identified in 67 probands with DP after whole exome sequencing. Variants are divided into those which were found to segregate with the DP trait within cohort pedigrees and those that did not segregate.

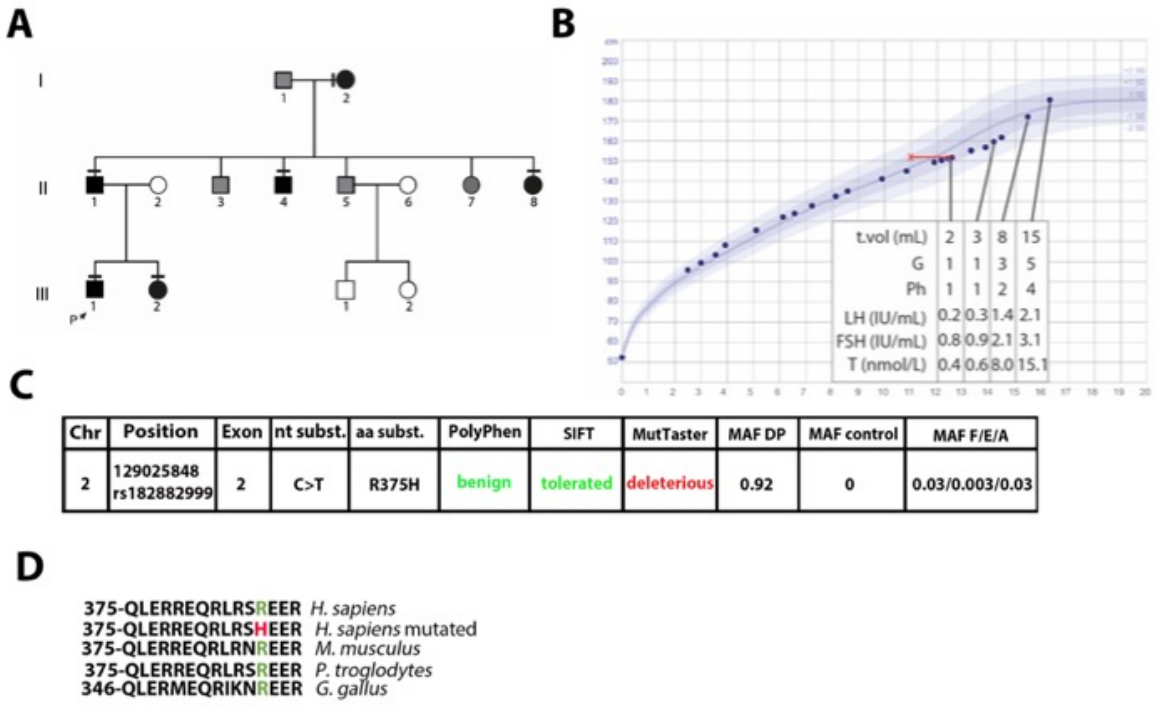

Chr	Position	Exon	nt subst.	aa subst.	PolyPhen	SIFT	MutTaster	MAF DP	MAF control	MAF F/E/A
2	129025848 rs182882999	2	C>T	R375H	benign	tolerated	deleterious	0.92	0	0.03/0.003/0.03

Figure 1 – *HS6ST1* gene mutation has been found in a family from a self-limited DP cohort. (A) Family tree of the proband carrying the R375H mutation. Males are represented in squares while circles indicate females family members. Clinically affected family members are in black, grey symbols represent family members with unknown phenotype, unaffected individuals are marked in white. The arrow labelled 'P' indicates the proband in the family. A horizontal black line above or adjacent to an individual's symbol indicates that they are heterozygous for the mutation. **(B)** Clinical details of the proband. Height chart for the proband shows reduction in growth velocity from 12 years of age, with associated delayed bone age shown in red. The subject was prepubertal until 14.1 years of age. This was followed by spontaneous onset of puberty and subsequent development over 2 years to normal adult testosterone levels and testicular volume. **(C)** *In silico* analysis of *HS6ST1* mutation PolyPhen-2, SIFT and Mutation Taster were used to predict structural and functional effects of R375H amino acid substitution. **(D)** Alignment of partial protein sequences of vertebrate *HS6ST1* orthologues shows that the R375 residue is evolutionarily conserved in humans and several other vertebrate species. Abbreviations: T vol, testicular volume; G, Tanner genital stage; Ph, Tanner pubic hair stage; LH, luteinising hormone; FSH, follicular stimulating hormone; T – testosterone.

sequencing did not validate the existence of these variants, therefore only R375H variant was considered.

Pedigree with a potentially pathogenic HS6ST1 variant displayed an autosomal dominant inheritance pattern and classical self-limited DP.

The pedigree harbouring the R375H variant display several family members with typical features of self-limited DP (Figure 1A). The proband was first investigated for growth delay at 12.8 years, when his bone age was 11 years (Figure 1B). Clinical examination at this stage found him to be prepubertal, with bilateral testis volumes of 2 mL and no pubic hair development. His blood biochemistry analysis showed a typical picture of functional hypogonadism. However, spontaneous onset of puberty was first observed around 14.3 years of age and over the next 2.4 years, he achieved normal adult range testis volume and testosterone levels. His sister's age at menarche was 15 years. Both siblings had normal birth weight and birth length. Their father and paternal uncle and aunt also displayed DP with delayed pubertal growth spurt. All family members with DP had self-reported normal olfactory behaviours.

Hs6st1 is expressed within the adult hypothalamus and olfactory bulbs

In the adult brain, GnRH neurons are dispersed in a bilateral continuum between the OB and the MPOA of the hypothalamus, where most cell bodies reside (Merchenthaler et al., 1984). By ISH experiments, we found that *Hs6st1* mRNA is highly expressed in the granular, mitral and glomerular layers of adult OB (Figure 2A) and more diffusely in the MPOA (Figure 3B, upper panel). *Hs6st1* expression was also observed in the ARC of the hypothalamus, where reside neurons essential for GnRH secretion such as KNDy neurons (Figure 2B, lower panel). However, by combining ISH with immunofluorescence, we found that *Hs6st1* transcript did not localize with $GnRH^+$ neurons (Figure 2C). Hence, these observations suggest that *Hs6st1* is expressed by hypothalamic cells different from GnRH neurons.

Normal positioning and number of GnRH neurons in the MPOA of Hs6st1 heterozygous mice.

To determine whether Hs6st1 is required for the normal development of the GnRH neuron system, we compared mice heterozygous for a single *Hs6st1* null allele ($Hs6st1^{+/-}$) to their wild type littermates ($Hs6st1^{+/+}$). Interestingly, we did not observe gross differences in brains or OB morphology between both genotypes (Figure 3A-B). Moreover, there were no obvious and significant differences in both positioning and number of GnRH neurons in the MPOA as well

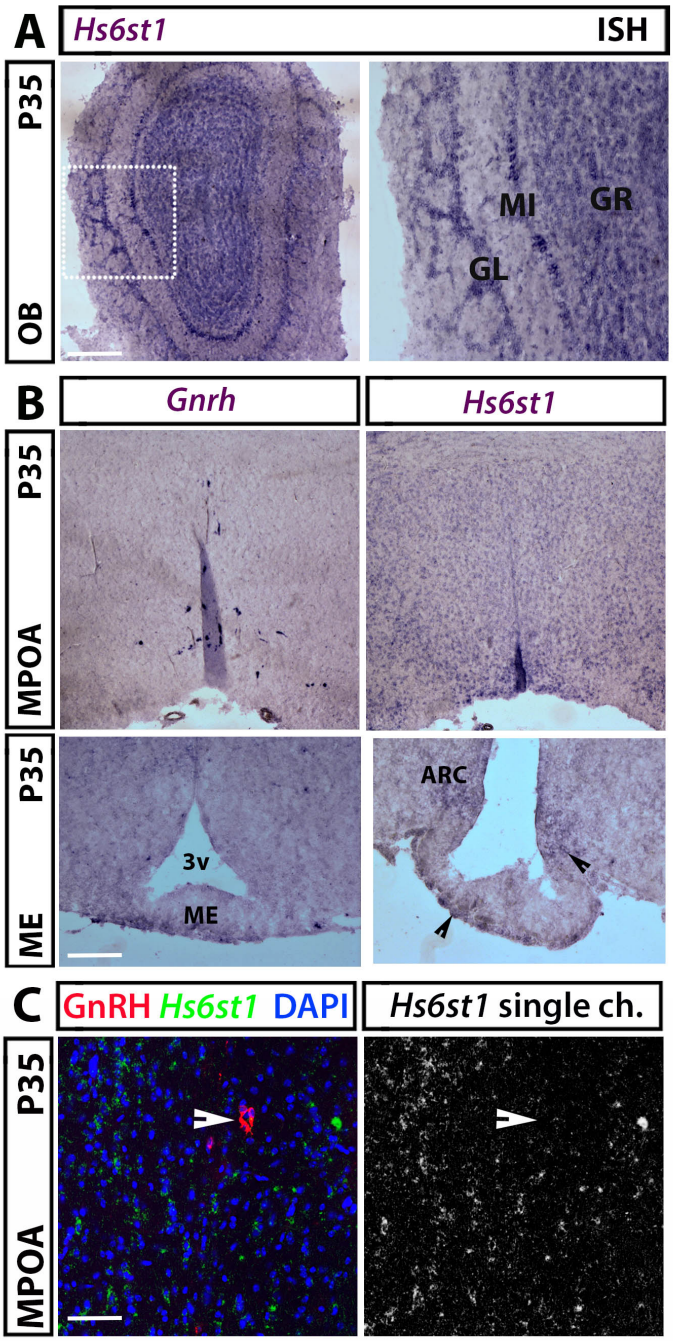

Figure 2 – *In situ* hybridization revealed *Hs6st1* transcript expression in territories relevant to GnRH function at postnatal day (P) 35. (A) Coronal sections of adult mouse OB were labelled with a specific riboprobe for *Hs6st1* mRNA; dotted box represents high magnification area. **(B)** Contiguous coronal sections of adult mouse hypothalamus representing the MPOA (upper panels) and the ME and ARC (lower panels) were labelled with riboprobes for *Gnrh* and *Hs6st1*; arrowheads indicate *Hs6st1* expression in the ARC and ME. **(C)** Coronal sections of MPOA were double labelled with riboprobe for *Hs6st1* (in green) and a specific antibody for Gnrh (in red); no expression of H*s6st1* in GnRH-positive neurons (example of GnRH neuron is indicated with a solid arrowhead). Abbreviations: GL, glomerular layer; MI, mitral layer; GR, granular layer; 3v, third ventricle; ARC, arcuate nucleus; ME, median eminence; 3v, third ventricle; MPOA, medial preoptic area; OB, olfactory bulb. Scale bars: 125 µm (A, B upper panels), 50 µm (B lower panels), 25 µm (C).

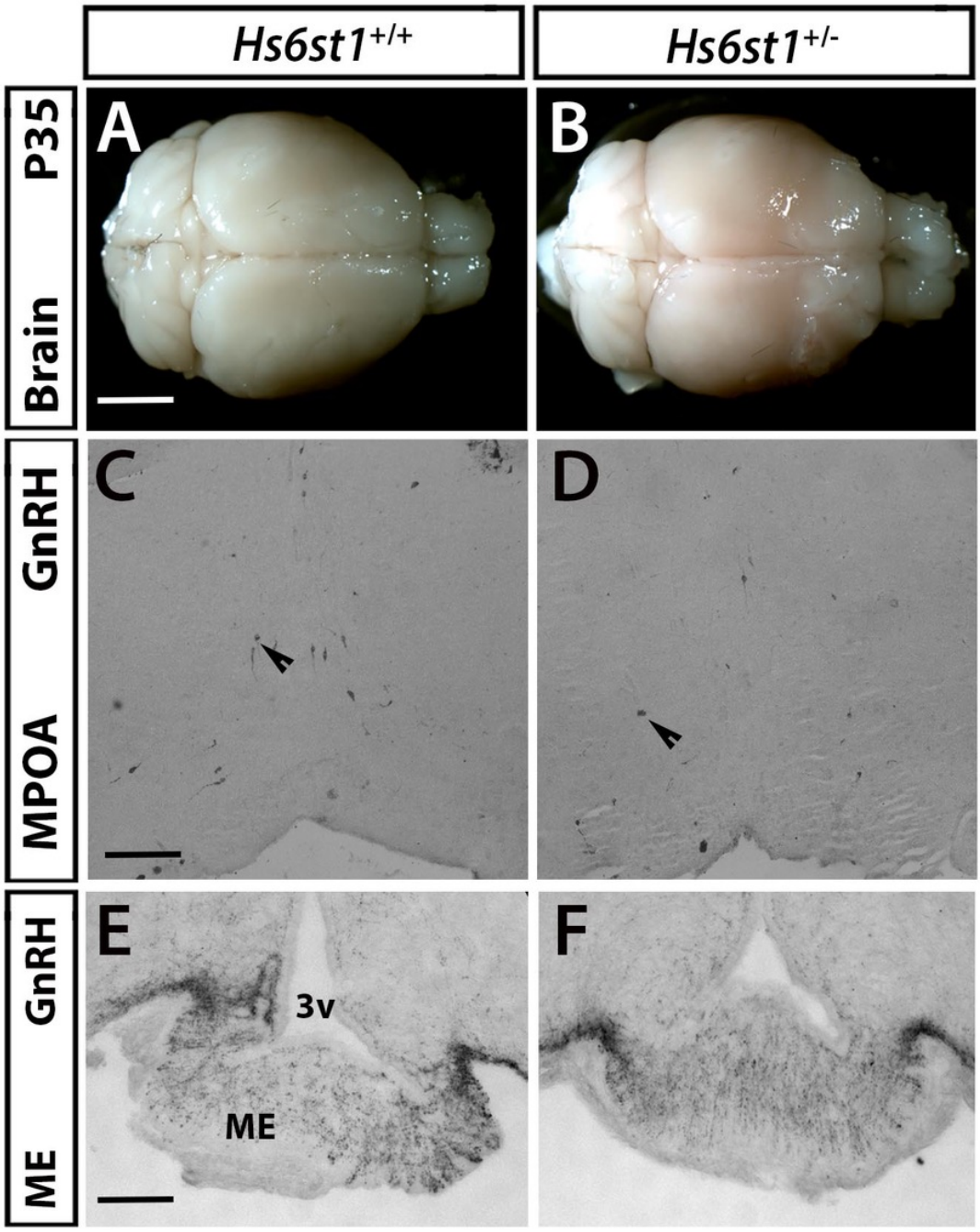

Figure 3 – *Hs6st1*$^{+/-}$ mice showed no defects in olfactory bulbs morphology nor in the number and projections of GnRH neurons. (A-B) Perfused adult *Hs6st1*$^{+/+}$ (A) and *Hs6st1*$^{+/-}$ (B) brains showed no obvious defects in OB morphology. **(C-D)** Coronal sections of adult mouse MPOA were immunostained for GnRH; arrowheads indicate examples of GnRH neurons that are normally present in *Hs6st1*$^{+/+}$ (C) and *Hs6st1*$^{+/-}$ (D). **(E-F)** Immunostaining for GnRH in coronal sections of adult mouse ME showed that GnRH neurons project similarly to the ME in *Hs6st1*$^{+/+}$ (E) and *Hs6st1*$^{+/-}$ (F) mice. Abbreviations: OB, olfactory bulb; MPOA, medial preoptic area; ME, median eminence; 3v, third ventricle. Scale bar: 3 mm (A, B), 125 µm (C, D), 50 µm (E, F).

(Figure 3C-D; number of $GnRH^+$ cells ± s.e.m.: *Hs6st1*$^{+/-}$: 341.2±24.2 vs. *Hs6st1*$^{+/+}$: 378.3±30.2, n=5 each; P>0.05; Student's t-test). In agreement, GnRH neurons in *Hs6st1*$^{+/-}$ mice also projected similarly to the ME, the site where they normally release GnRH into the hypophyseal blood portal system and the pixel intensity of GnRH-stained neurites was similar in both genotypes (Figure 3E-F; % stained neurite area ± s.e.m.: *Hs6st1*$^{+/+}$: 2.9±0.4 vs. *Hs6st1*$^{+/-}$: 3.1±0.3, n=5 each; P>0.05, Student's t-test).

Hs6st1$^{+/-}$ *mice show significantly delayed puberty onset*

To determine whether heterozygous loss of Hs6st1 is sufficient to cause delayed puberty onset, we compared the timing of puberty in *Hs6st1*$^{+/-}$ (n=13) and *Hs6st1*$^{+/+}$ (n=12) female mice by identifying the day of vagina opening (VO), a proxy measurement for pubertal activation of the HPG axis in mice (Messina et al., 2016). We found that VO was delayed by on average 1.88±0.82 days in *Hs6st1*$^{+/-}$ compared to *Hs6st1*$^{+/+}$ females (Figure 4A, left panel; postnatal day (P) of VO ± s.e.m.: *Hs6st1*$^{+/+}$: 30.2±0.7 vs. *Hs6st1*$^{+/-}$: 31.9±0.5; P<0.05, Student's t-test; mice were pooled form 6 different litters). DP in *Hs6st1*$^{+/-}$ females was not due to overall delayed development, as they were not smaller than *Hs6st1*$^{+/+}$ littermate females around the time of VO (weight at P30 ± s.e.m.: *Hs6st1*$^{+/+}$: 14.12±0.58 g vs. *Hs6st1*$^{+/-}$: 13.67±0.58 g; P>0.05, Student's t-test). Instead, and consistent with DP, there was an insignificant trend towards larger weight at the time of VO in *Hs6st1*$^{+/-}$ compared to *Hs6st1*$^{+/+}$ females within the cohort examined (Figure 4A, right panel; body weight on the day of VO ± s.e.m.: *Hs6st1*$^{+/+}$: 14.9±0.3 g vs. *Hs6st1*$^{+/-}$: 15.5±0.3 g; P>0.05, Student's t-test).

Despite DP, the fertility of young adult *Hs6st1*$^{+/-}$ males and females of both sexes appeared normal: they seared litters without obvious delay and of normal litter size when paired to WT mice at 4-6 months of age (litter size ± s.e.m.: *Hs6st1*$^{+/-}$ x *Hs6st1*$^{+/+}$: 7.2±0.95 pups per litter in 6 litters, vs. *Hs6st1*$^{+/+}$ x *Hs6st1*$^{+/+}$: 7.3±0.71 in 7 litters; P>0.05) and *Hs6st1*$^{+/-}$ mice were born at the expected Mendelian ratio. Accordingly with the ability to father litters of normal size, testes appeared normal in young adult (P35) *Hs6st1*$^{+/-}$ (n=6) and *Hs6st1*$^{+/+}$ males (n=8) (Figure 4B; testes length (mm) ± s.e.m.:, *Hs6st1*$^{+/+:}$ 8.31±0.17 mm vs. *Hs6st1*$^{+/-}$: 8.30±0.16 mm; P>0.05). Moreover, testes showed normal organisation of germ cells and interstitial Leydig cells and contained a similar number of seminiferous tubules per area (Figure 5B-C; seminiferous/mm^2 ± s.e.m.: *Hs6st1*$^{+/+}$: 14.53±0.91 vs. *Hs6st1*$^{+/-}$: 14.69±0.62; n=5 each; P>0.05). Overall, *in vivo* analysis on mice lacking one *Hs6st1* allele proved that HS6ST1 haploinsufficiency delays puberty albeit fertility in adults was not compromised.

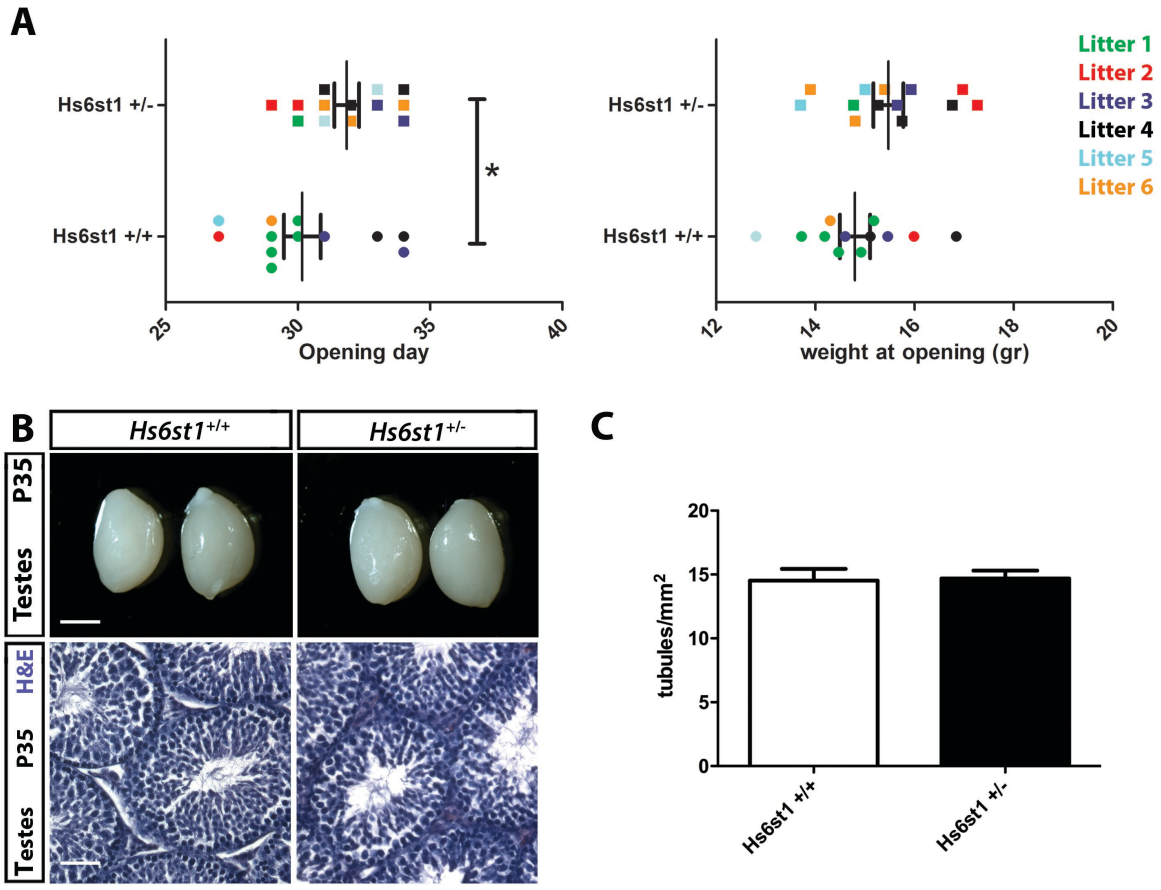

Figure 4 – Peripubertal female *Hs6st1*$^{+/-}$ mice show delayed vaginal opening while young adult male *Hs6st1*$^{+/-}$ mice showed normal testes morphology. (A) Age (left graph) and weight (right graph) at the time of the vaginal opening in female *Hs6st1*$^{+/+}$ (n=12) and *Hs6st1*$^{+/-}$ (n=13) mice. Values for littermates are shown in the same colour. * indicates $p<0.05$. **(B-C)** *Hs6st1*$^{+/+}$ and *Hs6st1*$^{+/-}$ mice have similar testes size (upper panels of B), normal spermatogenesis after H&E staining of paraffin sections (lower panels of B) and similar number of seminiferous tubules (C). Scale bars: 3 mm (B upper panels), 25 µm (B lower panels).

3.3 Discussion

The inheritance of DP is under strong genetic influence, with a clear autosomal dominant segregation pattern within families with complete or incomplete penetrance (Sedlmeyer and Palmert, 2002), and thus represents a useful basis for the investigation of puberty genetics (Wehkalampi et al., 2008b). However, only a few genes responsible for self-limited DP have been identified. In agreement with a partial overlap between the genetic pattern underlying DP and IGD, screening self-limited DP patients for mutations in already known IGD genes appears a prudent strategy. Yet, the genetic overlap between the two conditions is to date minimal (Zhu et al., 2015) and some observed differences in inheritance patterns and penetrance between the two conditions have been recently reported (Cassatella et al., 2018; Howard, 2018).

IGD is genetically heterogenous with almost 40 different genes identified as causative and incomplete penetrance can be often observed within pedigrees; the high genetic variability echoes in a wide spectrum of phenotypes (Pitteloud et al., 2007a; Raivio et al., 2007; Sidhoum et al., 2014). Progresses in the knowledge of genetic basis underlying self-limited DP and IGD, together with advances in genetic testing technologies, will help to establish a definitive diagnosis in adolescent patients presenting with delayed onset of puberty.

Here, we have identified a deleterious non-synonymous mutation, R375H, in the IGD causative gene *HS6ST1*. This variant is likely the causal factor for self-limited DP diagnose in one pedigree of our cohort of patients with familial DP. *HS6ST1* mutations have been previously identified in up to 2% of patients with nHH and KS (Pitteloud et al., 2006a; Tornberg et al., 2011), but have not previously been reported in pedigrees segregating with the trait of self-limited DP. We hypothesized a model in which the sole *HS6ST1* heterozygous mutation causes DP, whilst potentially *HS6ST1* homozygosity or, consistently with oligogenicity observed in IGD, a 'second-hit' in a different gene, may produce the phenotype of IGD.

Our studies in a murine model corroborate haploinsufficiency of *Hs6st1* as a cause of delayed pubertal timing without compromised fertility. *Hs6st1*$^{+/-}$ mice were born at normal Mendelian ratios without obvious defects in GnRH neuron or testes development, but peripubertal females showed delayed VO. The question of sex bias in self-limited DP is still object of debate, as it is diagnosed in up to 83% of boys and 30% of girls presenting with pubertal delay (Lawaetz et al., 2015; Sedlmeyer and Palmert, 2002; Varimo et al., 2017). Although, the underlying reasons for gender difference are not clear, it may partially be due to ascertainment bias. Indeed, a

previous study has shown a near equal sex ratio consistent with autosomal dominant inheritance when all of the affected individuals from our large cohort were examined, as opposed to the probands only (Wehkalampi et al., 2008b).

In our murine model of *Hs6st1*$^{+/-}$ mice, we did not find any evidence of a sex difference in anatomical studies and only females were examined for timing of pubertal onset by measuring VO as it represent a reliable and robust marker of pubertal onset in female mice. Male mice were not assessed for the timing of puberty, but post-pubertal (P35) mice were analysed to evaluate testicular morphology, including the presence of spermatogenesis as normal spermatogenesis reflects reproductive competence and excludes GnRH deficiency. In post-pubertal female mice, the reproductive competence was in turn assessed as fertility of the females. With these methods, GnRH deficiency was excluded in both sexes of *Hs6st1*$^{+/-}$ mice. To exclude poor growth as underlying cause for pubertal delay heterozygous *Hs6st1* mice were weighted and did not appear significantly smaller or lighter than their wild type littermates. Our expression studies in wild type mice indicate that Hs6st1 mRNA is expressed in several tissues relevant to normal GnRH neuron migration or function, including the OB and the MPOA, ARC and PVN of the hypothalamus. Yet, no obvious abnormalities in OB morphology, GnRH neuron number in the MPOA or in GnRH neuron innervation of the ME were reported in Hs6st1$^{+/-}$ mice compared to wild type littermates. Interestingly, *Hs6st1* expression in the ARC and PVN, where KNDy neurons and tanycytes modulate GnRH secretion and function (Parkash et al., 2015; Pielecka-Fortuna et al., 2008), may suggest that Hs6st1 haploinsufficiency could affect the regulation of GnRH neuron secretion by altering the GnRH pulse generator machinery. Moreover, Hs6st1 is required for the correct function of Anos1 and Fgfr1, two genes that are essential for normal HPG axis function (Tornberg et al., 2011). In a *C. elegans* model, it was demonstrated that *hst-6* (i.e. the *C. elegans* ortholog gene for *Hs6st1*) regulates neural branching in concert with Anos1 and Fgfr1 (Tornberg et al., 2011). Specifically in GnRH neuron system, Anos1 was demonstrated to be able to enhance Fgfr1 signalling in a HS-dependent manner in immortalised human GnRH neurons suggesting that this interaction may promote GnRH neuron development (Hu et al., 2009). Hs6st1 mutations may also impact HPG axis establishment via Anos1-independent pathways, as HS modifications of many different proteoglycans in the extracellular matrix have the potential to affect multiple signalling pathways (Bishop et al., 2007) previously implicated in the neuroendocrine control of fertility (Condomitti and de Wit, 2018).

To summarize, we have identified a novel pathogenic mutation in *HS6ST1* gene as the probable cause of DP in a pedigree from our extensive patient cohort, with no other pathogenic mutations in genes known to cause IGD identified in our cohort. These findings strengthen the idea that, with the exception of a few genes like *HS6ST1*, the genetic background of IGD and DP is either largely different or is due to mutations in as yet undiscovered genes (Cassatella et al., 2018; Howard, 2018). Our findings may differ from those in previous publications, in which up to 14% of DP probands were reported to carry potentially pathogenic variants in known causative IGD genes (Zhu et al., 2015), but previous results display some limitations and therefore prior estimates of IGD mutation rates in DP patients may have been over-estimated. For instance, they have not been adjusted for segregation with the DP trait within families, nor have the variants been tested for pathogenicity. Indeed, prior to adjustment for segregation, our results suggested that 17.9% of DP probands had potentially pathogenic variants in IGD genes, highlighting the value of familial data in identification of causal variants in a condition such as DP. Although further pedigrees with familial DP need to be studied to identify additional causative genes and provide accurate estimates of the genetic IGD and DP overlap, our findings provide evidence that perturbations in a single allele of a gene regulating the HPG axis is sufficient to cause self-limited DP. In contrast, available evidence suggests that more deleterious alterations in the same gene, or in combination with additional genes, are required to cause more severe IGD phenotypes.

SECTION IV
Materials and methods

1. Mutational analysis: procedures in patients and *in silico* methods

1.1 Homozygosity mapping and Whole Exome Sequencing: SEMA3G case

Genetic analysis was performed by our collaborators at Great Ormond Street Children Hospital in London. The blood samples were collected from the family through Great Ormond Street Hospital's NHS Trust. Genomic DNA was isolated through standard techniques at the UCL Genomics centre, and the samples were stored for long term at a temperature of -80°C until analysis. HZM was conducted by the UCL Genomics services. The Illumina microarray platform was used for the genotyping, following the Infinium HD Ultra Assay protocol (Rev B, 2010, Illumina Inc.). Results were generated using the Illumina Genomestudio software, and copy number variation and loss of heterozygosity data was generated (cnvPartition v3.1.6, Illumina). The minimum homozygous region size was 1 Mb, with a minimum of 50 consecutive SNPs.

WES was conducted on the 2 patients and their unaffected siblings at the Genetic Medicine Department, St Mary's Hospital, University of Manchester. Patients #2 WES data, due to higher quality and depth of the sequencing to other WES, were used in combination with HZM to identify the candidate gene/mutation lying within the homozygous regions. Filtering strategy to narrow down the list of variants is reported in Figure 1 and contemplates biological relevance (i.e. variants affecting protein structure), presence in shared homozygous regions and in a homozygous state and novelty (Figure 1). Sanger sequencing was performed to check mutation in the affected patients and their family. Primers was designed using the online Primer3 software. The sequencing reaction was conducted using the BigDye Terminator V1.1 Cycle Sequencing kit (Applied Biosystems). The sequences were compared to a reference sequence using the Sequencher® 5.3 software.

1.2 Self-limited DP patient cohort

The patients selected for this study belong to a previously described and accurately phenotyped Finnish DP cohort, for which diagnosis is based on objective evidence of a delayed pubertal growth spurt rather than self-recall (Wehkalampi et al., 2008a). Patients were referred with DP to specialist pediatric care in central and southern Finland from 1982 to 2004. All patients (n = 492) met the diagnostic criteria for self-limited DP, defined as the onset of Tanner genital stage II (testicular volume > 3 mL) > 13.5 years in boys or Tanner breast stage II >13.0 years in girls (i.e., 2 SD later than average pubertal development) (Palmert and Dunkel, 2012). Medical history, clinical examination, and routine laboratory tests were reviewed to exclude those with chronic illness. IGD, if suspected, was excluded by spontaneous pubertal development at follow-up. Normal fertility has been demonstrated in affected family members (Wehkalampi et al., 2008b). Families of the DP patients

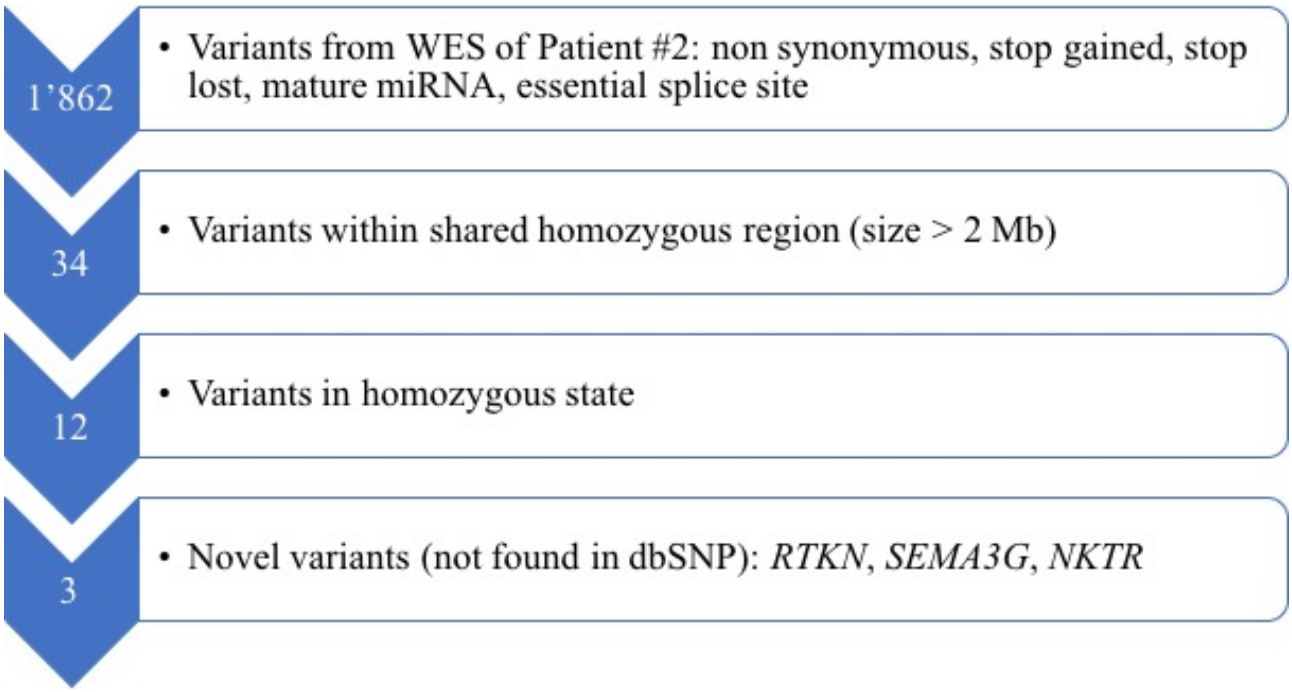

Figure 1 – Filtering strategy applied on WES data from Patient #2. Variants with a biological relevance (n=1.862) were filtered according to their presence in the two brothers shared homozygous regions that have been identified through HZM. Variants that were present in shared homozygous region with size >2 Mb (n=34) were then filtered according to their homozygous nature (n=12) and finally only variants that were not registered in SNPs databases were considered for further analysis (n=3).

were invited to participate via structured interviews and using archived height measurement records. The criteria for DP in probands' family members were: i) age at take-off; or ii) peak height velocity occurring 1.5 SD beyond the mean, that is, age at take-off >12.9 and 11.3 years, or age at peak height velocity > 14.8 and 12.8 years in males and females, respectively; or iii) age at attaining adult height > 18 or 16 years in males and females, respectively (Wehkalampi et al., 2008a).Written informed consent was obtained from all participants. The study protocol was approved by the Ethics Committee for Pediatrics, Adolescent Medicine and Psychiatry, Hospital District of Helsinki and Uusimaa (570/E7/2003). UK ethical approval was granted by the London–Chelsea National Research Ethics Service committee (13/LO/0257). The study was conducted in accordance with the guidelines of the Declaration of Helsinki.

1.3 Whole Exome Sequencing and Targeted Exome Sequencing: HS6ST1 case

Genetic analysis was performed by our collaborators at Queen Mary University of London. Genetic analysis was performed in 160 individuals from those 67 families with the greatest number of affected individuals in our cohort (125 affected family members: males, n=76; females, n=49; 35 of their unaffected family members (male, n = 13; female, n = 22). WES was performed on DNA extracted from peripheral blood leukocytes of these 160 individuals, using a Nimblegen v.2 or Agilent v.5 platform and Illumina HiSeq 2000 sequencing. The exome sequences were aligned to the University of California Santa Cruz hg19 reference genome. Picard tools and the Genome Analysis Toolkit were used to mark PCR duplicates, realign around indels, recalibrate quality scores, and call variants. Variants were analysed and filtered for potential causal variants using filters for quality control, predicted function, minor allele frequency (MAF), and segregation with DP trait (Figure 2). Filtering by MAF included only variants with MAF <1% in the 1000 Genomes database, the National Heart, Lung, and Blood Institute exome variant server and the ExAC and gnomAD databases. Biological relevance filtering allowed prioritization of variants according to known IGD causative genes based on previously published studies and using pathway analysis with MetaCore (GeneGo/Thomson Reuters). The segregation with trait filter retained only variants present in ≥ n-1 affected individuals (where n indicates the number of affected individuals in a given pedigree) and not present in more than one unaffected individual. Targeted exome sequencing (Fluidigm) of the remaining candidate gene postfiltering was performed in a further 42 families from the same cohort (288 individuals; 178 with DP: males n=106; females n=72; 110 controls: males, n=55; females, n=55), with filtering performed as previously described (Howard et al., 2016). Whole-gene rare variant burden testing was performed after sequencing. A multiple comparison adjustment was applied post hoc using the Benjamini–Hochberg method (Benjamini et al., 2001), as detailed in Howard et al. (Howard et al., 2016). All variants identified were confirmed via Sanger sequencing.

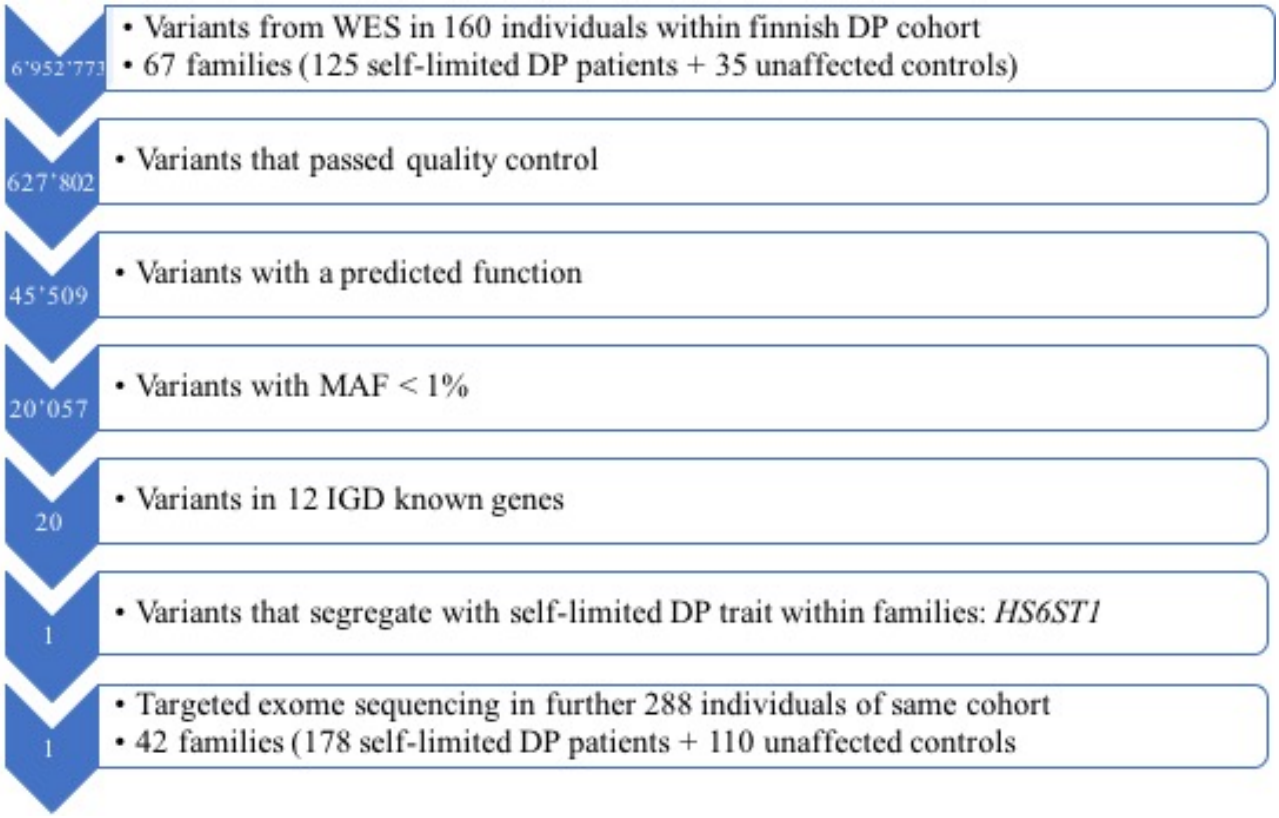

Figure 2 – Filtering strategy applied on WES data from DP cohort individuals. Variants found in 160 individuals (n=6.952.773) were prior filtered according to quality control (n=627.802) and biological relevance (i.e. affecting protein structure, n=45.509). Variants with MAF>1% were filtered out and the remaining variants (n=20.057) were checked in a list of 28 known IGD causative genes. Only variants affecting these genes (n=20) and segregating with DP trait within families were considered for further analysis (n=1). Targeted exome sequencing confirmed the presence of the remaining variant in other individuals of the cohort.

1.4 Prediction tools

In silico mutational analysis was performed to predict the effect of *SEMA3G*, *NKTR*, *RTKN* and *HS6ST1* mutations, as previously described (Cariboni et al., 2015). Specifically, we took advantage from the free online software SIFT (http://sift.bii.a-star.edu.sg/) (Ng and Henikoff, 2003), MutationTaster2 http://www.mutatontaster.org/) (Schwarz et al., 2014) and PolyPhen-2 http://genetics.bwh.harvard.edu/pph2) (Adzhubei et al., 2010).

2. *In vitro* methods

1. Expression vectors and conditioned media

The expression vector encoding for human SEMA3G (pAPtag5-hSEMA3G) was kindly provided by Prof. Hellmut Augustin; the vector contains sequence encoding for the placental AP and c-Myc tag in frame with SEMA3G coding sequence. The p.Gly166Val point mutation was introduced by PCR mediated mutagenesis (QuickChange Lightning Site-Directed Mutagenesis Kit, Agilent Technologies), using specific the primers SEMA3G_G166V (Table 1). Expression vectors were transiently transfected into COS-7 cells using Lipofectamine 2000 (Invitrogen). Conditioned media (CM) were collected 48 hours after transfection and concentrated by diafiltration with Microcon-30 kDa Centrifugal Filter Unit (Millipore) prior to chemotactic and immunoblotting assays.

2.2 Immunocytochemistry

Cells were fixed with 4% paraformaldehyde (PFA) for 15 minutes and were incubated with phosphate buffered saline (PBS) containing 0.1% TritonX-100 and a serum-free blocking solution (Dako). The primary antibody mouse anti-cMyc (1:200 in PBS 0.1% TritonX-100, overnight incubation at 4°C; Thermo Fisher Scientific) was used to detect the presence of WT or mutated human SEMA3G. A secondary antibody 488-conjugated goat anti-mouse IgG (1:200 in PBS 0.1% TritonX-100, 2 hours incubation at room temperature (RT); Jackson Immuno.) was used. Nuclei were counterstained with DAPI (1:10000; Sigma).

2.3 Immunoblotting

Cells were lysed in 150 mM NaCl, 50 mM Tris-HCl (pH 7.4) and 1% Triton X-100, supplemented with protease and phosphatase inhibitors (Roche). Lysates were centrifuged at 13000 rpm for 10 min at 4°C and protein concentration determined with the Bradford assay (Bio-Rad). Concentrated CM of transfected COS-7 cells were diluted 1:4 in Laemmli sample buffer (Cariboni et al., 2004). 20 μg of protein lysate or 20 μL of concentrated CM were used for SDS-PAGE. Proteins were transferred to nitrocellulose membrane (Bio-Rad). After incubation with 5% BSA in PBS-T (PBS 0.1%-Tween

Gene	Sequence 5'->3'		Amplicon size (bp)	Temperature of annealing (°C)
Gapdh	FW REV	TGGCATTGTGGAAGGGCTCATGAC ATGCCAGTGAGCTTCCCGTTCAGC	189	66
Hs6st1_MUT genotyping	FW REV	ACAGCTGCCAGGATCCTAAA CAAGCCAATGGTCTGGAAGT	200	58
Hs6st1_WT genotyping	FW REV	ATGGTGACTGTGACCCACAA GGGATATAGGGGACCTTGGA	200	58
Nktr_ISH	FW REV	CCACTCGAGTTTGGTGACGA **ggtaatacgactcactatagggGCCTTCACATCCAGAGCACT**	692	60
Nrp1	FW REV	TTCCGCAGCGACAAATGTGG. TACTTGCAGTCTCTGTCCTC	188	58
Nrp2	FW REV	CGAATTCCAAAGATGCTGGC GGAGCCTGAGGAGATGATGG	260	58
Plxna1	FW REV	CCAGGCCAAGCTCTTCGTG CGTGTCTAGCTGCAGGGTGA	250	61
Plxna1_MUT genotyping	FW REV	GCATGCCTGTGACACTTGGCTCACT CCATTGCTCAGCGGTGCTGTCCATC	600	63
Plxna1_WT genotyping	FW REV	CCTGCAGATTGATGACGACTTCTGC TCATGCAGACCCAGTCTCCCTGTCA	200	63
Plxna2	FW REV	ATCAATTCAGCTGGAGACCT TGCTGGTGGTATACAGGGTC	485	57
Plxna3	FW REV	CATCAACACCCCTCTGCAGA GCACCTTCTTCAAATTACCGCT	195	59
Plxna3_MUT genotyping	FW REV	GCCAAGTTCTAATTCCATCAGA CACCTGCTTCTCACTCAGGA	300	55
Plxna3_WT genotyping	FW REV	CCCTGAATAGGGTGTAATAACTT CACCTGCTTCTCACTCAGGA	500	55
Plxna4	FW REV	AGTCCGCCCAGATGACGACC AAGTCATGCGGTCCCTGTCTTCTGT	320	65
Rtkn_ISH	FW REV	CAAGAGGCTTGCCACCAAAC **ggtaatacgactcactatagggATCCAGTTCTGCAGGGCTTC**	594	60
SEMA3G_G166V mutagenesis	FW REV	ACCGCCCCCGGACACTTTCCACACTGC GCAGTGTGGAAAGTGTCCGGGGGCGGT	-	-
Sema3g_ISH	FW REV	CCTTCATCACAGTGGGGCAT **ggtaatacgactcactatagggATAGGGTCCCCACTGATGCT**	680	60
Sema3g_MUT genotyping	FW REV	TTGCCAAGTTCTAATTCCAT AGTTCTGGACTCCTCTTTCC	203	57.5
Sema3g_WT genotyping	FW REV	ATGACGCAGGAAACTACACT AGTTCTGGACTCCTCTTTCC	490	57.5

Table 1 - List of primers. Bold letters represent T7 promoter sequence used in ISH probe design.

20) for 60 min, the membrane was immunoblotted with the following antibodies: mouse anti-cMyc (1:1000; Thermo Fisher Scientific), rabbit anti-Gapdh antibody (1:2500; Abcam), rabbit anti-pAkt (Ser473), rabbit anti-Akt (1:1000 each; Cell Signalling) followed by horseradish peroxidase-conjugated anti-rabbit or anti-mouse antibodies (1:10000; Sigma-Aldrich). Blots were washed with PBS-T three times and developed with the ECL system (Amersham Biosciences) according to the manufacturer's protocols.

2.4 AP-fusion protein-binding assay.

GN11 cells were fixed for 5 minutes in methanol, washed 5 times with PBS, incubated in PBS containing 10% FBS for 30 minutes, and then incubated with AP mix (200 µL of conditioned media containing AP fusion proteins, 56 µL 10% FBS $MgCl_2$, 10.7 µL 0.5 M HEPES pH 7.0) for 1 hour at room temperature. Cells were then washed for 5 minutes each with PBS, fixed with 4% PFA for 2 minutes at room temperature, and washed again. Endogenous AP was heat inactivated by incubation at 65°C for 2 hours. Cell-bound, heat-stable recombinant SEMA3G-AP activity was detected as an insoluble reaction product after incubation with 4-nitro blue tetrazolium chloride (NBT) and 5-bromo-4-chloro-3-indolyl phosphate (BCIP) (Roche).

2.5 Migration assays.

Subconfluent GN11 cells were used for chemotaxis experiments using a 48-well Boyden's chamber (Neuro Probe). For these experiments, GN11 cells were suspended in serum-free medium (100.000 cells/50 µL) and placed in the upper compartment of the Boyden chamber. Compartments were separated by a polycarbonate porous membrane (8 µm pores) pre-coated with gelatin (0.2 mg/mL). 28 µL of the concentrated conditioned media from untransfected COS-7 cells or COS-7 cells transfected with expression vectors for SEMA3G WT or SEMA3G G166V were placed into the lower compartment of the chamber. The chamber was kept in an incubator at 37°C for 2 hours. After 2 hours, cells that had migrated through the membrane separating the two compartments of the chamber were fixed in methanol and thiazine-eosin stained using the Diff-Quick kit (Biomap, Italy).

2.6 RT-PCR on GN11 cells

Total RNA was extracted from subconfluent GN11 with TRIzol (Life Technologies). 1 µg of single-stranded cDNA was synthesized with High-Capacity cDNA Reverse Transcription kit (Applied Biosystems). PCR was performed on 100 ng of cDNA with Platinum SuperFi PCR Master Mix (Invitrogen) according to manufacturer indications with specific primers for murine *Nrp1*, *Nrp2*, *Plxna1*, *Plxna2*, *Plxna3*, *Plxna4* and *Gapdh* (see Table 1). PCR products were analyzed by electrophoresis on a 1% agarose gel and bands visualized under UV illumination after Midori Green staining (Nippon Genetics).

3. *In vivo* methods

3.1 Mouse strains and procedures

Mice were housed in individually ventilated cages under pathogen-free conditions. Animals had free access to food and water and were kept in a 12-hour light-dark cycle. All animal procedures were performed in accordance with institutional UK Home Office and German Home Office guidelines.

Sema3g. Genotyping of *Sema3g* wild type or knock out mice was performed by PCR with specific primers (Table 1); mice were bred on C57Bl/6 background (Kutschera et al., 2011).

Plxna1 and Plxna3. Plxna1 and *Plxna3* mice were maintained on a C57Bl/6 background by pairing heterozygous partners. Double mutant mice were generated by pairing double heterozygous partners. Genotyping was performed using specific primers (Table 1).

Hs6st1. The *Hs6st1*$^{+/-}$ mice have been previously described as well as genotyping protocol (Table 1) (Tillo et al., 2016) and were maintained on a C57BL/6J background by pairing with wild type partners.

Embryo. To obtain embryos of defined gestational stages, mice were mated in the evening, and the morning of vaginal plug formation was counted as E0.5. Time pregnant mouse at the desired stage were terminated with CO_2 followed by cervical dislocation. The abdomen was cut and the embryo-filled uterus was removed from the body cavity and placed in a tissue culture dish filled with fresh ice-cold PBS. Under dissecting microscope, embryos were removed from the uterus and the amniotic sack and then placed in a clean dish with ice-cold PBS. Heads were separated from the embryo and placed in a 24-well plate with fresh ice-cold PBS; tails were kept for genotyping, if needed. Heads were washed 3 times in PBS and then fixed in 4% PFA for 3 hours at 4°C on an orbital shaker. After fixation, heads were washed 2 times in PBS, cryopreserved in a 30% sucrose solution for 24 hours at 4°C and finally embedded in OCT (Leica) or in paraffin.

Adult. Mice were anesthetized with CO_2 and checked for the absence of sensibility. An abdominal incision was performed and after the removal of the sternum, the heart was exposed in order to allow perfusion. A needle was inserted in the left ventricle and perfusion was performed firstly with PBS and then with 4% PFA using a peristaltic pump Gilson Miniplus 2 with a speed of 5 mL/min. Brain and testes were harvested from perfused mice and immersed in 4% PFA overnight at 4°C for additional fixation. Brains were cryopreserved in 30% sucrose solution and embedded in OCT (Leica). Testes were dehydrated through an alcohol series (10%-25%-50%-70%-96%-100% EtOH) and xylene and finally embedded in paraffin.

Vaginal opening. Hs6st1$^{+/+}$ and Hs6st1$^{+/-}$ female mice were checked daily for vaginal opening (VO) and weight after weaning, that is, from 21 days of age (Caligioni, 2009; Messina et al., 2016) (Figure 3).

3.2 In situ hybridization

Probe synthesis. Mouse *Sema3g*, *Nktr* and *Rtkn* antisense probes were synthetized form mouse cDNA. Primers were designed with Primer 3 Plus software (http://biotools.umassmed.edu/cgi-bin/primer3plus/primer3plus.cgi) in order to obtain a 500-800 bp amplicon; the reverse primer was modified with the addition of a T7 promoter at the 5' end (5'-**ggtaatacgactcactataggg**-3'). Primers were resuspended in molecular grade H_2O (Euroclone) at a 100 µM concentration for long term storage and were used at a 10 µM concentration. Oligonucleotides used to generate *Sema3g*, *Nktr*, *Rtkn* probes are listed in Table 1. cDNA produced from mRNA extracted from a sample that expresses the gene of interest was used as a template for a high-fidelity PCR reaction at following conditions (Phusion High Fidelity DNA polymerase, NeB):

Phusion High-Fidelity PCR	
Reagent	**Volume (µL)**
5X HF buffer	10
DMSO	2.5
FW primer (10 µM)	4
REV primer (10 µM)	4
dNTPs (10 mM)	1
cDNA	0.5
Phusion Taq DNA polymerase	0.3
H_2O	28

PCR programme	
Temperature (°C)	**Time**
98	30 s
98	10 s x 35 cycles
60	20 s x 35 cycles
72	20 s x 35 cycles
72	7 min
10	hold

The product of PCR #1 was run on a 1% agarose gel and the band corresponding to the desired amplicon was extracted using the Gel Extraction Kit (Qiagen). A second PCR program was run exactly like the first one but using as template 2.5 µL from the PCR #1 product. PCR #2 product was purified using the PCR Purification Kit (Qiagen). PCR #2 product was quantified by OD (Nanodrop2000, Thermo Scientific) and checked on a 1% agarose gel. For the probe synthesis, 200 ng of PCR #2 product were used as template for T7 RNA polymerase *in vitro* transcription (DIG RNA labelling kit, Roche). Mouse *Gnrh* (SacII/T3; gift from Dr. Memi), *Plxna1* (EcoRI/T7; Addgene plasmid #58237), *Plxna2* (NotI/SP6; Addgene plasmid #62353), *Plxna3* (XhoI/SP6; Addgene plasmid #58238), *Plxna4* (SalI/SP6; Addgene plasmid #58239) (Schwarz et al., 2008) and *Hs6st1* (EcoRI/T3) (Tillo et al., 2016). Antisense probes were synthetized from plasmids containing cDNA of the gene of interest. Sense probe were generated as specificity controls (Figure 4).

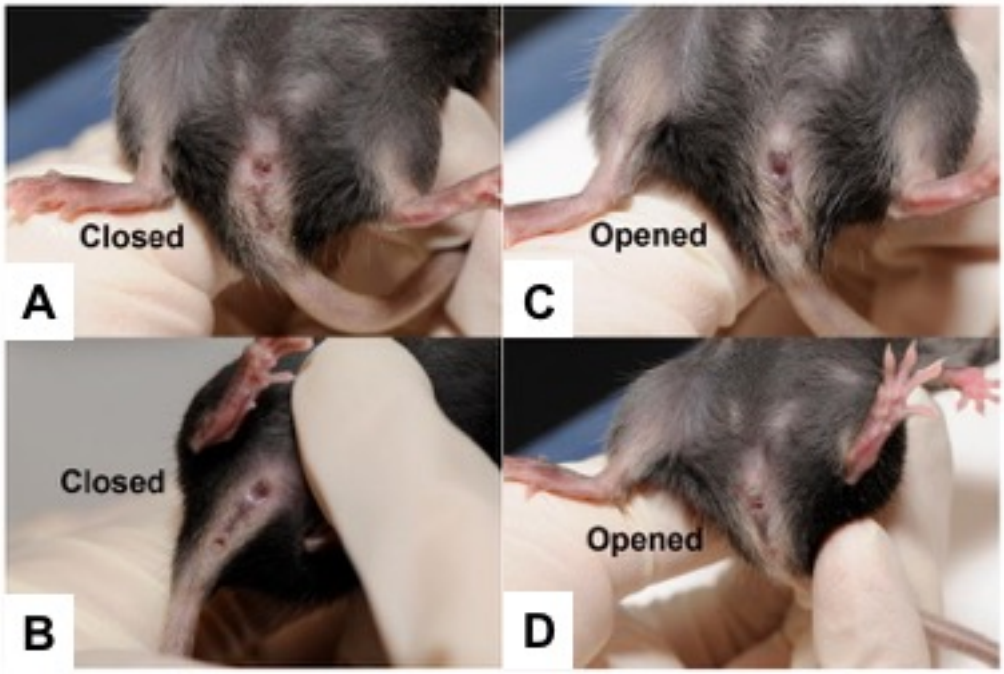

Figure 3 – Vaginal opening check. (A-D) Vaginal opening in mice at approximately postnatal day 26 (P26), showing closed vaginal cavity (A,B) and opened vaginal cavity (C,D).

Adapted from "Assessing reproductive status/stages in mice" by C.S. Caligioni, 2009, *Curr Protoc Neurosci*, Appendix 4-I. Copyright 2009 by the author.

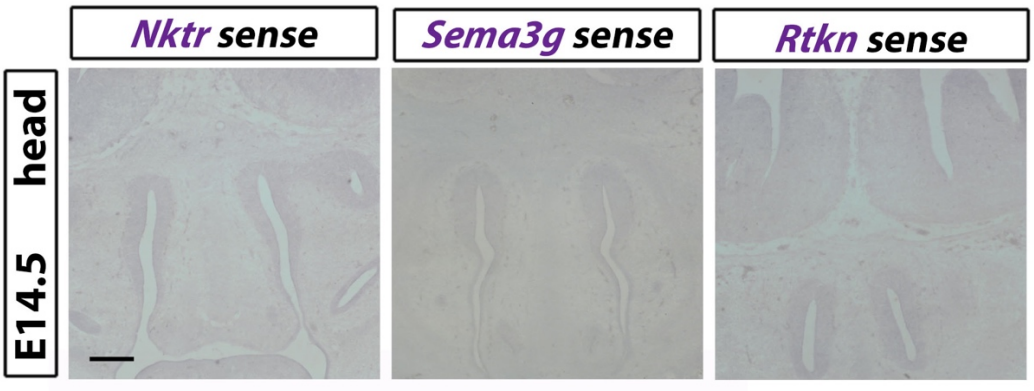

Figure 4 – *In situ* hybridization probes specificity. Coronal sections of mouse embryo heads were RNA-labelled with sense probes against *Nktr*, *Sema3g* and *Rtkn*. No signals can be detected for each sense probe, confirming the specificity of antisense probes that will be used in further experiments.

Briefly, 4 µg of plasmid was linearized with the specific restriction enzyme (NeB) for 2 hours at 37°C in buffer CutSmart 10X (NeB). Linearized plasmids were checked on 1% agarose gel and purified with PCR Purification Kit (Qiagen). 1 µg of linearized plasmid was used as template for *in vitro* transcription, using either T7, SP6 or T3 RNA polymerase (DIG RNA labelling kit, Roche).

Probes were checked on 1% agarose gel and then purified by adding 1 µL of glycogen, 2.5 µL of LiCl 4M and 75 µL of 100% EtOH and incubating overnight at -20°C. Probes were pelleted (centrifuge at 4°C, 13'000 G, 15 minutes), washed with 70% EtOH and pelleted again (centrifuge at 4°C, 13'000 G, 5 minutes). Probe pellets were resuspended in 21.5 µL of molecular grade H_2O, incubated 10 minutes at 55°C to dissolve RNA and then stored in aliquots at -80°C.

Hybridization and detection. PFA-fixed cryosections were incubated with DIG-labelled antisense riboprobes (2 µg/mL). Hybridization step was performed in hybridization buffer (50% formamide, 0.3 M NaCl, 20 mM Tris-HCl, 5mM EDTA, 10% Dextran sulphate, 1x Denhardt's solution, 0.25 mg/mLTorula yeast tRNA) overnight at 65°C in a wet chamber. Sections were washed with saline sodium citrate (SSC) buffer (50% Formamide, 1X Saline Sodium Citrate buffer, 0,1% Tween20), blocked with blocking buffer (100 mM Maleic acid, 150 mM NaCl, 0.1% Tween20, 2% blocking reagent (Roche), 10% Normal Goat Serum (Sigma-Aldrich)) and then incubated overnight with AP-conjugated anti-DIG antibody (1:1500; Roche). mRNA expression was revealed by colorimetric staining using 4-Nitro blue tetrazolium chloride solution and 5-Bromo-4-chloro-3-indolyl phosphate disodium salt (NBT/BCIP, Roche) in a staining solution (100 mM NaCl, 50 mM $MgCl_2$, 100 mM Tris-HCl pH 9.8, 1% Tween20, 5% poly-vinyl-alcohol) at 37°C. Colorimetric reaction was checked after 6 hours and if no coloured precipitate was detected, new staining solution was added and left overnight. The reaction was stopped with MilliQ H_2O and slides were mounted with aqueous mounting media Mowiol 4-88 (Sigma-Aldrich).

3.3 Immunostaining

De-waxing was performed by rehydrating microtome-cut sections through xylene washes and a decrescent alcohol series (100%-96%-70%-50% EtOH). Antigen retrieval was performed before immunostaining in citrate buffer pH 6.0 (10mM Sodium citrate, 0.05% Tween20) at 98°C for 20 minutes.

PFA-fixed cryosections or paraffin embedded sections were washed twice with PBS and permeabilized with PBS containing 0.1% TritonX-100 (Sigma-Aldrich). Aspecific sites were blocked with 10% NGS or serum-free blocking reagent (Dako) according to the primary antibody for 1 hour. For immunoperoxidase labelling (IHC), an additional 20 minutes-block with Bloxall (Vector Lab.) was performed to quench endogenous peroxidases. Sections were incubated with primary antibodies

diluted in PBS 0.1% TritonX-100 overnight at 4°C (Table 1). After washes with PBT, sections were incubated for 2 hours with secondary antibodies conjugated with biotin (for IHC) or fluorophores (for immunofluorescence) diluted in PBS 0.1% TritonX-100 (Table 2). For IHC, sections were developed with the ABC kit for 2 hours (Vector Lab.) and 3,3-diaminobenzidine (Sigma-Aldrich). For IF, nuclei counterstained with DAPI (1:10000; Sigma-Aldrich). Slides were finally mounted with aqueous mounting media Mowiol 4-88.

In some experiments, we performed ISH (Memi et al., 2013) for *Sema3g* before immunostaining for GnRH.

3.4 Histological analysis

Haematoxylin and eosin (H&E). For testes analysis, 10 µm paraffin embedded testes sections were cut with a microtome and processed as previously described (Macchi et al., 2017). Briefly, sections were rehydrated through xylene and a decrescent alcohol series (100%-96%-70%-50%- H_2O) and stained with haematoxylin for 1 minute and eosin for 3 minutes (Bio-Optica). Sections were then dehydrated with a crescent alcohol series (H_2O-50%-70%-96%-100%) and xylene and mounted with the synthetic mounting media BioMount (Bio-Optica).

Alcian blue. Alcian blue staining was performed as previously described (Cohen et al, 2012). Briefly, sections were incubated with 0.2% alcian blue (Sigma-Aldrich) in acid/ethanol solution (0.37% HCl, 70% EtOH) for 30 minutes, washed in acid/ethanol and then cleared with KOH/glycerol (1% KOH m/v in H_2O, 50% glycerol v/v). Slides were mounted with aqueous mounting media Mowiol 4-88.

4. Image processing, quantifications and statistics

4.1 Image processing

To acquire bright-field images, we used a Zeiss Axioskop2 plus microscope equipped with a TCH-5.0ICE digital camera or a Leica DM5500B microscope equipped with a DCF295 camera (Boyden's chamber assay, AP assay, ISH and DAB stained sections, H&E and alcian blue stained sections). We used a Leica TCS SPE1 confocal microscope to acquire fluorescence images of COS-7 transfected cells and mouse tissues. All images were processed using Photoshop CS6 (Adobe Inc.). In some experiments, we acquired brightfield images of ISH patterns and confocal images of immunofluorescence staining and converted the bright-field images to RGB color mode for superimposition onto the confocal images.

Primary Antibody antigen	Host	Dilution	Company
mouse Gnrh	Rabbit	1:1000 IHC/1:400 IF	Immunostar
mouse Peripherin	Rabbit	1:200	Millipore
mouse CD31	Rabbit	1:50	Abcam
mouse Endomucin	Rat	1:300	Santa Cruz
mouse Sox9	Rabbit	1:1000	gift Prof. Wegner
mouse Cyp17a1	Mouse	1:100	Santa Cruz
mouse Plxna1	Goat	1:200	R&D
mouse Plxna3	Goat	1:200	R&D
mouse Tuj1	Rabbit	1:500	Covance
mouse S100	Rabbit	1:400	Dako
Biotinylated Isolectin B4	-	1:50	Vector Lab.

Table 1 - List of primary antibodies used for immunohistochemistry.

Secondary Antibody	Host	Dilution	Company
anti Rabbit IgG-488	Donkey	1:200	Jackson Immuno.
anti Rabbit IgG-biotin	Goat	1:400	Vector Lab.
anti Rabbit IgG-Cy3	Donkey	1:200	Jackson Immuno.
anti Mouse IgG-488	Donkey	1:200	Jackson Immuno.
anti Goat IgG-Cy3	Donkey	1:200	Jackson Immuno.
anti Rat IgG-biotin	Goat	1:400	Vector Lab.
Streptavidin-488	-	1:200	Jackson Immuno.

Table 2 – List of secondary antibodies used for immunocytochemistry.

4.2 Quantifications

Transfection efficiency. Transfection efficiency of COS-7 cells with WT or mutated SEMA3G containing plasmids was determined from 3 independent transfections as a ratio of fluorescent positive cells to the total of DAPI positive cells number.

Boyden's chamber assay. Images were taken with a 20x objective and analysed with ISCapture software. Three random fields of stained cells were counted for each well, and the mean number of migrating cells/field for each experimental condition was calculated.

Densitometric analysis immunoblotting. Densitometric analysis of band intensity was performed using the ImageJ software (NIH) and the mean pixel intensity calculated. Optical density (O.D.) values were normalized on Gapdh values and the O.D. ratio pAKT/AKT was calculated.

Immunostaining analysis. To determine the total number of GnRH neurons in E14.5 mouse heads or in postnatal mouse brains, 20 μm sagittal sections through each entire head/brain were immunolabelled for GnRH and all GnRH-positive cells counted in each section, as previously described (Cariboni et al., 2011). For each experimental condition, at least n = 3 heads/brains were analysed. To compare the abundance of $GnRH^+$ neurites at the ME of wild types and mutants, we measured the pixel intensity of GnRH staining in 20 μm sagittal sections through the ME of n=3 mice for each genotype at 10x magnification. To quantify the number of Sertoli and Leydig cells in the testes, we counted the number of $Sox9^+$ e Cyp^+ cells per tubule or in the interstitial space of wils type and mutant testes, respectively, in 12 independent images acquired with a 20x objective.

4.3 Statistics

A Fisher's exact test was used to compare the prevalence of deleterious variants in our cohort with the Finnish population, using the ExAC browser (Exome Aggregation Consortium, Cambridge, MA).

For *in vitro* and *in vivo* experiments, we calculated the mean of at least three independent samples. Data are expressed as mean ± standard error of the mean (s.e.m.) or as mean ± standard deviation (s.d.). To determine statistical significance, we used the two-way Student's unpaired t-test or, for multiple comparison, a one-way ANOVA followed by a Dunnett's post-hoc test. For VO analysis we used a one-way Student's paired t-test. A p-value of $P<0.05$ (one asterisk) was considered significant; a p-value of $P<0.01$ was indicated with 2 asterisks; a p-value of $P<0.001$ with 3 asterisks. Statistical analysis was performed using Prism4 software (GraphPad Software).

SECTION V
Discussion and future perspectives

IGD represents a complex and heterogenous disorder from both clinical and genetic points of view with many different clinical manifestations characterized by nHH along with other non-reproductive symptoms, and up to 35 genes identified to cause a pathological phenotype. In addition, recent observations highlight the high variability in the inheritance pattern of IGD, which can be Mendelian (i.e. autosomal recessive or dominant, X-linked recessive) or oligogenic, with two or more genes implicated. Moreover, genetic causes for IGD are still largely unknown, with the 50% of overall cases being idiopathic (Stamou and Georgopoulos, 2017). All these features create a complex genetic architecture underlying this disorder and hampered genotype-phenotype correlations, making IGD hard to be diagnosed. Thus, a timely and precise diagnosis is necessary to guarantee an early treatment aimed at restoring the HPG axis functionality and to prevent the onset of co-morbidities such as osteoporosis, psychosocial disturbs and type II diabetes (Boehm et al., 2015). The identification of novel genes implicated in IGD will certainly help to ameliorate treatment and this can be achieved by using two strategies. First, an accurate screening of patients affected by IGD may identify mutations in novel genes that must be studied in experimental models in order to confirm their biological function; second, the phenotypic analysis of genetically modified mouse models could predict novel candidate genes to be screened in patients affected by IGD. Here, we successfully applied both approaches to increase our knowledge on the genetic architecture underlying IGD. Moreover, we had the opportunity to collaborate with clinicians who study the genetic causes of self-limited DP in a large and well-characterized cohort of patients. In this context, we proved that IGD causative genes may also be involved in the pathogenesis of self-limited DP, providing evidences of common genetic pathways underlying these rare disorders.

First, thanks to a collaboration with clinicians from Great Ormond Street Children Hospital, we studied a novel form of syndromic IGD characterized by nHH, mental retardation and facial dysmorphic features, whose genetic causes were still unrecognized. This rare disorder was shared by two brothers born from a consanguineous marriage thus we combined HZM with WES to search for homozygous mutations in novel candidate genes. We found three novel homozygous variants lying in shared homozygous regions harboured by *SEMA3G*, *RTKN* and *NKTR* genes. We next studied the biological relevance of these mutations in well-established experimental models, such as wild type and genetically modified mouse models, immortalized GnRH neurons and bioinformatic tools for mutational predictions. We focussed our efforts first on class 3 semaphorin member SEMA3G as this class of molecules has been deeply studied along with GnRH neuron development and olfactory system formation. Interestingly, we confirmed the essential recruitment of a functional Sema3g signalling in the development of GnRH neurons both *in vitro* and *in vivo*. Still, our mouse model lacking *Sema3g* gene display defective GnRH neuron migration but did not recapitulate the other

phenotypic feature, i.e. mental retardation and facial dysmorphism, characterizing the novel form of syndromic IGD exhibited by our patients. Thus, we performed preliminary expression analysis on wild-type mice to study the potential involvement of *NKTR* and *RTKN* in the pathogenesis of this disorder. In agreement with our hypothesis, *Nktr* seemed to be expressed by cartilaginous tissues of the head and therefore it may have a role in the correct formation of head's bones and cartilages; in turn, *Rtkn* was found to be expressed by proliferative zones of ventral and dorsal FB, suggesting a possible involvement in neuronal progenitor development and subsequently dysfunctional Rtkn may underlie mental retardation. Although our expression studies provide insights into a hypothetical recruitment of NKTR and RTKN in the development of embryonic head and therefore may endorse them as concurrent causative genes together with SEMA3G for our form of syndromic IGD, these studies are not conclusive and further experiments will elucidate the biological function of NKTR and RTKN. In the future, we will perform functional studies on a transgenic zebrafish line carrying a point mutation that cause a premature stop codon in *nktr* orthologue gene (*nktr*^{sa37872}); moreover, this mutation affects a residue that in conserved across species and it lies in the same domain of the mutation found in our patients which is conserved in zebrafish as well. This mutant line combined with wild type fishes will allow us to easily study cartilage development in zebrafish embryos lacking a functional *nktr* gene by performing ISH analysis to confirm the expression of *nktr* in cartilaginous tissues and Alcian blue staining to visualize altered cartilages. On the other side, we will perform *in utero* electroporation of shRNA for mouse Rtkn in mouse embryo to knock-down gene function and thereafter we will assess the presence of abnormal cortical development by histological examinations.

On the other hand, the aim of this dissertation was also the identification of signalling receptor for Sema3a in the context of GnRH neurons and olfactory system development. *SEMA3A* is a well-recognized gene underlying IGD as mutations have been found in up to 6% of overall cases (Balasubramanian and Crowley, 1993) and mice lacking either *Sema3a* or its co-receptors *Nrp1*^{sema}*/Nrp*2 exhibited abnormal olfactory system formation and defective GnRH neuron migration (Cariboni et al., 2011). Class 3 semaphorins signalling receptors Plxna1-4 are redundantly expressed and co-operate in different complexes to transduce signals into the cells depending on tissues and developmental stage. The role of PlxnAs in the context of nasal compartment has been only recently described. The functional involvement of Plxna1 in olfactory/GnRH neuron system development was demonstrated and mutations in *PLXNA1* gene were found in patients affected by KS (Marcos et al., 2017). Yet, *Plxna1*-null mice showed at low penetrance a pathological phenotype and mutations in patients have been found in heterozygous state concomitantly with other mutated genes. Thus, we hypothesized a possible compensative role of other PlxnAs. First, we studied the expression of all four PlxnAs during mouse embryonic development in order to identify the best candidates to control

OLF/VN nerves formation and therefore GnRH neuron migration together with Plxna1 and we found that Plxna1 and Plxna3 are expressed by peripherin-expressing neuronal cells. Then, by taking advantage from genetically mouse models we studied the functional role of this two isoforms and accordingly we found that only compound *Plxna1;Plxna3*-null mice present defective GnRH neuron migration due to misrouting of VN nerves and to the absence of cVN/TN nerves. So far, adult mice have not been available, and we were able to confirm the severe phenotype only in P10 mice, which exhibited a less innervated ME compared to their wild type littermates. Therefore, further analysis will be needed on post-pubertal mice to assess their reproductive capacity and gonadal functionality. To this purpose, it will be important to analyse whether the nearly absence of GnRH neurons in the MPOA of embryonic *Plxna1;Plxna3* compound-null mice will have an impact on the fertility of adult mice. The preliminary analysis performed on P10 mice suggests that GnRH deficiency persists also during postnatal development as ME of compound knock out mice showed a decreased innervation by GnRH neurons. However, it will be necessary to analyse post-pubertal mice in order to assess the impact of GnRH neuron loss on gonadal size and morphology and on reproductive capacity. Overall, our findings in mouse embryos and the preliminary experiments on P10 mice indicate PLXNA3 as a novel putative gene underlying IGD and therefore mutations in *PLXNA3* gene may be screened in patients. Furthermore, by taking advantage from human foetus tissues provided by HDBR facility in London, UK, we were able to demonstrate that PLXNA1 and PLXNA3 are expressed with a conserved pattern in human foetus heads as well. In future, it would be interesting to identify the nature of PLXNA1- and PLXNA3-positive cells in humans by double immunofluorescence experiments using antibodies specific for each PLXNA isoform and markers for GnRH neurons, OLF nerves, VN/TN nerves and OECs. These studies will ameliorate our understanding on how the olfactory and GnRH neuron systems develop in humans and will strengthen the possibility that PLXNA3 play a pivotal role for HPG axis functionality in humans. Finally, we demonstrated the efficacy of basic research-driven approach in predicting novel candidate genes underlying IGD.

The third part of this dissertation was aimed at better understanding the genetic architecture that determine self-limited DP, which represents the extreme end of normal pubertal timing and is the principal cause of DP. Familial self-limited DP is a highly heritable condition, which often segregates in an autosomal dominant pattern in the majority of families. Although self-limited DP has a clear genetic basis, the underlying genetic regulation has been largely unknown (Howard, 2018). Recent studies have discovered a novel gene that lead to familial self-limited DP, such as *IGSF10* (Howard et al., 2016) and further understanding on self-limited DP has come from sequencing genes known to cause GnRH deficiency, NGS studies in patients with early puberty and from large-scale genome wide association studies in the general population (Howard and Dunkel, 2018). These studies

suggested that the genetic basis of DP is highly heterogeneous and may be partially overlapping with the genetics underlying IGD (Zhu et al., 2015). On this basis, in collaboration with clinicians from Queen Mary University in London, UK, we analysed WES data from 160 individuals from a large cohort of Finnish self-limited DP patients in search for mutations in IGD causative genes. We only found one heterozygous rare variant (R375H) in *HS6ST1* gene that segregates with self-limited DP trait within families. To confirm the pathogenic potential of *HS6ST1* haploinsufficiency, we performed *in vivo* experiments on wild type and *Hs6st1*$^{+/-}$ mice. We found that *Hs6st1* is expressed within the MPOA and ARC of adult mice. Peri-pubertal female mice exhibited delayed VO whilst post-pubertal heterozygous mice do not show any defects due to spontaneous, although delayed, puberty onset. Our results strengthen the idea that self-limited DP and IGD shared, at least in part, a common genetic architecture. In addition, we demonstrated that *HS6ST1* haploinsufficiency is sufficient to cause self-limited DP both in mice and in humans and self-limited DP patients with an unknown genetic cause should be screened for mutations in *HS6ST1*. However, molecular mechanisms through which Hs6st1 deficiency cause either IGD or self-limited DP have not been elucidated yet. Heparan sulphate modifications of many different proteoglycans in the extracellular matrix have the potential to affect multiple signalling pathways and accordingly mutations in Hs6st1 may impact HPG axis at very different levels. For these reasons, we may hypothesize that Hs6st1 exert a dual role in the development of GnRH neurons, which if defective leads to IGD, and in their function within the adult hypothalamus, causing self-limited DP if altered. In the future, we will extend *Hs6st1* mRNA expression studies to embryonic stages and we will analyse *Hs6st1*-null mice to assess the recruitment of this enzyme for the correct development of GnRH neurons. Moreover, we will evaluate possible compensative mechanisms exerted by other genes, such as *Hs6st2* and *Hs6st3*, by analysing their expression patterns in wild type mice and the compound loss of different enzyme modifying heparan sulphate in genetically modified mice.

In conclusion, our studies identified *SEMA3G*, *NKTR* and *RTKN* as underlying genes for a novel form of syndromic IGD, proposed *PLXNA3* as a novel gene to be screened in KS patients and demonstrated the essential requirement of fully functional *HS6ST1* in puberty onset. Overall, the results obtained during my PhD thesis provided novel insights into the molecular mechanisms and genetics controlling GnRH neuron biology and associated reproductive disorders, confirming that the combination of patients screening and experimental *in silico*, *in vitro* and *in vivo* models are effective in the discovering novel genes implicated in rare and complex inherited disorders such as IGD.

SECTION VI
References

Abraham, E., Palevitch, O., Gothilf, Y. and Zohar, Y. (2009). The zebrafish as a model system for forebrain GnRH neuronal development. *Gen. Comp. Endocrinol.* **164**, 151–160.

Abreu, A. P. and Kaiser, U. B. (2016). Pubertal development and regulation. *lancet. Diabetes Endocrinol.* **4**, 254–264.

Abreu, A. P., Trarbach, E. B., de Castro, M., Frade Costa, E. M., Versiani, B., Matias Baptista, M. T., Garmes, H. M., Mendonca, B. B. and Latronico, A. C. (2008). Loss-of-Function Mutations in the Genes Encoding Prokineticin-2 or Prokineticin Receptor-2 Cause Autosomal Recessive Kallmann Syndrome. *J. Clin. Endocrinol. Metab.* **93**, 4113–4118.

Adams, R. H., Lohrum, M., Klostermann, A., Betz, H. and Püschel, A. W. (1997). The chemorepulsive activity of secreted semaphorins is regulated by furin-dependent proteolytic processing. *EMBO J.* **16**, 6077–86.

Adzhubei, I. A., Schmidt, S., Peshkin, L., Ramensky, V. E., Gerasimova, A., Bork, P., Kondrashov, A. S. and Sunyaev, S. R. (2010). A method and server for predicting damaging missense mutations. *Nat. Methods* **7**, 248–9.

Aerts, S., Lambrechts, D., Maity, S., Van Loo, P., Coessens, B., De Smet, F., Tranchevent, L.-C., De Moor, B., Marynen, P., Hassan, B., et al. (2006). Gene prioritization through genomic data fusion. *Nat. Biotechnol.* **24**, 537–44.

Alto, L. T. and Terman, J. R. (2017). Semaphorins and their Signaling Mechanisms. *Methods Mol. Biol.* **1493**, 1–25.

Amoss, M., Burgus, R., Blackwell, R., Vale, W., Fellows, R. and Guillemin, R. (1971). Purification, amino acid composition and N-terminus of the hypothalamic luteinizing hormone releasing factor (LRF) of ovine origin. *Biochem. Biophys. Res. Commun.*

Anderson, S. K., Gallinger, S., Roder, J., Frey, J., Young, H. a and Ortaldo, J. R. (1993). A cyclophilin-related protein involved in the function of natural killer cells. *Proc. Natl. Acad. Sci. U. S. A.* **90**, 542–6.

Antipenko, A., Himanen, J.-P., van Leyen, K., Nardi-Dei, V., Lesniak, J., Barton, W. A., Rajashankar, K. R., Lu, M., Hoemme, C., Püschel, A. W., et al. (2003). Structure of the semaphorin-3A receptor binding module. *Neuron* **39**, 589–98.

Ardouin, O., Legouis, R., Fasano, L., David-Watine, B., Korn, H., Hardelin, J. P. and Petit, C. (2000). Characterization of the two zebrafish orthologues of the KAL-1 gene underlying X chromosome-linked Kallmann syndrome. *Mech. Dev.* **90**, 89–94.

Ba, W., van der Raadt, J. and Nadif Kasri, N. (2013). Rho GTPase signaling at the synapse: Implications for intellectual disability. *Exp. Cell Res.* **319**, 2368–2374.

Bagri, A., Cheng, H.-J., Yaron, A., Pleasure, S. J. and Tessier-Lavigne, M. (2003). Stereotyped pruning of long hippocampal axon branches triggered by retraction inducers of the semaphorin family. *Cell* **113**, 285–99.

Balasubramanian, R. and Crowley, W. F. (1993). *Isolated Gonadotropin-Releasing Hormone (GnRH) Deficiency*.

Balasubramanian, R. and Crowley, W. F. (2017). Reproductive endocrine phenotypes relating to CHD7 mutations in humans. *Am. J. Med. Genet. C. Semin. Med. Genet.* **175**, 507–515.

Bamberg, J. A., Baumgartner, S., Betz, H., Bolz, J., Chedotal, A., Christensen, C. R. L., Comoglio, P. M., Culotti, J. G., Doherty, P., Drabkin, H., et al. (1999). Unified nomenclature for the semaphorins/collapsins. Semaphorin Nomenclature Committee. *Cell* **97**,

551–2.

Bamshad, M. J., Ng, S. B., Bigham, A. W., Tabor, H. K., Emond, M. J., Nickerson, D. A. and Shendure, J. (2011). Exome sequencing as a tool for Mendelian disease gene discovery. *Nat. Rev. Genet.* **12**, 745–55.

Barraud, P., St John, J. A., Stolt, C. C., Wegner, M. and Baker, C. V. H. (2013). Olfactory ensheathing glia are required for embryonic olfactory axon targeting and the migration of gonadotropin-releasing hormone neurons. *Biol. Open* **2**, 750–9.

Beate, K., Joseph, N., Nicolas, D. R. and Wolfram, K. (2012). Genetics of isolated hypogonadotropic hypogonadism: role of GnRH receptor and other genes. *Int. J. Endocrinol.* **2012**, 147893.

Bellon, A., Luchino, J., Haigh, K., Rougon, G., Haigh, J., Chauvet, S. and Mann, F. (2010). VEGFR2 (KDR/Flk1) signaling mediates axon growth in response to semaphorin 3E in the developing brain. *Neuron* **66**, 205–19.

Benjamini, Y., Drai, D., Elmer, G., Kafkafi, N. and Golani, I. (2001). Controlling the false discovery rate in behavior genetics research. *Behav. Brain Res.* **125**, 279–84.

Bergman, J. E. H., Bosman, E. A., van Ravenswaaij-Arts, C. M. A. and Steel, K. P. (2010). Study of smell and reproductive organs in a mouse model for CHARGE syndrome. *Eur. J. Hum. Genet.* **18**, 171–7.

Bhattacharyya, S. and Bronner-Fraser, M. (2008). Competence, specification and commitment to an olfactory placode fate. *Development* **135**, 4165–77.

Bianco, S. D. C. and Kaiser, U. B. (2009). The genetic and molecular basis of idiopathic hypogonadotropic hypogonadism. *Nat. Rev. Endocrinol.* **5**, 569–76.

Bishop, J. R., Schuksz, M. and Esko, J. D. (2007). Heparan sulphate proteoglycans fine-tune mammalian physiology. *Nature* **446**, 1030–7.

Bless, E., Raitcheva, D., Henion, T. R., Tobet, S. and Schwarting, G. A. (2006). Lactosamine modulates the rate of migration of GnRH neurons during mouse development. *Eur. J. Neurosci.* **24**, 654–60.

Boehm, U., Bouloux, P.-M., Dattani, M. T., de Roux, N., Dodé, C., Dunkel, L., Dwyer, A. A., Giacobini, P., Hardelin, J.-P., Juul, A., et al. (2015). Expert consensus document: European Consensus Statement on congenital hypogonadotropic hypogonadism--pathogenesis, diagnosis and treatment. *Nat. Rev. Endocrinol.* **11**, 547–64.

Bouilly, J., Messina, A., Papadakis, G., Cassatella, D., Xu, C., Acierno, J. S., Tata, B., Sykiotis, G., Santini, S., Sidis, Y., et al. (2018). DCC/NTN1 complex mutations in patients with congenital hypogonadotropic hypogonadism impair GnRH neuron development. *Hum. Mol. Genet.* **27**, 359–372.

Bouligand, J., Ghervan, C., Tello, J. A., Brailly-Tabard, S., Salenave, S., Chanson, P., Lombès, M., Millar, R. P., Guiochon-Mantel, A. and Young, J. (2009). Isolated familial hypogonadotropic hypogonadism and a GNRH1 mutation. *N. Engl. J. Med.* **360**, 2742–8.

Brand, J. S., Rovers, M. M., Yeap, B. B., Schneider, H. J., Tuomainen, T.-P., Haring, R., Corona, G., Onat, A., Maggio, M., Bouchard, C., et al. (2014). Testosterone, sex hormone-binding globulin and the metabolic syndrome in men: an individual participant data meta-analysis of observational studies. *PLoS One* **9**, e100409.

Brock, O. and Bakker, J. (2013). The two kisspeptin neuronal populations are differentially

organized and activated by estradiol in mice. *Endocrinology* **154**, 2739–2749.

Bülow, H. E., Berry, K. L., Topper, L. H., Peles, E. and Hobert, O. (2002). Heparan sulfate proteoglycan-dependent induction of axon branching and axon misrouting by the Kallmann syndrome gene kal-1. *Proc. Natl. Acad. Sci. U. S. A.* **99**, 6346–51.

Caligioni, C. S. (2009). Assessing reproductive status/stages in mice. *Curr. Protoc. Neurosci.* **Appendix 4**, Appendix 4I.

Campbell, R. K., Satoh, N. and Degnan, B. M. (2004). Piecing together evolution of the vertebrate endocrine system. *Trends Genet.* **20**, 359–66.

Campbell, R. E., Gaidamaka, G., Han, S.-K. and Herbison, A. E. (2009). Dendro-dendritic bundling and shared synapses between gonadotropin-releasing hormone neurons. *Proc. Natl. Acad. Sci.* **106**, 10835–10840.

Capparuccia, L. and Tamagnone, L. (2009). Semaphorin signaling in cancer cells and in cells of the tumor microenvironment--two sides of a coin. *J. Cell Sci.* **122**, 1723–36.

Cariboni, A., Pimpinelli, F., Colamarino, S., Zaninetti, R., Piccolella, M., Rumio, C., Piva, F., Rugarli, E. I. and Maggi, R. (2004). The product of X-linked Kallmann's syndrome gene (KAL1) affects the migratory activity of gonadotropin-releasing hormone (GnRH)-producing neurons. *Hum. Mol. Genet.* **13**, 2781–91.

Cariboni, A., Rakic, S., Liapi, A., Maggi, R., Goffinet, A. and Parnavelas, J. G. (2005). Reelin provides an inhibitory signal in the migration of gonadotropin-releasing hormone neurons. *Development* **132**, 4709–18.

Cariboni, A., Maggi, R. and Parnavelas, J. G. (2007a). From nose to fertility: the long migratory journey of gonadotropin-releasing hormone neurons. *Trends Neurosci.* **30**, 638–644.

Cariboni, A., Hickok, J., Rakic, S., Andrews, W., Maggi, R., Tischkau, S. and Parnavelas, J. G. (2007b). Neuropilins and their ligands are important in the migration of gonadotropin-releasing hormone neurons. *J. Neurosci.* **27**, 2387–95.

Cariboni, A., Davidson, K., Rakic, S., Maggi, R., Parnavelas, J. G. and Ruhrberg, C. (2011a). Defective gonadotropin-releasing hormone neuron migration in mice lacking SEMA3A signalling through NRP1 and NRP2: implications for the aetiology of hypogonadotropic hypogonadism. *Hum. Mol. Genet.* **20**, 336–44.

Cariboni, A., Davidson, K., Dozio, E., Memi, F., Schwarz, Q., Stossi, F., Parnavelas, J. G. and Ruhrberg, C. (2011b). VEGF signalling controls GnRH neuron survival via NRP1 independently of KDR and blood vessels. *Development* **138**, 3723–33.

Cariboni, A., Andrews, W. D., Memi, F., Ypsilanti, A. R., Zelina, P., Chedotal, A. and Parnavelas, J. G. (2012). Slit2 and Robo3 modulate the migration of GnRH-secreting neurons. *Development* **139**, 3326–31.

Cariboni, A., André, V., Chauvet, S., Cassatella, D., Davidson, K., Caramello, A., Fantin, A., Bouloux, P., Mann, F. and Ruhrberg, C. (2015). Dysfunctional SEMA3E signaling underlies gonadotropin-releasing hormone neuron deficiency in Kallmann syndrome. *J. Clin. Invest.* **125**, 2413–28.

Casoni, F., Hutchins, B. I., Donohue, D., Fornaro, M., Condie, B. G. and Wray, S. (2012). SDF and GABA interact to regulate axophilic migration of GnRH neurons. *J. Cell Sci.* **125**, 5015–25.

Casoni, F., Malone, S. A., Belle, M., Luzzati, F., Collier, F., Allet, C., Hrabovszky, E., Rasika,

S., Prevot, V., Chédotal, A., et al. (2016). Development of the neurons controlling fertility in humans: new insights from 3D imaging and transparent fetal brains. *Development* **143**, 3969–3981.

Cassatella, D., Howard, S. R., Acierno, J. S., Xu, C., Papadakis, G. E., Santoni, F. A., Dwyer, A. A., Santini, S., Sykiotis, G. P., Chambion, C., et al. (2018). Congenital hypogonadotropic hypogonadism and constitutional delay of growth and puberty have distinct genetic architectures. *Eur. J. Endocrinol.* **178**, 377–388.

Chachlaki, K., Malone, S. A., Qualls-Creekmore, E., Hrabovszky, E., Münzberg, H., Giacobini, P., Ango, F. and Prevot, V. (2017). Phenotyping of nNOS neurons in the postnatal and adult female mouse hypothalamus. *J. Comp. Neurol.* **525**, 3177–3189.

Chan, Y.-M., de Guillebon, A., Lang-Muritano, M., Plummer, L., Cerrato, F., Tsiaras, S., Gaspert, A., Lavoie, H. B., Wu, C.-H., Crowley, W. F., et al. (2009). GNRH1 mutations in patients with idiopathic hypogonadotropic hypogonadism. *Proc. Natl. Acad. Sci. U. S. A.* **106**, 11703–8.

Chauvet, S., Cohen, S., Yoshida, Y., Fekrane, L., Livet, J., Gayet, O., Segu, L., Buhot, M.-C., Jessell, T. M., Henderson, C. E., et al. (2007). Gating of Sema3E/PlexinD1 signaling by neuropilin-1 switches axonal repulsion to attraction during brain development. *Neuron* **56**, 807–22.

Christian, C. A. and Moenter, S. M. (2010). The neurobiology of preovulatory and estradiol-induced gonadotropin-releasing hormone surges. *Endocr. Rev.* **31**, 544–77.

Chung, W. C. J. and Tsai, P.-S. (2010). Role of fibroblast growth factor signaling in gonadotropin-releasing hormone neuronal system development. *Front. Horm. Res.* **39**, 37–50.

Clarke, I. J. (2011). Control of GnRH secretion: one step back. *Front. Neuroendocrinol.* **32**, 367–75.

Clarke, I. J. and Arbabi, L. (2016). New concepts of the central control of reproduction, integrating influence of stress, metabolic state, and season. *Domest. Anim. Endocrinol.* **56**, S165–S179.

Clarkson, J. and Herbison, A. E. (2016). Hypothalamic control of the male neonatal testosterone surge. *Philos. Trans. R. Soc. Lond. B. Biol. Sci.* **371**, 20150115.

Clément, K., Vaisse, C., Lahlou, N., Cabrol, S., Pelloux, V., Cassuto, D., Gourmelen, M., Dina, C., Chambaz, J., Lacorte, J. M., et al. (1998). A mutation in the human leptin receptor gene causes obesity and pituitary dysfunction. *Nature* **392**, 398–401.

Cogliati, T., Delgado-Romero, P., Norwitz, E. R., Guduric-Fuchs, J., Kaiser, U. B., Wray, S. and Kirsch, I. R. (2007). Pubertal impairment in Nhlh2 null mice is associated with hypothalamic and pituitary deficiencies. *Mol. Endocrinol.* **21**, 3013–27.

Condomitti, G. and de Wit, J. (2018). Heparan Sulfate Proteoglycans as Emerging Players in Synaptic Specificity. *Front. Mol. Neurosci.* **11**, 14.

Conrotto, P., Valdembri, D., Corso, S., Serini, G., Tamagnone, L., Comoglio, P. M., Bussolino, F. and Giordano, S. (2005). Sema4D induces angiogenesis through Met recruitment by Plexin B1. *Blood* **105**, 4321–9.

Cordero, D. R., Brugmann, S., Chu, Y., Bajpai, R., Jame, M. and Helms, J. A. (2011). Cranial neural crest cells on the move: their roles in craniofacial development. *Am. J. Med. Genet. A* **155A**, 270–9.

Corradi, A., Croci, L., Broccoli, V., Zecchini, S., Previtali, S., Wurst, W., Amadio, S., Maggi, R., Quattrini, A. and Consalez, G. G. (2003). Hypogonadotropic hypogonadism and peripheral neuropathy in Ebf2-null mice. *Development* **130**, 401–10.

Cravo, R. M., Margatho, L. O., Osborne-Lawrence, S., Donato, J., Atkin, S., Bookout, A. L., Rovinsky, S., Frazão, R., Lee, C. E., Gautron, L., et al. (2011). Characterization of Kiss1 neurons using transgenic mouse models. *Neuroscience* **173**, 37–56.

d'Anglemont de Tassigny, X., Fagg, L. A., Dixon, J. P. C., Day, K., Leitch, H. G., Hendrick, A. G., Zahn, D., Franceschini, I., Caraty, A., Carlton, M. B. L., et al. (2007). Hypogonadotropic hypogonadism in mice lacking a functional Kiss1 gene. *Proc. Natl. Acad. Sci. U. S. A.* **104**, 10714–9.

Day, F. R., Elks, C. E., Murray, A., Ong, K. K. and Perry, J. R. B. (2015). Puberty timing associated with diabetes, cardiovascular disease and also diverse health outcomes in men and women: the UK Biobank study. *Sci. Rep.* **5**, 11208.

de Roux, N., Genin, E., Carel, J.-C., Matsuda, F., Chaussain, J.-L. and Milgrom, E. (2003). Hypogonadotropic hypogonadism due to loss of function of the KiSS1-derived peptide receptor GPR54. *Proc. Natl. Acad. Sci.* **100**, 10972–10976.

Dellovade, T. L., Pfaff, D. W. and Schwanzel-Fukuda, M. (1998). The gonadotropin-releasing hormone system does not develop in Small-Eye (Sey) mouse phenotype. *Brain Res. Dev. Brain Res.* **107**, 233–40.

Deng, S., Hirschberg, A., Worzfeld, T., Penachioni, J. Y., Korostylev, A., Swiercz, J. M., Vodrazka, P., Mauti, O., Stoeckli, E. T., Tamagnone, L., et al. (2007). Plexin-B2, but not Plexin-B1, critically modulates neuronal migration and patterning of the developing nervous system in vivo. *J. Neurosci.* **27**, 6333–47.

Diaczok, D., Romero, C., Zunich, J., Marshall, I. and Radovick, S. (2008). A novel dominant negative mutation of OTX2 associated with combined pituitary hormone deficiency. *J. Clin. Endocrinol. Metab.* **93**, 4351–9.

Diaczok, D., DiVall, S., Matsuo, I., Wondisford, F. E., Wolfe, A. M. and Radovick, S. (2011). Deletion of Otx2 in GnRH neurons results in a mouse model of hypogonadotropic hypogonadism. *Mol. Endocrinol.* **25**, 833–46.

Dodé, C. and Hardelin, J.-P. (2009). Kallmann syndrome. *Eur. J. Hum. Genet.* **17**, 139–46.

Dodé, C., Levilliers, J., Dupont, J.-M., De Paepe, A., Le Dû, N., Soussi-Yanicostas, N., Coimbra, R. S., Delmaghani, S., Compain-Nouaille, S., Baverel, F., et al. (2003). Loss-of-function mutations in FGFR1 cause autosomal dominant Kallmann syndrome. *Nat. Genet.* **33**, 463–5.

Dodé, C., Teixeira, L., Levilliers, J., Fouveaut, C., Bouchard, P., Kottler, M.-L., Lespinasse, J., Lienhardt-Roussie, A., Mathieu, M., Moerman, A., et al. (2006). Kallmann syndrome: mutations in the genes encoding prokineticin-2 and prokineticin receptor-2. *PLoS Genet.* **2**, e175.

Dubois, S. L., Acosta-Martínez, M., DeJoseph, M. R., Wolfe, A., Radovick, S., Boehm, U., Urban, J. H. and Levine, J. E. (2015). Positive, But Not Negative Feedback Actions of Estradiol in Adult Female Mice Require Estrogen Receptor α in Kisspeptin Neurons. *Endocrinology* **156**, 1111–1120.

Dwyer, A. A., Jayasena, C. N. and Quinton, R. (2016). Congenital hypogonadotropic hypogonadism: implications of absent mini-puberty. *Minerva Endocrinol.* **41**, 188–95.

Eckler, M. J. and Chen, B. (2014). Fez family transcription factors: controlling neurogenesis and cell fate in the developing mammalian nervous system. *Bioessays* **36**, 788–97.

Falardeau, J., Chung, W. C. J., Beenken, A., Raivio, T., Plummer, L., Sidis, Y., Jacobson-Dickman, E. E., Eliseenkova, A. V., Ma, J., Dwyer, A., et al. (2008). Decreased FGF8 signaling causes deficiency of gonadotropin-releasing hormone in humans and mice. *J. Clin. Invest.* **118**, 2822–31.

Farooqi, S. and O'Rahilly, S. (2006). Genetics of obesity in humans. *Endocr. Rev.* **27**, 710–18.

Farooqi, I. S., Volders, K., Stanhope, R., Heuschkel, R., White, A., Lank, E., Keogh, J., O'Rahilly, S. and Creemers, J. W. M. (2007). Hyperphagia and early-onset obesity due to a novel homozygous missense mutation in prohormone convertase 1/3. *J. Clin. Endocrinol. Metab.* **92**, 3369–73.

Ferreras, C., Rushton, G., Cole, C. L., Babur, M., Telfer, B. A., van Kuppevelt, T. H., Gardiner, J. M., Williams, K. J., Jayson, G. C. and Avizienyte, E. (2012). Endothelial heparan sulfate 6-O-sulfation levels regulate angiogenic responses of endothelial cells to fibroblast growth factor 2 and vascular endothelial growth factor. *J. Biol. Chem.* **287**, 36132–46.

Forni, P. E. and Wray, S. (2012). Neural Crest and Olfatory System: New Prospective. *Mol Neurobiol* **46**, 349–360.

Forni, P. E. and Wray, S. (2015). GnRH, anosmia and hypogonadotropic hypogonadism--where are we? *Front. Neuroendocrinol.* **36**, 165–77.

Forni, P. E., Taylor-Burds, C., Melvin, V. S., Williams, T., Williams, T. and Wray, S. (2011). Neural crest and ectodermal cells intermix in the nasal placode to give rise to GnRH-1 neurons, sensory neurons, and olfactory ensheathing cells. *J. Neurosci.* **31**, 6915–27.

Forni, P. E., Bharti, K., Flannery, E. M., Shimogori, T. and Wray, S. (2013). The indirect role of fibroblast growth factor-8 in defining neurogenic niches of the olfactory/GnRH systems. *J. Neurosci.* **33**, 19620–34.

Franco, B., Guioli, S., Pragliola, A., Incerti, B., Bardoni, B., Tonlorenzi, R., Carrozzo, R., Maestrini, E., Pieretti, M., Taillon-Miller, P., et al. (1991). A gene deleted in Kallmann's syndrome shares homology with neural cell adhesion and axonal path-finding molecules. *Nature*.

Frey, J. L., Bino, T., Kantor, R. R., Segal, D. M., Giardina, S. L., Roder, J., Anderson, S. and Ortaldo, J. R. (1991). Mechanism of target cell recognition by natural killer cells: characterization of a novel triggering molecule restricted to CD3- large granular lymphocytes. *J. Exp. Med.* **174**, 1527–36.

Fueshko, S. M., Key, S. and Wray, S. (1998a). GABA inhibits migration of luteinizing hormone-releasing hormone neurons in embryonic olfactory explants. *J. Neurosci.* **18**, 2560–9.

Fueshko, S. M., Key, S. and Wray, S. (1998b). Luteinizing hormone releasing hormone (LHRH) neurons maintained in nasal explants decrease LHRH messenger ribonucleic acid levels after activation of GABA(A) receptors. *Endocrinology* **139**, 2734–40.

Gamble, J. A., Karunadasa, D. K., Pape, J.-R., Skynner, M. J., Todman, M. G., Bicknell, R. J., Allen, J. P. and Herbison, A. E. (2005). Disruption of ephrin signaling associates with disordered axophilic migration of the gonadotropin-releasing hormone neurons. *J. Neurosci.* **25**, 3142–50.

Garaffo, G., Conte, D., Provero, P., Tomaiuolo, D., Luo, Z., Pinciroli, P., Peano, C., D'Atri, I., Gitton, Y., Etzion, T., et al. (2015). The Dlx5 and Foxg1 transcription factors, linked via miRNA-9 and -200, are required for the development of the olfactory and GnRH system. *Mol. Cell. Neurosci.* **68**, 103–119.

Geller, S., Kolasa, E., Tillet, Y., Duittoz, A. and Vaudin, P. (2013). Olfactory ensheathing cells form the microenvironment of migrating GnRH-1 neurons during mouse development. *Glia* **61**, 550–66.

Gherardi, E., Love, C. A., Esnouf, R. M. and Jones, E. Y. (2004). The sema domain. *Curr. Opin. Struct. Biol.* **14**, 669–78.

Giacobini, P., Kopin, A. S., Beart, P. M., Mercer, L. D., Fasolo, A. and Wray, S. (2004). Cholecystokinin modulates migration of gonadotropin-releasing hormone-1 neurons. *J. Neurosci.* **24**, 4737–48.

Giacobini, P., Messina, A., Wray, S., Giampietro, C., Crepaldi, T., Carmeliet, P. and Fasolo, A. (2007). Hepatocyte growth factor acts as a motogen and guidance signal for gonadotropin hormone-releasing hormone-1 neuronal migration. *J. Neurosci.* **27**, 431–45.

Giacobini, P., Messina, A., Morello, F., Ferraris, N., Corso, S., Penachioni, J., Giordano, S., Tamagnone, L. and Fasolo, A. (2008). Semaphorin 4D regulates gonadotropin hormone-releasing hormone-1 neuronal migration through PlexinB1-Met complex. *J. Cell Biol.* **183**, 555–66.

Giacobini, P., Parkash, J., Campagne, C., Messina, A., Casoni, F., Vanacker, C., Langlet, F., Hobo, B., Cagnoni, G., Gallet, S., et al. (2014). Brain endothelial cells control fertility through ovarian-steroid-dependent release of semaphorin 3A. *PLoS Biol.* **12**, e1001808.

Gibson, J., Morton, N. E. and Collins, A. (2006). Extended tracts of homozygosity in outbred human populations. *Hum. Mol. Genet.* **15**, 789–95.

Gill, J. C. and Tsai, P.-S. (2006). Expression of a dominant negative FGF receptor in developing GNRH1 neurons disrupts axon outgrowth and targeting to the median eminence. *Biol. Reprod.* **74**, 463–72.

Gill, J. C., Moenter, S. M. and Tsai, P.-S. (2004). Developmental regulation of gonadotropin-releasing hormone neurons by fibroblast growth factor signaling. *Endocrinology* **145**, 3830–9.

Gorbenko Del Blanco, D., Romero, C. J., Diaczok, D., De Graaff, L. C. G., Radovick, S. and Hokken-Koelega, A. C. S. (2012). A novel OTX2 mutation in a patient with combined pituitary hormone deficiency, pituitary malformation, and an underdeveloped left optic nerve. *Eur. J. Endocrinol.*

Gregory, S. J. and Kaiser, U. B. (2004). Regulation of Gonadotropins by Inhibin and Activin. *Semin. Reprod. Med.* **22**, 253–267.

Gu, C., Yoshida, Y., Livet, J., Reimert, D. V, Mann, F., Merte, J., Henderson, C. E., Jessell, T. M., Kolodkin, A. L. and Ginty, D. D. (2005). Semaphorin 3E and plexin-D1 control vascular pattern independently of neuropilins. *Science* **307**, 265–8.

Guo, H.-F. and Vander Kooi, C. W. (2015). Neuropilin Functions as an Essential Cell Surface Receptor. *J. Biol. Chem.* **290**, 29120–6.

Hanchate, N. K., Giacobini, P., Lhuillier, P., Parkash, J., Espy, C., Fouveaut, C., Leroy, C., Baron, S., Campagne, C., Vanacker, C., et al. (2012). SEMA3A, a gene involved in axonal pathfinding, is mutated in patients with Kallmann syndrome. *PLoS Genet.* **8**, e1002896.

Hardelin, J. P., Julliard, A. K., Moniot, B., Soussi-Yanicostas, N., Verney, C., Schwanzel-Fukuda, M., Ayer-Le Lievre, C. and Petit, C. (1999). Anosmin-1 is a regionally restricted component of basement membranes and interstitial matrices during organogenesis: implications for the developmental anomalies of X chromosome-linked Kallmann syndrome. *Dev. Dyn.* **215**, 26–44.

He, C., Zhang, C., Hunter, D. J., Hankinson, S. E., Buck Louis, G. M., Hediger, M. L. and Hu, F. B. (2010). Age at menarche and risk of type 2 diabetes: results from 2 large prospective cohort studies. *Am. J. Epidemiol.* **171**, 334–44.

Herbison, A. E. (2006). Physiology of the gonadotropin-releasing hormone neuronal network. In *Knobil and Neill's Physiology of Reproduction*, pp. 1415–1482.

Herbison, A. E. (2016). Control of puberty onset and fertility by gonadotropin-releasing hormone neurons. *Nat. Rev. Endocrinol.* **12**, 452–466.

Hide, T., Hatakeyama, J., Kimura-Yoshida, C., Tian, E., Takeda, N., Ushio, Y., Shiroishi, T., Aizawa, S. and Matsuo, I. (2002). Genetic modifiers of otocephalic phenotypes in Otx2 heterozygous mutant mice. *Development* **129**, 4347–57.

Hota, P. K. and Buck, M. (2012). Plexin structures are coming: Opportunities for multilevel investigations of semaphorin guidance receptors, their cell signaling mechanisms, and functions. *Cell. Mol. Life Sci.* **69**, 3765–3805.

Howard, S. R. (2018). Genes underlying delayed puberty. *Mol. Cell. Endocrinol.* **476**, 119–128.

Howard, S. R. and Dunkel, L. (2018). The Genetic Basis of Delayed Puberty. *Neuroendocrinology* **106**, 283–291.

Howard, S. R., Guasti, L., Ruiz-Babot, G., Mancini, A., David, A., Storr, H. L., Metherell, L. A., Sternberg, M. J., Cabrera, C. P., Warren, H. R., et al. (2016). IGSF10 mutations dysregulate gonadotropin-releasing hormone neuronal migration resulting in delayed puberty. *EMBO Mol. Med.* **8**, 626–42.

Hu, Y., Guimond, S. E., Travers, P., Cadman, S., Hohenester, E., Tumbull, J. E., Kim, S. H. and Bouloux, P. M. (2009). Novel mechanisms of fibroblast growth factor receptor 1 regulation by extracellular matrix protein anosmin-1. *J. Biol. Chem.* **284**, 29905–29920.

Hudson, M. L., Kinnunen, T., Cinar, H. N. and Chisholm, A. D. (2006). C. elegans Kallmann syndrome protein KAL-1 interacts with syndecan and glypican to regulate neuronal cell migrations. *Dev. Biol.* **294**, 352–65.

Hung, R.-J. and Terman, J. R. (2011). Extracellular inhibitors, repellents, and semaphorin/plexin/MICAL-mediated actin filament disassembly. *Cytoskeleton (Hoboken).* **68**, 415–33.

Hutchins, B. I., Kotan, L. D., Taylor-Burds, C., Ozkan, Y., Cheng, P. J., Gurbuz, F., Tiong, J. D. R., Mengen, E., Yuksel, B., Topaloglu, A. K., et al. (2016). CCDC141 Mutation Identified in Anosmic Hypogonadotropic Hypogonadism (Kallmann Syndrome) Alters GnRH Neuronal Migration. *Endocrinology* **157**, 1956–66.

Iwai, T., Saitoh, A., Yamada, M., Takahashi, K., Hashimoto, E., Ukai, W., Saito, T. and Yamada, M. (2012). Rhotekin modulates differentiation of cultured neural stem cells to neurons. *J. Neurosci. Res.* **90**, 1359–66.

Jackson, R. S., Creemers, J. W. M., Ohagi, S., Raffin-Sanson, M. L., Sanders, L., Montague, C. T., Hutton, J. C. and O'Rahilly, S. (1997). Obesity and impaired prohormone processing

associated with mutations in the human prohormone convertase 1 gene. *Nat. Genet.* **16**, 303–6.

Janssen, B. J. C., Robinson, R. A., Pérez-Brangulí, F., Bell, C. H., Mitchell, K. J., Siebold, C. and Jones, E. Y. (2010). Structural basis of semaphorin-plexin signalling. *Nature* **467**, 1118–22.

Jayakody, S. A., Andoniadou, C. L., Gaston-Massuet, C., Signore, M., Cariboni, A., Bouloux, P. M., Le Tissier, P., Pevny, L. H., Dattani, M. T. and Martinez-Barbera, J. P. (2012). SOX2 regulates the hypothalamic-pituitary axis at multiple levels. *J. Clin. Invest.* **122**, 3635–46.

Jongbloets, B. C. and Pasterkamp, R. J. (2014). Semaphorin signalling during development. *Development* **141**, 3292–7.

Jongmans, M. C. J., van Ravenswaaij-Arts, C. M. A., Pitteloud, N., Ogata, T., Sato, N., Claahsen-van der Grinten, H. L., van der Donk, K., Seminara, S., Bergman, J. E. H., Brunner, H. G., et al. (2009). CHD7 mutations in patients initially diagnosed with Kallmann syndrome--the clinical overlap with CHARGE syndrome. *Clin. Genet.* **75**, 65–71.

Kanasaki, H., Oride, A., Mijiddorj, T., Sukhbaatar, U. and Kyo, S. (2017). How is GnRH regulated in GnRH-producing neurons? Studies using GT1-7 cells as a GnRH-producing cell model. *Gen. Comp. Endocrinol.* **247**, 138–142.

Känsäkoski, J., Fagerholm, R., Laitinen, E.-M., Vaaralahti, K., Hackman, P., Pitteloud, N., Raivio, T. and Tommiska, J. (2014). Mutation screening of SEMA3A and SEMA7A in patients with congenital hypogonadotropic hypogonadism. *Pediatr. Res.* **75**, 641–4.

Kaprara, A. and Huhtaniemi, I. T. (2018). The hypothalamus-pituitary-gonad axis: Tales of mice and men. *Metabolism.* **86**, 3–17.

Katayama, K., Imai, F., Suto, F. and Yoshida, Y. (2013). Deletion of Sema3a or plexinA1/plexinA3 causes defects in sensory afferent projections of statoacoustic ganglion neurons. *PLoS One* **8**, e72512.

Kato, M., Ui-Tei, K., Watanabe, M. and Sakuma, Y. (2003). Characterization of voltage-gated calcium currents in gonadotropin-releasing hormone neurons tagged with green fluorescent protein in rats. *Endocrinology* **144**, 5118–25.

Kawauchi, S., Shou, J., Santos, R., Hébert, J. M., McConnell, S. K., Mason, I. and Calof, A. L. (2005). Fgf8 expression defines a morphogenetic center required for olfactory neurogenesis and nasal cavity development in the mouse. *Development* **132**, 5211–23.

Kelley, C. G., Lavorgna, G., Clark, M. E., Boncinelli, E. and Mellon, P. L. (2000). The Otx2 homeoprotein regulates expression from the gonadotropin-releasing hormone proximal promoter. *Mol. Endocrinol.* **14**, 1246–56.

Khan, F. I., Wei, D.-Q., Gu, K.-R., Hassan, M. I. and Tabrez, S. (2016). Current updates on computer aided protein modeling and designing. *Int. J. Biol. Macromol.* **85**, 48–62.

Kim, S. H. (2015). Congenital Hypogonadotropic Hypogonadism and Kallmann Syndrome: Past, Present, and Future. *Endocrinol. Metab. (Seoul, Korea)* **30**, 456–66.

Kim, H. H., Wolfe, A., Cohen, R. N., Eames, S. C., Johnson, A. L., Wieland, C. N. and Radovick, S. (2007). In vivo identification of a 107-base pair promoter element mediating neuron-specific expression of mouse gonadotropin-releasing hormone. *Mol. Endocrinol.* **21**, 457–71.

Kim, H.-G., Kurth, I., Lan, F., Meliciani, I., Wenzel, W., Eom, S. H., Kang, G. B.,

Rosenberger, G., Tekin, M., Ozata, M., et al. (2008). Mutations in CHD7, encoding a chromatin-remodeling protein, cause idiopathic hypogonadotropic hypogonadism and Kallmann syndrome. *Am. J. Hum. Genet.* **83**, 511–9.

King, J. C. and Anthony, E. L. P. (1984). LHRH neurons and their projections in humans and other mammals: Species comparisons. *Peptides*.

Klenke, U. and Taylor-Burds, C. (2012). Culturing embryonic nasal explants for developmental and physiological study. *Curr. Protoc. Neurosci.* **Chapter 3**, Unit 3.25.1-16.

Koppel, A. M. and Raper, J. A. (1998). Collapsin-1 covalently dimerizes, and dimerization is necessary for collapsing activity. *J. Biol. Chem.* **273**, 15708–13.

Kotan, L. D., Hutchins, B. I., Ozkan, Y., Demirel, F., Stoner, H., Cheng, P. J., Esen, I., Gurbuz, F., Bicakci, Y. K., Mengen, E., et al. (2014). Mutations in FEZF1 cause Kallmann syndrome. *Am. J. Hum. Genet.* **95**, 326–31.

Kramer, P. R. and Wray, S. (2000). Novel gene expressed in nasal region influences outgrowth of olfactory axons and migration of luteinizing hormone-releasing hormone (LHRH) neurons. *Genes Dev.* **14**, 1824–34.

Kruger, R. P., Aurandt, J. and Guan, K.-L. (2005). Semaphorins command cells to move. *Nat. Rev. Mol. Cell Biol.* **6**, 789–800.

Kuiri-Hänninen, T., Sankilampi, U. and Dunkel, L. (2014). Activation of the hypothalamic-pituitary-gonadal axis in infancy: Minipuberty. *Horm. Res. Paediatr.* **82**, 73–80.

Kutschera, S., Weber, H., Weick, A., De Smet, F., Genove, G., Takemoto, M., Prahst, C., Riedel, M., Mikelis, C., Baulande, S., et al. (2011). Differential endothelial transcriptomics identifies semaphorin 3G as a vascular class 3 semaphorin. *Arterioscler. Thromb. Vasc. Biol.* **31**, 151–9.

Laitinen, E.-M., Hero, M., Vaaralahti, K., Tommiska, J. and Raivio, T. (2012). Bone mineral density, body composition and bone turnover in patients with congenital hypogonadotropic hypogonadism. *Int. J. Androl.* **35**, 534–40.

Lalani, S. R., Safiullah, A. M., Molinari, L. M., Fernbach, S. D., Martin, D. M. and Belmont, J. W. (2004). SEMA3E mutation in a patient with CHARGE syndrome. *J. Med. Genet.* **41**, e94.

Lander, E. S. and Botstein, D. (1987). Homozygosity mapping: a way to map human recessive traits with the DNA of inbred children. *Science* **236**, 1567–70.

Landry, D., Cloutier, F. and Martin, L. J. (2013). Implications of leptin in neuroendocrine regulation of male reproduction. *Reprod. Biol.* **13**, 1–14.

Larder, R. and Mellon, P. L. (2009). Otx2 induction of the gonadotropin-releasing hormone promoter is modulated by direct interactions with Grg co-repressors. *J. Biol. Chem.* **284**, 16966–78.

Lawaetz, J. G., Hagen, C. P., Mieritz, M. G., Jensen, M. B., Petersen, J. H. and Juul, A. (2015). Evaluation of 451 Danish boys with delayed puberty: Diagnostic use of a new puberty nomogram and effects of oral testosterone therapy. *J. Clin. Endocrinol. Metab.* **100**, 1376–1385.

Layman, W. S., McEwen, D. P., Beyer, L. A., Lalani, S. R., Fernbach, S. D., Oh, E., Swaroop, A., Hegg, C. C., Raphael, Y., Martens, J. R., et al. (2009). Defects in neural stem cell proliferation and olfaction in Chd7 deficient mice indicate a mechanism for hyposmia in

human CHARGE syndrome. *Hum. Mol. Genet.* **18**, 1909–23.

Layman, W. S., Hurd, E. A. and Martin, D. M. (2011). Reproductive dysfunction and decreased GnRH neurogenesis in a mouse model of CHARGE syndrome. *Hum. Mol. Genet.* **20**, 3138–50.

Lee, J. M., Tiong, J., Maddox, D. M., Condie, B. G. and Wray, S. (2008). Temporal migration of gonadotrophin-releasing hormone-1 neurones is modified in GAD67 knockout mice. *J. Neuroendocrinol.* **20**, 93–103.

Leon, S. and Tena-Sempere, M. (2015). Dissecting the Roles of Gonadotropin-Inhibitory Hormone in Mammals: Studies Using Pharmacological Tools and Genetically Modified Mouse Models. *Front. Endocrinol. (Lausanne).* **6**, 189.

Lettieri, A., Oleari, R., Gimmelli, J., ANDRé, V. and Cariboni, A. (2016). The role of semaphorin signaling in the etiology of hypogonadotropic hypogonadism. *Minerva Endocrinol.* **41**, 266–78.

Lin, L., Conway, G. S., Hill, N. R., Dattani, M. T., Hindmarsh, P. C. and Achermann, J. C. (2006). A homozygous R262Q mutation in the gonadotropin-releasing hormone receptor presenting as constitutional delay of growth and puberty with subsequent borderline oligospermia. *J. Clin. Endocrinol. Metab.* **91**, 5117–21.

Liu, W., Li, J., Liu, M., Zhang, H. and Wang, N. (2015). PPAR-γ promotes endothelial cell migration by inducing the expression of Sema3g. *J. Cell. Biochem.* **116**, 514–23.

Liu, X., Uemura, A., Fukushima, Y., Yoshida, Y. and Hirashima, M. (2016). Semaphorin 3G Provides a Repulsive Guidance Cue to Lymphatic Endothelial Cells via Neuropilin-2/PlexinD1. *Cell Rep.* **17**, 2299–2311.

Love, C. A., Harlos, K., Mavaddat, N., Davis, S. J., Stuart, D. I., Jones, E. Y. and Esnouf, R. M. (2003). The ligand-binding face of the semaphorins revealed by the high-resolution crystal structure of SEMA4D. *Nat. Struct. Biol.* **10**, 843–8.

Macchi, C., Steffani, L., Oleari, R., Lettieri, A., Valenti, L., Dongiovanni, P., Romero-Ruiz, A., Tena-Sempere, M., Cariboni, A., Magni, P., et al. (2017). Iron overload induces hypogonadism in male mice via extrahypothalamic mechanisms. *Mol. Cell. Endocrinol.* **454**, 135–145.

Maeda, K., Ohkura, S., Uenoyama, Y., Wakabayashi, Y., Oka, Y., Tsukamura, H. and Okamura, H. (2010). Neurobiological mechanisms underlying GnRH pulse generation by the hypothalamus. *Brain Res.* **1364**, 103–115.

Maggi, R., Pimpinelli, F., Molteni, L., Milani, M., Martini, L. and Piva, F. (2000). Immortalized luteinizing hormone-releasing hormone neurons show a different migratory activity in vitro. *Endocrinology* **141**, 2105–12.

Magni, P., Dozio, E., Ruscica, M., Watanobe, H., Cariboni, A., Zaninetti, R., Motta, M. and Maggi, R. (2007). Leukemia inhibitory factor induces the chemomigration of immortalized gonadotropin-releasing hormone neurons through the independent activation of the Janus kinase/signal transducer and activator of transcription 3, mitogen-activated protein kinase/extrac. *Mol. Endocrinol.* **21**, 1163–74.

Maier, E. C., Saxena, A., Alsina, B., Bronner, M. E. and Whitfield, T. T. (2014). Sensational placodes: neurogenesis in the otic and olfactory systems. *Dev. Biol.* **389**, 50–67.

Manfredi-Lozano, M., Roa, J. and Tena-Sempere, M. (2017). Connecting metabolism and

gonadal function: Novel central neuropeptide pathways involved in the metabolic control of puberty and fertility. *Front. Neuroendocrinol.* **48**, 37–49.

Marcos, S., Monnier, C., Rovira, X., Fouveaut, C., Pitteloud, N., Ango, F., Dodé, C. and Hardelin, J.-P. (2017). Defective signaling through plexin-A1 compromises the development of the peripheral olfactory system and neuroendocrine reproductive axis in mice. *Hum. Mol. Genet.* **26**, 2006–2017.

Margolin, D. H., Kousi, M., Chan, Y.-M., Lim, E. T., Schmahmann, J. D., Hadjivassiliou, M., Hall, J. E., Adam, I., Dwyer, A., Plummer, L., et al. (2013). Ataxia, dementia, and hypogonadotropism caused by disordered ubiquitination. *N. Engl. J. Med.* **368**, 1992–2003.

Marín, O. and Rubenstein, J. L. R. (2003). Cell migration in the forebrain. *Annu. Rev. Neurosci.* **26**, 441–83.

Marino, M., Moriondo, V., Vighi, E., Pignatti, E. and Simoni, M. (2014). Central hypogonadotropic hypogonadism: genetic complexity of a complex disease. *Int. J. Endocrinol.* **2014**, 649154.

Martinez de la Escalera, G., Choi, A. L. and Weiner, R. I. (1992). Generation and synchronization of gonadotropin-releasing hormone (GnRH) pulses: intrinsic properties of the GT1-1 GnRH neuronal cell line. *Proc. Natl. Acad. Sci.* **89**, 1852–1855.

Mason, A. J., Hayflick, J. S., Zoeller, R. T., Young, W. S., Phillips, H. S., Nikolics, K. and Seeburg, P. H. (1986). A deletion truncating the gonadotropin-releasing hormone gene is responsible for hypogonadism in the hpg mouse. *Science (80-.).*

Matsumoto, S.-I., Yamazaki, C., Masumoto, K.-H., Nagano, M., Naito, M., Soga, T., Hiyama, H., Matsumoto, M., Takasaki, J., Kamohara, M., et al. (2006). Abnormal development of the olfactory bulb and reproductive system in mice lacking prokineticin receptor PKR2. *Proc. Natl. Acad. Sci. U. S. A.* **103**, 4140–5.

Matsuo, H., Baba, Y., Nair, R. M. G., Arimura, A. and Schally, A. V. (1971). Structure of the porcine LH- and FSH-releasing hormone. I. The proposed amino acid sequence. *Biochem. Biophys. Res. Commun.*

McCormack, S. E., Li, D., Kim, Y. J., Lee, J. Y., Kim, S.-H., Rapaport, R. and Levine, M. A. (2017). Digenic Inheritance of PROKR2 and WDR11 Mutations in Pituitary Stalk Interruption Syndrome. *J. Clin. Endocrinol. Metab.* **102**, 2501–2507.

Mellon, P. L., Windle, J. J., Goldsmith, P. C., Padula, C. A., Roberts, J. L. and Weiner, R. I. (1990). Immortalization of hypothalamic GnRH neurons by genetically targeted tumorigenesis. *Neuron* **5**, 1–10.

Memi, F., Abe, P., Cariboni, A., MacKay, F., Parnavelas, J. G. and Stumm, R. (2013). CXC chemokine receptor 7 (CXCR7) affects the migration of GnRH neurons by regulating CXCL12 availability. *J. Neurosci.* **33**, 17527–37.

Merchenthaler, I., Görcs, T., Sétáló, G., Petrusz, P. and Flerkó, B. (1984). Gonadotropin-releasing hormone (GnRH) neurons and pathways in the rat brain. *Cell Tissue Res.* **237**, 15–29.

Merlo, G. R., Mantero, S., Zaghetto, A. A., Peretto, P., Paina, S. and Gozzo, M. (2007). The role of Dlx homeogenes in early development of the olfactory pathway. *J. Mol. Histol.* **38**, 347–58.

Messina, A. and Giacobini, P. (2013). Semaphorin signaling in the development and function of the gonadotropin hormone-releasing hormone system. *Front. Endocrinol. (Lausanne).* **4**, 133.

Messina, A., Ferraris, N., Wray, S., Cagnoni, G., Donohue, D. E., Casoni, F., Kramer, P. R., Derijck, A. A., Adolfs, Y., Fasolo, A., et al. (2011). Dysregulation of Semaphorin7A/β1-integrin signaling leads to defective GnRH-1 cell migration, abnormal gonadal development and altered fertility. *Hum. Mol. Genet.* **20**, 4759–74.

Messina, A., Langlet, F., Chachlaki, K., Roa, J., Rasika, S., Jouy, N., Gallet, S., Gaytan, F., Parkash, J., Tena-Sempere, M., et al. (2016). A microRNA switch regulates the rise in hypothalamic GnRH production before puberty. *Nat. Neurosci.* **19**, 835–44.

Miller, A. M., Treloar, H. B. and Greer, C. A. (2010). Composition of the migratory mass during development of the olfactory nerve. *J. Comp. Neurol.* **518**, 4825–41.

Minoux, M. and Rijli, F. M. (2010). Molecular mechanisms of cranial neural crest cell migration and patterning in craniofacial development. *Development* **137**, 2605–21.

Miraoui, H., Dwyer, A. A., Sykiotis, G. P., Plummer, L., Chung, W., Feng, B., Beenken, A., Clarke, J., Pers, T. H., Dworzynski, P., et al. (2013). Mutations in FGF17, IL17RD, DUSP6, SPRY4, and FLRT3 are identified in individuals with congenital hypogonadotropic hypogonadism. *Am. J. Hum. Genet.* **92**, 725–43.

Miura, K., Acierno, J. S. and Seminara, S. B. (2004). Characterization of the human nasal embryonic LHRH factor gene, NELF, and a mutation screening among 65 patients with idiopathic hypogonadotropic hypogonadism (IHH). *J. Hum. Genet.* **49**, 265–8.

Moody, S. A. and LaMantia, A.-S. (2015). Transcriptional Regulation of Cranial Sensory Placode Development.pp. 301–350.

Morgan, N. V., Gissen, P., Sharif, S. M., Baumber, L., Sutherland, J., Kelly, D. A., Aminu, K., Bennett, C. P., Woods, C. G., Mueller, R. F., et al. (2002). A novel locus for Meckel-Gruber syndrome, MKS3, maps to chromosome 8q24. *Hum. Genet.* **111**, 456–61.

Mori-Akiyama, Y., Akiyama, H., Rowitch, D. H. and de Crombrugghe, B. (2003). Sox9 is required for determination of the chondrogenic cell lineage in the cranial neural crest. *Proc. Natl. Acad. Sci. U. S. A.* **100**, 9360–5.

Müller, F. and O'Rahilly, R. (2004). Olfactory structures in staged human embryos. *Cells Tissues Organs*.

Murakami, S. and Arai, Y. (2002). Migration of LHRH neurons into the spinal cord: evidence for axon-dependent migration from the transplanted chick olfactory placode. *Eur. J. Neurosci.* **16**, 684–92.

Murakami, Y., Suto, F., Shimizu, M., Shinoda, T., Kameyama, T. and Fujisawa, H. (2001). Differential expression of plexin-A subfamily members in the mouse nervous system. *Dev. Dyn.* **220**, 246–58.

Muscatelli, F. (2000). Disruption of the mouse Necdin gene results in hypothalamic and behavioral alterations reminiscent of the human Prader-Willi syndrome. *Hum. Mol. Genet.*

Navarro, V. M., Gottsch, M. L., Chavkin, C., Okamura, H., Clifton, D. K. and Steiner, R. A. (2009). Regulation of Gonadotropin-Releasing Hormone Secretion by Kisspeptin/Dynorphin/Neurokinin B Neurons in the Arcuate Nucleus of the Mouse. *J. Neurosci.* **29**, 11859–11866.

Ng, P. C. and Henikoff, S. (2003). SIFT: Predicting amino acid changes that affect protein function. *Nucleic Acids Res.* **31**, 3812–4.

Oh, W.-J. and Gu, C. (2013). The role and mechanism-of-action of Sema3E and Plexin-D1 in

vascular and neural development. *Semin. Cell Dev. Biol.* **24**, 156–62.

Okubo, K. and Nagahama, Y. (2008). Structural and functional evolution of gonadotropin-releasing hormone in vertebrates. *Acta Physiol.* **193**, 3–15.

Palevitch, O., Kight, K., Abraham, E., Wray, S., Zohar, Y. and Gothilf, Y. (2007). Ontogeny of the GnRH systems in zebrafish brain: in situ hybridization and promoter-reporter expression analyses in intact animals. *Cell Tissue Res.* **327**, 313–22.

Palevitch, O., Abraham, E., Borodovsky, N., Levkowitz, G., Zohar, Y. and Gothilf, Y. (2009). Nasal embryonic LHRH factor plays a role in the developmental migration and projection of gonadotropin-releasing hormone 3 neurons in zebrafish. *Dev. Dyn.* **238**, 66–75.

Palmert, M. R. and Dunkel, L. (2012). Clinical practice. Delayed puberty. *N. Engl. J. Med.* **366**, 443–53.

Parkash, J., Messina, A., Langlet, F., Cimino, I., Loyens, A., Mazur, D., Gallet, S., Balland, E., Malone, S. A., Pralong, F., et al. (2015). Semaphorin7A regulates neuroglial plasticity in the adult hypothalamic median eminence. *Nat. Commun.* **6**, 6385.

Parker, M. W., Guo, H.-F., Li, X., Linkugel, A. D. and Vander Kooi, C. W. (2012). Function of members of the neuropilin family as essential pleiotropic cell surface receptors. *Biochemistry* **51**, 9437–46.

Pasterkamp, R. J. and Giger, R. J. (2009). Semaphorin function in neural plasticity and disease. *Curr. Opin. Neurobiol.* **19**, 263–74.

Pavlov, M. I., Sautier, J.-M., Oboeuf, M., Asselin, A. and Berdal, A. (2003). Chondrogenic differentiation during midfacial development in the mouse: in vivo and in vitro studies. *Biol. cell* **95**, 75–86.

Perälä, N., Peitsaro, N., Sundvik, M., Koivula, H., Sainio, K., Sariola, H., Panula, P. and Immonen, T. (2010). Conservation, expression, and knockdown of zebrafish plxnb2a and plxnb2b. *Dev. Dyn.* **239**, 2722–34.

Perälä, N., Sariola, H. and Immonen, T. (2012). More than nervous: the emerging roles of plexins. *Differentiation.* **83**, 77–91.

Pielecka-Fortuna, J., Chu, Z. and Moenter, S. M. (2008). Kisspeptin acts directly and indirectly to increase gonadotropin-releasing hormone neuron activity and its effects are modulated by estradiol. *Endocrinology* **149**, 1979–1986.

Pierce, A., Bliesner, B., Xu, M., Nielsen-Preiss, S., Lemke, G., Tobet, S. and Wierman, M. E. (2008). Axl and Tyro3 modulate female reproduction by influencing gonadotropin-releasing hormone neuron survival and migration. *Mol. Endocrinol.* **22**, 2481–95.

Pitteloud, N., Meysing, A., Quinton, R., Acierno, J. S., Dwyer, A. A., Plummer, L., Fliers, E., Boepple, P., Hayes, F., Seminara, S., et al. (2006a). Mutations in fibroblast growth factor receptor 1 cause Kallmann syndrome with a wide spectrum of reproductive phenotypes. *Mol. Cell. Endocrinol.* **254**–**255**, 60–69.

Pitteloud, N., Acierno, J. S., Meysing, A., Eliseenkova, A. V., Ma, J., Ibrahimi, O. A., Metzger, D. L., Hayes, F. J., Dwyer, A. A., Hughes, V. A., et al. (2006b). Mutations in fibroblast growth factor receptor 1 cause both Kallmann syndrome and normosmic idiopathic hypogonadotropic hypogonadism. *Proc. Natl. Acad. Sci. U. S. A.* **103**, 6281–6.

Pitteloud, N., Quinton, R., Pearce, S., Raivio, T., Acierno, J., Dwyer, A., Plummer, L., Hughes, V., Seminara, S., Cheng, Y. Z., et al. (2007a). Digenic mutations account for variable

phenotypes in idiopathic hypogonadotropic hypogonadism. *J. Clin. Invest.* **117**, 457–463.

Pitteloud, N., Zhang, C., Pignatelli, D., Li, J.-D., Raivio, T., Cole, L. W., Plummer, L., Jacobson-Dickman, E. E., Mellon, P. L., Zhou, Q.-Y., et al. (2007b). Loss-of-function mutation in the prokineticin 2 gene causes Kallmann syndrome and normosmic idiopathic hypogonadotropic hypogonadism. *Proc. Natl. Acad. Sci. U. S. A.* **104**, 17447–52.

Plant, T. M. (2015a). Neuroendocrine control of the onset of puberty. *Front. Neuroendocrinol.* **38**, 73–88.

Plant, T. M. (2015b). 60 YEARS OF NEUROENDOCRINOLOGY: The hypothalamo-pituitary–gonadal axis. *J. Endocrinol.* **226**, T41–T54.

Pratt, T., Conway, C. D., Tian, N. M. M.-L., Price, D. J. and Mason, J. O. (2006). Heparan sulphation patterns generated by specific heparan sulfotransferase enzymes direct distinct aspects of retinal axon guidance at the optic chiasm. *J. Neurosci.* **26**, 6911–23.

Prevot, V. (2014). Puberty in Mice and Rats. In *Knobil and Neill's Physiology of Reproduction: Two-Volume Set*, .

Prosser, H. M., Bradley, A. and Caldwell, M. A. (2007). Olfactory bulb hypoplasia in Prokr2 null mice stems from defective neuronal progenitor migration and differentiation. *Eur. J. Neurosci.* **26**, 3339–44.

Pugliese-Pires, P. N., Fortin, J. P., Arthur, T., Latronico, A. C., Mendonca, B. B., Villares, S. M. F., Arnhold, I. J. P., Kopin, A. S. and Jorge, A. A. L. (2011). Novel inactivating mutations in the GH secretagogue receptor gene in patients with constitutional delay of growth and puberty. *Eur. J. Endocrinol.*

Pyott, S. M., Schwarze, U., Christiansen, H. E., Pepin, M. G., Leistritz, D. F., Dineen, R., Harris, C., Burton, B. K., Angle, B., Kim, K., et al. (2011). Mutations in PPIB (cyclophilin B) delay type I procollagen chain association and result in perinatal lethal to moderate osteogenesis imperfecta phenotypes. *Hum. Mol. Genet.* **20**, 1595–609.

Quennell, J. H., Mulligan, A. C., Tups, A., Liu, X., Phipps, S. J., Kemp, C. J., Herbison, A. E., Grattan, D. R. and Anderson, G. M. (2009). Leptin indirectly regulates gonadotropin-releasing hormone neuronal function. *Endocrinology* **150**, 2805–12.

Radovick, S., Wray, S., Lee, E., Nicols, D. K., Nakayama, Y., Weintraub, B. D., Westphal, H., Cutler, G. B. and Wondisford, F. E. (1991). Migratory arrest of gonadotropin-releasing hormone neurons in transgenic mice. *Proc. Natl. Acad. Sci. U. S. A.* **88**, 3402–6.

Raivio, T., Falardeau, J., Dwyer, A., Quinton, R., Hayes, F. J., Hughes, V. A., Cole, L. W., Pearce, S. H., Lee, H., Boepple, P., et al. (2007). Reversal of idiopathic hypogonadotropic hypogonadism. *N. Engl. J. Med.* **357**, 863–73.

Rance, N. E., Young, W. S. and McMullen, N. T. (1994). Topography of neurons expressing luteinizing hormone-releasing hormone gene transcripts in the human hypothalamus and basal forebrain. *J. Comp. Neurol.* **339**, 573–86.

Ravindran, E., Hu, H., Yuzwa, S. A., Hernandez-Miranda, L. R., Kraemer, N., Ninnemann, O., Musante, L., Boltshauser, E., Schindler, D., Hübner, A., et al. (2017). Homozygous ARHGEF2 mutation causes intellectual disability and midbrain-hindbrain malformation. *PLoS Genet.* **13**, e1006746.

Rehman, S. U., Baig, S. M., Eiberg, H., Rehman, S. U., Ahmad, I., Malik, N. A., Tommerup, N. and Hansen, L. (2011). Autozygosity mapping of a large consanguineous Pakistani family

reveals a novel non-syndromic autosomal recessive mental retardation locus on 11p15-tel. *Neurogenetics* **12**, 247–51.

Ritte, R., Lukanova, A., Tjønneland, A., Olsen, A., Overvad, K., Mesrine, S., Fagherazzi, G., Dossus, L., Teucher, B., Steindorf, K., et al. (2013). Height, age at menarche and risk of hormone receptor-positive and -negative breast cancer: A cohort study. *Int. J. Cancer* **132**, 2619–2629.

Rogers, C. D. and Nie, S. (2018). Specifying neural crest cells: From chromatin to morphogens and factors in between. *Wiley Interdiscip. Rev. Dev. Biol.* **7**, e322.

Sabado, V., Barraud, P., Baker, C. V. H. and Streit, A. (2012). Specification of GnRH-1 neurons by antagonistic FGF and retinoic acid signaling. *Dev. Biol.* **362**, 254–62.

Salian-Mehta, S., Xu, M., Knox, A. J., Plummer, L., Slavov, D., Taylor, M., Bevers, S., Hodges, R. S., Crowley, W. F. and Wierman, M. E. (2014). Functional consequences of AXL sequence variants in hypogonadotropic hypogonadism. *J. Clin. Endocrinol. Metab.* **99**, 1452–60.

Sanlaville, D., Etchevers, H. C., Gonzales, M., Martinovic, J., Clément-Ziza, M., Delezoide, A.-L., Aubry, M.-C., Pelet, A., Chemouny, S., Cruaud, C., et al. (2006). Phenotypic spectrum of CHARGE syndrome in fetuses with CHD7 truncating mutations correlates with expression during human development. *J. Med. Genet.* **43**, 211–217.

Sarrazin, S., Lamanna, W. C. and Esko, J. D. (2011). Heparan sulfate proteoglycans. *Cold Spring Harb. Perspect. Biol.* **3**, a004952–a004952.

Sato, Y., Miyasaka, N. and Yoshihara, Y. (2005). Mutually exclusive glomerular innervation by two distinct types of olfactory sensory neurons revealed in transgenic zebrafish. *J. Neurosci.* **25**, 4889–97.

Schulz, Y., Wehner, P., Opitz, L., Salinas-Riester, G., Bongers, E. M. H. F., van Ravenswaaij-Arts, C. M. A., Wincent, J., Schoumans, J., Kohlhase, J., Borchers, A., et al. (2014). CHD7, the gene mutated in CHARGE syndrome, regulates genes involved in neural crest cell guidance. *Hum. Genet.* **133**, 997–1009.

Schwanzel-Fukuda, M. (1999). Origin and migration of luteinizing hormone-releasing hormone neurons in mammals. *Microsc. Res. Tech.*

Schwanzel-Fukuda, M. and Pfaff, D. W. (1989). Origin of luteinizing hormone-releasing hormone neurons. *Nature*.

Schwanzel-Fukuda, M., Bick, D. and Pfaff, D. W. (1989). Luteinizing hormone-releasing hormone (LHRH)-expressing cells do not migrate normally in an inherited hypogonadal (Kallmann) syndrome. *Mol. Brain Res.*

Schwarting, G. A., Kostek, C., Bless, E. P., Ahmad, N. and Tobet, S. A. (2001). Deleted in colorectal cancer (DCC) regulates the migration of luteinizing hormone-releasing hormone neurons to the basal forebrain. *J. Neurosci.* **21**, 911–9.

Schwarting, G. A., Raitcheva, D., Bless, E. P., Ackerman, S. L. and Tobet, S. (2004). Netrin 1-mediated chemoattraction regulates the migratory pathway of LHRH neurons. *Eur. J. Neurosci.* **19**, 11–20.

Schwarting, G. A., Henion, T. R., Nugent, J. D., Caplan, B. and Tobet, S. (2006). Stromal cell-derived factor-1 (chemokine C-X-C motif ligand 12) and chemokine C-X-C motif receptor 4 are required for migration of gonadotropin-releasing hormone neurons to the forebrain. *J.*

Neurosci. **26**, 6834–40.

Schwarz, Q., Waimey, K. E., Golding, M., Takamatsu, H., Kumanogoh, A., Fujisawa, H., Cheng, H. and Ruhrberg, C. (2008). Plexin A3 and plexin A4 convey semaphorin signals during facial nerve development. *Dev. Biol.* **324**, 1–9.

Schwarz, J. M., Cooper, D. N., Schuelke, M. and Seelow, D. (2014). MutationTaster2: mutation prediction for the deep-sequencing age. *Nat. Methods* **11**, 361–2.

Sedita, J., Izvolsky, K. and Cardoso, W. V. (2004). Differential expression of heparan sulfate 6-O-sulfotransferase isoforms in the mouse embryo suggests distinctive roles during organogenesis. *Dev. Dyn.* **231**, 782–94.

Sedlmeyer, I. L. and Palmert, M. R. (2002). Delayed puberty: analysis of a large case series from an academic center. *J. Clin. Endocrinol. Metab.* **87**, 1613–20.

Sedlmeyer, I. L., Hirschhorn, J. N. and Palmert, M. R. (2002). Pedigree analysis of constitutional delay of growth and maturation: determination of familial aggregation and inheritance patterns. *J. Clin. Endocrinol. Metab.* **87**, 5581–6.

Seminara, S. B., Messager, S., Chatzidaki, E. E., Thresher, R. R., Acierno, J. S., Shagoury, J. K., Bo-Abbas, Y., Kuohung, W., Schwinof, K. M., Hendrick, A. G., et al. (2003). The GPR54 Gene as a Regulator of Puberty. *N. Engl. J. Med.* **349**, 1614–1627.

Sharma, A., Verhaagen, J. and Harvey, A. R. (2012). Receptor complexes for each of the Class 3 Semaphorins. *Front. Cell. Neurosci.* **6**, 28.

Shi, C.-H., Schisler, J. C., Rubel, C. E., Tan, S., Song, B., McDonough, H., Xu, L., Portbury, A. L., Mao, C.-Y., True, C., et al. (2014). Ataxia and hypogonadism caused by the loss of ubiquitin ligase activity of the U box protein CHIP. *Hum. Mol. Genet.* **23**, 1013–24.

Shivers, B. D., Harlan, R. E., Morrell, J. I. and Pfaff, D. W. (1983). Absence of oestradiol concentration in cell nuclei of LHRH-immunoreactive neurones. *Nature* **304**, 345–347.

Sidhoum, V. F., Chan, Y. M., Lippincott, M. F., Balasubramanian, R., Quinton, R., Plummer, L., Dwyer, A., Pitteloud, N., Hayes, F. J., Hall, J. E., et al. (2014). Reversal and relapse of hypogonadotropic hypogonadism: Resilience and fragility of the reproductive neuroendocrine system. *J. Clin. Endocrinol. Metab.* **99**, 861–870.

Siebold, C. and Jones, E. Y. (2013). Structural insights into semaphorins and their receptors. *Semin. Cell Dev. Biol.* **24**, 139–45.

Spergel, D. J., Kruth, U., Hanley, D. F., Sprengel, R. and Seeburg, P. H. (1999). GABA- and glutamate-activated channels in green fluorescent protein-tagged gonadotropin-releasing hormone neurons in transgenic mice. *J Neurosci* **19**, 2037–2050.

Spergel, D. J., Krüth, U., Shimshek, D. R., Sprengel, R. and Seeburg, P. H. (2001). Using reporter genes to label selected neuronal populations in transgenic mice for gene promoter, anatomical, and physiological studies. *Prog. Neurobiol.* **63**, 673–686.

Spicer, O. S., Wong, T.-T., Zmora, N. and Zohar, Y. (2016). Targeted Mutagenesis of the Hypophysiotropic Gnrh3 in Zebrafish (Danio rerio) Reveals No Effects on Reproductive Performance. *PLoS One* **11**, e0158141.

Stainier, D. Y. R., Raz, E., Lawson, N. D., Ekker, S. C., Burdine, R. D., Eisen, J. S., Ingham, P. W., Schulte-Merker, S., Yelon, D., Weinstein, B. M., et al. (2017). Guidelines for morpholino use in zebrafish. *PLoS Genet.* **13**, e1007000.

Stamou, M. I. and Georgopoulos, N. A. (2018). Kallmann syndrome: phenotype and genotype of hypogonadotropic hypogonadism. *Metabolism.* **86**, 124–134.

Stamou, M. I., Cox, K. H. and Crowley, W. F. (2015). Discovering Genes Essential to the Hypothalamic Regulation of Human Reproduction Using a Human Disease Model: Adjusting to Life in the "-Omics" Era. *Endocr. Rev.* **36**, 603–21.

Steventon, B., Mayor, R. and Streit, A. (2014). Neural crest and placode interaction during the development of the cranial sensory system. *Dev. Biol.* **389**, 28–38.

Strobel, A., Issad, T., Camoin, L., Ozata, M. and Strosberg, A. D. (1998). A leptin missense mutation associated with hypogonadism and morbid obesity. *Nat. Genet.* **18**, 213–5.

Strzelecka-Kiliszek, A., Mebarek, S., Roszkowska, M., Buchet, R., Magne, D. and Pikula, S. (2017). Functions of Rho family of small GTPases and Rho-associated coiled-coil kinases in bone cells during differentiation and mineralization. *Biochim. Biophys. Acta - Gen. Subj.*

Suter, K. J., Song, W. J., Sampson, T. L., Wuarin, J. P., Saunders, J. T., Dudek, F. E. and Moenter, S. M. (2000). Genetic targeting of green fluorescent protein to gonadotropin-releasing hormone neurons: characterization of whole-cell electrophysiological properties and morphology. *Endocrinology* **141**, 412–419.

Suto, F., Murakami, Y., Nakamura, F., Goshima, Y. and Fujisawa, H. (2003). Identification and characterization of a novel mouse plexin, plexin-A4. *Mech. Dev.* **120**, 385–96.

Suto, F., Tsuboi, M., Kamiya, H., Mizuno, H., Kiyama, Y., Komai, S., Shimizu, M., Sanbo, M., Yagi, T., Hiromi, Y., et al. (2007). Interactions between plexin-A2, plexin-A4, and semaphorin 6A control lamina-restricted projection of hippocampal mossy fibers. *Neuron* **53**, 535–47.

Suzuki, J. and Osumi, N. (2015). Neural crest and placode contributions to olfactory development. *Curr. Top. Dev. Biol.*

Suzuki, A., Sangani, D. R., Ansari, A. and Iwata, J. (2016). Molecular mechanisms of midfacial developmental defects. *Dev. Dyn.* **245**, 276–93.

Swiercz, J. M., Kuner, R., Behrens, J. and Offermanns, S. (2002). Plexin-B1 directly interacts with PDZ-RhoGEF/LARG to regulate RhoA and growth cone morphology. *Neuron* **35**, 51–63.

Sykiotis, G. P., Pitteloud, N., Seminara, S. B., Kaiser, U. B. and Crowley, W. F. (2010a). Deciphering genetic disease in the genomic era: the model of GnRH deficiency. *Sci. Transl. Med.* **2**, 32rv2.

Sykiotis, G. P., Plummer, L., Hughes, V. A., Au, M., Durrani, S., Nayak-Young, S., Dwyer, A. A., Quinton, R., Hall, J. E., Gusella, J. F., et al. (2010b). Oligogenic basis of isolated gonadotropin-releasing hormone deficiency. *Proc. Natl. Acad. Sci. U. S. A.* **107**, 15140–4.

Takahashi, T., Fournier, A., Nakamura, F., Wang, L. H., Murakami, Y., Kalb, R. G., Fujisawa, H. and Strittmatter, S. M. (1999). Plexin-neuropilin-1 complexes form functional semaphorin-3A receptors. *Cell* **99**, 59–69.

Takamatsu, H. and Kumanogoh, A. (2012). Diverse roles for semaphorin-plexin signaling in the immune system. *Trends Immunol.* **33**, 127–35.

Tamagnone, L., Artigiani, S., Chen, H., He, Z., Ming, G. I., Song, H., Chedotal, A., Winberg, M. L., Goodman, C. S., Poo, M., et al. (1999). Plexins are a large family of receptors for transmembrane, secreted, and GPI-anchored semaphorins in vertebrates. *Cell* **99**, 71–80.

Tang, H., Liu, Y., Luo, D., Ogawa, S., Yin, Y., Li, S., Zhang, Y., Hu, W., Parhar, I. S., Lin, H., et al. (2015). The kiss/kissr systems are dispensable for zebrafish reproduction: evidence from gene knockout studies. *Endocrinology* **156**, 589–99.

Taniguchi, M., Masuda, T., Fukaya, M., Kataoka, H., Mishina, M., Yaginuma, H., Watanabe, M. and Shimizu, T. (2005). Identification and characterization of a novel member of murine semaphorin family. *Genes Cells* **10**, 785–92.

Taroc, E. Z. M., Prasad, A., Lin, J. M. and Forni, P. E. (2017). The terminal nerve plays a prominent role in GnRH-1 neuronal migration independent from proper olfactory and vomeronasal connections to the olfactory bulbs. *Biol. Open* **6**, 1552–1568.

Tata, B., Huijbregts, L., Jacquier, S., Csaba, Z., Genin, E., Meyer, V., Leka, S., Dupont, J., Charles, P., Chevenne, D., et al. (2014). Haploinsufficiency of Dmxl2, encoding a synaptic protein, causes infertility associated with a loss of GnRH neurons in mouse. *PLoS Biol.* **12**, e1001952.

Teixeira, L., Guimiot, F., Dodé, C., Fallet-Bianco, C., Millar, R. P., Delezoide, A. and Hardelin, J. (2010). Defective migration of neuroendocrine GnRH cells in human arrhinencephalic conditions. *J. Clin. Invest.* **120**, 3668–72.

Terasawa, E. and Fernandez, D. L. (2001). Neurobiological Mechanisms of the Onset of Puberty in Primates 1. *Endocr. Rev.* **22**, 111–151.

Thumkeo, D., Watanabe, S. and Narumiya, S. (2013). Physiological roles of Rho and Rho effectors in mammals. *Eur. J. Cell Biol.* **92**, 303–15.

Tillo, M., Charoy, C., Schwarz, Q., Maden, C. H., Davidson, K., Fantin, A. and Ruhrberg, C. (2016). 2- and 6-O-sulfated proteoglycans have distinct and complementary roles in cranial axon guidance and motor neuron migration. *Development* **143**, 1907–13.

Tobet, S. A., Hanna, I. K. and Schwarting, G. A. (1996). Migration of neurons containing gonadotropin releasing hormone (GnRH) in slices from embryonic nasal compartment and forebrain. *Brain Res. Dev. Brain Res.* **97**, 287–92.

Topaloglu, A. K., Reimann, F., Guclu, M., Yalin, A. S., Kotan, L. D., Porter, K. M., Serin, A., Mungan, N. O., Cook, J. R., Imamoglu, S., et al. (2009). TAC3 and TACR3 mutations in familial hypogonadotropic hypogonadism reveal a key role for Neurokinin B in the central control of reproduction. *Nat. Genet.* **41**, 354–358.

Topaloglu, A. K., Lomniczi, A., Kretzschmar, D., Dissen, G. A., Kotan, L. D., McArdle, C. A., Koc, A. F., Hamel, B. C., Guclu, M., Papatya, E. D., et al. (2014). Loss-of-function mutations in PNPLA6 encoding neuropathy target esterase underlie pubertal failure and neurological deficits in Gordon Holmes syndrome. *J. Clin. Endocrinol. Metab.* **99**, E2067-75.

Topaloğlu, A. K. (2017). Update on the Genetics of Idiopathic Hypogonadotropic Hypogonadism. *J. Clin. Res. Pediatr. Endocrinol.* **9**, 113–122.

Tornberg, J., Sykiotis, G. P., Keefe, K., Plummer, L., Hoang, X., Hall, J. E., Quinton, R., Seminara, S. B., Hughes, V., Van Vliet, G., et al. (2011). Heparan sulfate 6-O-sulfotransferase 1, a gene involved in extracellular sugar modifications, is mutated in patients with idiopathic hypogonadotrophic hypogonadism. *Proc. Natl. Acad. Sci. U. S. A.* **108**, 11524–9.

Tsai, P.-S., Moenter, S. M., Postigo, H. R., El Majdoubi, M., Pak, T. R., Gill, J. C., Paruthiyil, S., Werner, S. and Weiner, R. I. (2005). Targeted expression of a dominant-negative fibroblast growth factor (FGF) receptor in gonadotropin-releasing hormone (GnRH) neurons

reduces FGF responsiveness and the size of GnRH neuronal population. *Mol. Endocrinol.* **19**, 225–36.

Tsutsui, K., Saigoh, E., Ukena, K., Teranishi, H., Fujisawa, Y., Kikuchi, M., Ishii, S. and Sharp, P. J. (2000). A novel avian hypothalamic peptide inhibiting gonadotropin release. *Biochem. Biophys. Res. Commun.* **275**, 661–7.

Turan, I., Hutchins, B. I., Hacihamdioglu, B., Kotan, L. D., Gurbuz, F., Ulubay, A., Mengen, E., Yuksel, B., Wray, S. and Topaloglu, A. K. (2017). CCDC141 Mutations in Idiopathic Hypogonadotropic Hypogonadism. *J. Clin. Endocrinol. Metab.* **102**, 1816–1825.

Ubuka, T., Son, Y. L., Bentley, G. E., Millar, R. P. and Tsutsui, K. (2012). Gonadotropin-inhibitory hormone (GnIH), GnIH receptor and cell signaling. *Gen. Comp. Endocrinol.* **190**, 10–17.

Ubuka, T., Son, Y. L. and Tsutsui, K. (2016). Molecular, cellular, morphological, physiological and behavioral aspects of gonadotropin-inhibitory hormone. *Gen. Comp. Endocrinol.* **227**, 27–50.

Uchida, Y., James, J. M., Suto, F. and Mukouyama, Y.-S. (2015). Class 3 semaphorins negatively regulate dermal lymphatic network formation. *Biol. Open* **4**, 1194–205.

Vaaralahti, K., Wehkalampi, K., Tommiska, J., Laitinen, E. M., Dunkel, L. and Raivio, T. (2011). The role of gene defects underlying isolated hypogonadotropic hypogonadism in patients with constitutional delay of growth and puberty. *Fertil. Steril.* **95**, 2756–2758.

Valverde, F., Santacana, M. and Heredia, M. (1992). Formation of an olfactory glomerulus: Morphological aspects of development and organization. *Neuroscience*.

Vannelli, G. B., Ensoli, F., Zonefrati, R., Kubota, Y., Arcangeli, A., Becchetti, A., Camici, G., Barni, T., Thiele, C. J. and Balboni, G. C. (1995). Neuroblast long-term cell cultures from human fetal olfactory epithelium respond to odors. *J. Neurosci.* **15**, 4382–94.

Varimo, T., Hero, M., Laitinen, E.-M., Sintonen, H. and Raivio, T. (2015). Health-related quality of life in male patients with congenital hypogonadotropic hypogonadism. *Clin. Endocrinol. (Oxf).* **83**, 141–3.

Varimo, T., Miettinen, P. J., Känsäkoski, J., Raivio, T. and Hero, M. (2017). Congenital hypogonadotropic hypogonadism, functional hypogonadotropism or constitutional delay of growth and puberty? An analysis of a large patient series from a single tertiary center. *Hum. Reprod.* **32**, 147–153.

Vázquez, M. J., Romero-Ruiz, A. and Tena-Sempere, M. (2015). Roles of leptin in reproduction, pregnancy and polycystic ovary syndrome: consensus knowledge and recent developments. *Metabolism.* **64**, 79–91.

Vilensky, J. A. (2014). The neglected cranial nerve: Nervus terminalis (cranial nerve N). *Clin. Anat.*

Vodrazka, P., Korostylev, A., Hirschberg, A., Swiercz, J. M., Worzfeld, T., Deng, S., Fazzari, P., Tamagnone, L., Offermanns, S. and Kuner, R. (2009). The semaphorin 4D-plexin-B signalling complex regulates dendritic and axonal complexity in developing neurons via diverse pathways. *Eur. J. Neurosci.* **30**, 1193–208.

Wang, S., Haynes, C., Barany, F. and Ott, J. (2009). Genome-wide autozygosity mapping in human populations. *Genet. Epidemiol.* **33**, 172–80.

Wang, H., Graham, I., Hastings, R., Gunewardena, S., Brinkmeier, M. L., Conn, P. M.,

Camper, S. A. and Kumar, T. R. (2015). Gonadotrope-specific deletion of Dicer results in severely suppressed gonadotropins and fertility defects. *J. Biol. Chem.* **290**, 2699–714.

Wehkalampi, K., Widén, E., Laine, T., Palotie, A. and Dunkel, L. (2008a). Association of the timing of puberty with a chromosome 2 locus. *J. Clin. Endocrinol. Metab.* **93**, 4833–4839.

Wehkalampi, K., Widén, E., Laine, T., Palotie, A. and Dunkel, L. (2008b). Patterns of inheritance of constitutional delay of growth and puberty in families of adolescent girls and boys referred to specialist pediatric care. *J. Clin. Endocrinol. Metab.* **93**, 723–8.

Wetsel, W. C., Valença, M. M., Merchenthaler, I., Liposits, Z., López, F. J., Weiner, R. I., Mellon, P. L. and Negro-Vilar, A. (1992). Intrinsic pulsatile secretory activity of immortalized luteinizing hormone-releasing hormone-secreting neurons. *Proc. Natl. Acad. Sci. U. S. A.* **89**, 4149–53.

Whitlock, K. E. (2005). Origin and development of GnRH neurons. *Trends Endocrinol. Metab.* **16**, 145–151.

Wierman, M. E., Kiseljak-Vassiliades, K. and Tobet, S. (2011). Gonadotropin-releasing hormone (GnRH) neuron migration: initiation, maintenance and cessation as critical steps to ensure normal reproductive function. *Front. Neuroendocrinol.* **32**, 43–52.

Wray, S. (2010). From nose to brain: development of gonadotrophin-releasing hormone-1 neurones. *J. Neuroendocrinol.* **22**, 743–53.

Wray, S., Nieburgs, A. and Elkabes, S. (1989a). Spatiotemporal cell expression of luteinizing hormone-releasing hormone in the prenatal mouse: evidence for an embryonic origin in the olfactory placode. *Dev. Brain Res.*

Wray, S., Grant, P. and Gainer, H. (1989b). Evidence that cells expressing luteinizing hormone-releasing hormone mRNA in the mouse are derived from progenitor cells in the olfactory placode. *Proc. Natl. Acad. Sci. U. S. A.* **86**, 8132–6.

Wu, S., Wilson, M. D., Busby, E. R., Isaac, E. R. and Sherwood, N. M. (2010). Disruption of the single copy gonadotropin-releasing hormone receptor in mice by gene trap: severe reduction of reproductive organs and functions in developing and adult mice. *Endocrinology* **151**, 1142–52.

Wyatt, A., Bakrania, P., Bunyan, D. J., Osborne, R. J., Crolla, J. A., Salt, A., Ayuso, C., Newbury-Ecob, R., Abou-Rayyah, Y., Collin, J. R. O., et al. (2008). Novel heterozygous OTX2 mutations and whole gene deletions in anophthalmia, microphthalmia and coloboma. *Hum. Mutat.* **29**, E278-83.

Xu, C. and Fan, C.-M. (2007). Allocation of paraventricular and supraoptic neurons requires Sim1 function: a role for a Sim1 downstream gene PlexinC1. *Mol. Endocrinol.* **21**, 1234–45.

Xu, C., Messina, A., Somm, E., Miraoui, H., Kinnunen, T., Acierno, J., Niederländer, N. J., Bouilly, J., Dwyer, A. A., Sidis, Y., et al. (2017). KLB, encoding β-Klotho, is mutated in patients with congenital hypogonadotropic hypogonadism. *EMBO Mol. Med.* **9**, 1379–1397.

Yanicostas, C., Herbomel, E., Dipietromaria, A. and Soussi-Yanicostas, N. (2009). Anosmin-1a is required for fasciculation and terminal targeting of olfactory sensory neuron axons in the zebrafish olfactory system. *Mol. Cell. Endocrinol.* **312**, 53–60.

Yazdani, U. and Terman, J. R. (2006). The semaphorins. *Genome Biol.* **7**, 211.

Yoshida, K., Tobet, S. a, Crandall, J. E., Jimenez, T. P. and Schwarting, G. a (1995). The migration of luteinizing hormone-releasing hormone neurons in the developing rat is associated with a transient, caudal projection of the vomeronasal nerve. *J. Neurosci.* **15**, 7769–

77.

Yoshida, K., Rutishauser, U., Crandall, J. E. and Schwarting, G. A. (1999). Polysialic acid facilitates migration of luteinizing hormone-releasing hormone neurons on vomeronasal axons. *J. Neurosci.* **19**, 794–801.

Yoshida, Y., Han, B., Mendelsohn, M. and Jessell, T. M. (2006). PlexinA1 signaling directs the segregation of proprioceptive sensory axons in the developing spinal cord. *Neuron* **52**, 775–88.

Young, J., Metay, C., Bouligand, J., Tou, B., Francou, B., Maione, L., Tosca, L., Sarfati, J., Brioude, F., Esteva, B., et al. (2012). SEMA3A deletion in a family with Kallmann syndrome validates the role of semaphorin 3A in human puberty and olfactory system development. *Hum. Reprod.* **27**, 1460–5.

Yuasa, K., Nagame, T., Dohi, M., Yanagita, Y., Yamagami, S., Nagahama, M. and Tsuji, A. (2012). cGMP-dependent protein kinase I is involved in neurite outgrowth via a Rho effector, rhotekin, in Neuro2A neuroblastoma cells. *Biochem. Biophys. Res. Commun.* **421**, 239–44.

Zhang, Y., Proenca, R., Maffei, M., Barone, M., Leopold, L. and Friedman, J. M. (1994). Positional cloning of the mouse obese gene and its human homologue. *Nature*.

Zhang, G., Li, J., Purkayastha, S., Tang, Y., Zhang, H., Yin, Y., Li, B., Liu, G. and Cai, D. (2013). Hypothalamic programming of systemic ageing involving IKK-β, NF-κB and GnRH. *Nature* **497**, 211–6.

Zhou, X., Ma, L., Li, J., Gu, J., Shi, Q. and Yu, R. (2012). Effects of SEMA3G on migration and invasion of glioma cells. *Oncol. Rep.* **28**, 269–75.

Zhu, J., Choa, R. E. Y., Guo, M. H., Plummer, L., Buck, C., Palmert, M. R., Hirschhorn, J. N., Seminara, S. B. and Chan, Y.-M. (2015). A shared genetic basis for self-limited delayed puberty and idiopathic hypogonadotropic hypogonadism. *J. Clin. Endocrinol. Metab.* **100**, E646-54.

APPENDIX

I. List of figures and tables

SECTION I – Introduction

Figure 1 – Schematic diagram of GnRH neuron pathway showing hypothalamic neural networks that regulate GnRH secretion and feedback mechanisms 3

Figure 2 – Periods of activation of HPG axis 7

Figure 3 – Schematic illustration showing the different GnRH paralogs expressed by vertebrate species 10

Figure 4 – Schematic diagram illustrating the structural organization of GNRH1 gene 10

Figure 5 – Schematic representation of GnRH neuron migration 12

Figure 6 – Olfactory placode formation 14

Figure 7 – Schematic diagram of VN nerve pathways 18

Figure 8 – Neurodevelopmental and neuroendocrine regulation of GnRH neurons 26

Table 1 – List of known IGD causative genes 27-28

Figure 9 – Phase-contrast photomicrographs of immortalized GnRH neuron lines 43

Figure 10 – GnRH3 neuron development observed in a live Tg(*gnrh3*:EGFP) zebrafish larva 47

Figure 11 – Phylogenetic tree of semaphorin sequences 50

Figure 12 – Schematic representation of the protein structure of semaphorin and their receptors 51

Figure 13 – Semaphorin-Plexin complexes signalling pathways 57

Figure 14 – *Sema3a*-deficient mice aberrant phenotype 61

Figure 15 – LacZ staining revealed *Sema3g* expression during mouse development 65

Figure 16 – HSPG have multiple activities in cells and tissues 68

Figure 17 – HSPG structure and enzymatic modifications 69

SECTION III – Results and discussion

Paragraph 1 – Semaphorin 3G

Figure 1 – HZM identifies a SEMA3G mutation in two brothers with syndromic IGD 78

Table 1 – List of all homozygous regions identified in affected patients 80

Table 2 – List of variants obtained from Patient #2 WES 81

Figure 2 – Diminished signalling activity of SEMA3G protein harbouring G166V mutation 83

Figure 3 – *Sema3g* mRNA expression during GnRH neuron development 86

Figure 4 – Reduced GnRH neuron numbers in the *Sema3g*-null embryos 87

Figure 5 – Sema3g is dispensable for axonal and vascular patterning in the embryonic nose 89

Figure 6 – Sema3g deficiency reduces GnRH neuron projections to the ME and impairs testes function 90

Figure 7 – *Rtkn* and *Nktr* mRNAs are expressed in the mouse embryonic head in the brain and in chondrogenic areas, respectively 92

Paragraph 2 – Class A plexins

Figure 1 – Differential expression of *Plxna1-4* transcripts during mouse embryonic development in the nasal region 100

Figure 2 – Plxna1 and Plxna3 are expressed by neuronal progenitors and not by OECs 101

Figure 3 – Expression of Plxna1 and Plxna3 on VN nerves 102

Figure 4 – Expression of PLXNA1 and PLXNA3 in human foetus at CS19 104

Figure 5 – Abnormal migration of GnRH neurons in the nose and decreased GnRH neuron number in the developing hypothalamus of *Plxna1;Plxna3* compound-null mutants 105

Table 1 – Total and partial numbers of GnRH+ neurons at E14.5 mouse heads 106

Figure 6 – Combined but not single loss of Plxna1 and Plxna3 reduces GnRH neuron innervation of the ME 106

Figure 7 – Aberrant VN nerves patterning and GnRH neuron migration in *Plxna1;Plxna3* compound-null mice 108

Paragraph 3 – Heparan Sulphate 6-O Sulpho-Transferase 1

Table 1 – IGD genes filtering 113

Figure 1 – *HS6ST1* gene mutation has been found in a family from a self-limited DP cohort 114

Figure 2 – ISH revealed *Hs6st1* mRNA expression in territories relevant to GnRH function at P35 116

Figure 3 – *Hs6st1*$^{+/-}$ mice showed no defects in OB morphology nor in the number and projections of GnRH neurons 117

Figure 4 – Peripubertal female *Hs6st1*$^{+/-}$ mice showed delayed VO while young adults male *Hs6st1*$^{+/-}$ mice showed normal testes morphology 119

SECTION IV – Materials and methods

Figure 1 – Filtering strategy applied on WES data from Patient #2 125

Figure 2 – Filtering strategy applied on WES data from DP cohort individuals 127

Table 1 – List of primers 129

Figure 3 – Vaginal opening check 133

Figure 4 – *In situ* hybridization probes specificity 133

Table 2 – List of primary antibodies used for immunohistochemistry 136

Table 3 – List of secondary antibodies used for immunohistochemistry 136

II. List of frequent abbreviations

3v – third ventricle

AOB – accessory olfactory bulb

AP – alkaline phosphatase

AR – androgen receptor

ARC – arcuate nucleus

AVPV – anteroventral periventricular nucleus

BV – blood vessels

cAMP – cyclic adenosine monophosphate

CDGP – constitutional delay of growth and puberty

CM – conditioned medium

CNS – central nervous system

CP – cribriform plate

CPHD – combined pituitary hormone deficiency

CS – Carnegie stage

DMH – dorsomedial nucleus

DP – delayed puberty

E – embryonic day

E_2 – estradiol

ERα – estrogen receptor alpha

FSH – follicle-stimulating hormone

GABA – γ-aminobutyric acid

(E)GFP – (enhanced) green fluorescent protein

GH – growth hormone

GnIH – gonadotropin-inhibiting hormone

GnRH – gonadotropin-releasing hormone

GnRHR – GnRH receptor

GW – gestational week

hCG – human chorionic gonadotropin

(h/d)pf – hours/days post-fertilization

HPG axis – hypothalamus-pituitary-gonad axis

HZM – homozygosity mapping

IB4 – isolectin B4

IGD – Isolated GnRH Deficiency

ISH – *in situ* hybridisation

KNDy neurons – kisspeptin-neurokinin B-dynrohpin A neurons

KS – Kallmann Syndrome

LH – luteinizing hormone

MAF – minor allele frequency

ME – median eminence

MOB – main olfactory bulb

MM – migratory mass

MPOA – medial preoptic area

mRNA – messenger RNA

NC – neural crest

NCC – neural crest cell

NFJ – nasal-forebrain junction

NGS – next generation sequencing

nHH – normosmic hypogonadotropic hypogonadism

NRP - neuropilin

NS – nasal septum

OB – olfactory bulb

OE – olfactory epithelium

OEC – olfactory ensheathing cell

OLF nerve – olfactory nerve

OP – olfactory placode

OSN – olfactory sensory neuron

P – postnatal day

POMC – pro-opio-melanocortin

PNS – peripheral nervous ystem

PSI – Plexin-Semaphorin-Integrin

RFRP3 – RF-amide related peptide 3

SOD – septo-optic dysplasia

TN nerve – terminal nerve

VNO – vomeronasal organ

(c)VN nerve – (caudal) vomeronasal nerve

WES – whole exome sequencing